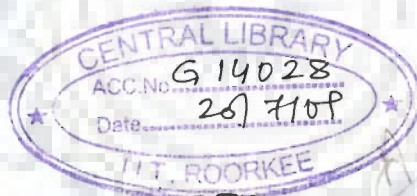# TREATMENT OF TEXTILE MILL WASTEWATER

A THESIS

Submitted in partial fulfilment of the
requirements for the award of the degree

of

DOCTOR OF PHILOSOPHY

in

CHEMICAL ENGINEERING

by

PRADEEP KUMAR

DEPARTMENT OF CHEMICAL ENGINEERING
INDIAN INSTITUTE OF TECHNOLOGY ROORKEE
ROORKEE-247 667 (INDIA)
JULY, 2007

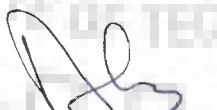# INDIAN INSTITUTE OF TECHNOLOGY ROORKEE
ROORKEE

CANDIDATE'S DECLARATION

I hereby certify that the work which is being presented in the thesis entitled **TREATMENT OF TEXTILE MILL WASTEWATER** in partial fulfilment of the requirements for the award of the degree of Doctor of Philosophy and submitted in the Department of Chemical Engineering, Indian Institute of Technology Roorkee, Roorkee is an authentic record of my own work carried out during a period from January 2003 to July 2007 under the supervision of Dr. Shri Chand, Professor & Head, Department of Chemical Engineering and Dr. B. Prasad, Associate Professor, Department of Chemical Engineering, Indian Institute of Technology Roorkee, Roorkee.

The matter presented in this thesis has not been submitted by me for the award of any other degree of this or any other Institute.

(PRADEEP KUMAR)

This is to certify that the above statement made by the candidate is correct to the best of our knowledge.

(B. PRASAD)
Supervisor

(SHRI CHAND)
Supervisor

Date: July 24, 2007

The Ph.D. Viva-Voce Examination of **Mr. PRADEEP KUMAR**, Research Scholar, has been held on ....

Signature of Supervisors   Signature of External Examiner

ABSTRACT

Textile industry is one of the most polluting industries. Treating textile effluent is a challenging task as it contains a variety of chemicals, organics, fibers, etc. Major pollutants in cotton textile wastewater come from natural impurities extracted from the fiber, the processing chemicals and dyes. The removal of color from textile mill wastewater is of great environmental concern. More than half of the nearly 90 dyestuffs used in textile mills (e.g. reactive blue 21, direct blue 80 and vat violet etc. at specific COD/BOD ratios) are non-biodegradable. There are about 706 cotton textile mills in India mainly located in Mumbai, Ahmedabad, Coimbatore and Kanpur. Out of these, 291 are composite mills and 415 are spinning mills. The composite effluent discharged from these textile mills varies from 1 to 10 million liters per day depending upon the quantity of cloth produced and the manufacturing processes employed (Swaminathan and Subhramanyam, 1982; Verma and Mishra, 2006; Toor et al., 2006; Sirianuntapiboon and Srisornsak, 2007).

Among the various treatment methods, catalytic thermolysis (thermal treatment) and coagulation are the most promising ones. Thermolysis is a chemical process by which a substance is decomposed in to other substances by use of heat. During catalytic thermolysis, two mechanisms, both in parallel but complementary to each other, take place simultaneously. The organic molecules, both small and large, present in the effluent undergo chemical and thermal breakdown and complexation, forming insoluble particles, which settle down. Further, during thermolysis larger molecules also undergo breakdown into smaller molecules, which are soluble. Work has already been done to reduce COD and color of other effluents like distillery wastewater and pulp and paper mill waste in sufficient amount using thermolysis. A maximum reduction in COD and BOD observed for alcohol distillery effluent were 70% and 83% respectively (Chaudhari et al., 2005). For pulp and paper mill effluent, the COD and color

ii

reductions were 63.3% and 92.5%, respectively (Garg et al., 2005, 2007). After the success of thermolysis process in treating other wastewaters, the present work is aimed to undertake treatment of textile mill wastewaters using thermolysis, coagulation and thermolysis accompanied with coagulation for the three different effluents; desizing waste, dyeing waste and composite waste.

The objectives set for the present work were (a) to conduct thermolysis of the effluents at moderate temperatures and atmospheric pressure conditions in presence of different catalysts and study the effect of treatment parameters such as pH, time, temperature and catalyst concentration on COD and color removal (b) to study the kinetics of thermolysis process (c) to study the effectiveness of various coagulants for COD and color reduction (d) to study the settleability of the solid residue and the filterability of treated effluent and the effect of pH on these processes (e) the thermal degradation characteristics and characterization of the solid residue by FTIR, CHNS and proximate analysis to see their suitability of being used as solid fuel and (f) to study the mechanism of coagulation process.

The experimental studies for thermolysis were carried out in a 0.5 l three-necked glass reactor. The pH of the waste water was adjusted to the desired value by adding 0.1 N HCl or 0.1 N NaOH solution before it was transferred to the three-necked glass reactor. Thereafter, the catalyst was added to the solution. The temperature of the reaction mixture was raised using a hot plate to the desired value by a P.I.D. temperature controller, which was fitted in one of the necks through the thermocouple. The raising of the temperature of the waste water from ambient to 95 ^{o}C took about 30 min. A vertical water-cooled condenser was attached to the middle neck of the reactor to prevent any loss of vapor. The time taken to attain the desired temperature was the heating time. Further heating was done at the desired temperature and the time was measured by subtracting heating time from the total time. Thus, heating time was taken as zero for further heating. The reaction mixture was agitated using a magnetic stirrer. The samples were withdrawn at periodic intervals for the measurement of COD,

iii

color and pH. The samples were centrifuged to decant the supernatant. The final pH of the solution after the reaction was also observed. The treated effluent including sludge was then rapidly mixed and the slurry so formed was used to study the settling and filterability characteristics.

The thermolysis operation of composite wastewater (COD_O=1960 mg/l, color = 2250 PCU) was carried out in presence of catalysts $CuSO_4$, $FeSO_4$, $FeCl_3$, CuO, ZnO and PAC. Among these copper sulfate was found to be most active in giving 77.9% COD and 92.85% color reductions, at a catalyst concentration of 6 kg/m^3, pH 12 and temperature 95 $^\circ$C. During coagulation aluminum potassium sulfate is found to be the most active among other coagulants (commercial alum, $FeSO_4$, $FeCl_3$ and PAC) tested resulting in 88.62% COD reduction and 95.4% color reduction, at pH 8 and a coagulant concentration of 5 kg/m^3. Coagulation of clear fluid (supernatant) obtained after catalytic thermolysis (at above mentioned operating conditions except at a lower coagulant concentration of 3 kg/m^3) resulted in a reduction of 97.3% COD and close to 100% of color. Thermolysis followed by coagulation, thus, is found to be the most effective process in reduction of COD as well as color at a lower dose (3 kg/m^3) of coagulant. The residual COD was found to be 11.7 mg/l in the final effluent, whereas, the COD/BOD_3 ratio was 1.67. A value of less than 2 of COD/BOD_3 ratio is desirable to make the effluent biodegradable. The sludge produced from the coagulation unit would contain lower inorganic mass coagulant, requiring reduces disposal problems, whereas the solid residue from the thermolysis, which is rich in organics, can be used as a solid fuel with high calorific value of about 16 MJ/kg, close to that of Indian coal.

During catalytic thermolysis of the fresh dyeing wastewater (COD_O = 5744 mg/l, color = 3840 PCU) copper sulfate has been found to be most active catalyst giving 66.85% COD as well as 71.4% color reductions, at a catalyst concentration of 5 kg/m^3, pH 8 and 95 $^\circ$C temperature. During treatment by coagulation process, commercial alum was found to be the best among the other coagulants tested, resulting in 58.57% COD and 74% color reductions, at pH 4 and a coagulant dose of 5 kg/m^3.

Coagulation of the supernatant obtained after catalytic thermolysis at above mentioned operating conditions (except at a lower coagulant concentration of 2 kg/m^3) resulted in a reduction of 89.91% COD and 94.4% color. The final COD and color was found to be 192 mg/l and 61.5 PCU, respectively in the treated effluent. The COD/BOD$_3$ ratio was 1.88.

In case of desizing wastewater (COD$_O$ = 2884 mg/l, color = 520 PCU) the catalytic thermolysis at moderate temperatures (60-95 °C) and atmospheric pressure in the presence of a CuSO$_4$ catalyst showed a maximum removal of 71.6% of COD and 87.2% of color at a catalyst concentration of 4 kg/m^3, 95 °C and initial pH 4. The results on the effect of variation of catalyst mass loading revealed that 4 kg/m^3 is the critical catalyst concentration. The maximum COD and color reductions by coagulation were 58.34% and 85 %, respectively, at a coagulant dose of 5 kg/m^3 and pH 4. The application of coagulation to the supernatant obtained after thermolysis show a removal of 87.96 % COD and 96.0 % color at above mentioned conditions except at a coagulant dose of 1 kg/m^3. The amount of inorganic sludge obtained due to the addition of coagulant is, thus, drastically reduced due to the reduced amount (almost 25%) of coagulant. The COD and color of the final effluent were found to be 98.6 mg/l and 2.67 PCU, respectively and the COD/BOD$_3$ ratio was 1.36.

The thermogravimetric studies (TGA, DTA and DTGA) were conducted for the precipitated sludges of the dyeing, desizing and composite waste waters in order to study the combustion characteristics and the prospect of being used as a solid fuel. The information on the temperature of dehydration and volatilization (removal of volatiles), their rates and heats evolved/consumed during the process were obtained. The kinetic analysis and reaction mechanisms of thermal degradation and oxidation have been proposed for residue degradation using thermogravimetry. For a one step irreversible reaction model, differential and integral methods have been suggested for the determination of kinetic parameters, the order of reaction, frequency factor, the specific reaction rate constant, activation energy, change in entropy, enthalpy and Gibb's free

energy, steric factor and its dependence on temperature using Arrhenius equation (Jalan and Srivastava, 1994, 1999; Gangavati et al., 2005).

The chemical aspects of coagulation has been explained by an examination of the hydrolysis of metal ions. The hydrolytic reactions of metal ions have been used extensively to explain coagulation mechanisms (Hundt and O'Melia, 1988; Dempsey *et al.,* 1984; Edwards and Amirtharajah, 1985; Mangravite *et al.,* 1975). The particular form of the metal present at a given pH is assumed to be responsible for the actual coagulation process. The effect of pH_0 on the color reduction of dyeing waste, for example, could be explained by the combined effect of (i) the ionization of amino, hydroxy and sulpho groups present in the dye molecules which increases with pH in the acidic range, and (ii) the decrease in the concentration of dissolved hydrolysis products. Aluminum based coagulants show better results than that of iron based coagulants in the removal of COD and color of the dyeing wastewater.

Kinetic studies of catalytic thermolysis process of composite, dyeing and desizing wastewater reveal that the kinetics, in general, can be represented adequately by the first order processes. A two-step reaction mechanism was suggested. The activation energy, E for the first and second steps for composite wastewater were found to be 8.34 and 19.24 kJ/mol, respectively. The corresponding values of the frequency factor were 0.098 and 0.065 m^{-1} respectively. The values of E for first and second step in case of dyeing wastewater were found to be 23.00 and 39.57 kJ/mol; and for desizing wastewater 36.64 and 42.36 kJ/mol respectively. The values of the frequency factors for first and second steps were 12.59 and 429.92 m^{-1} for dyeing and 614.96 and 1057.17 m^{-1} for desizing wastewater, respectively.

The FTIR of the dried wastewater and the residues obtained after treatment showed useful information on the type and intensity of various bonds and groups present. Composite wastewater after drying at ~38 °C for 36 h exhibits a broad band due to $\nu(OH)$, $\delta(OH)$, conjugated C=C bond and a weak bond of CH_2 groups in waste. The waste material also exhibits medium intensity band of sulphate group. On

treatment with copper sulphate by thermolysis most of the IR peaks become intense. The sharp band of sulphato group was possibly present in the coordinated form, $\nu(OH)$, $\delta(OH)$, $\nu(C=C)$ and $\nu(CH_2)$. The presence of two to three medium intensity bands in the 400-600 cm^{-1} in both the above samples possibly suggest that hydroxyl groups are coordinated to metal ions present in the sample. Similar results were also obtained and explained with other effluents before and after treatment.

In order to study the effectiveness of various process parameters, the settling and filtration characteristics of the treated effluent were studied. The parameters such as sedimentation velocity (u_c) and sedimentation flux and area of sedimentation tank in case of settling experiments and specific cake resistance and filter medium resistance in case of filterability studies were calculated. The treatment variables have strong effect on the quality and texture of the particles present in final slurry vis-à-vis their settling and filtration characteristics.

On the basis of above results, it is concluded that the catalytic thermolysis followed by coagulation is an effective process for the treatment of textile mill wastewaters to remove COD and color. The advantages include : (i) The treatment temperature of 95°C during catalytic thermolysis can be easily maintained in case of dyeing and desizing waste as these streams evolve at temperatures close to this from the plant, (ii) Substantial reduction of COD and color during thermolysis results in reduced coagulant requirement in the subsequent process, thus producing much less inorganic sludge to be disposed, (iii) The final liquid effluents are within the disposable norms as prescribed by Central Pollution Control Board, India, (iv) Thermolysis sludge containing organics can be used as a solid fuel (after drying) with good calorific value.

ACKNOWLEDGEMENTS

Dr. Rashmi and my cousins Abhinendra and Udita. I would like to acknowledge them for their prayers, for the encouragement they have given me whenever I was depressed and for the support they have rendered me throughout my life and especially throughout this work. I put on record to express my love and affection to my wife Praveen, daughter Ananya and son Pranjal, for their love and support during the last stages of this tedious journey. I would highly appreciate my in-laws for their cooperation and encouragement.

I would like to acknowledge Mr. Sandeep Jain for typing and bringing the final shape to this thesis.

I want to express my sincere thanks to all those who directly or indirectly helped me at various stages of this work.

Finally, I bow to the Almighty God that blessed me in the moments of need.

PRADEEP KUMAR

CONTENTS

LIST OF FIGURES

LIST OF TABLES

NOMENCLATURE

ABBREVIATIONS

AGR	Atmospheric glass reactor
A. R.	Analytical reagent
BOD_5	5 day – Biochemical oxygen demand (mg/l)
ccc	Critical coagulant concentration (kg/m^3)
CF	Coagulation – Flocculation
COD	Chemical oxygen demand (mg/l)
COD_0	Initial COD (mg/l)
C_w	Catalyst/coagulant mass loading (kg/m^3)
D1	One way transport diffusion model
D2	Two way transport diffusion model
D3	Three dimensional diffusion model
DLVO	Derjaguin, Landau, Verwey and Overbeek Theory
F1	Chemical Reaction First order
GAC	Granular Activated Carbon
K_p	Slope
P	Atmospheric pressure
PAC	Poly aluminum chloride
PCU	Platinum-Cobalt Unit
pH_0	Initial pH
PID	Proportional Integral Differential
PVA	Polyvinyl alcohol
SR	Settling Rate
TDW	Textile dye wastewater
TE	Treatment efficiency
T_A	Ambient temperature
T_R	Reaction temperature
TDS	Total dissolved solids (mg/l)
TOC	Total organic carbon (mg/l)

TSS	Total suspended solids (mg/l)
VOCs	Volatile Organic Compounds
WAO/CWAO	Wet air oxidation/ Catalytic wet air oxidation
WO/CWO	Wet oxidation/ Catalytic wet oxidation
ZD	Zhuravlev diffusion model

NOTATIONS

A	Area of tank (m^2)
A_f	Area of filtration (m^2)
C	Concentration of solids in waste water (kg/m^3)
C_0	Initial solids concentration (kg/m^3)
C(t)	Concentration of solids at time t (kg/m^3)
C_u	Concentration of the solids required in the underflow (kg/m^3)
C_w	Catalyst or coagulant mass loading or concentration (kg/m^3)
E	Activation energy (kJ/mol)
e	Neper number (= 2.7183)
h	Plank constant
k	Specific rate constant
k_1, k_2	First order kinetic constants
k_0	Frequency factor
k_B	Boltzmann constant
n'	Order of thermal degradation reaction
P	Total pressure (MPa)
P_s	Steric Factor
pH_0	Initial value of pH
pH_f	Final value of pH
Q_0	Feed rate (m^3/min)
R	Gas constant (= 8.314 J/mol K)
R_m	Resistance of filter medium (m^{-1})
r^2	Correlation factor
T	Temperature (^{o}C or K)
T_p	DTG peak temperature (^{o}C)

t	Time (h)
t_h	Heating time (h)
u_c	Sedimentation velocity
V	Cumulative average volume of filtrate collected up to that time interval (m^3)
v_f	Volumetric flow rate of effluent (m^3/s)

GREEK LETTERS

α_c	Specific cake resistance (m kg^{-1})
α_d	Deactivation function, dimensionless function
α'	Degree of transformation, Fractional pyrolysis of the biomass
β	Intercept
μm	Micron meter
χ	Transmission coefficient
μ	Viscosity of the filtrate (Pa.s)
β'	A constant
ΔG	Gibbs free energy (kJ/mol)
$\Delta G^{\#}$	Gibbs free energy for the active complex formation
ΔH	Change of the enthalpy (kJ/mol)
$\Delta H^{\#}$	Change of the enthalpy for the active complex formation
ΔP	The pressure drop across the filter (Pa)
ΔS	Change in entropy (J/mol K)
$\Delta S^{\#}$	Change in entropy for the active complex formation
Δt	Time interval of filtration (s)
ΔV	Volume of filtrate collected during Δt (m^3)

Chapter-1

INTRODUCTION
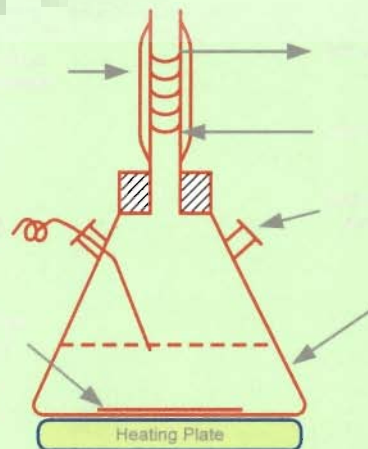
Chapter – 1

INTRODUCTION

1.1   GENERAL

Textile industry is one of the most polluting industries. Treating textile effluent is a challenging task as it contains a variety of chemicals, organics, dyes and colorants, fibers, etc. There are about 706 cotton textile mills in India mainly located in Mumbai, Ahmedabad, Coimbatore and Kanpur. Out of these, 291 are composite mills and 415 are spinning mills. The composite effluent discharged from the textile mills varies from 1 to 10 million liters per day depending upon quantity of cloth produced and various manufacturing processes employed. Table 1.1 shows the pollution characteristics of certain typical Indian industries (Garg, 2005).

The concern for environmental quality has led to enactment of different acts, rules and regulations, wherein clear stipulations have been made to preserve the quality of the environment with sustainable development. These laws make it mandatory for the industries to meet the discharge standards of the effluents as also the quality of the ambient environment. In India, the water (Prevention and Control of Pollution) Act, 1974 and the Environment (Protection) Act, 1986 and the Rules and Regulations framed thereunder limit the total discharge of wastewater and prescribe the discharge water quality to be met before the effluents are permitted to be discharged either on land or in surface water. The quality parameters and the effluent quality vary from industry to industry (Swaminathan and Subhramanyam, 1982). The tolerance limits of some parameters for industrial effluents discharged into the Inland surface water, public sewerage and agricultural lands are shown in Table 1.2 (Choudhury, 2006).

Table 1.1 Major pollutants in typical Indian industries (Garg, 2005)

S. No.	Industry type	Pollution characteristics
1.	Pulp and paper	Lignin, low nitrogen, color, suspended fibre, low BOD/COD ratio
2.	Oil refinery	Free oils, phenolic compounds, H_2S and RSH, emulsified oils
3.	Petrochemical	Phenolic compounds, oil and pH
4.	Distillery	BOD, COD, high color, chlorides and sulphate
5.	Textile	Color, suspended solids, high or low pH, chromium and sodium
6.	Fertilizer (ammonium)	Nitrogen, phosphorous, arsenic, oils
7.	Dairy	Oil and grease, dissolved and suspended solids, nitrogen, putrescible
8.	Sugar mill	High volatile acids and low pH
9.	Pharmaceutical	Low or high pH, total solids, low BOD/COD ratio
10.	Tannery	High pH, chromium, chloride, high persistent color and tannin

Table 1.2 Discharge standards for industrial effluents into the inland surface waters, public sewerage and agricultural land as prescribed by the Bureau of Indian Standards, Govt. of India [IS: 2490, Part I, 1974, amended in 1985] (Choudhury, 2006)

S. No.	Characteristic of the effluent	Tolerance limit for discharge (mg/l, max)		
		Inland surface waters	Public sewerage	Agricultural land
1.	BOD_5	30	350	500
2.	COD	250	-	-
3.	pH	53.9	5.5 – 9	5.5 – 9
4.	Suspended solids	100	600	200
5.	Chlorides (as Cl)	1000	1000	600
6.	Sulphate (as SO_4)	1000	1000	1000
7.	Oil and grease	10	20	10
8.	Lead (as Pb)	0.1	1	-
9.	Copper (as Cu)	3	3	-
10.	Temperature, °C	40	45	-

1.2 TEXTILE MANUFACTURING PROCESS

The textile industries produce and process textile-related products for further processing into home furnishings and industrial goods. Textile industries receive and prepare fibres; transform into yarn, thread or webbing; convert the yarn into fabric or related product; and dye and finish these materials at various stags of production. There are primarily four processing stages in textile mills, as shown in Figure 1.1.

```
┌──────────────┐      ┌──────────────┐      ┌──────────────┐      ┌──────────────┐
│    Yarn      │ ───> │   Fabric     │ ───> │    Wet       │ ───> │ Fabrication  │
│  formation   │      │  formation   │      │  processing  │      │              │
└──────────────┘      └──────────────┘      └──────────────┘      └──────────────┘
```
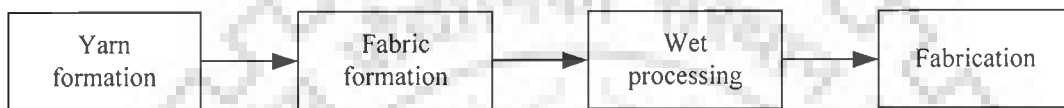
Figure 1.1 The processing stages in textile mills

1.2.1 Yarn Formation

Textile fibres are processed into yarn by grouping and twisting operations used to bind them together. Although most textile fibres are processed using spinning operations, the processes leading to the spinning vary depending on whether the fibres are natural or man-made. Natural fibres, known as staple when harvested, include animal and plant fibres, such as cotton, silk and wool. These fibres must go through a series of preparation steps before they can be spun into yarn, including opening, blending, scouring, carding, combing and drafting. Man made fibres may be processed into filament yarn or staple-length fibres so that they can be spun.

1.2.2 Fabric Formation

The major methods for fabric manufacture are weaving and knitting. Weaving or interlacing yarns, is a common process used to create fabric. Knitting is another method of fabric construction. Manufacturers of knit fabrics also consume a sizeable amount of textile fibres.

1.2.3 Wet Processing

Wet processing enhances the appearance, durability, and serviceability of fabrics by converting un-dried and unfinished goods into finished consumer goods. Collectively known as finishing, wet processing has been broken down into four stages.

These stages involve treating grey goods with chemical baths and often require additional washing, rinsing and drying steps as shown in Figure 1.2.
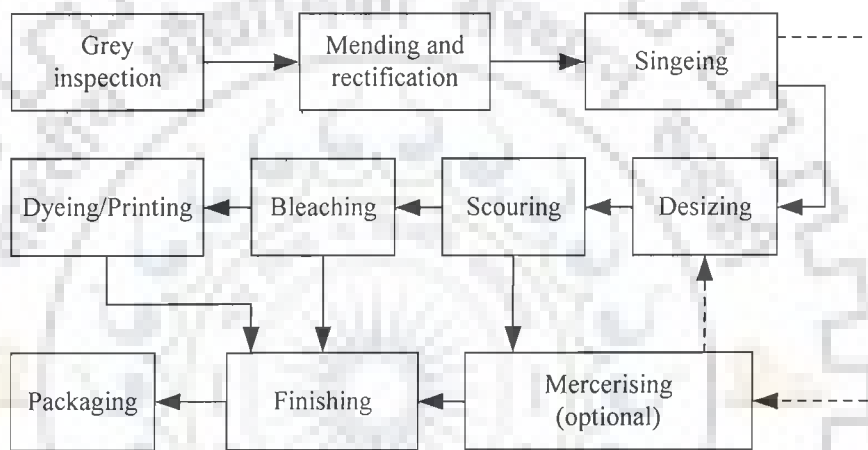
Figure 1.2 Sequence of operations in cotton fabric processing

Much of the waste from the industry is produced during the wet processing stages. Most fabric that is dyed, printed or finished must first be prepared. There are many preparation techniques, some of which are listed below:

1.2.3.1 Singeing

Singeing is essential to impart smooth finish to the fabric. It is a dry process used on woven goods that removes fibres protruding from yarn or fabrics. Passing burns off the fibres over a flame or over heated copper plates. Singeing, thus, improves the surface appearance of woven goods and reduces pilling.

1.2.3.2 Desizing

Desizing is used to remove sizing agents applied prior to weaving. Natural fibres such as cotton are most often sized with water-insoluble starches or mixtures of starch and other material. Removing starch before scouring is necessary because they can react and cause color changes when exposed to sodium hydroxide in scouring. The proportion of water considered in this process is comparatively small. The effluents of this process are high BOD, high TDS, and pH around 7 and some suspended solids.

1.2.3.3 Scouring

Scouring is a cleaning process, which uses alkali, typically sodium hydroxide, to break down natural oils and surfactants and to emulsify and suspend remaining impurities in the scouring bath.

1.2.3.4 Bleaching

Bleaching eliminates unwanted colored matter from fibres, yarns, or cloth. Various bleaching agents commonly used include hydrogen peroxide, sodium hypochlorite, sodium chloride, as well as alkalis and acids. Except peroxide, other oxidizing agents have to be reduced or neutralized.

1.2.3.5 Mercerizing

Mercerization is a continuous chemical process used for cotton and cotton/polyester goods to increase dye ability, lustre and appearance. During mercerising, the fabric is passed through a cold 15 to 20 percent solution of caustic soda, and then stretched out on a tender frame where hot water sprays remove most of the caustic solution. It can be collected separately at source, and some recovered or reused. The remaining liquor must be neutralized before disposal.

1.2.3.6 Dyeing

Dyeing is used to add color and intricacy to textiles and increase product value. The components common to most of the dyes are dye residues and the dyeing assistants, usually agents with surface-active properties. Dyes are classified as acid, basic, direct, disperse, reactive, sulfur and vat dyes. In addition, certain dyes contain substances, which can be troublesome in purification. Sulphur dyes contain sodium sulphide, which must be removed or diluted before treatment. The metal containing dyes, such as, chrome dye liquors interfere seriously in biochemical processes.

1.2.3.7 Printing

In textile fabric printing, a decorative pattern or design is applied to constructed fabric by roller, fat screen or rotary screen methods. Most common pollutants in fabric printing are volatile organic compounds (VOCs) from mineral spirit solvents in print pastes or ink. Concentrated paste may be collected and treated separately and the used water may be treated with other streams.

1.2.4 Finishing

Finishing processes include chemical or mechanical treatments performed on fibre, yarn or fabric to improve appearance, texture and performance. Mechanical finishing involves brushing and ironing to increase the lustre of textiles. The other common chemical finishing includes permanent press, and stain resistant finishes. Drying, curing and cooling steps usually follow chemical finishes. The effluent from a finishing unit may contain a wide variety of chemicals. Various starches used as filling agents are found in large quantities as residues.

1.3 WATER CONSUMPTION IN TEXTILE MILL

Cotton textile mills use approximately $0.2 - 0.3$ m^3 of water/kg cloth produced. In a typical textile mill, 45% water is consumed in bleaching and finishing, 23% in dyeing and printing, 15% in boilers, 15% in spinning and weaving and 9% in domestic and sanitary purpose. The large quantity of water is required for different processes to manufacture the cloth.

1.3.1 Textile Mill Effluent

The wastewaters originating from wet processes are generally characterized by the high content of color caused by the dyestuffs, salts, chemical oxygen demand (COD) deriving from additives, such as, acetic acid, detergents and complexing agents, suspended solids including fibres; high temperature and broadly fluctuating pH. Textile industries typically generate $0.2 - 0.3$ m^3 of wastewater per kg of finished product resulting in an average pollution of 0.1 kg COD per kg of fabric. Various pollutants present in the textile effluent may be classified into three main groups based on their detrimental effects

(1)   The pollutants, which are toxic or harmful.

(2)   Pollutants which contribute to oxygen depletion

(3)   Inert materials as suspension or in soluble state which are harmless as such but can be detrimental if present in high concentration, e.g.

(a) By way of deposition on the plant

(b) By covering the surface of water, preventing oxygen penetration.

(c) Dyes and coloring agents can prevent the entry of light in the water

Dissolved solids clogging the pores of soil where the effluent is discharged.

Figure 1.3 gives the idea of wastewater treatment in a textile mill.
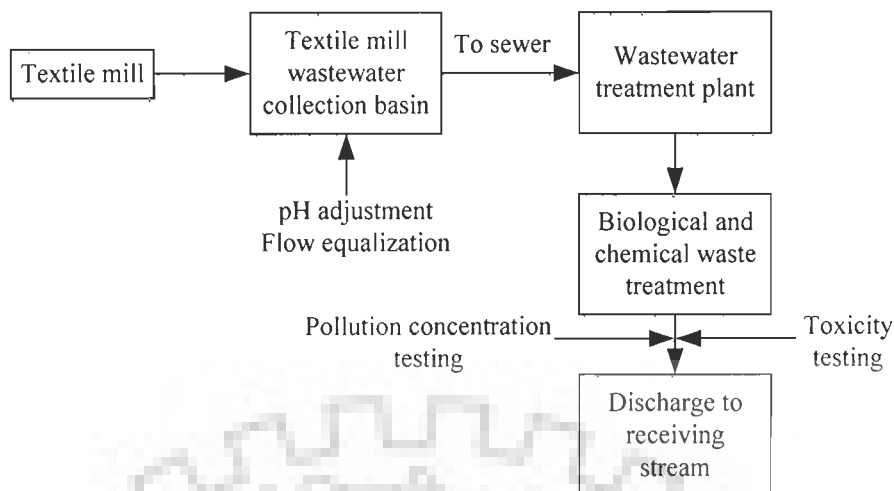
Figure 1.3 Wastewater treatment in a textile mill

Table 1.3 lists the typical pollution characteristics of the effluent from the textile industry.

Table 1.3 Effluent characteristics of the textile industry waste (Barclay and Buckley, 2000)

Process	Composition	Nature
Sizing	Starch, waxes, carboxymethyl cellulose, polyvinyl alcohol	High BOD and COD
Desizing	Starch, glucose, carboxymethyl cellulose, polyvinyl alcohol, fats and waxes	High BOD, COD, suspended solids, dissolved solids
Scouring	Caustic soda, waxes, grease, soda ash, sodium silicate, fibres, surfactants, sodium phosphate	Dark colored, high pH, high COD, dissolved solids
Bleaching	Hypochlorite, chlorine, caustic soda, hydrogen peroxide, acids, surfactants, sodium silicate, sodium phosphate	Alkaline, suspended solids
Mercerizing	Caustic soda	High pH, low COD, high dissolved solids
Dyeing	Various dyes, mordant, reducing agents, acetic acid, soap	Strongly colored, high COD, dissolved solids, low suspended solids, heavy metals
Printing	Pastes, starch, gums, oil mordant, acids, soaps	Highly colored, high COD, oily appearance, suspended solids
Finishing	Inorganic salts, toxic compounds	Slightly alkaline, low BOD

8

1.4   TREATMENT TECHNIQUES

The treatment of textile mill wastewater has been tried on laboratory scale and full-scale basis using various treatment techniques.

Preliminary	Primary	Secondary	Tertiary
→ Equalization	→ Screening	→ Chemical separation	→ Chemical oxidation
	→ Sedimentation	→ Coagulation	→ Gamma radiation
→ Neutralization	→ Flotation	→ Biological oxidation	→ Foam fractionation
→ Disinfection	→ Flocculation		→ Reverse osmosis
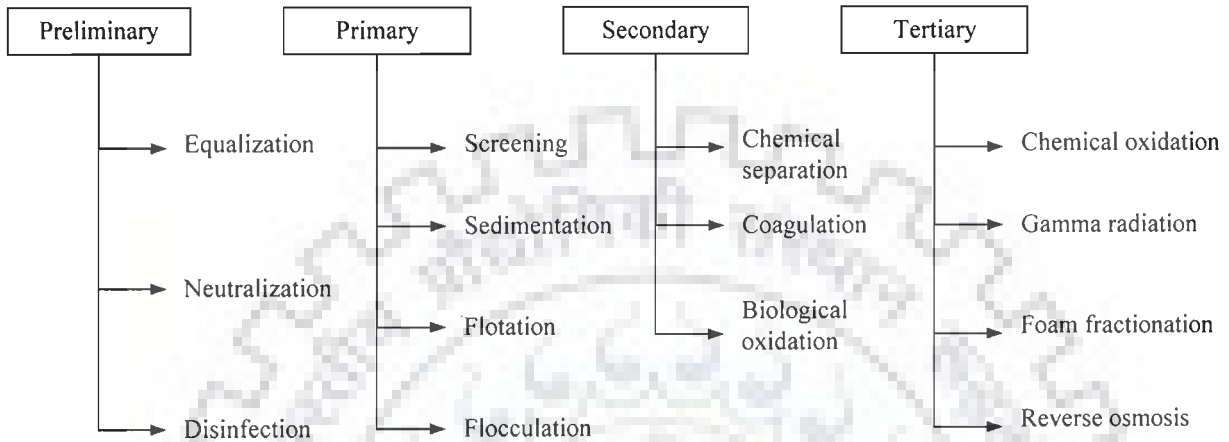
Figure 1.4 Treatment techniques for textile mill wastewater (Mckay, 1979)

1.4.1   Preliminary/Primary/Secondary Treatment Processes

The quality of effluents may vary in terms of nature of pollutants, their concentrations, treatment and disposal methods required. The contents of effluents may vary from totally inorganic to highly toxic organics or combination of both. The treatment of these effluents by the normal methods of treating wastewaters depends upon the quantum, concentration, toxicity and presence of non-biodegradable organics in an industrial wastewater. Its treatment may consist of any one or more of the following processes:

1.4.1.1 Equalization

Mixing of wastewater (from different sources) for some predetermined period in a mixing basin to produce a uniform wastewater carries out Equalization. This is

necessary when the wastewater produced by the industry varies in characteristics and quantity over the entire day. If the waste streams are not controlled lagoons used for equalization can be odoriferous and objectionable to the surrounding community.

1.4.1.2 Neutralization

In this process, the excessive acidity or alkalinity of the particular wastewater is neutralized by adding base or acid, respectively. But because of odour and air pollution problem, this method is not generally practiced.

1.4.1.3 Disinfection

When the disinfectant is added before the primary treatment, its effect is two fold; it can destroy some of the wastes that can be toxic to the microbes in the secondary process and secondly, it can prevent septic floc, pathogenic organisms and undesirable algae from reaching and receiving stream. When the disinfectant is added in the final treatment step it is usually for the latter reason. The chemicals that are most commonly used as disinfectants are chlorine and its derivatives (Garg, 2005).

1.4.2   Physical Treatments

1.4.2.1 Coagulation/Flocculation

Coagulation/Flocculation is widely used for the removal of colloidal and suspended particles present in water or the wastewater. Inorganic salts like alum, $FeCl_3$, $FeSO_4$, etc. are generally used for the coagulation and flocculation of suspensions, whereas organic polymers, polyelectrolytes and surfactants are employed, both as flocculants and dispersants. The suspended particles vary considerably in their source composition, charge density, particle size, shape and density. The application of coagulation and flocculation process and the selection of the coagulants depend upon

10

understanding of the interaction of the particles with the coagulants and the environmental factors such as pH and temperature.

The mechanism of coagulation follows the neutralization of charged particles, resulting in the lowering of the DLVO energy barrier, called destabilization. Coagulation and flocculation are successive steps. Flocculation refers to the successful collisions that occur when the destabilized particles are driven towards each other by the hydraulic shear forces in the rapid mix and flocculation basins. The agglomeration of colloids quickly bridges together to form microflocs which grow and adhere together to make visible floc masses.

The wastewater generally contains negative charged colloidal particles and suspended particles which repel one another due to their having similar charges. When a coagulant containing positive charge is added to the wastewater, the negative charge is neutralized since the physical force of attraction (the van der Waals force) exceeds the electrical force of repulsion, causing the particles to coagulate.

Salts of aluminum and iron are most commonly used in water and wastewater treatment. They are usually low-cost and easily available materials. The inorganic metal hydroxides which are formed produce short polymer chains which enhance microfloc formation. Inorganic coagulants are also capable of removing a portion of the organic precursors which may combine with chloride to form disinfection by-products. The large volume of the floc produced entrap microbial mass as they settle. These inorganic flocculants may alter the pH of the water because they consume alkalinity. Due to their acidic nature, corrosion resistant equipment are generally required.

In wastewater treatment, long chain and high-molecular weight polymers are widely used as coagulants. The polymers may be used alone or with inorganic

coagulants. Polymers are effective over a wider range of pH than the inorganic coagulants. They can be applied at lower doses, and they do not consume alkalinity much. They produce smaller volume of more concentrated, rapidly settling floc and produce a cleaner effluent. The high cost of polymers and certain environmental conditions restrict their usage in some cases. Polymers as flocculants pass through several elementary process as schematically given in Figure 1.5.
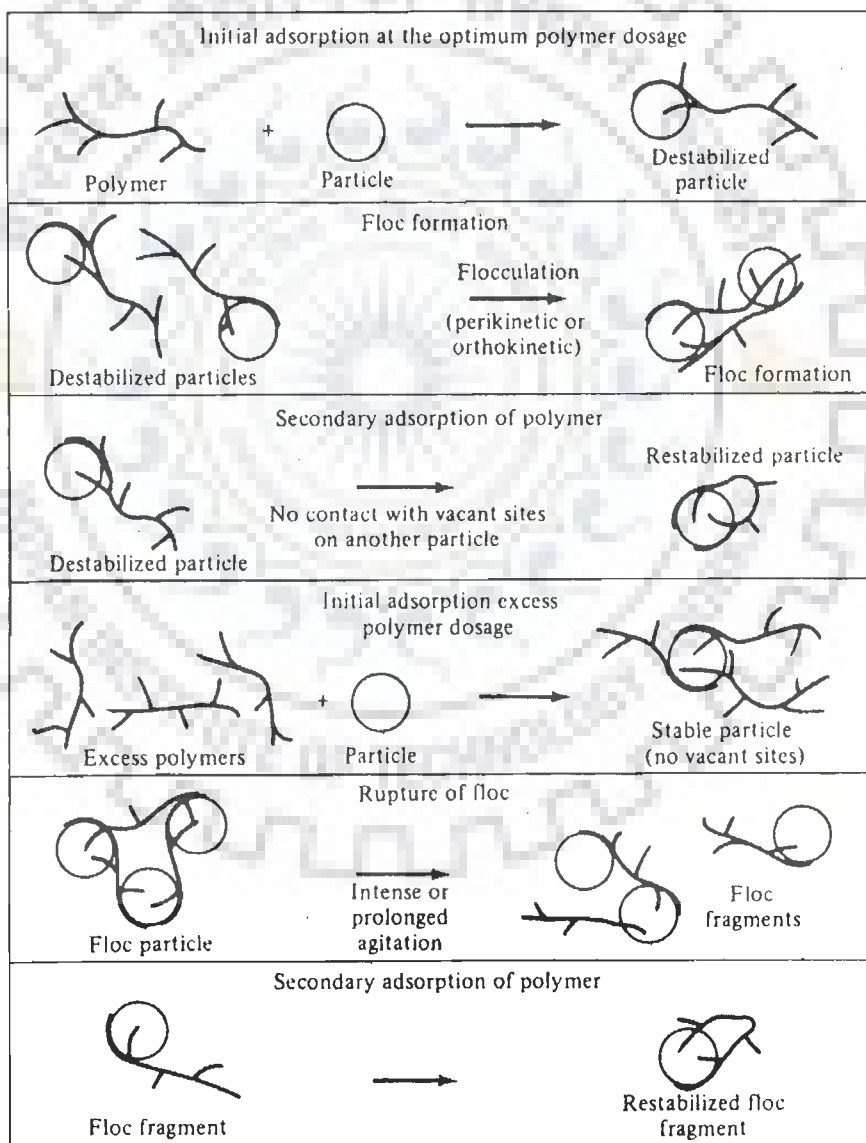
Figure 1.5 Interparticle bridging with polymers. (Peavy et al., 1985)

These are :

- Initial adsorption at the optimum polymer dosage leading to destabilized particles.

- Floc formation

- Secondary adsorption of polymer leading to restabilized particles.

- Initial adsorption excess polymer dosage leading to stable particles.

- Rupture of floc

- Rearrangement and break-up of the structure of a floc.

All these elementary processes occur simultaneously under turbulent flow conditions.

The destabilization of particles is important in order to aggregate them. Chemical coagulation can destablize colloidal particles by four distinct mechanisms, double layer compression, charge neutralization, enmeshment in a precipitate and intra-particle binding. More than one mechanism may operate simultaneously depending on the nature of the particle surface and the polymer. It is understood that the rate of flocculation by bridging is an order of magnitude greater than that by either charge path neutralization or simple charge neutralization.

1.4.2.2 Adsorption

Adsorption techniques have gained favour recently due to their efficiency in the removal of pollutants too stable for conventional methods. Adsorption produces high quality product and is a process, which is economically feasible (Choy et al., 1999; Verma and Mishra, 2006). Decolorization is a result of two mechanisms: adsorption and ion exchange, and is influenced by many physico-chemical factors, such as, dye-sorbent interaction, sorbent surface area, particle size, temperature, pH and contact time

(Sloker et al., 1997; Kumar et al., 1998; Annaduraj, 2002; Papic et al., 2004). Physical adsorption occurs when weak inter particle bonds exist between the adsorbate and adsorbent. In the majority of cases, physical adsorption is easily reversible (Singh and Tiwari, 1997). Chemical adsorption occurs when strong inter particle bonds are present between the adsorbate and adsorbent due to an exchange of electrons. Chemisorption is deemed to be irreversible in the majority of cases (Allen et al., 2005).

Activated carbon is the main adsorbent used in textile industry. Different physical forms of activated carbons are produced depending on their application: granular (GAC) forms to be used in adsorption columns and powder forms for use in batch adsorption followed by filtration (Rajagopal et al., 1991; Mishra & Tripathy, 1993). Chitin is the second most abundant natural carbohydrate polymer next to cellulose. Chitin is a naturally occurring derivative of cellulose, where the C_2 hydroxyl group has been replaced by the acetyl amino group-$NHCOCH_3$. Adsorption can occur through van der Waals attraction, hydrogen bonding and Coulombic attraction (Figueiredo et al., 2005; Meshko et al., 2001; Rama Krishna, 1997).

A combination of fly ash and coal is being used recently. A high fly ash concentration increases the adsorption rates of the mixture due to increasing the surface area available for adsorption. This combination may be substituted for activated carbon, with a ratio of fly ash: coal 1: 1 (Gupta et al., 1990). The cellular structure of peat makes it an ideal choice as an adsorbent. Peat is a low-grade carbonaceous fuel containing lignin, cellulose and humic acids as its major constituents. It has the ability to adsorb transition metals and polar organic compounds from dye-containing effluents. Peat may be seen as a viable adsorbent in countries where it is widely available. Peat is shown to be a particularly effective adsorbent for basic dyes but has a lower capacity for acid dyes (Uddin et al., 2003).

1.4.2.3 Membrane filtration

This process is suitable to clarify, concentrate and also to separate dye continuously from effluent (Mishra and Tripathy, 1993; Xu and Lebrun, 1999). It has some additional features in comparison to other processes; resistance to temperature, and adverse chemical environment, and microbial attack. The disadvantages of this process include: concentrated residue left after separation posing disposal problems and high capital cost and the possibility of clogging and membrane replacement. This method of filtration is suitable for water recycling within a textile dye plant if the effluent contains low concentration of dyes, but it is unable to reduce the dissolved solid content, which makes water reuse a difficult task (Fersi et al., 2005; Varioniene, 2003).

1.4.2.4 Ion Exchange

Ion exchange has not been widely used for the treatment of dye-containing effluents, mainly due to the opinion that ion exchangers can not accommodate a wide range of dyes. Wastewater is passed over the ion exchange resin until the available exchange sites are saturated. Both cat ion and anion dyes can be removed from dye containing effluent this way. Advantages of this method include no loss of adsorbent on regeneration, reclamation of solvent after use and the removal of soluble dyes. A major disadvantage is cost. Organic solvents are expensive, and the ion exchange method is not very expensive (Slokar, 1997, Mishra and Tripathi, 1993).

1.4.3   Chemical Methods

1.4.3.1 Oxidative Processes

This is the most commonly used method of decolorization by chemical means. This is mainly due to its simplicity of application. The main oxidizing agent is usually

hydrogen peroxide (H_2O_2). This agent needs to be activated by some means, for example, ultraviolet light. Many methods of chemical decolorization vary depending on the way in which the H_2O_2 is activated. Chemical oxidation removes the dye from the dye-containing effluent by oxidation resulting in aromatic ring cleavage of the dye molecules.

1.4.3.2 Fenton's Reagent

Fenton's reagent is a suitable chemical means of treating wastewaters, which are resistant to biological treatment or are poisonous to live biomass. Chemical separation uses the action of sorption or bonding to remove dissolved dyes from wastewater and has been shown to be effective in decolorizing both soluble and insoluble dyes. One major advantage of this method is sludge generation through flocculation of the reagent and the dye molecules. The sludge, which contains the conventionally been incinerated to produce power, but such disposal is seen by some to be far from environmentally friendly. The performance is dependent on the final floc formation and its settling quality, although cationic dyes do not coagulate at all. Acid, direct vat, mordant and reactive dyes usually coagulate, but the resulting floc is of poor quality and does not settle well, yielding mediocre results.

1.4.3.3 Advanced Oxidation Process (AOPs)

Advanced oxidation processes are characterized by production of OH radicals and selectivity of attack, which is a useful attribute for an oxidant. The versatility of AOP is also enhanced by the fact that they offer different possible ways for OH^- radicals. A list of the different possibilities offered by AOP is given in Table 1.4.

Table 1.4 Advanced oxidation processes (Kdasi et al., 2004)

$H_2O_2/UV/Fe^{2+}$ (photo assisted Fenton)

H_2O_2/Fe^{2+} (Fenton)

Ozone/UV

Ozone/H_2O_2

Ozone/UV/H_2O_2

Ozone/TiO_2/Electron-beam irradiation

Ozone/TiO_2/H_2O_2

Ozone + electron-beam irradiation

Ozone/ultrasonics

H_2O_2/UV

Combining O_3, H_2O_2, TiO_2, UV radiation, electron beam irradiation and ultrasound commonly accelerates generation of HO. Of these, O_3/H_2O_2, O_3/UV and H_2O_2/UV hold the greatest promise to oxidize textile wastewater (Kdasi et al., 2004).

1.4.3.4 Ozonation

Ozonation is a powerful technique in removing residual color in the textile effluent. The instability of ozone makes it a powerful oxidizing agent with oxidation potential of 2.07 volts as compared to chlorine, which has oxidation potential of 1.36 volts. The placement of the ozonation stage in the wastewater treatment process can affect its efficiency. Ozonation works best as a tertiary treatment process following an activated sludge process since ozone is not effective at oxidizing soluble organic at a preliminary stage (Alaton and Alaton, 2007).

Some classes of dyes respond more readily to oxidation by ozone than others. Reactive dyes are degraded to the greatest extent and ozonation is moderately successful in treating wastewaters containing sulfur, azoic and basic dyes. However, disperse dyes have poor responses to ozone. According to one study, wastewater from a

printing dye works was treated to 95% decolorization. Ozone also can aid in removing some other pollutants like surfactants and carriers that are commonly found in textile wet processing wastewaters. It helps decompose detergents, chlorinated hydrocarbons, phenols, pesticides and aromatic hydrocarbons.

Use of ozone to renovate spent dye baths from reactive dyeing of cotton is technically feasible. Reuse of ozonated water saves chemicals (mainly salt), water, wastewater treatment expense and energy.

1.4.3.5 Photochemical

This method degrades dye molecules to CO_2 and H_2O by UV treatment in the presence of H_2O_2 (Peralto-Zamora et al., 1999). Degradation is caused by the production of high concentrations of hydroxyl radicals. UV light may be used to activate chemicals, such as H_2O_2 and the rate of dye removal is influenced by the intensity of the UV radiation, pH, dye structure and the dye bath composition. This may be set up in a bath or continuous column unit. Depending on initial materials and the extent of the decolorization treatment, additional by-products, such as halides, metals, inorganic acids, organic aldehydes and organic acids, may be produced. There are advantages of photochemical treatment of dye-containing effluent; no sludge is produced and foul odors are greatly reduced (Robinson et al., 2001; Toor et al., 2006).

1.4.3.6 Electrochemical Precipitation

In this method, an electrical cell with two or more plates is used and an electrical current is passed through it. This releases the iron and the hydroxide ions into the solution. The reactions taking place are as follows:

Anode reaction	:	$Fe \rightarrow Fe^{+2} + 2e^-$
Cathode reaction	:	$2H_2O + 2e^- \rightarrow H_2 + 2OH^-$
Solution reaction	:	$Fe^{2+} + 2OH^- \rightarrow Fe(OH)_2$

18
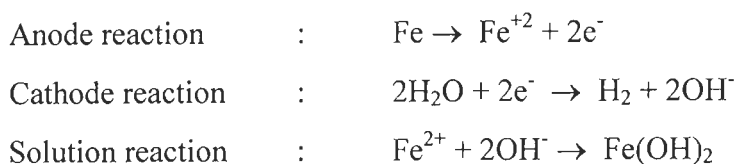
Most of the dyes can be removed by electrochemical precipitation and decolorization is quick to the order of seconds to minutes. Hence, this method is useful for treating large volumes of wastes. However, larger amounts of electricity and expensive equipments are required to set up and maintain this process. Also, there is a problem of sludge disposal.

Electrocoagulation (EC) has been proposed in recent years as an effective method to treat various wastewaters such as: Landfill leachate (Tsai et al., 1997), restaurant wastewater (Chen et al., 2000), saline wastewater (Lin et al., 1998), tar and oil shale wastewater (Renk, 1988), urban wastewater (Pouet and Grasmick, 1995), laundry wastewater (Ge et al., 2004). Nitrate and arsenic bearing wastewater (Kumar et al. 2004) and chemical-mechanical polishing wastewater (Lai and Lin, 2004).

EC treatment of textile dye-containing solutions or wastewater samples has been tested on a laboratory scale and good removal of COD, color, turbidity and dissolved solids at varying operating conditions were obtained (Kim et al., 2002; Kobya et al., 2003; Mollah et al., 2004).

1.4.3.7 Wet Air Oxidation

Wet air oxidation has been demonstrated to be a viable process for the treatment of desizing, scouring, dyeing and printing wastewater from the textile industry. Wet air oxidation requires high temperature (at 300 $^{\circ}$C) and high pressure (over 10 MPa) (Lei et al., 1997, 1998, 2000). The CWAO process is capable of converting all organic contaminants ultimately to carbon dioxide and water, and can also remove oxidizable inorganic components such as cyanides and ammonia. The process uses air as the oxidant, which is mixed with the effluent and passed over a catalyst at elevated temperatures and pressures. If complete COD removal is not required, the air rate, temperature and pressure can be reduced, therefore reducing the operating cost.

CWAO is particularly cost-effective for effluents that are highly concentrated (chemical oxygen demands of 10,000 to over 100,000 mg/l) or which contain components that are not readily biodegradable or are toxic to biological treatment systems. CWAO process plants also offer the advantage that they can be highly automated for unattended operation, have relatively small plant footprints, and are able to deal with variable effluent flow rates and compositions.

The process is not cost-effective compared with other advanced oxidation processes or biological processes for lightly contaminated effluents (COD less than about 5,000 mg/l).The CWAO process is a development of the wet air oxidation (WAO) process.

Organic and some inorganic contaminants are oxidised in the liquid phase by contacting the liquid with high pressure air at temperatures which are typically between 120°C and 310°C. In the CWAO process the liquid phase and high pressure air are passed co-currently over a stationary bed catalyst. The operating pressure is maintained well above the saturation pressure of water at the reaction temperatures (usually about 15-60 bar) so that the reaction takes place in the liquid phase. This enables the oxidation processes to proceed at lower temperatures than those required for incineration. Residence times are from 30 minutes to 90 minutes, and the chemical oxygen demand removal may typically be about 75% to 99%. The effect of the catalyst is to provide a higher degree of COD removal than is obtained by WAO at comparable conditions (over 99% removal can be achieved), or to reduce the residence time.

Organic compounds may be converted to carbon dioxide and water at the higher temperatures; nitrogen and sulphur heteroatoms are converted to to molecular nitrogen and sulphates. The process becomes autogenic at COD levels of about 10,000 mg/l, at which the system will require external energy only at start-up (Mishra et al., 1995).

1.4.3.8 Catalytic Thermolysis

The primary function of thermal treatment is to convert the waste to a stable and usable end product and reduce the amount that requires final disposal in landfills. Catalytic thermolysis (thermal pretreatment) is a chemical process by which a substance is decomposed into other substances by use of heat. During catalytic thermolysis, two mechanisms, both in parallel but complementary to each other, take place simultaneously. The organic molecules, both smaller and large, present in the effluent undergo chemical and thermal breakdown and complexation, forming insoluble particles, which settle down. Further, during catalytic thermolysis larger molecules also undergo breakdown into smaller molecules, which are soluble. A maximum reduction in COD and BOD observed for alcohol distillery effluent were 70% and 83% respectively (Chaudhari et al., 1995). For pulp and paper mill effluent, the COD and color reductions were 63.3% and 92.5%, respectively (Garg et al., 1995, 2007), whereas for textile desizing wastewater the corresponding values were 71.6% and 87.2% respectively (Kumar et al., 2007).

1.4.4 Biological Treatment

Aerobic treatment can be carried out in stabilization ponds, aerated lagoons, activated sludge or percolating filters. Aerobic treatment uses oxygen dissolved in the wastewater together with microorganisms in the activated sludge to convert the wastes to more microorganisms and CO_2.

Organic matter is partially oxidized and some of the energy produced is used for making new cells with formation of flocs. The flocs are allowed to settle and then removed as sludge (Laing, 1991). A proportion of the sludge removed is recycled back to the aeration tank to maintain the colony of microorganisms and the remainder of the sludge can either be disposed off or further reduced by anaerobic treatment. Disposal of the sludge can be through agricultural use as a fertilizer, in landfill or by drying and

incineration (although, disposal to agriculture is prohibited by law in many countries because of the presence of heavy metals).

Anaerobic treatment occurs in sealed tanks and converts the waste into methane and carbon dioxide. Where nitrogenous and sulphide-containing pollutants are present, ammonical substances and hydrogen sulphide are produced. Considerable heat is produced from anaerobic treatment and after the extraction of heat through heat exchangers, the hot water can be used to heat administration buildings during winter seasons.

For biological treatment to succeed there must be sufficient nitrogen and phosphorous present in the effluent. It may be necessary to add these nutrients in an industrial treatment plant. At a STW where domestic effluent is mixed with industrial effluent, these nutrients should appear in high enough concentrations to keep the microorganism population healthy. Table 1.5 shows other conditions that are necessary to ensure the success of biological treatment.

Table 1.5 Conditions necessary for biological treatment (Laing, 1991)

Variable	Condition
Temperature	35°C maximum (can be higher for anaerobic treatment)
Ratio BOD: nitrogen	Approx. 17: 1
Ratio BOD: phosphorus	Approx. 100: 1
pH	6.5 – 9 (preferably 7 maximum)
Metals (Zn, Cu, Cr)	Less than 10 mg/dm^3

1.4.5 Comparison of Various Methods

Out of several technologies to treat industrial wastewater, not all are important for textile effluents in view of difficult contaminants and cost of treatment. The most important of all is color contamination. Various important technologies used for removal of color are compared in the Table 1.6 shown below.

Table 1.6 Textile effluent treatment methods

Method	Process	Advantages	Disadvantages
Filtration	Nanofiltration	Excellent color, TDS and organics removal BOD/COD reduction Heavy metal removal High recovery of process water and salt Water suitable for reuse	Require prefiltration Highly concentrated residual Requires treatment and disposal
Color separation	Precipitation/floc culation followed by filtration	Good color removal Other contaminants removed with sludge Water suitable for some uses	Equipment size High chemical costs Sludge requires disposal
	Activated carbon adsorption	Good color removal Removes organics Low capital cost	Requires prefiltration Short run time between back flushing Back flushing water requires treatment and disposal Activated carbon recovery is costly
	Chlorination	Inexpensive Removes color No sludge generation	Aquatic toxicity, Lowers pH Does not treat heavy metals Does not remove salts Requires dosage control
Color Destruction	Ozonation	No sludge generation No toxicity	High capital and operating costs Requires long residence time Does not destroy heavy metals Marginal efficiency
	Biological degradation	Removes color, BOD/COD	Requires a very large system, area, and tight control Sludge requires disposal
Fenton reagent		Effective decolorization of both soluble and insoluble dyes	Sludge generation
Ozonation		Applied in gaseous state: no alteration of volume	Short half-life (20 min)
Photochemical		No sludge production	Formation of by-products
NaOCl		Initiates and accelerates azo-bond cleavage	Release of aromatic amines
Cucurbituril		Good sorption capacity for various dyes	High cost
Electrochemical destruction		Breakdown compounds are non-hazardous	High cost of electricity
Activated carbon		Good removal of wide variety of dyes	Very expensive
Peat		Good adsorbent due to cellular structure	Specific surface areas for adsorption are lower than activated carbon
Wood chips		Good sorption capacity for acid dyes	Requires long retention times
Silica gel		Effective for basic dye removal	Side reactions prevent commercial application
Membrane filtration		Removes all dye types	Concentrated sludge production
Ion exchange		Regeneration: no adsorbent loss	Not effective for all dyes
Irradiation		Effective oxidation at lab scale	Requires a lot of dissolved O_2
Electrokinetic coagulation		Economically feasible	High sludge production

1.5   AIM OF THE PRESENT WORK

As can be seen in Chapter II, not much work has been done on the treatment of textile mill wastewater using catalytic thermolysis accompanied with/without coagulation. In our laboratory, work on catalytic thermolysis accompanied with/without coagulation has already been investigated to reduce COD and color of industrial effluents from distilleries and pulp and paper mills. In view of the work done in the laboratory, the present work is aimed to undertake treatment of textile mill wastewaters using catalytic thermolysis, coagulation and catalytic thermolysis accompanied by coagulation of the wastewaters from desizing and dyeing streams and the composite wastewater. The following objectives were set for the present work:

i.   To characterize the effluent obtained from different sections of a cotton textile mill.

ii.   To use catalytic thermolysis at moderate temperatures and atmospheric pressure conditions with various catalysts, such as, copper sulfate, ferric chloride, ferrous sulfate, zinc oxide, copper oxide and PAC to treat these wastewaters.

iii. To study the effect of such parameters as temperature, pH and catalyst concentration on the COD and color reduction during catalytic thermolysis.

iv.   To study the kinetics of catalytic thermolysis process.

v.   To study the effectiveness of various coagulants, such as commercial alum, ferrous sulfate, ferric chloride, PAC and aluminum potassium sulfate to remove COD and color.

vi.   To study the treatment of the three effluents using catalytic thermolysis followed by coagulation.

vii. To study the settleability of the solid residue and the filterability of the treated effluent.

viii. To study the thermal degradation characteristics of solid residue obtained from catalytic thermolysis and coagulation of the textile wastewater.

ix. To characterize the solid residue by FTIR, CHNS analyzer and proximate analysis.

Chapter-2

LITERATURE REVIEW
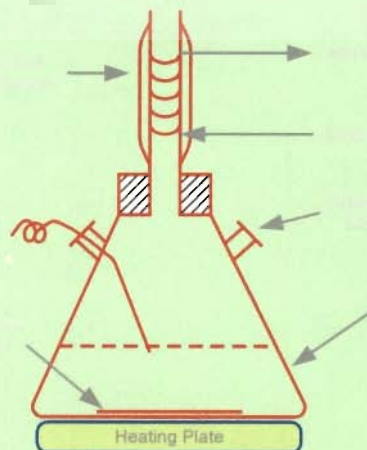
Chapter – 2

LITERATURE REVIEW

2.1 GENERAL

A concise review of the existing literature on treatment of textile mill wastewater is presented in this chapter. The information on catalytic thermolysis (thermal treatment) is very scarce. Literature on other treatment methods, such as coagulation, oxidation, adsorption and biological treatment have been presented in different sections.

2.2 CATALYTIC THERMOLYSIS

The first work reported on the catalytic thermolysis process was by Daga et al. (1986) for the treatment of distillery wastewater. Daga et al. (1986) thermally treated the distillery wastewater with a COD of 100 kg/m^3 by heating at temperatures in the range of 150-230 °C. They reported a decrease in the COD with an increase in temperature and autogenous pressure. 30% COD reduction at 150 °C and 50% COD reduction at 230 °C at the end of 6 h treatment period were found. The process kinetics was described by a two step COD reduction with the initial step being faster than the second one. The first order rate constants were found to be 9.72, 12.96 and 14.35 min^{-1} at 150, 170 and 190 °C for the first step, and 1.46, 1.32 and 1.66 min^{-1} for the second step, respectively.

Lele et al. (1989) performed the catalytic thermolysis of distillery wastewater at temperature in the range of 160-250 °C and autogenous pressure. It was observed that the COD reduction is linear with treatment time and that after 2 h, further COD reduction was not observed. The authors reported a zero order COD reduction kinetics.

The zero order rate was evaluated as 6.67, 10.40, 10.8 and 14.40 kg/m^{3}h at 160 °C, 200 °C, 230 °C and 250 °C respectively. Their work supported the work of Daga et al. (1986) in that an increase in temperature results in an increase in COD reduction. The filterability of the treated effluent was also studied by using a simple gravity filtration on an ordinary filter paper. The cake and medium resistances at different temperatures reported were maximum at 160 °C and lowest at 250 °C. Thus, the filterability of the slurry was found to increase with an increase in the treatment temperature. The color of the final filtrate was dark brown at 160 °C and was light orange at 250 °C. They also studied the effect of pH on catalytic thermolysis of DWW at 230 °C and reported that the low pH (~1) is favourable to the catalytic thermolysis. The neutral pH was found to have poor performance on the reaction, while moderate improvement in COD reduction was observed at basic conditions. The COD reductions observed were 59.3%, 51.9%, 53.7%, 25.9%, 38.9% and 40.7% respectively at initial pH (pH$_0$) 1, 3, 4.5, 7, 9 and 12 at end of reaction time (t$_R$) = 2 h. The corresponding energy recoveries were 52.5%, 49.5%, 49.5%, 31.7%, 36% and 37%, respectively in terms of charred residue obtained after the treatment. The residue was found to have a heating value equivalent to that of lignite. Under acidic and basic conditions, significant amounts of charred residues were observed, and the COD reduction was attributed mainly to the formation of the solid residue.

The catalytic thermolysis of mature timothy grass based distillery wastewater was studied by Belkacemi et al. (1999, 2000). The total organic carbon (TOC) of wastewater was 22.5 kg/m^3. A significant amount of TOC reduction was observed during a short heating period. TOC reduction was found to be 37 %, 46 % and 54 % at 200 °C, 220 °C and 240 °C, respectively, at t$_R$ = 10 min, initial pH (pH$_0$) 4.5 and autogenous pressure.

The thermolysis process for biodigester effluent was reported by Dhale and Mahajani (2000), where the effluent was heated in absence of air at 150 °C resulting in

a 35% COD reduction in $t_R = 0.6$ h. The thermally treated effluent was further treated by flocculation using iron-based synthetic flocculent followed by catalytic wet air oxidation, in which $FeSO_4$ was used as catalyst.

Chen et al. (2003) presented the treatment of printing and dyeing wastewater from the textile industry by thermal treatment and wet air oxidation (WAO). The range of operating temperatures examined was between 150 and 300 ^oC. Thermal decomposition during preheating was found to play a significant role in the COD removal with up to 18% COD removed at an operating temperature of 300 ^oC.

Chaudhari et al. (2005) have reported the catalytic catalytic thermolysis of biodigester effluent in temperature range of 100-140 ^oC and autogeneous pressure. COD reductions of 43% and 70% of initial COD ($COD_0 = 34000$ mg/dm^3) at 100 and 140 ^oC, respectively at $pH_0 = 1$ and autogenous pressure in presence of CuO catalyst. After the treatment, a considerable amount of organic solid residue was obtained, the amount of which increased with increasing temperature. The residue was found to have a medium heating value ~18 MJ/kg.

Garg et al. (2005) studied catalytic thermochemical precipitation of black liquor at low temperatures (60-95^oC) using copper sulphate catalyst. This operation has resulted in the formation of settleable solid residue. 61.4% reduction of initial COD ($COD_0 = 7000$ mg/dm^3) was obtained at 95 ^oC, pH_0 5 and 2 h heating period. The residue after drying had medium heating value ~19 MJ/kg. The treated effluent was found to have good settling and filtration properties.

Pradeep et al. (2007) reported catalytic thermolysis (thermal treatment) for the reduction of COD and color of the desizing wastewater under moderate temperature and atmospheric pressure conditions using various catalysts. The homogeneous copper sulfate catalyst was found to be the most active in comparison to other catalysts used. A removal of about 71.6% chemical oxygen demand (COD) and 87.2% color of desizing wastewater was obtained with a catalyst concentration of 4 kg/m^3 at pH 4. The pH_0 value of the wastewater showed a pronounced effect on the precipitation process.

Table 2.1 Previous works on the catalytic thermolysis

Authors	Substrate and catalyst used	Catalyst used	System used for reaction	Results	Remarks
Daga et al. (1986)	Cane based DWW $COD_0 = 65{-}100 \ kg/m^3$	Nil	Stainless Steel (S.S. 316) autoclave	33 % and 55 % COD reductions were found at 150 °C and 230 °C respectively at pH_0 4 and autogenous pressure.	A two-step COD reduction was noted. The COD reduction was fast during initial period of reaction. Thereafter, the hydrolysis proceeds slowly. The COD reduction was found to be first order for both the steps with respect to COD.
Lele et al. (1989)	Cane based DWW $COD_0 = 108 \ kg/m^3$	Nil	Stainless Steel (S.S. 316) autoclave	28 % and 53.7 % COD reductions were obtained at 160 °C and 230 °C respectively and autogeneous pressures. The pH_0 for the process was 4.5. The COD reduction was a strong function of the pH_0 of the wastewater. 59.3 %, 25.9 % and 40.7 % COD reductions were observed at $pH_0 = 1, 7, 12$ respectively at 230 °C and autogeneous pressure.	The COD reductions were due to formation of solid residues, which were obtained at bottom of reactor after the experiments. A single step zero order kinetic described the COD reduction. The filterability of the treated effluent were best when treated at acidic conditions followed by basic and neutral pH.
Belkacemi et al. (1999, 2000)	Timothy grass based DWW $TOC_0 = 22.5 \ kg/m^3$ $pH_0 = 4.5$	Nil	Stainless Steel (S.S. 316) autoclave	37 %, 46 % and 54 % COD reductions were obtained at 200 °C, 220 °C and 240 °C respectively at $t_R = 10$ min and autogenous pressure.	The authors have reported that the solid residues were obtained during the process. The kinetics incorporated the effect of catalyst deactivation during the process. The first order TOC reduction was noted.

Dhale and Mahajani (2000)	BDE from the cane based DWW treatment plant $COD_0 = 34.0$ kg/m^3 pH_0 = alkaline	Nil	Stainless Steel (S.S. 316) autoclave	35 % COD reduction was found at 150 ^{o}C for 0.67 h heating under autogenous pressure and pH_0 8.	The total dissolved solids decreased from 3.43 % (w/v) to 1.52 % (w/v). The COD reduction was reported to be due to separation of solids contained in BDE.
Chen et al. (2003)	Printing and dyeing wastewater	Nil	Stainless Steel (S.S. 316) autoclave	18 % COD removal at 846 ^{o}C, oxygen partial pressure = 1.69 MPa, activation energy = 37.5 KJ/mol K.	The authors have reported that the results were obtained during process are useful to design WAO reactor and prediction of WAO performance in treating printing and dyeing wastewater
Chaudhari et al. (2005)	BDE from the cane based DWW treatment plant $COD_0 = 34.0$ kg/m^3 pH_0 = 7.8	CuO	Stainless Steel (S.S. 316) autoclave	62% and 70% COD reductions were found at 140°C and pH_0 = 1 for reaction times 2 h and 6 h, respectively, under autogenous pressure.	A two step COD reduction was obtained. Considerable amount of solid residue was obtained after the treatment, having the heating value equivalent to lignite. The treated effluent has been found to have good filtration property.
Garg et al. (2005)	Black liquor	CuSO$_4$	Glass reactor used for thermolysis and SS autoclave for WAO.	63.3% COD and 92.5% color removal was reported at catalyst concentration of 5 kg/m^3 and 2 kg/m^3, during thermochemical pretreatment.	The authors have reported the residual copper in the supernatant works as a good catalyst for wet air oxidation process.
Pradeep et al. (2007)	Desizing wastewater	CuSO$_4$	Glass reactor used for thermolysis 0.5 L capacity.	71.6% COD and 87.2% color of desizing wastewater was obtained at a catalyst concentration of 4 kg/m^3.	The authors have reported the residue obtained after catalytic thermolysis is useful in agricultural field.

2.3 TREATMENT OF TEXTILE MILL WASTE WATER BY COAGULATION

Lin and Peng (1996) studied the treatment of textile wastewaters from a large dyeing and finishing mill by a continuous process of combined chemical coagulation, electrochemical oxidation and activated sludge treatment. Operating variables, such as the wastewater flow rate, conductivity, pH, applied current and amount of poly aluminum chloride (PAC) were explored to determine their respective effects on the efficiency of the electrochemical oxidation of the textile wastewater. Economic evaluation of the combined treatment method indicates that it is highly competitive in comparison to the conventional treatment method practiced in the textile industry.

Lin and Chen (1997) investigated possible reuse of wastewater effluent from the secondary wastewater treatment plant of a dyeing and finishing mill using electrochemical method, chemical coagulation and ion exchange. To enhance the efficiency of electrochemical method, addition of a small amount of hydrogen peroxide is found to be highly beneficial. Experimental results throughout the present study have indicated that the combined chemical treatment methods are very effective and are capable of elevating the water quality of the treated waste effluent to the reuse standard of the textile industry. In the Fenton process, a weight $FeSO_4/H_2O_2$ ratio of 3 : 4 was found to yield very good treatment results for COD and color reduction.

The treatment of simulated desizing wastewater by the Fenton process along with chemical coagulation was investigated by Lin and Lo (1997). The simulated wastewater contained less than 0.2% polyvinyl alcohol (PVA) and Blue G (a direct dye) or Black B (a reactive dye). Chemical coagulation using polyaluminum chloride and polymer was found to complement the Fenton treatment process in reducing the floc settling time, enhancing color removal and reducing Fe ion concentration. A two-

31

step Fenton treatment process intended separately for chemical coagulation and chemical oxidation was observed to be only marginally better than the single-step one.

Tan et al. (2000) studied the removal of dyes from industrial dye wastes using magnesium chloride. Magnesium chloride, as compared to alum and polyaluminum chloride (PAC) is a less commonly used coagulant in the field of wastewater treatment, with a cost in between alum and PAC. The results show that $MgCl_2$ is capable of removing more than 90% of the coloring material at a pH of 11 and a dose of 4 g $MgCl_2$/l of dye solution. $MgCl_2$ is shown to be more effective in removing reactive dye than alum and PAC in terms of settling time and amount of alkalinity required. Wastewaters of a dyeing and printing mill on different days have been treated by $MgCl_2$ aqueous solution in bench scale. The treatment of the industrial waste has shown a reduction of 88% in COD and 95% of suspended solids.

Arslan et al. (2001) presented the treatability of a simulated disperse dye-bath by ferrous iron coagulation, ozonation, and ferrous iron-catalyzed ozonation at varying pH (3–13) and Fe(II)-ion doses (0.09–18 mM) (COD_0 = 3784 mg/l; TOC_0 = 670 mg/l; $BOD_{5,0}$ = 58 mg/l). The simulated effluent more closely resembled an actual dyehouse effluent than an aqueous disperse dye solution. Coagulation with 5000 mg/l $FeSO_4 \cdot 7H_2O$ (18mM Fe^{2+}) at pH 11 removed up to 97% color and 54% COD, whereas oxidation via ozonation alone (applied ozone dose = 2300 mg/l) was only effective at pH 3, resulting in 77% color and 11% COD removal.

Removal of phenolic compounds from rubber–textile wastewaters by physico-chemical process was investigated by Ozbelge et al. (2002) using four different types of coagulants ($Al_2(SO_4)_3$, $Fe_2(SO_4)_3$, $FeSO_4$, $FeCl_3$) with or without lime ($Ca(OH)_2$) addition, in jar-test experiments. The optimum results were obtained by using 50%

FeCl$_3$ solution and lime at various dosages at 23 °C, which satisfy the decision criterion of high treatment efficiency (TE) in removing the phenolic compounds, good settling rate (SR) of the flocs, and a reasonably low cost of treatment. The achieved TE are over 94% in most of the cases. First adding lime and then the coagulant yield better results in terms of the treatment efficiency and settling behavior of the formed flocs. One minute rapid mixing after the addition of lime and coagulant, followed by 30-min gentle mixing were applied in the experiments successfully. The optimum pH of coagulation was found to be around 12. Bes-Pia et al. (2002) carried out the jar test experiments with different coagulants and flocculants, at different concentrations and pH and obtained that the combination of the physico-chemical treatment and the nanofiltration leads to a COD removal of almost 100%.

Kim et al. (2002) studied the performance of pilot scale combined process of fluidized biofilm process, chemical coagulation and electrochemical oxidation for textile wastewater treatment. In order to enhance biological treatment efficiency, two species of microbes, which can degrade textile wastewater pollutants efficiently, were isolated and applied to the system with supporting media. FeCl$_3$.6H$_2$O, pH 6 and 3.25 x 10^{-3} mol/l were determined as optimal chemical coagulation condition and 25mM NaCl of electrolyte concentration, 2.1 mA/cm^2 of current density and 0.7 l/min of flow rate were chosen for the most efficient electrochemical oxidation at pilot scale treatment.

Bes-Pia et al. (2003) studied the feasibility of the combination of physico-chemical treatment with nanofiltration to reuse wastewater of a printing, dyeing and finishing textile industry. For the physico-chemical treatment two coagulants (one containing Al^{3+} and another containing Fe^{2+}) were compared by carrying out jar-tests

using different chemical concentrations and pH values. After that, nanofiltration experiments with physico-chemically treated wastewater were performed at different operating pressures and cross-flow velocities. The results showed that the COD and conductivity of the nanofiltration permeates were lower than 100 mg/l/l and 1000 µS/cm respectively.

Georgiou et al. (2003) presented textile wastewater treatment towards the destruction of the wastewater's color by means of coagulation/ flocculation using ferrous sulfate and/or lime. Treatment with lime alone proved to be very effective in removing the color (70–90%) and part of the COD (50–60%). The treatment with ferrous sulfate regulating the pH in the range 9.07 ± 0.5 using lime was equally effective. Finally, the treatment with lime in the presence of increasing doses of ferrous sulfate was tested successfully, however; it proved to be very costly mainly due to the massive production of solids that precipitated. Kim et al. (2003) showed the effectiveness of biological pretreatment involving appropriate microorganisms and suitable support media in a combined process. The combined process consisted of biological pretreatment, chemical coagulation and electrochemical oxidation. COD and color were reduced by 95.4% and 98.5% by the combined process, respectively.

Damas et al. (2005) studied of preozonation influence on the physical-chemical treatment of textile wastewater. Initially the ozonation influence on the coagulation-flocculation process was studied in textile wastewater from a dyeing, printing and finishing industry. Several jar-tests were carried out using wastewater before and after an ozonation process, with reaction times of 30 and 60 min. It was highlighted that a short time preozonation enhanced the coagulation process, achieving after sedimentation COD and turbidity reductions of 57% and 95%, respectively.

Selcuk et al. (2005) evaluated and compared the performance of ferrous and aluminum sulfate coagulations and ozonation treatment techniques. The evaluation of treatment efficiency was made using the parameters of oxygen demand (COD), color absorbances at 436 nm, 525 nm and 620 nm and Daphnia magna toxicity test. Approximately 50-60% color, 60% COD and 70-80% toxicity were removed at 1000 mg/l and 1500 mg/l[1] ferrous and aluminum sulfate, respectively. However, these required doses for optimum toxicity reduction are not economical due to the chemical sludge production. The toxicity of wastewater reduced after color degradation by 85% at the transferred ozone (TrO_3) concentration of 82.3 mg/.

Color removal by $MgCl_2$ when treating synthetic waste containing pure dyes was studied by Gao et al. (2007). The color removal efficiency of $MgCl_2/Ca(OH)_2$ was compared with that of $Al_2(SO_4)_3$, polyaluminum chloride (PAC) and $FeSO_4/Ca(OH)_2$. The mechanism of color removal by $MgCl_2$ was also investigated. It was shown that the color removal efficiency of $MgCl_2$ is related to the type of dye and depends on the pH of the waste and the dosage of the coagulants used. Treatment of waste containing reactive dye or dispersed dye with $MgCl_2$ yielded an optimum color removal ratio when the pH of the solution was equal to or above 12.0. For both the reactive and dispersed dye waste, $MgCl_2/Ca(OH)_2$ was shown to be superior to $MgCl_2/NaOH$, $Al_2(SO_4)_3$, PAC and $FeSO_4/Ca(OH)_2$ for color removal.

Gao et al. (2007) adopted a new composite coagulant, which was prepared by polyferric chloride (PFC) premixed with polydimethyldiallylammonium chloride (PDMDAAC) to treat the simulated dye water and the actual textile wastewater. The color removal results treated by the composite coagulant (PFC–PDMDAAC) were compared with those treated by PFC, PDMDAAC and PFC followed by PDMDAAC

(PFC/PDMDAAC), respectively. It was found that the synergy between PFC and PDMDAAC increases zeta potential of PFC–PDMDAAC and reduces the effect of pH on zeta potential and Fe(III) species of PFC–PDMDAAC. Treatment with PFC–PDMDAAC is very effective in removing disperse blue HGL (98%) and reactive blue STE (86%).

Bali and Karagozoglu (2007) evaluated the Fenton process (involving oxidation and coagulation), ferric coagulation and H_2O_2/pyridine/Cu(II) system for the removal of color from a synthetic textile wastewater containing polyvinyl alcohol and a reactive dyestuff, Remazol Turquoise Blue G-133. A decolorization efficiency of 96% was achieved with Fenton's reagent at an optimum [Fe(II)]:[H_2O_2] molar ratio of 1.21:1. However, 27% of initial Fe(II) was still in the effluent which required further treatment. Optimum pH and coagulant dose were found to be 7 and 100-125 mg/l, respectively, and the corresponding efficiency was 100%. Cationic polyelectrolyte was found to be the most suitable type and 2 mg/l of it enhanced the decolorization by 10% and 75% for filtered and non-filtered samples, respectively. The maximum efficiency achieved by H_2O_2/pyridine/Cu(II) system was about 92% with a high initial reaction rate different from the H_2O_2/pyridine system which also led to 92% removal. However, the required H_2O_2 dosage was very high in this system with a low Cu(II).

2.4 TREATMENT OF TEXTILE MILL WASTE WATER BY OXIDATION PROCESSES

Lin and Ho (1996) treated desizing wastewater by catalytic wet-air oxidation. Experiments were conducted to investigate the effects of temperature and catalyst dosage ($CuSO_4$ and $Cu(NO_3)_2$) on the pollutant (chemical oxygen demand or COD) removal. It is observed that over 80% of the COD removal can be realized in an hour of

the catalytic WAO process. A kinetic model was also developed and a two-stage, first-order kinetic expression was found to represent well the treatment reaction. The correlations between the reaction rate coefficients and the temperature and catalyst dosage were also determined.

Treatability of mixed raw, coagulated and biologically pretreated textile and pulp wastewater and effluents from different process stages by enhanced heterogenous photocatalytic oxidation process was investigated by Balcioglu and Arslan (1998). Treatment performances were evaluated in terms of COD, TOC, BOD_5, and color removal. Results indicate that photocatalytic oxidation process enhanced with 15 mM H_2O_2 was more efficient in removal of pollutants for pretreated wastewater samples. By the application of photocatalytic treatment, 52 and 87% COD removals were obtained for biotreated Kraft bleaching and textile effluents, respectively. Addition of only 1 mM ferric ion speeded up the oxidation time of the textile effluent significantly, but it had no impact on total COD reduction. While complete color removal of the textile wastewater was achieved within the first h of photocatalytic treatment, complete decolorisation could not be obtained for pulp effluents, except for the coagulated wastewater throughout the reaction period. Biologically pretreated textile wastewater was found to have potential for reuse after photocatalytic treatment.

The photodegradation and biodegradability of four non-biodegradable azo dyes were investigated by Chun and Yizhong (1999). The color removal of dyes solution and dyeing wastewater reached to above 90% within 20-30 min of photocatalytic treatment. BOD was found to increase. While COD, TOC decreased, so that the ratio of BOD_4/COD of the wastewater increased from original zero up to 0.75. The result implies that photocatalytic oxidation enhanced the biodegradability of the dye-

containing wastewater and therefore relationship between decolorization and biodegradability exists. When the color disappeared completely, the wastewater biodegraded normally and could be discharged for further treatment. The experimental results demonstrate that it is possible to combine photocatalysis with conventional biological treatment for the remedy of wastewater containing generally non-biodegradable azo dyes.

Vlyssides et al. (2000) treated textile dye wastewater (TDW) from a reactive azo dyeing process by an electrochemical oxidation method using Ti/Pt as anode and stainless steel 304 as cathode. Due to the strong oxidizing potential, the chemicals produced chlorine, oxygen, hydroxyl radicals and other oxidants. When the wastewater was passed through the electrolytic cell, the organic pollutants were oxidized to carbon dioxide and water. The biodegradability of the wastewater was improved because the COD/BOD ratio decreased from 2.16 to 1.52. These results indicate that this electrolytic method could be used for effective TDW oxidation or as a feasible detoxification and color removal pretreatment stage for biological post treatment.

Szpyrkowicz et al. (2001) performed experimental studies on the destruction of disperse dyes by chemical oxidation using ozone, hypochlorite and Fenton reagent (H_2O_2 + Fe^{2+}) and compared with the data obtained by electrochemical oxidation. While the results obtained during hypochlorite oxidation were not satisfactory (only 35% reduction of color was achieved at a dose of 6 g/l), ozonation enabled color to be reduced by up to 90% (ozone dose 0.5 g/l). High decolorisation was, however, accompanied by a low removal (10% efficiency) of chemical oxygen demand (COD).

The photocatalytic degradation of various dyes were studied by Hachem et al. (2001), using P25 Degussa as catalyst. All dye solutions underwent a decolorization.

The kinetics of reaction have been studied and were found to be zero or first order with respect to the dyes. This was compared with the adsorption properties. The effect of the addition of hydrogen peroxide was studied. An enhancement of the rate was observed in all cases and the order with respect to the additive was found to be almost zero.

The photodegradation of three non hydrolysed reactive azo dyes in aqueous solution was investigated by Neamtu et al. (2002) in a laboratory-scale batch photoreactor equipped with an immersed low pressure mercury lamp. Six different doses of hydrogen peroxide, at constant initial concentration of the substrate (100 mg/l) were used. The pseudo-first order rate constants were calculated from the experimental kinetic curves, for the three azo dyes. These rate constants have extreme values of the order of 0.1 min^{-1} at a H_2O_2 dose of 24.5 mmol/l. The effectiveness of the UV/H_2O_2 process has been evaluated by the degree mineralization of the TOC, as a complementary indicator of the treatment efficiencies. The results confirm the suitability of the UV/H_2O_2 process as a textile wastewater pre-treatment step, once optimum operating conditions and cost effectiveness of the method are established.

Baban et al. (2003) studied the treatment of effluents from dyeing processes of woolen textile finishing industries highly polluted with recalcitrant compounds and compared to effluents from rinsing and finishing processes. Oxidation of woolen textile dyeing effluent consisting of wastewater generated from spent dye baths and first and second rinses (remaining composite wastewater) were investigated. Ozone oxidation (C_{O3} = 18.5 mg/l; input rate) was applied on remaining composite wastewater, before and after the biological treatment, for various time intervals. Treatment efficiency was monitored by decolorization and by COD removal rates. Additionally, toxicity tests (bioluminescence test) were carried out to determine the effect of oxidation process.

The results indicated that 40 minutes ozonation of biologically treated wastewater yielded almost colorless effluent with a decolorization efficiency of around 98–99% and with a corresponding ozone absorption rate of 58.0 mg/l. Biological treatment followed by 10 min ozone oxidation reduced the overall toxicity significantly (92%). However, ozonation was found to have only slight effect on COD removal.

Chen et al. (2003) presented the results of a study on the treatment of printing and dyeing wastewater from the textile industry by wet air oxidation (WAO). The range of operating temperatures examined was between 423 and 573 K at an oxygen partial pressure of 1.69 MPa standardized at 298 K. The extent of COD removal by the oxidation process increases with temperature until 523 K. Thermal decomposition during preheating was found to play a significant role in the COD removal with up to 18% COD removed at an operating temperature of 573 K. A first order kinetic model has been proposed and tested for the removal of COD by WAO.

Polyvinyl alcohol (PVA), known as the dominant contributor of chemical oxygen demand (COD) in textile wastewater, is very difficult to decompose by conventional treatment technologies. Kim et al. (2003) studied the electrochemical oxidation using a RuO_2/Ti anode to treat a PVA solution. The mechanisms of PVA degradation and COD destruction were investigated, while the operating parameters affecting the mechanisms were also studied. The parameters investigated included current density, PVA concentration in waste stream, the rate of electrolyte consumption of sodium chloride, and the feed rate of wastewater.

Kusvuran et al. (2004) studied UV/TiO_2, electro-Fenton (EF), wet-air oxidation (WAO), and UV/electro-Fenton (UV/EF) advanced oxidation processes (AOPs) to degrade Reactive Red 120 (RR120) dye in aqueous solution. The most efficient method

on decolorization and mineralization of RR120 was observed to be WAO process. Photocatalytic degradation of RR120 by UV/TiO$_2$ have been studied at different pH values. At pH 3 photocatalytic degradation kinetics of RR120 successfully fitted to Langmuir–Hinshelwood (L–H) kinetics model. Decolorization efficiency observed in the order of WAO > UV/TiO$_2$ = UV/EF > EF while WAO > UV/TiO2 > UV/EF > EF order was observed in TOC removal (mineralization). For all AOPs, it was found that degradation products in reaction mixture can be disposed safely to environment after 90 min treatment.

Neamtu et al. (2004) evaluated the degradation of a reactive azo dye, Procion Marine H-EXL, by catalytic wet hydrogen peroxide oxidation (CWHPO). The catalyst was prepared by ion-exchange of a commercially available ultrastable Y zeolite. The results indicate that after only 10 min at 50 °C, 20 mmol/l H$_2$O$_2$ and 1g/l FeY, the color removal was as high as of 97% at pH = 3 and 53% at pH = 5. More than 96% removal of the dye could be attained in 30 min at pH = 5, t = 50 °C, 20 mmol/l H$_2$O$_2$ and 1 g/l FeY which corresponds to about 76% reduction of the COD$_0$ and 37% removal of the initial TOC.

Degradation of Reactive Black 5 (RB5), a well-known non-biodegradable disazo dye was studied by Kusvurana et al. (2005) using UV/TiO$_2$, wet-air oxidation (WAO), electro-Fenton (EF) and UV/electro-Fenton (UV/EF) advanced oxidation processes (AOPs). The efficiency of substrate decolorization and mineralization in each process were comparatively discussed by decreases in concentration and total organic carbon content of RB5 solutions. The most efficient method on decolorization and mineralization was observed to be WAO process. Mineralization efficiency was observed in the order of WAO> UV/TiO$_2$ > UV/EF > EF. Photocatalytic degradation

kinetics of RB5 successfully fitted to Langmuir–Hinshelwood (L–H) kinetics model. The values of second order degradation rate constant (k") and adsorption constant (K) were determined as 5.085 mg/l min and 0.112 l/mg, respectively.

H_2O_2 , an environmentally friendly oxidant, was used by El-Daly et al. (2005) to oxidize and decolorize two of the direct dyes that fulfill an outstanding demand. These dyes are C. I. Direct Green 28 (14155), I, and C. I. Direct Blue 78 (34200), II. The oxidation of I does not occur in acidic medium. The reaction is slow in neutral medium. The reaction rate increases with pH till it reaches a maximum at 10.17. The oxidation of I is characterized by an autocatalytic behavior. The oxidation of II does not take place in alkaline medium. The reaction was carried out in acidic phosphate buffer medium at pHZ5.0 in the presence of Cu (II) as a catalyst. The oxidation reaction of I showed a first order kinetics for H_2O_2 and zero-order kinetics for Dye. The oxidation reaction of II showed a first order kinetics for both dye and Cu (II) and a zero-order kinetics for H_2O_2. The Cu (II)-catalyzed oxidation reaction of II showed an autocatalytic behavior in acidic phosphate/citric acid buffer medium and the reaction rate reaches a maximum at pH=4.15.

Wu et al. (2006) investigated decomposition kinetics of basic dye in a photocatalytic slurry reactor. The dye decomposition kinetics by nano-size TiO_2 suspension at natural solution pH was experimentally studied by varying the agitation speed (50–200 rpm), TiO_2 suspension concentration (0.25–1.71 g/l/l), initial dye concentration (10–50 ppm), temperature (10–50 ∘C), and UV power intensity (0–96 W). The experimental results show the agitation speed, varying from 50 to 200 rpm, has a slight influence on the dye decomposition rate and the pH history; the dye decomposition rate increases with the TiO_2 suspension concentration up to 0.98 g/l/l,

then decrease with increasing TiO_2 suspension concentration; the initial dye decomposition rate increases with the initial dye concentration up to a certain value depending upon the temperature, then decreases with increasing initial dye concentration.

Grimau and Gutierrez (2006) focused on the optimization of the electrochemical decolorisation of textile effluents containing reactive dyes. The decolorisation yield was dependent on the dyeing electrolyte (NaCl or Na_2SO_4). Dyeing effluents which contained from 0.5 to 20 g/l of NaCl reached a high decolorisation yield, depending on the current density, immediately after the electrochemical process. These results were improved when the effluents were stored for several hours under solar light. After the electrochemical treatment, the effluents were stored in a tank and exposed under different lighting conditions: UV light, solar light and darkness. A TOC removal of 81% was obtained when high current density was applied for a prolonged treatment with recirculation. This treatment required a high electrical consumption.

Rajkumar and Kim (2006) revealed that all the reactive dyes were degraded in chlorine mediated electrochemical oxidation. Titanium based dimensionally stable anode (DSA) was used for in situ generation of chlorine in the dye solution. All classes of reactive dyes (100 mg/l/l) showed a complete color removal at a supporting electrolyte concentration of 1.5 g/l/l NaCl and 36.1 mA/cm^2 current density. The COD and TOC removals were from 39.5 to 82.8% and from 11.3 to 44.7%, respectively, for different reactive dyes. It can be concluded in general that the triazine containing higher molecular weight diazo compounds takes more time for complete de-colorization than the mono azo or anthraquinone containing dye compounds. The degradation rate of mixed dye compounds was affected by reaction temperature, current density, NaCl

43

concentration and initial dye concentration. However, the pH_0 of the dye solution ranging from 4.3 to 9.4 did not show significant effect on de-colorization. A complete color removal with 73.5% COD and 32.8% TOC removals were obtained for mixed reactive dyes (200 mg/l/l) at the end of 120 min of electrolysis under the optimum operating conditions of 4 g/l/l NaCl concentration and 72.2 mA/cm^2 current density.

Andrade et al. (2007) investigated the electrochemical performance of pure Ti–Pt/β-PbO$_2$ electrodes, or doped with Fe and F (together or separately), in the oxidation of simulated wastewaters containing the Blue Reactive 19 dye (BR-19), using a filter-press reactor, and then compared with that of a boron-doped diamond electrode supported on a niobium substrate (Nb/BDD). The electro-oxidation of the dye simulated wastewater (volume of 0.1 l, with a BR-19 initial concentration of 25 mg/l) was carried out under the following conditions: current density of 50 mA cm^{-2}, volume flow rate of 2.4 l/h, temperature of 25 $^{\circ}$C and electrode area of 5 cm^2. The performances of the electrodes in the dye decolorization were quite similar, achieving 100% decolorization, and in some cases 90% decolorization was achieved by applying only ca. 0.3 A h/l (8 min of electrolysis). The reduction of the simulated wastewater organic load, monitored by its TOC, was greater for the Ti–Pt/β-PbO$_2$–Fe,F electrode obtained from an electro-deposition bath containing 1 mM Fe^{3+} and 30 mM F^{-}.

2.5 TREATMENT OF TEXTILE MILL WASTE WATER BY FENTON PROCESS

Treatment of wastewater effluent from the secondary wastewater treatment plant of a dyeing and finishing mill was investigated by Lin and Chen (1997) for possible reuse employing Fenton process, chemical coagulation and ion exchange. The Fenton process and chemical coagulation are intended primarily to remove color,

turbidity (NTU) and COD concentration of wastewater effluent while ion exchange is used to further lower the COD and Fe ion concentrations, total hardness, conductivity, alkalinity, SS and TDS of wastewater. Experimental results indicated that the combined chemical treatment methods are very effective and are capable of elevating water quality of the treated wastewater effluent to the reuse standard of the textile industry.

Arslan and Balcloglu (1999) demonstrated the application of UV/Fenton, near-UV-visible/Fenton, dark Fenton and H_2O_2/UV reactions to treat simulated dye-house effluents representing wastewater from the textile dyeing and rinsing process. Lab-scale photochemical reactor using concentrations of 0.5 - 25 mM H_2O_2, 0.04 - 0.5 mM Fe^{2+} - ion and different dilutions of textile wastewater was used. Comparative evaluation of the obtained results revealed that the decolorization rate increased with applied H_2O_2 and Fe^{2+} - ion dose as well as the strength of the synthetic textile wastewater. The best results were obtained by the near - UV/visible/Fenton process with a decolorization rate constant of 1.57 min^{-1}, a UV_{254nm} reduction of 97 % and a DOC removal of 41% at relatively low doses of the H_2O_2 oxidant and Fe^{2+} - ion catalyst within 60 min treatment time.

Kang et al. (2000) described the use of photo-fenton process for color removal from textile wastewater stream. The wastewater sample to be treated was simulated by using colorless polyvinyl alcohol (PVA) and reactive dyestuff of R94H. As a result, the hydroxyl radical (HO•) oxidation could effectively remove color, but the chemical oxygen demand (COD) was removed in a slight degree. The color removal is markedly related with the amount of HO• formed. The optimum pH for both the OH• formation and color removal occurs at pH 3-5. Up to 96% of color can be removed within 30 min under the studied conditions.

Kang et al. (2002) evaluated the Fenton process, involving oxidation and coagulation, for the removal of color and chemical oxygen demand (COD) from synthetic textile wastewater containing polyvinyl alcohol and a reactive dyestuff, R94H. The experimental variables studied include dosages of iron salts and hydrogen peroxide, oxidation time, mixing speed and organic content. The results showed that the color was removed mainly by Fenton oxidation. The color removal reached a maximum of 90% at a reaction time of 5 min under low dosages of H_2O_2 and Fe^{2+}. In contrast, the COD was removed primarily by Fenton coagulation, rather than by Fenton oxidation. The ratio of removal efficiency between Fenton process and ferric coagulation was 5.6 for color removal and 1.2 for COD removal. It is concluded that Fenton process for the treatment of textile wastewater favors the removal of color rather than COD.

The simultaneous use of Fenton reagent and irradiation for the treatment of textile wastewaters generated during a hydrogen peroxide bleaching process was investigated by Perez et al. (2002). The experimental conditions tested during this study provide the simultaneous occurrence of Fenton, Fenton-like and photo-Fenton reactions. Concentrations of Fe(II) between 0 and 400 ppm, and H_2O_2 between 0 and 10,000 ppm were used. Temperatures above 25 ^{o}C and up to 70 ^{o}C show a beneficial effect on organic load reduction. A set of experiments was conducted under different light sources with the aim to ensure the efficiency of using solar light irradiation. The combination of Fenton, Fenton-like and photon-Fenton reactions has been proved to be highly effective for the treatment of such a type of wastewaters, and several advantages for the technique application arise from the study.

Xu et al. (2004) studied the degradation of 20 different dyes in aqueous solutions by the Fenton process. The dyes included 6 types: acidic, reactive, direct,

cationic, disperse and vat dyes. The former four types of dyes were decolorized and their TOC values were decreased greatly, while the color and TOC removals of the latter two types were lower. The catalytic activities of four metal ions on the degradation efficiencies of Vat Blue BO, which was chosen as a model dye because of its lowest color and TOC removals, were compared in the dark and under the ultraviolet light irradiation. The catalytic ability of different metals was $Fe^{2+} > Cu^{2+} > Mn^{2+} > Ag^+$ in the dark, and the same sequence was obtained under irradiation condition with greater degradation efficiency. Furthermore, the efficiencies of three oxidation processes, including H_2O_2/UV, Fe^{2+}/H_2O_2 and $Fe^{2+}/H_2O_2/UV$ were compared. The results showed that the oxidation by $Fe^{2+}/H_2O_2/UV$ was the strongest, and even greater than the arithmetic sum of the other two processes, which suggests the synergistic effect of ultraviolet and ferrous ions on the degradation reaction.

The photocatalytic organic content reduction of two selected synthetic wastewater from the textile dyeing industry were studied by the use of heterogeneous and homogeneous photocatalytic methods under solar irradiation. The effect of two different TiO_2 modifications with oxidants such as H_2O_2 and $Na_2S_2O_8$ on the decolorisation and the dissolved organic content reduction (DOC) of the wastewater was examined by Kositzi et al. (2004). The TiO_2/H_2O_2 system seems to be more efficient in comparison to the synergetic action that appears when using persulphate and TiO_2 in this specific wastewater. By an accumulated energy of 50 kJ/l the synergetic effect of TiO_2 P-25 with H_2O_2 and $Na_2S_2O_8$ leads to a 70% and 57% DOC reduction, respectively, in the case of cotton synthetic wastewater, while the decolorisation was almost complete.

Meric et al. (2005) studied the effectiveness of Fenton's oxidation (FO) process and ozone (O_3) oxidation and compared with a coagulation–flocculation (CF) process

to remove effluent toxicity as well as color and COD from a textile industry wastewater. Daphnia magna was used to test acute toxicity in raw and pre-treated wastewater. The operational parameters for each process were determined on the basis of complete toxicity removal. The FO process removed COD at a higher rate (59%) than O_3 (33%), while color removal was similar (89% and 91%, respectively). The CF process removed both COD and color at rates similar to the FO process. A color range of 150–250 platin–cobalt (Pt–Co) unit was assessed for toxicity.

Dantas et al. (2006) used new composites as adsorbents and/or heterogeneous catalysts for Fenton oxidation. The composites with high iron oxides content were effective to adsorb contaminants in textile wastewater, and the adsorptive capacity increased with the superficial iron concentration. These solids were also used as heterogeneous Fenton catalysts and had the advantage of being effective at pH 3.0 with a consumption of hydrogen peroxide lower than required by the homogeneous Fenton process.

The feasibility of employing different photoxidation systems, like Fenton/UV-C and ferrioxalate/H_2O_2/solar light in the decolorization and mineralization of an azo dye were investigated by Lucas and Peres (2007). The experiments indicate that RB5 can be effectively decolorized using Fenton/UV-C and ferrioxalate/H_2O_2/solar light processes with a small difference between the two processes, 98.1% and 93.2%, respectively, after 30 min. Although there is lesser difference in dye decolorization, significant increment in TOC removal was found with Fenton/UV-C process (46.4% TOC removal) relative to ferrioxalate/ H_2O_2/solar light process (29.6% TOC removal). This fact reveals that UV-C low-pressure mercury lamp although with its small effect on dye decolorization is particularly important in dye mineralization, when compared to solar light.

Bandala et al. (2007) investigated the decolorisation of synthetic and real textile wastewater containing benzidine-based azo dyes using dark Fenton reaction and solar driven photo-Fenton process. Experimental runs with synthetic wastewater were used to identify the best conditions to perform real wastewater decolorisation. It was found that, using solar energy to promote the advanced oxidation process (AOP) proposed, the reaction kinetic is increased by almost twice, compared with dark Fenton reaction. With solar driven photo-Fenton, decolorisation of 90% was achieved using 1mM of Fe^{2+} and 50mM of H_2O_2 with only 12 kJ/l/l. When these conditions were tested for real wastewater, 56% of color removal was obtained and 62.6% of the organic matter found initially in the effluent (measured as chemical oxygen demand, COD) was eliminated after 16 kJ/l.

2.6 TREATMENT OF TEXTILE MILL WASTE WATER BY ADSORPTION

Malik and Taneja (1994) utilized fly ash from thermal power plants, steel mills, etc. for color removal of dye effluents. Since fly ash is a rich source of silica, alumina, and other oxides, it was explored for the removal of color from dye effluents. Different classes of dyes were studied at varying dye concentration and quantity of adsorbent. Much better results were obtained in the case of a diluted sample as compared to a concentrated dye solution, although an increasing quantity of adsorbent has shown no significant improvement.

Jia et al. (1999) utilized active carbon fiber as electrodes to treat several simulated dyeing wastewater and factual textile-dyeing wastewater from a textile-dyeing operation. This method was found to be quite effective and highly competitive in contrast with Fenton's reagent. Several operating variables, such as voltage, pH and
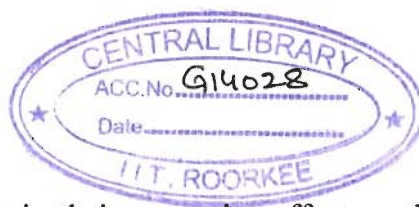
salt added were studied to ascertain their respective effect on the treatment efficacy. According to the experiment, nearly all the wastewater's chromaticity removals were higher than 90%, with COD removals within ca. 40±80%

Karcher et al. (2001) tested various sorption filters, such as zeolites, polymeric resins, ion exchangers and granulated ferric hydroxide (GEH) for the removal of different reactive dyes (M 600–1500 g/mol). Zeolites and microporous resins were not suitable due to extremely low sorption capacities. The macroporous resins without functional groups showed moderate maximum loadings (100–400 mmol/g or 100–400 mg/g) but low affinity and were not suitable for large dyes (>1000 g/mol). Loadings on anion exchangers were high but regeneration was difficult for the strong basic type (S6328a, Bayer). Catalytic oxidative regeneration of GEH is possible using H_2O_2.

Silva et al. (2004) used spent brewery grains (SWG) for the adsorption of acid orange 7 dye in aqueous solutions (AO_7), a monoazo acid dye currently used in paper and textile industries. The presence of AO_7 in these effluents causes obvious environmental problems. Kinetics studies of adsorption of AO_7 to SBG (3.75%, m/v) were carried out at 20 °C, using aqueous solutions with different AO_7 concentrations (30–834 mg/l). The adsorption process followed a pseudo-first order model. The equilibrium process showed to be well described by both Freundlich and Langmuir isotherm models, at 20 and 30 °C. The maximum adsorption capacity was estimated to be 30.5 mg AO_7/g SBG, at 30 °C. Free energy of adsorption ($\Delta G°$), enthalpy ($\Delta H°$), and entropy ($\Delta S°$) changes were calculated to predict the nature of adsorption. The estimated values for $\Delta G°$ were −22.78 and −24.53 kJ/mol, respectively, at 293.3K (20 °C) and 303.3K (30 °C), which are rather low indicating that a spontaneous process

occurred. The enthalpy changes and entropy of adsorption were 28.66 and 175.36 J/mol K, respectively. The positive value for ΔH° indicates that the adsorption of AO_7 dye to SBG is an endothermic process. The positive value of entropy reflects the affinity of the adsorbent for AO_7 dye. The obtained results were very promising since: (i) high levels of color removal (>90%) were achieved with low contact times adsorbent/dye (less than 1 h contact); and (ii) the whole SBG can be successfully used as adsorbent of AO_7 dye in aqueous solution without needing any previous treatments such as milling and/or sieving. Spent grains, being a cheap, and easily available material, could be an alternative for more costly adsorbents used for dye removal in wastewater treatment processes.

Sayan et al. (2006) studied the optimization and modeling of decolorization and COD reduction of reactive dye solutions by ultrasound-assisted adsorption. The removal of reactive dye rifacion yellow HE4R was studied by using both ultrasound and combined ultrasound/activated carbon. The effects of relevant parameters, namely; ultrasound power, temperature, time, activated carbon concentration, dye concentration and pH_0 have been investigated on the decolorization and COD reduction by using the fractional factorial design and the orthogonal central composite design. A model has been obtained among decolorization, COD reduction and relevant parameters by means of variance analysis and obtained model was optimized. 80.62% decolorization efficiency was accomplished by ultrasound. Afterwards, combined ultrasound/activated carbon were applied to remove all dye color and COD from synthetic textile wastewater. The efficiencies of decolorization and COD reduction were accomplished at optimum conditions as 99.9% and 85.22%, respectively.

Ozer and Dursun (2006) studied the removal of methylene blue from aqueous solution by dehydrated wheat bran carbon. Dyes are usually present in the effluent

water of many industries, such as textiles, leather, paper, printing and cosmetics. The effectiveness of dye adsorption from wastewater has made to get alternative different low cost adsorbent to other expensive treatment methods. The adsorption of methylene blue onto dehydrated wheat bran (DWB) was investigated at temperatures (25–45 °C), initial methylene blue (MB) concentrations (100–500 mg/l) and adsorbent dosage at the given contact time for the removal of dye. The optimum adsorption conditions were found to be as medium pH of 2.5 and at the temperature of 45 °C for the varying adsorbent dosage. Equilibrium isotherms were analyzed by Freundlich, Langmuir and Redlich-Peterson isotherm equations using correlation coefficients. Adsorption data were well described by the Langmuir model, although they could be modeled by the Freundlich and Redlich-Peterson model as well. The pseudo-first order and pseudo-second order kinetic models were applied to test the experimental data. It was concluded that the pseudo-second order kinetic model provided better correlation of the experimental data rather than the pseudo-first order model. The mass transfer model as intraparticle diffusion was applied to the experimental data to examine the mechanisms of rate controlling step. It was found that at the higher initial MB concentration, intraparticle diffusion is becoming significant controlling step. The thermodynamic constants of the adsorption process were also evaluated by using the Langmuir constants related to the equilibrium of adsorption at temperatures varied in the range 25–55 °C.

Andrzejewska et al. (2007) investigated the removal of an anionic reactive dye, C.I. Reactive Blue 19, from aqueous solution using a commercial, highly dispersed precipitate, Syloid® 244 silica. The adsorption resulted in blue pigmentation of the silica carrier; the ensuing pigment was subjected to a comprehensive physicochemical

analysis, including particle size, particle size distribution, polydispersity, tendency to form primary and secondary agglomerates and the morphology of the particle surface. It was found that a preliminary surface modification of the silica adsorbent with an NH_2-silane compound was necessary. The aminosilane-modified silica could be used as a selective adsorbent in the purification of waste dye solutions; its application secured highly efficient removal of dye from solutions (in most cases over 90% and in some cases even 100%). The silica-carrier product was then used as a pigment within an exterior acrylic paint.

2.7   MEMBRANE SEPARATION

Chen et al. (1997) treated desizing wastewaters from the bleaching and dyeing industry by nanofiltration (NF) membrane separation on a pilot scale in the pressure controlled region. The two brown colored wastewaters had chemical oxygen demand (COD) of 14,000 mg/l and 5430 mg/l, respectively. Permeate flux and COD retention were investigated in relation to trans-membrane pressure drop, temperature, and feed-solution concentration. The permeate flux was found to increase significantly with transmembrane pressure drop and to decrease with feed concentration. Higher permeate flux was found for wastewater with higher pH. A minor increase in COD retention was found for the increase in trans-membrane pressure drop as well as operating temperature. The COD retention was about 95% for wastewater with pH 10.2, and 80-85% for wastewater with pH 5.5.

Bruggen et al. (2001) investigated the removal of dye compounds from color baths used in the textile industry by the application of nanofiltration. Retention of two reactive dyes (reactive blue 2 and reactive orange 16) was studied in separate baths and with different concentrations of Na_2SO_4, Na_2CO_3, NaOH and a surfactant. Different

nanofiltration membranes (UTC-60, NF70 and NTR 7450) were used. The water flux in each of the experiments was monitored.

Sand filtration and ultrafiltration (UF) as pre-treatments for a membrane process of nanofiltration (NF) or reverse osmosis (RO) was reported by Marcuccl et al. (2001). The UF module tested works at low operating pressure (that involves low energy costs) and guarantees a constant permeate (feed of the next membrane process of NF or RO). The RO permeate can be reused in the dyeing processes as demonstrated by many yarn dyeing tests on the industrial scale. NF does not reach the retention behavior of RO (total hardness removal of 75% and >90% for NF and RO, respectively). Marcucci et al. (2002) applied different membrane technologies, supported by clariflocculation and ozonization, for textile wastewater reuse. In the first case the pilot plant used sand filtration and microflitration (MF) as pre-treatments for nanofiltration (NF). The MF and NF membranes tested were of the spiral wound type. The NF permeate can be reused in all production steps, including dyeing with light coloration. In the second case, the chemical-physical pre-treatment and the advanced treatment of water have been experimented for different kind of wastewater. The most interesting experimental results were obtained from the treatment of wastewater from the carbonising process.

Bes-Pia et al. (2003) focused on the advanced treatment of the biologically treated wastewater of a textile plant. Both nanofiltration experiments at different operating conditions and oxidation reactions with ozone and ozone/UV irradiation were performed to evaluate the final water quality for its reuse. It was concluded that a high COD removal was obtained with chemical oxidation with ozone and with ozone/UV. The advantage of this technique in comparison with nanofiltration is that there is no reject stream generation. Nevertheless, the oxidation does not reduce the water

conductivity. Thus, the reuse of the treated water is not possible. Bes-Pia et al. (2004) indicated that nanofiltration (NF) membrane permeates could be reused in some processes of finishing, dyeing and printing in the textile industry. In this work, biologically treated textile wastewaters were subjected to ozonation as a pre-treatment stage to NF. The aim was to reduce organic matter in order to prevent membranes from fouling and to oxidize organic wastewater compounds that could damage the membrane material. NF experiments were carried out in a laboratory plant equipped with a pressure vessel containing one spiral-wound membrane element (2.51 m 2 of active surface). With ozonation, wastewater COD was reduced up to three different levels (160, 135 and 82 mg/l). NF experiments with wastewaters of different organic matter concentrations were carried out studying the effect of increasing the feed concentration periodically. Conductivity retentions higher than 65% were achieved, with no significant flux decay observed during the experiments.

Banat et al. (2005) treated the waters colored with methylene blue dye by vacuum membrane distillation. The objective of the study was to examine the potential use of the vacuum membrane distillation process for the treatment of dyed solutions. Batch experiments were conducted on dilute MB-water mixtures using a tubular polypropylene membrane module. The impact of operating variables such as feed temperature, flow rate and initial dye concentration was investigated.

Bes-Pia et al. (2005) used nanofiltration as a pre-treatment step for textile industry wastewater along with chemical neutralization, physicoehemical treatment and membranes. Neutralization studies were conducted in order to select the most appropriate neutralizing agent in terms of conductivity of the neutralized wastewater. For the physicoehemical treatment, four coagulants from the Cibaa Company

(Mangaso15389, Mangaso16348, Zetag 7103 and Alcy1955) were compared by carrying out jar tests using different concentrations and pH values. After that, nanofiltration experiments of the physicochemically treated wastewater were performed in a laboratory plant equipped with a pressure vessel containing one spiral-wound membrane element ($A = 2.51 \ m^2$). The operating conditions were: transmembrane pressure of 20 bar, cross-flow velocity of 1.66 m/s and a temperature of 25°C. As a result, the combination of physicochemical treatment and nanofiltration provided treated water with good enough quality to be reused in the industry.

The treatment of textile wastewater for reuse using an electrochemical oxidation step combined with a membrane filtration step was reported by Chen et al. (2005). Two testing sequences of electrochemical oxidation and membrane filtration were studied in a sequential batch order. The results show clearly that fibres welded in an arc-shape can enhance the mechanical properties of the fibres effectively and that electrochemical oxidation and membrane filtration as sequential processes are feasible. Electrochemical oxidation has a high removal (89.8% efficiency) of the chemical oxygen demand (COD) of the wastewater while the membrane filter can almost totally remove the total suspended solids (TSS) (nearly 100% reduction) and turbidity (98.3% elimination) in it. Coincidentally, their advantages make up for their disadvantages. After these two steps, all the wastewater indices decrease to low levels; in particular, COD levels are reduced to 18.2 mg/l. The treated water can be reused in many production areas of the textile dyehouse factory.

Żyłła et al. (2006) studied the model and real post-dyeing wastewater concentrated by nanofiltration (NF). In this process a filtrate characterised by an over 98% color reduction, expressed in DFZ (spectral absorption coefficient) and a

concentrate of high organic load were obtained. Further on, the NF concentrate was subjected to anoxic biodegradation. In the anoxic biodegradation of real wastewater, the degree of COD reduction was 50% on average. The filtrate coming from NF of wastewater was reused as process water in repeated dyeing processes. As a result of the end-use properties of the dyed products, it was found that the purified filtrate could be applied as process water for dyeing.

Textile industry utilizes thousands of tons of various chemicals for wet and dry processing. Effluents from wet processing, for instance, are characterized by the presence of coloring, hazardous and toxic pollutants. Numerous studies indicated several opportunities for membrane based interventions for reuse/recovery of water and chemicals. ElDefrawy and Shaalan (2007) proposed a hybrid treatment–recycling approach for decision making in the textile industry. This approach comprises the segregation of wastewater streams and the selection of the treatment–recycling scheme on the basis of reported performance data and updated cost indicators using a program tailored for this purpose. The program is validated for several scenarios representing typical actual scenarios from the textile industry. Results indicate that the use of membrane systems within the treatment–recycling scheme reduces the wastewater treatment cost through the recovery of chemicals and water. Further, the developed program proved to be sound software for decision making in the textile industry.

Qin et al. (2007) investigated the feasibility for recovering the wastewater from a specific dyeing facility by nanofiltration (NF). Process review at the dyeing facility was conducted and wastewater streams were characterized. A bench scale unit with total membrane area of 465 cm2 was used in this study. Trials were conducted to recover the wastewater using three types of NF membranes. The results indicated that

the NF membrane process performed high efficiency of >99% for dye removal and NE-70 membrane showed better performance in terms of flux and separation than Desal-5 membrane. Turbidity, hardness, TOC and color of the treated water were less than 0.2 NTU, 60 mg/l as $CaCO_3$, 10 mg/l and 5 HU, respectively. It was concluded that it is feasible to recover 70% of the wastewater from the dyeing facility using a NF membrane process and the quality of the treated water could meet the requirements of dyeing process.

Ranganathan et al. (2007) studied recycling of wastewaters and analysis of the cost of water recovery for textile dyeing industries discharging effluents ranging between 80 and $200m^3$/t of production. Hypochlorite, the commonly used bleaching chemical is being gradually phased out by alkaline hydrogen peroxide solution that generates less effluent and fewer solids in the effluents. Coloring of yarn/cloth takes place in the presence of high concentration of sodium chloride or sodium sulphate (25–75 kg/m^3) in dye solutions. Dye bath wastewaters and wash waters are the process effluents of dyeing industry which are collected separately or together and follow the advanced treatment for maximum recycling of recovered waters. After treating the dye bath water by sand and nanofiltration (NF), the permeate is used in process for dye bath preparation and the reject of about 20–30% is sent to multi effect evaporator (MEE)/solar evaporation pond (SEP).Wash waters treated using a sequence of physicochemical and biological unit processes are passed into two stages reverse osmosis (RO) membrane systems and then the permeate is reused in the processes. The removal of total dissolved solids (TDS), chemical oxygen demand (COD), chloride and sodium were in the range of 80–97%, 91–97%,76–97% and 96%, respectively.

2.8 TREATMENT OF TEXTILE MILL WASTE WATER BY BIODEGRADATION

Polar organic pollutants in textile wastewaters may give rise to problems in biological wastewater treatment. For the most part they are non-biodegradable, and their elimination is incomplete. The behaviour of these pollutants was reported by Schrader et al. (1996). Biological, chemical and physicochemical wastewater treatment was followed with the help of substance-specific detection methods - liquid chromatography-mass spectrometry (LC-MS), flow-injection analysis-mass spectrometry (FIA-MS) and tandem mass spectrometry (MS-MS). No elimination was observed using biochemical and adsorptive procedures and there were insufficient results from the physico-chemical treatment.

Panswad and Luangdilok (2000) showed that the reactive dyes are problematic compounds in textile wastewaters as they are water-soluble and cannot be easily removed by conventional aerobic biological wastewater treatment systems. Anaerobic systems could reduce the color intensity more satisfactorily than the aerobic processes. However, the intermediate products are carcinogenic aromatic amines which need to be further decomposed by an aerobic treatment. An anaerobic/aerobic SBR system was used to treat a synthetic dye wastewater with glucose and acetic acid (1000 mg/l COD) as carbon sources, together with 20 mg/l of four different reactive dyes; i.e., bisazo vinylsulphonyl, anthraquinone vinylsulphonyl, anthraquinone monochlorotriazinyl and oxazine. The color reduction of the first three dyes was 63, 64 and 66%, respectively. More color removal was achieved in the anaerobic phase than in the aerobic step. The initial decolorization rate was 11.9, 0.37 and 0.48 SU/h for the first three dyes, respectively. Though the system comprised anaerobic and aerobic tanks, the color reduction did not rely on phosphorus accumulating organisms (PAOs).

59

Navarro et al. (2001) determined LC_{50} of the different process stages of the textile industry toxic discharges using bioassays with daphnids. The sensitivity of daphnids to chemicals was assayed using sodium dodecyl sulfate and was similar to other reports (14.6 ±6.8 vs 14.5±2.3 mg/l). All effuents from the five company samples were toxic in terms of LC_{50} and exhibited very high toxicity with acute toxicity unit (ATU) levels between 2.2 and 960, indicating that the five textile industries produced toxic water. The sensory characteristics indicated that the dyes contributed to overall sample toxicity at all process stages. The most toxic contaminant seemed to be ClO_2 at levels between 0.2 and 6.8 mg/l, suggesting that further research is needed on the economic costs of stage-by-stage and total effluent treatments.

Palaa and Tokat (2002) also indicated that due to the low biodegradability of many dyes and textile chemicals the biological treatment is not always successful in the treatment of cotton textile wastewater, in terms of color removal. A specific organic flocculant (Marwichem DEC), powdered activated carbon (PAC), bentonite, activated clay and commercial synthetic inorganic clay (Macrosorb) were directly added into the activated sludge laboratory pilot plant model. Before dosage, the optimum sludge retention time and hydraulic retention time were determined as 30 days and 1.6 days, respectively. The Monod kinetic constants were determined. Under these conditions the average COD removal was 94% and color removal was 36%. The addition of these materials did not change COD removal significantly. The most effective materials were found to be DEC and PAC for color removal. While the color removal efficiency for 120 mg/l DEC addition was 78%, it was 65% for 100 mg/l, 77% for 200 mg/l and 86% for 400 mg/l PAC addition.

Chang et al. (2002) applied a biological aerated filter (BAF) to treat textile wastewater. The performance of two lab-scale biofilters was monitored for 7 months to

compare the effect of natural zeolite with sand as media. Under organic load varying from 1.2 to 3.3 kg COD/m^3 day, the overall chemical oxygen demand (COD) reductions of the biofilter supported by natural zeolite and sand averaged 88 and 75%, respectively. Higher nitrogen removal in the biofilter with natural zeolite was attributable to its ion exchange capacity with NH_4^+. The results of cell counting showed that the numbers of nitrifying bacteria within the biofilm were higher on natural zeolite than on sand. Both biofilters were able to remove about 97% of suspended solids (SS) with loading of 1–3 kg SS/m^3 day. A pilot-scale BAF supported by natural zeolite with capacity to treat up to 12 m^3/day of textile wastewater was also monitored for 5 months. This system was able to remove about 99% biochemical oxygen demand, 92% COD, 74% SS, and 92% T-N with hydraulic load of 1.83 m^3/m^2 h.

Manu and Chaudhari (2003) reported the decolorization of simulated wastewater containing vat dye (C.I. vat blue 1: indigo) and azo dyes (Reactive blue H3R and Reactive red HE 7B) under anaerobic conditions using mixed bacterial cultures with long hydraulic retention times (HRT). Laboratory scale semicontinuous reactors were operated using simulated cotton dyeing wastewater at ambient temperatures (24-28 °C) by maintaining 10-day HRT for azo dyes and 5-day HRT for indigo dye. Influent dye concentration in wastewater was maintained at 100 mg/l and the reactors were operated for a period of 58 days. The performance of the bioreactors was evaluated by monitoring oxidation-reduction potential (ORP) in the reactor, color and chemical oxygen demand (COD) removal. COD removal of up to 95, 90 and 92% was achieved in a control (no dye), blue and red dye containing reactors. Color removal of 98-99% could be achieved in both the azo dye containing reactors. In the indigo dye containing reactor COD removal of 90% and color removal of up to 95% could be achieved.

Fongsatitkul et al. (2004) investigated the potential of biological treatment as a single process as well as in association with chemical oxidation to treat a textile wastewater. The experimental part incorporated the following three schemes: biological treatment only (stage 1), chemical oxidation prior to biological treatment (stage 2), and biological treatment followed by chemical oxidation (stage 3). Biodegradation was accomplished employing three identical sequencing batch reactors (SBRs), each having a liquid volume of 10 L, while chemical treatment involved the addition of Fenton's reagent in the range 25–300 mg/l, in a batch-type operation. Following an acclimation period of approximately 60 days, biological treatment resulted in a high percent reduction in chemical oxygen demand (COD), total Kjeldahl nitrogen (TKN), and total phosphorus (TP), and in a moderate decrease in color.

The impact of different redox mediators on color removal of azo dye model compounds and textile wastewater by thermophilic anaerobic granular sludge (55 $^{\circ}$C) was investigated by Santos et al. (2004) in batch assays. Additionally, a comparative study between mesophilic (30 $^{\circ}$C) and thermophilic (55 $^{\circ}$C) color removal was performed with textile wastewater, either in the presence or absence of a redox mediator. The present work clearly evidences the advantage of color removal at 55 $^{\circ}$C compared with 30 $^{\circ}$C when dealing with azo colored wastewaters.

Kapdan and Alparslan (2005) used a sequential anaerobic packed column reactor and an activated sludge unit operated continuously for treatment of a textile industry wastewater. Metal sponges were used as support material in anaerobic unit and pre-activated textile dyestuff biodegrading PDW facultative anaerobic bacterial culture was immobilized on the support particles. Effects of hydraulic retention times in anaerobic unit ($\theta_{Hanaerobic}$ = 12–72 h) and initial COD concentration (COD$_0$ = 3000±200

mg/l and 800±100 mg/l) at $\theta_{Hanaerobic} = 24$ h on color and COD removal performance of the system were investigated. The results indicated that over 85% decolorization and about 90% COD removal efficiency can be obtained up to $\theta_{Hanaerobic} = 48$ h but higher retention times causes decreasing in decolorization efficiency. Operating the system with real wastewater without adding any nutrients at $\theta_{Hanaerobic} = 24$ h resulted in over 60% improvement in color removal in studied wastewater compared to existing treatment plant.

A synthetic textile effluent containing an hetero-bireactive dye (Cibacron Red FN-R, 250 mg/l) was treated by coupling photo-Fenton process with an aerobic sequencing batch reactor (SBR). Montano et al. (2006) focused on the selection of suitable mild photo-Fenton conditions (Fe(II)/H$_2$O$_2$ reagents and irradiation time) that perform as a pre-treatment of a secondary biological treatment. Decolorisation (Abs$_{542.5}$), biodegradability enhancement (determined by BOD$_5$/COD index and respirometric methods) and dye degradation intermediates toxicity (Biotox1 technique) were the parameters employed to verify the chemical stage effectiveness. From different assessed photo-Fenton conditions, a Fenton reagent concentration of 20 mg/l Fe(II) and 250 mg/l H$_2$O$_2$, applied for an irradiation time of 90 min, was found to be an effective process to bio-compatibilize the studied wastewater. The SBR, working under steady conditions in a 24 h-cycle mode, made available an 80% COD removal in the combined oxidation system.

Sandhya and Swaminathan (2006) analyzed the kinetic of treatment of textile wastewater in hybrid column upflow anaerobic fixed bed reactor. Treatment of textile wastewater is considered to be difficult by traditional systems. The present study is related to treatment of textile wastewater in an anaerobic reactor. The study showed the

effectiveness of biological treatment of wastewater involving appropriate microorganism and suitable support media in a hybrid column, upflow anaerobic fixed bed (UAFB) reactor. COD and color were reduced to 84.80%, and 90% for textile wastewater. The reactor was operated at $1.038–8.21$ g COD/m^{3}d^1 of loading and found that 81.58% COD and 86.22% color removal at the highest loading rate. At steady state under anaerobic condition, color was effectively removed.

The effects of a reductant and carbon source on the decolorization of the disazo dye C.I. Reactive Black 5 and real textile wastewater were reported by Kim et al. (2006) in an anaerobic sludge system. The color removal without sulfide was about 94% at 35 °C during 72 h. The intermittent addition of sulfide (10 mg/ll) led to an increase in the microbial decolorization of more than 9% during 48 h in comparison with the case where no sulfide was added. In the treatment of real textile wastewater, the unsatisfactory removal of COD (57.8%) and color was obtained during 12 h, due to the lack of readily degradable COD for the azo dye decolorization and the toxic effect of the wastewater.

Sirianuntapiboon and Srisornsak (2007) reported the removal of disperse dyes from textile wastewater using bio-sludge. Granular activated carbon (GAC) did not show any significant adsorption ability on the disperse dyes, while resting (living) biosludge of a domestic wastewater treatment plant showed high adsorption abilities on both disperse dyes and organic matter. The dye adsorption ability of bio-sludge increased by approximately 30% through acclimatization with disperses dyes, and it decreased by autoclaving. The deteriorated bio-sludge could be reused after being washed with 0.1 N NaOH solutions. Disperse Red 60 was more easily adsorbed onto the bio-sludge than Disperse Blue 60. The GAC–SBR system could be applied to treat

textile wastewater (TWW) containing disperse dyes with high dye, BOD_5, COD, and TKN removal efficiencies of $93.0 \pm 1.1\%$, $88.0 \pm 3.1\%$, $92.2 \pm 2.7\%$ and $51.5 \pm 7.0\%$, respectively without any excess bio-sludge production under an organic loading of 0.18 kg $BOD5/m^3$ d.

In view of easy availability of the plant and high demand of seed gums throughout the world, the investigations were carried out by Sanghi et al. (2007) for possible exploitation of Ipomoea seeds as potential source of commercial gum. Graft co-polymerization with acrylamide was done to modify the seed gums for the favourable properties. The aqueous solutions of three highly colored different anionic dyes (reactive, acid and direct dye) were taken for decolorization studies. Although synthetic polyelectrolytes like PAC provide better dewatering characteristics in the sludge produced, their long-term effects on human health is not well understood. The role of natural seed gums and their grafted co-polymer on color removal was investigated by comparing two treatments: (i) PAC alone and (ii) PAC/seed gum in combination. The seed gums and their grafted co-polymers were found to be good working substitutes alone as well as in conjunction with a very low dose of PAC, for the decolorization of the dyes in varying ratios. Compared to PAC alone treatment, the use of seed gum as coagulant aids in combination with PAC was highly efficient in color removal. The results indicate that the use of seed gums as aids with PAC could be a very beneficial system in dye wastewater treatment.

Chapter-3

EXPERIMENTAL PROGRAMME
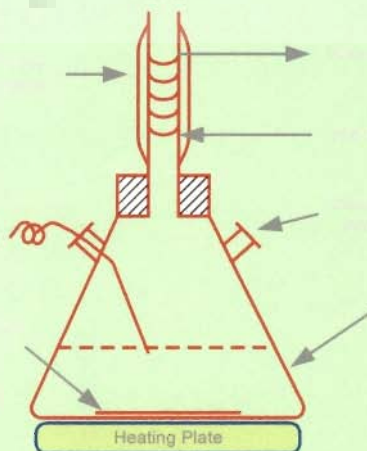
Chapter – 3

EXPERIMENTAL PROGRAMME

This chapter deals with the experimental set-up, materials, analytical procedures adopted during the experimental studies on the treatment of textile mill effluent. The treatment steps include catalytic thermolysis and coagulation. In addition, studies on settling characteristics and filterability of the treated waste were also carried out.

3.1 EXPERIMENTAL SETUP

3.1.1 Catalytic Thermolysis

The experimental studies were carried out in a 0.5 l three-necked glass reactor. Initially, the pH of the wastewater was adjusted by adding 0.1 N HCl or 0.1 N NaOH solution and then the wastewater was shifted to the three-necked glass reactor as shown in Figure 3.1. Thereafter, the catalyst/ coagulant/ chemical was added to the solution. The temperature of the reaction mixture was raised using a hot plate to the desired value and maintained by a P.I.D. temperature controller, which was fitted in one of the necks through the thermocouple. The raising of the temperature of the wastewater from ambient to 95 °C took about 30 min (t_h). A vertical water-cooled condenser was attached to the middle neck of the reactor to prevent any loss of vapor. The time taken to attain the desired temperature is the heating time, t_h. Further heating was done at the desired temperature and the time was measured by subtracting t_h from the total time. The reaction mixture was agitated using a magnetic stirrer. Experimental runs with different chemicals (catalysts) were conducted at 95 °C and the reactor samples were taken at periodic intervals. The samples were centrifuged to decant the

supernatant. Then, the supernatant was tested for the COD and color. The final pH of the solution after the reaction was also observed. After completion of the run, the effluent was allowed to cool down and settle for 2 h. The treated effluent including sludge was then rapidly mixed and the slurry so formed was used to study the settling and filterability characteristics of the sludge.
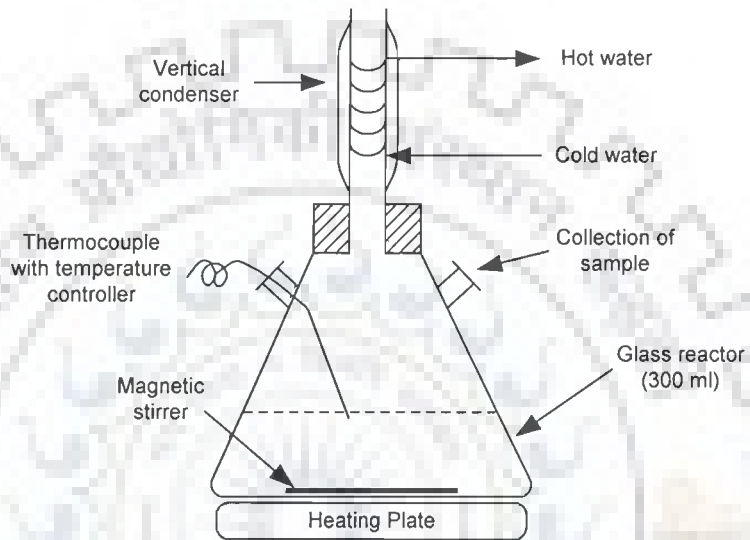
Figure 3.1. Experimental setup for catalytic thermolysis

3.1.2 Coagulation (Jar Test)

Jar tests have been used to evaluate the effectiveness of various coagulants and flocculants under a variety of operating conditions for wastewater treatment. Jar tests are used in these procedures to provide information of the most effective flocculant, optimum doses, effect of dosage on removal efficiencies and effect of settling times. In the jar test procedure, various coagulants such as commercial alum, aluminum potassium sulfate, PAC, $FeCl_3$, $FeSO_4$ have been used in a six jar tester as shown in Fig. 3.2. The result of this procedure can help optimize the performance of the best coagulant.

67
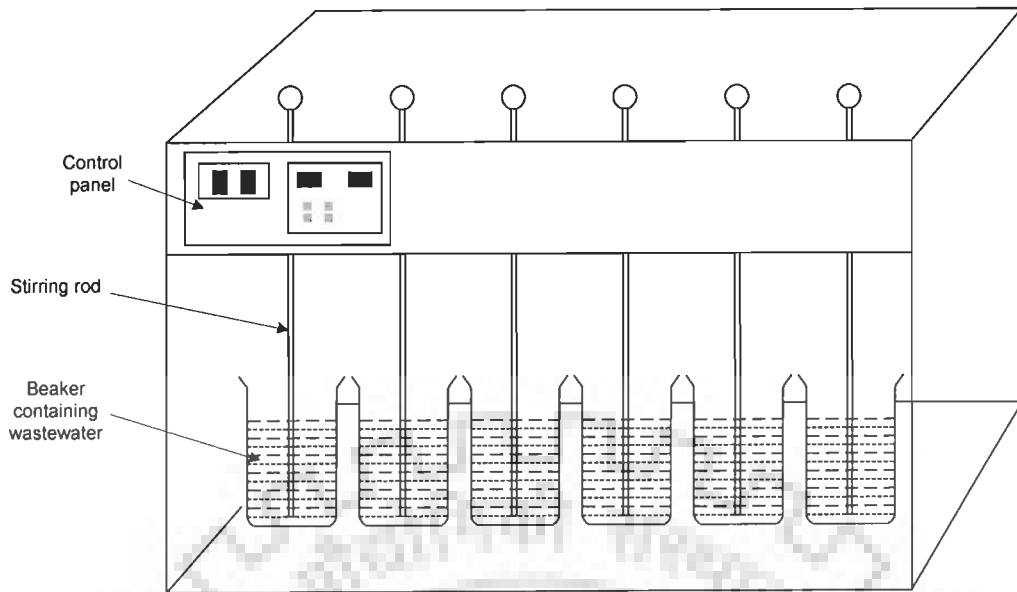
Fig. 3.2 Jar test

The procedure comprised of the following steps :

- The runs at ambient temperature were taken in a 0.5 l beaker.

- The wastewater was put into the beaker after adjusting the desired pH and at the same time the coagulant/ chemical was added to the beaker.

- The reaction mixture was agitated for 30 min at slow speed and for next 30 min rigorously using a paddle agitator. The wastewater was then allowed to settle for 2 h.

- Thereafter a small amount of sample was taken out to determine the color and COD of the treated sample.

- The solution left was again mixed rapidly for 5 min to make it a homogeneous solution and then it was examined for the settling and filterability characteristics.

The flow chart of the coagulation/thermal pretreatment is shown in Figure 3.3.
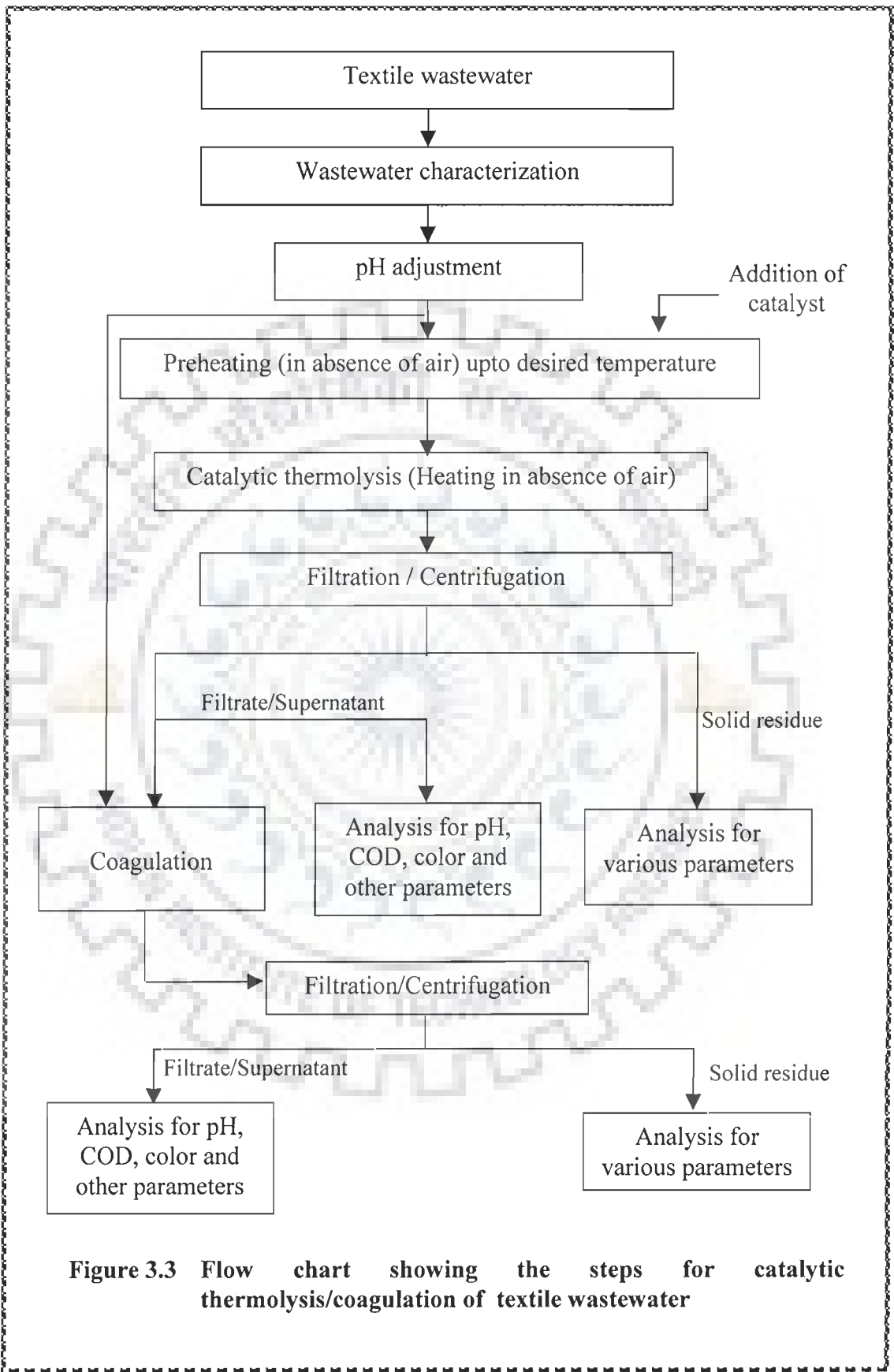
Figure 3.3 Flow chart showing the steps for catalytic thermolysis/coagulation of textile wastewater

3.2 MATERIALS

3.2.1 Wastewater Sample

The textile mill wastewater was obtained from a textile mill in Ghaziabad (U.P.) India and stored at a low temperature (3-4 $^{\circ}$C) in a freezer. The samples of effluents were analyzed as per Standard Methods (APHA, AWWA and WPCF, 1989) and other relevant methods, as described later. Typical analyses of the effluents are presented in Table 3.1.

Table 3.1 Typical composition of textile mill wastewater

Parameters	Composite wastewater	Dyeing wastewater	Desizing wastewater	Printing wastewater	Mercerizing wastewater
pH	9.1	10.3	4	7.17	11.86
Total Suspended Solids (TSS)	964.81	152.1	56.7	6.7	29.7
Total Dissolved Solids (TDS)	1698	325	126	-	-
COD	1960	5744	2884	392	62
BOD$_3$	420	1525	1075	51	97
COD/BOD ratio	4.67	3.77	2.68	7.69	0.64
Oil and Grease	221.29	62.4	145.9	1.42	18.1
Total iron (as Fe)	1.81	0.447	2.37	0.63	0.296
Phenolics as C$_6$H$_5$OH	Not detectable	Not detectable	Not detectable	Not detectable	Not detectable
Lead (as Pb)	Not detectable	Not detectable	Not detectable	Not detectable	Not detectable
Chlorides (as Cl)	650	60	950	550	544.43
Sulphates (as SO$_4^{2-}$)	164.47	306.74	520.94	135.17	200.16
Copper (as Cu^{2+})	0.653	0.046	0.038	0.013	0.014
Mercury (as Hg)	Not detectable	Not detectable	Not detectable	Not detectable	Not detectable
Nickel (as Ni)	Not detectable	Not detectable	Not detectable	Not detectable	Not detectable
Chromium (as Cr)	Not detectable	Not detectable	Not detectable	Not detectable	Not detectable
Manganese (as Mn^{2+})	0.46	-	0.64	0.141	-
Zinc (as Zn^{2+})	0.116	0.048	0.364	0.155	0.057
Turbidity (NTU)	480	191	207	193	143
Color	Blue	Orange	Light brown	Off-white	Colorless
Pt-Co Method	2250	3840	520	-	-

Note: All the values except pH and turbidity are in mg/l

3.2.2 Chemicals

The chemicals used as catalysts and as coagulants were of analytical reagent grade. Copper sulphate ($CuSO_4.5H_2O$), copper oxide (CuO) and potassium dichromate ($K_2Cr_2O_7$) were procured from S.D. Fine Chemicals Ltd., Mumbai, India, whereas, zinc oxide (ZnO), ferric chloride ($FeCl_3$) and ferrous sulphate ($FeSO_4.7H_2O$) were obtained from Qualigens Fine Chemicals, Mumbai, India. Ammonia solution, silver sulphate (Ag_2SO_4), mercury sulphate ($HgSO_4$) and aluminum potassium sulphate [$KAl(SO_4)_2.16H_2O$] were procured from Ranbaxy Fine Chemicals Ltd., Mumbai, India and PAC [$Al_2(OH)_nCl_{6-n}]_m$, with n = 2-5 and m = 4-10 was obtained from Vam Organics Ltd., Gajraula, U.P., India. Commercial alum [$Al_2(SO_4)_3.nH_2O$] was obtained from local market.

3.3   ANALYSIS OF RAW EFFLUENTS AND TREATED EFFLUENTS

The COD of the sample was determined by the standard dichromate reflux method using a Photometer and a digester (Aqualytic, Germany). The BOD of the samples was determined by incubating the seeded sample for 3 days at $27^{o}C$ following the method prescribed by the MOEF. The elemental (C, H, N and S) analysis was done using an elemental analyzer model Vario EL III (Elementar, Germany). The ash content was evaluated by combustion in a muffle furnace at 925 ^{o}C for 7 min. The amount of metal ions leached out in the solution and those fixed in the solid residue were determined by using an atomic absorption spectrometer (model Avanta; GBC, Australia). Thermal analyses (TGA/DTGA/DTA) of the wastewater and residue left after the treatment were carried out using a TG analyzer Perkin Elmer (Pyris Diamond). Color of textile wastewater was determined by color meter (Hanna Instruments, Singapore).

3.3.1 Biological Oxygen Demand

The method of BOD determination as prescribed by the Central Pollution Control Board, Delhi and the Ministry of Environment and Forests is different in terms of the time and temperature of incubation. This method is detailed below :

Apparatus

1. BOD bottles of 300 ml capacity

2. BOD Incubator - controlled at 27 $^{\circ}$C

Reagents

1. Phosphate buffer solution : Dissolve 8.5 g KH_2PO_4, 21.75 g K_2HPO_4, 33.4 g $Na_2HPO_4.7H_2O$ and 1.7 g NH_4Cl in about 500 ml distilled water and dilute to 1 L. The pH should be 7.2.

2. Magnesium sulfate solution : Dissolve 22.5 g $MgSO_4.7H_2O$ in distilled water and dilute to 1 L.

3. Calcium chloride solution : Dissolve 27.5 g $CaCl_2$ in distilled water and dilute to 1 L.

4. Ferric chloride solution : Dissolve 0.25 g $FeCl_3.6H_2O$ in distilled water and dilute to 1 L.

5. Sodium sulphite solution (0.025 N) : Dissolve 1.575 g Na_2SO_3 in 1000 ml distilled water. This solution is not stable, therefore it should be prepared daily.

Procedure

The required volume (4 liters) of distilled water was aerated in a container by bubbling compressed air for 1-2 days to attain DO saturation. Then 4 ml each of phosphate buffer, magnesium sulfate, calcium chloride and ferric chloride solutions

were added to 4 liters of dilution water and the mixture was mixed. The seed source from the domestic sewage was added to provide the population of microorganism for oxidizing the biodigester organic matter. The pH of the sample was maintained at around 7.0. 1 liter was siphoned out as blank and 3 bottles were filled with the blank in order to measure the O_2 consumption in dilution water. Then 3 liters were simultaneously siphoned out into separate measuring cylinders and 1ml, 3ml and 5ml of the effluent solution (untreated or treated) were added to the separate 1 liter solutions to obtain 1%, 3% and 5% diluted samples. The 1%, 3% and 5% diluted solutions were siphoned off immediately into 3 labeled bottles, each 1 bottle was kept for determining the initial DO and the other 2 DO bottles were incubated at 27 °C for 3 days. DO in the sample and the blank was determined on the initial day and after 3 days.

Calculation:

$$BOD \text{ in mg/L} = \frac{\text{DO consumed in the test by the diluted sample} \times 200}{\% \text{ of dilution}}$$

3.3.2 Chemical Oxygen demand (COD)

COD is the amount of a specified oxidant that reacts with the sample under controlled conditions. To examine the COD's of the effluent waters an AQUALYTIC COD reactor and ET 100 (a direct reading spectrophotometer) were used. The oxidant measured is the dichromate ion $(Cr_2O_7^{2-})$ reduced to the chromic ion (Cr^{3+}). The dichromate ion are strongly absorbed at 400 nm but nearly zero at 600 nm. The chromic ion has its strongest absorbance at 600 nm thus allowing measurement of the reduction from the dichromate to the chromic ion. Pre-prepared solutions of the COD solution were obtained from AQUALYTIC Company (Germany).

73

The COD reactor was preheated to 150 °C. The sample vials were prepared as the reactor was getting heated. The COD digestion reagent vials used came in three concentrations. The first set read 0-150 mg/l, second 0-1500 mg/l and the third set read 0-15000 mg/l. To prepare the 0-150 and 0-1500 mg/l vials 2 ml of each sample was added to its own vial. The 0-15000 mg/l vials only required 0.2 ml because each vial contained a built-in dilution factor of ten. The vials containing the samples were sealed tightly and shaken. They were then put into the heated COD reactor and allowed to digest for two hours. At the end of two hours, the vials were cooled and read in the spectrophotometer. The spectrophotometer-stored programs were used to read the vials. Wavelength 430 nm was used to read low range COD's and for high range COD's, a wavelength of 605 nm is used. These programs take the amount of absorption and insert it into an internal calculation to determine mg/l of COD. The spectrophotometer was first zeroed with a blank that contained de-ionized water with the digestion solution. Each sample's exterior was wiped clean and read with results recorded in mg/l COD.

3.3.3 Color

HANNA (Singapore) made colorimeter was used for true and apparent color test runs on the textile effluent samples. True color refers to filtered water in which the turbidity has been removed, whereas apparent color refers to the untreated water. A filtering apparatus consisting of Millipore 0.45-micron membrane filter, filter holder, filter flask, and a suction pump was assembled to test the true color or apparent color of the samples. A similar volume of de-ionized water was also filtered and used as a blank for analysis. The filtered samples were then put into vials that were compatible with the vial receptacle of the HI 93727 which was used to analyze the samples. Color of the

samples was read at a wavelength of 470 nm. The exterior of the sample vials was wiped clean and then inserted into the colorimeter. The blank was inserted first in order to adjust the reading of the colorimeter to zero. Each sample was read and the results were recorded in platinum-cobalt units (PCU).

3.3.4 Total Suspended Solids

The total suspended solids (TSS) concentration was determined by filtration of the water samples. Each sample was filtered through Millipore 0.45-micron filters. Each filter was weighed to obtain the initial weight. The filters containing the particulates were put into a 50 °C oven overnight to allow them to dry. At the end of 24 h, the filters were weighed again to obtain the dry weight of the filters. The initial weight was subtracted from the dry weight to determine the TSS. The TSS was recorded in mg/l units.

3.3.5 Analysis of Solid Residue

The proximate analysis of the sludge produced during the coagulation and catalytic thermolysis step and the dried sample of textile mill wastewater was carried out as per procedure laid down in IS: 1350 (Part – I) – 1984. The moisture content, ash, volatile solids and fixed carbon in the solid residue were determined. The procedure of proximate analysis is given in next section.

Elemental analysis for C, H, N and S was carried out by using Elementar Vario EL III (Elementar Analysensysteme GmbH, Germany). The heating value of the precipitated sludge was determined by preparing a suitable pellet and combusting it in a standard adiabatic bomb calorimeter (Karr, 1978).

Thermo-gravimetric analysis (TGA) of the residue left after the treatment was carried out at the Institute Instrumentation Centre, IIT, Roorkee using TGA analyzer

from Perkin Elmer (Pyris Diamond). In the present study, the weight changes in the solid residues were continuously monitored due to drying, volatilization and gasification, as the sample followed a linear heating program. DTA and DTG curves were also recorded continuously in terms of weight % loss per minute and temperature difference in mV (which could be converted as per calibration chart to obtain temperature difference between the alumina sample and solid residue at any temperature under temperature programmed heating (from 0 to 100 K/min). In the present study, the operating pressure was kept slightly positive, the purge gas (air) flow rate was maintained at 300 ml/min (in some runs 200 ml/min). The sample was uniformly spread over the crucible base in all the experiments and the quantity of sample taken was about 10 mg in all the runs.

The concentration of metal ions in the sludge and the solution was determined using an atomic absorption spectrometer (AAS) (Avanta GBC, Australia). The FTIR spectra of the dried black liquor and solid residue formed after the pretreatment with copper sulfate and commercial alum were recorded on a FTIR Spectrometer (Thermo Nicolet, USA, Software used: NEXUS) in the 4000 – 500 cm^{-1} wave number range using KBr pellets.

3.3.6 Procedure for Proximate Analysis

The proximate analysis of textile mill wastewater and solid residues formed as a result of catalytic thermolysis /coagulation was done according to the IS-1350 (Part-I)-1984. The parameters determined during the proximate analysis include moisture content, volatile matter, ash and fixed carbon. Volatile matter, ash and fixed carbon are calculated on "air dried" basis. The methods of determining the above mentioned parameters are as follows:

1. **Moisture content:** The moisture content of the sample was determined by a two stage method. In this procedure, the sample is first applied to the air-drying followed by oven drying at $108 \pm 2\ ^{o}C$ temperature. During the air-drying period, the drying is assumed to be complete when the loss in mass during an hour is less than 0.1% of the sample. The total moisture content of the original sample is calculated according to the following formula:

   Total moisture content of the original sample = X + Y [1- (X/100)]

   where, X = percentage loss in mass of the original sample in air drying

   Y = percentage loss in mass of the air dried sample on oven drying

2. **Volatile matter:** Volatile matters present in a dried sample are determined by heating the sample in an air free atmosphere at $925\ ^{o}C$ for a period of 7 min. The test is conducted in a cylindrical silica crucible with a well fitting lid. The volatile matter was determined from the equation:

   Volatile matter (%) = $[(M_3 - M_2)\ /(M_2 - M_1)]$ x 100

   where, M_1 = Mass of the empty crucible with lid

   M_2 = Mass of crucible + sample before heating

   M_3 = Mass of crucible + sample after heating

3. **Ash:** The sample is heated at $500\ ^{o}C$ in 30 min and then from 500 to $815\ ^{o}C$ for a further 30 to 60 min in the presence of air and then this temperature is maintained until no further change in mass takes place.

   In mathematical form,

   Ash (%) = $[(M_4 - M_1) - (M_2 - M_1)]$ x 100

   where, M_1 and M_2 are the same as defined above,

   M_4 = Mass of crucible + sample after heating in the presence of air

4. **Fixed carbon:** Fixed carbon is calculated by deducting from 100 the sum of the moisture content, volatile matter and ash, expressed as percent.

   Fixed carbon (%) = 100 – (Moisture content + Volatile matter + Ash)

Table 3.2 **Analytical techniques/instruments used for the determination of various parameters**

Sl. No.	Parameter	Analytical Technique/Method
1.	pH	Digital pH meter with combined electrode
2.	Total Suspended Solids (TSS)	Total suspended solid dried at 50 ^{o}C
3.	Total Dissolved Solids (TDS)	Total dissolved solids dried at 108°C (APHA 2540-D)
4.	COD	Closed reflux colorimetric method (APHA 5220-D)
5.	BOD_3	Incubation method, 27°C, 3 days (IS:3025)
6.	Oil and Grease	Partition-Gravimetric method (APHA 5520-B)
7.	Total iron (as Fe)	Atomic Absorption Spectrometric Method (APHA 3111-B)
8.	Chlorides (as Cl)	Argentometric method (APHA 4500-B)
9.	Sulphates (as SO_4^{2-})	Turbidimetric method (APHA 4500-E)
10.	Copper (as Cu^{2+})	Atomic Absorption Spectrometric Method (APHA 3111-B)
11.	Manganese (as Mn^{2+})	Atomic Absorption Spectrometric Method (APHA 3111-B)
12.	Zinc (as Zn^{2+})	Atomic Absorption Spectrometric Method (APHA 3111-B)
13.	Turbidity (NTU)	Nephelometric Method (APHA 2130-B)
14.	Color, Pt-Co Method	Colorimeter
15.	CHNS	CHNS analyzer
16.	Heating value of residue	Bomb calorimeter
17.	Oxidation characteristics of residues	TGA/DTA analyzer
18.	Functional groups	FTIR Spectrometer

Chapter-4

RESULTS AND DISCUSSION
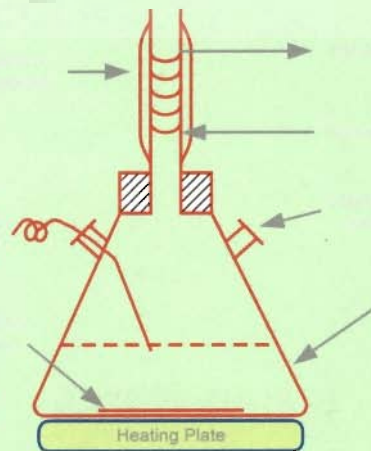
Chapter – 4

RESULTS AND DISCUSSION

4.0   GENERAL

The thermo-chemical precipitation (or catalytic thermolysis) undergoes complex reactions over the reaction time, thereby affecting the pH of the reactor mass. The compounds probably undergo hydrolysis to a limited extent with the formation of small amounts of lower carboxylic acids. This leads to the change in the pH. Complexation of the organics with metal catalyst making them insoluble and thereby precipitating the organics seems to play a major role in COD reduction.

The wastewaters viz., composite, dyeing and desizing wastewaters, were filtered, using the ordinary filter paper. Some color was removed during the filtration, adhering and adsorbed on the filter. The filtrate was used for further treatment.

4.1   TREATMENT OF COMPOSITE WASTEWATER OF A COTTON TEXTILE MILL BY CATALYTIC THERMOLYSIS AND COAGULATION

The experiments were planned to treat the undiluted composite wastewater (COD_0 = 1960 mg/l) by catalytic thermal treatment followed by coagulation. The catalyst used during catalytic thermolysis were $CuSO_4$, $FeSO_4$, $FeCl_3$, CuO, ZnO and poly aluminum chloride (PAC) whereas the coagulants used in the subsequent process included commercial alum, aluminum potassium sulfate, PAC, $FeCl_3$ and $FeSO_4$. The two processes (catalytic thermolysis and coagulation) were optimized with respect to the process parameters, such as, pH, catalyst/coagulant concentration, etc.

4.1.1 Catalytic Thermolysis

4.1.1.1 Effect of Initial pH (pH_0)

Figure 4.1(a) shows the effect of pH_0 at 25 $^{\circ}$C on the COD and color reduction of composite wastewater by catalytic thermolysis using various catalysts, such as $CuSO_4$, $FeSO_4$, $FeCl_3$, CuO, ZnO, PAC and without catalyst at a C_w of 6 kg/m^3. Different pH_0 values maintained during the experiments were 2, 4, 6, 8, 10 and 12, and the reaction was conducted at 95 $^{\circ}$C for 4 h. A portion of the resulting mixture after treatment was taken out and centrifuged for 10 min at a speed of 10000 rpm. The supernatant was separated and its COD was measured. The figure shows an identical trend of increasing percent COD reduction with increase in the value of pH_0 from 1 to 12 for all the catalysts. The reduction in COD was faster upto pH 8 in comparison to rate of reduction in the pH range 8-12. A maximum COD reduction of 77.9% was obtained using $CuSO_4$ as catalyst at pH 12. The final pH after the treatment were also measured and a decrease in pH was observed in all the cases. The reduction in pH after the treatment has been shown in Table 4.1. The decrease in pH may be due to the dissociation of the sulfurous and chlorine bearing compounds into sulphate/chloride ions, as the case may be, and also the formation of lower carboxylic acids. The sulphate/chloride ions after combining with H$^+$ ions present in wastewater form H_2SO_4/HCl which reduce the pH of the solution. The carboxylic acids are formed from the degradation of high molecular weight hydrocarbons. The pH_0 adjustment of the composite waste has been found to reduce the COD of the solution. A value of pH 12 yielded in a precipitation of the solution (at room temperature) with about 22% COD reduction in the supernatant. When the composite waste at pH 12 was thermally heated without any catalyst, the COD decrease observed was 34.5%. This clearly shows that the thermal pretreatment has better effect on precipitation than the change in pH.

80

Table 4.1 pH change after the treatment of composite wastewater with/without catalyst at 95 °C for 4 h

pH_0	Final pH (pH_f) after treatment with						
	$CuSO_4$	$FeSO_4$	$FeCl_3$	CuO	ZnO	PAC	Without catalyst
2	1.95	1.65	1.85	1.13	1.72	1.62	1.98
4	3.65	2.94	3.14	3.36	3.75	3.83	3.95
6	5.42	5.92	5.64	5.86	5.57	5.62	5.90
8	8.54	7.95	7.62	7.73	7.54	7.86	7.98
10	9.02	9.12	9.24	9.92	9.64	9.57	9.99
12	10.96	10.54	10.74	10.54	11.64	11.52	11.85

Figure 4.1(b) shows the effect of different catalysts at varying pH_0 on percent color reduction of composite wastewater. The reaction conditions were the same as in the previous case. For all the catalysts the percent color reduction increases with an increase in pH_0. The increase was fast at lower pH_0, whereas for $pH_0 > 10$. the color reduction was nearly constant. The reduction in COD without catalyst was much lower than that observed with a catalyst. $CuSO_4$ is found to be the best catalyst giving 92.85% color reduction at pH_0 12.
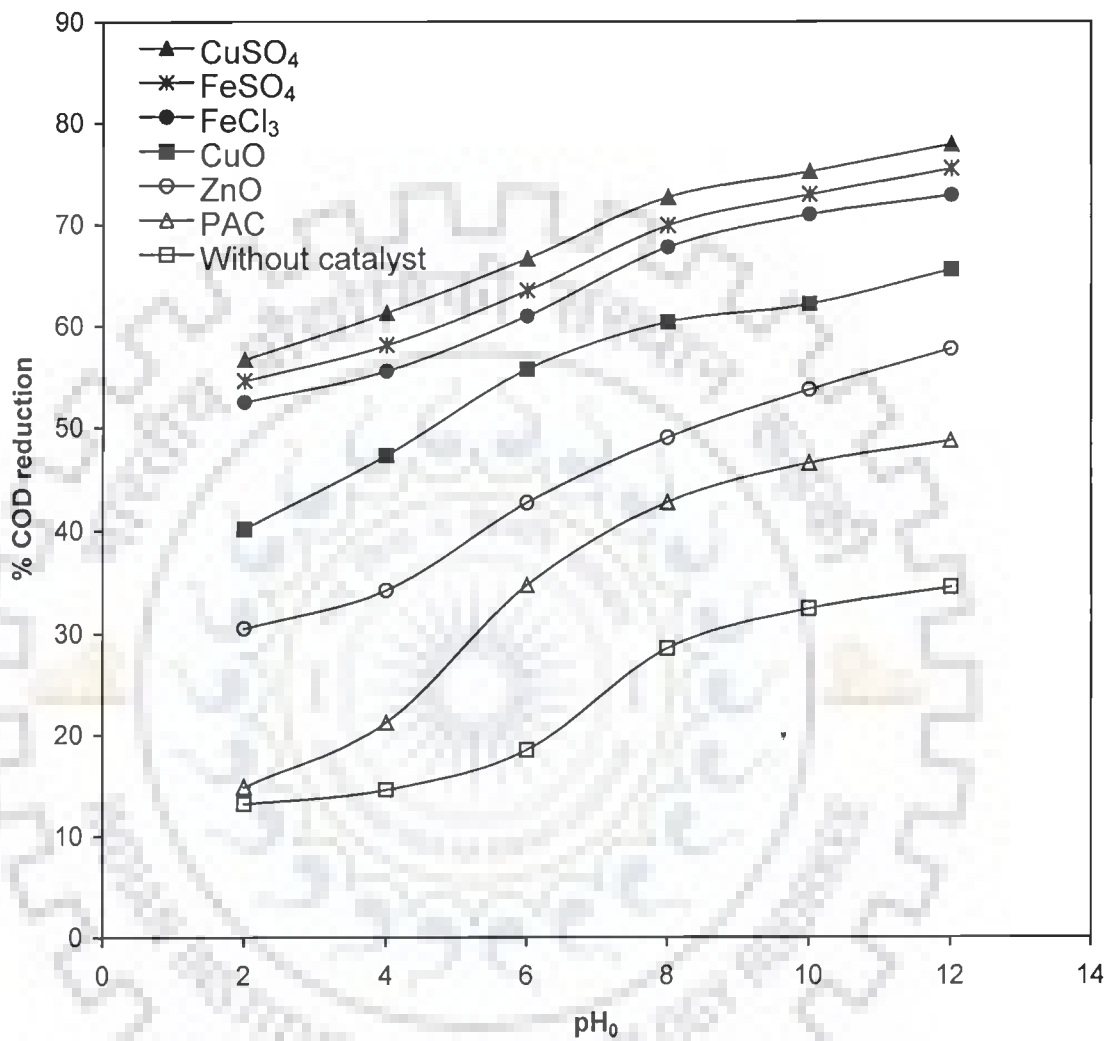
Figure 4.1(a) Effect of pH_0 on COD reduction of the composite wastewater by catalytic thermolysis

COD$_0$ = 1960 mg/l, T_R = 95°C, P = atmospheric, t_R = 4 h,

C_w = 6 kg/m^3

Figure 4.1(b) Effect of pH_0 on color reduction of the composite wastewater by catalytic thermolysis

COD_0 = 1960 mg/l, T_R = 95°C, P = atmospheric, t_R = 4 h,

C_w = 6 kg/m^3, Initial color concentration = 2250 PCU

4.1.1.2 Effect of temperature

Figure 4.2(a) shows the effect of treatment temperature on the COD and color reduction at pH_0 12. The concentration of $CuSO_4$ catalyst was 2 kg/m^3 and the temperature varied from 60 °C to 95 °C. The increase in temperature does not increase the reduction in color appreciably. The reduction in COD, however, was found to increase with temperature, giving a maximum of 72.9% reduction at 95°C. The maximum color removal at these conditions was 85.5%. The higher percentage removal of color in comparison of COD removal may be attributed to the ease in hydrolysis of molecules present in the dye and thereby disappearance of the color.

Figure 4.2(b) presents the COD reduction as a function of treatment temperature and time. For all the temperatures, a treatment time of 4 h seems to be the optimum. The values of COD removal corresponding to zero treatment time are indicative of the COD reduction during attainment of the desired treatment temperature. It is observed that the COD reduction gradually increases with time up to 240 min and thereafter there is no further increase. In all further studies on the effect of different process parameters, the treatment time was kept fixed at 4 h. An identical phenomenon has also been observed in the case of treatment of dyeing (Figure 4.13b) and desizing wastewaters (Figure 4.24).
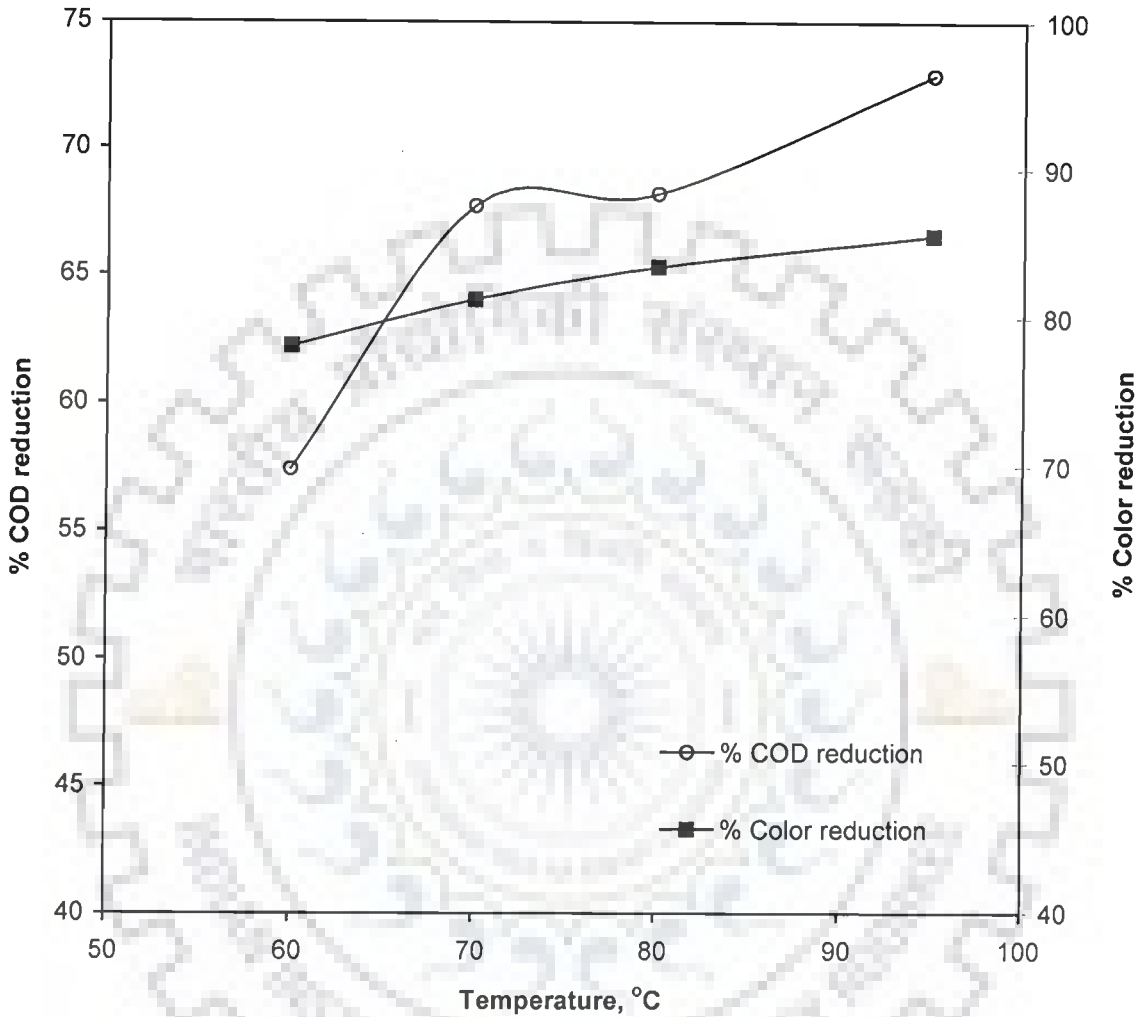
Figure 4.2(a) Effect of temperature on COD and color reduction of the composite wastewater by catalytic thermolysis with copper sulphate. $COD_0 = 1960$ mg/l, $t_R = 4$ h, P = atmospheric, $pH_0 = 12$, $C_w = 2$ kg/m^3, Initial color concentration = 2250 PCU
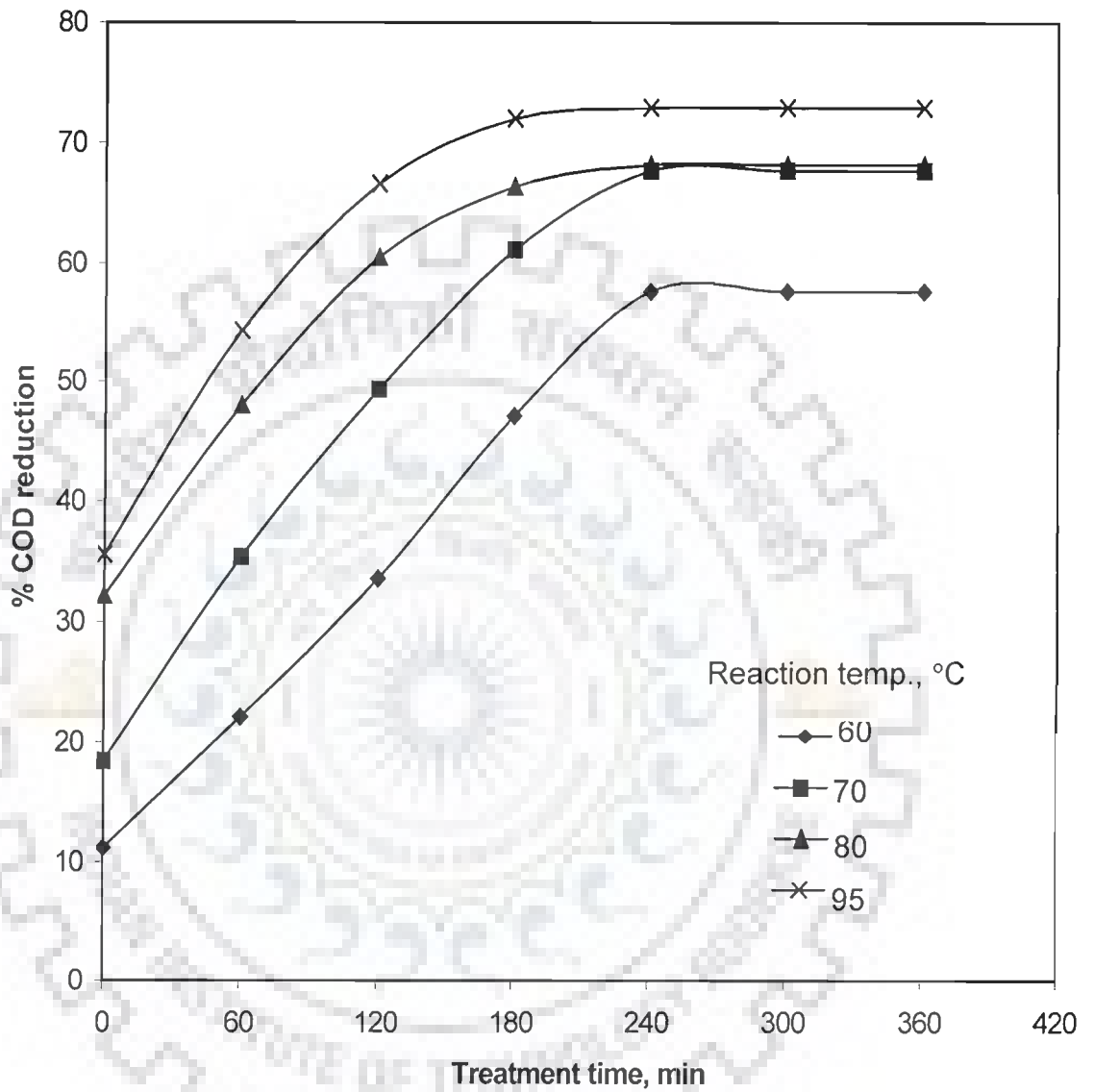
Figure 4.2(b) Effect of temperature on COD reduction of the composite wastewater by catalytic thermolysis

COD_0 = 1960 mg/l, t_R = 4 h, P = atmospheric pressure, pH_0 = 12, C_w = 2 kg/m³, catalyst = copper sulphate

4.1.1.3 Effect of Catalyst Mass Loading (C_w)

The effect of catalyst mass loading on the COD as well as color reduction of composite wastewater ($COD_0 = 1960$ mg/l and initial color $= 2250$ PCU) was observed during catalytic thermolysis at 95 °C for 4 h as shown in Figure 4.3. $CuSO_4$, being the best among all the catalysts, was chosen for further studies. The C_w was varied from 1 to 12 kg/m^3 while the pH_0 was adjusted at 12 for all the experimental runs. With $C_w = 1$ kg/m^3, a 62.5% reduction in COD was observed which increased to 77.9% at $C_w = 6$ kg/m^3. Further increase in C_w did not increase the COD reduction. The color reduction under similar conditions increased from 83.65% at $C_w = 1$ kg/m^3 to 92.85% at $C_w = 6$ kg/m^3.

4.1.2 Coagulation

Figure 4.4(a-b) shows the COD and color reduction during coagulation of the fresh composite wastewater. The coagulants used included aluminum potassium sulphate, commercial alum, $FeSO_4$, $FeCl_3$ and PAC. A general trend of increase in COD reduction with an increase in pH_0 (from 2 to 12) was observed. The major increase was from pH_0 4 to pH_0 10. PAC and $FeSO_4$, however, did not follow this trend. The curve showing COD reduction without any coagulant, however, shows 48.9% reduction only. By pH adjustment, the decrease in COD is much higher under alkaline conditions that that under acidic condition. A similar trend was also observed for color reduction with PAC and $FeSO_4$.

Aluminum potassium sulphate was found to be the best coagulant giving 84-88% COD reduction and about 95% color reduction at pH_0 8. Figure 4.5 depicts the effect of coagulants dose (C_w) on COD and color reduction of the composite waste at pH_0 8. For a number of coagulants, pH_0 8 happens to be the optimum pH for both COD

and color reduction. The results in Figure 4.5 show a sharp increase in COD and color reductions with an increase in coagulant dose from 1 to 5 kg/m^3. Beyond this, there was almost no change in COD and color. Coagulant dose of 5 kg/m^3, may thus be called as the critical coagulant concentration (CCC). At coagulant dose of 5 kg/m^3 and $pH_0 = 8$, the maximum COD and color reduction were 88.62% and 95.4%, respectively.

4.1.3 Catalytic Thermolysis followed by Coagulation

In another series of experiments catalytic thermolysis was followed by coagulation. The coagulation (using aluminum potassium sulphate) was done to the supernatant obtained from the catalytic thermolysis (using $CuSO_4$). Figure 4.6 depicts the COD and color reductions and compares the results of coagulation with/without catalytic thermolysis. Coagulation has significant effect on increasing the removal of COD and color when applied after catalytic thermolysis. An COD reduction of 97.3 % is achieved when the supernatant of the thermally treated effluent is subjected to coagulation. Color reduction in the treated effluent was nearly 100%. The results, thus, show that the catalytic thermolysis (using $CuSO_4$) followed by coagulation (using aluminum potassium sulphate) is the most effective method of treatment of composite wastewater of a cotton textile mill. The COD and color in the final treated effluent were 11.7 mg/l and non-detectable color, respectively. The COD/BPD_3 ratio was 1.67. Both these values are within the range prescribed by Central Pollution Control Board, India. It may be noted that an effluent to become biodegradable, COD/BOD_3 must be less than 2.
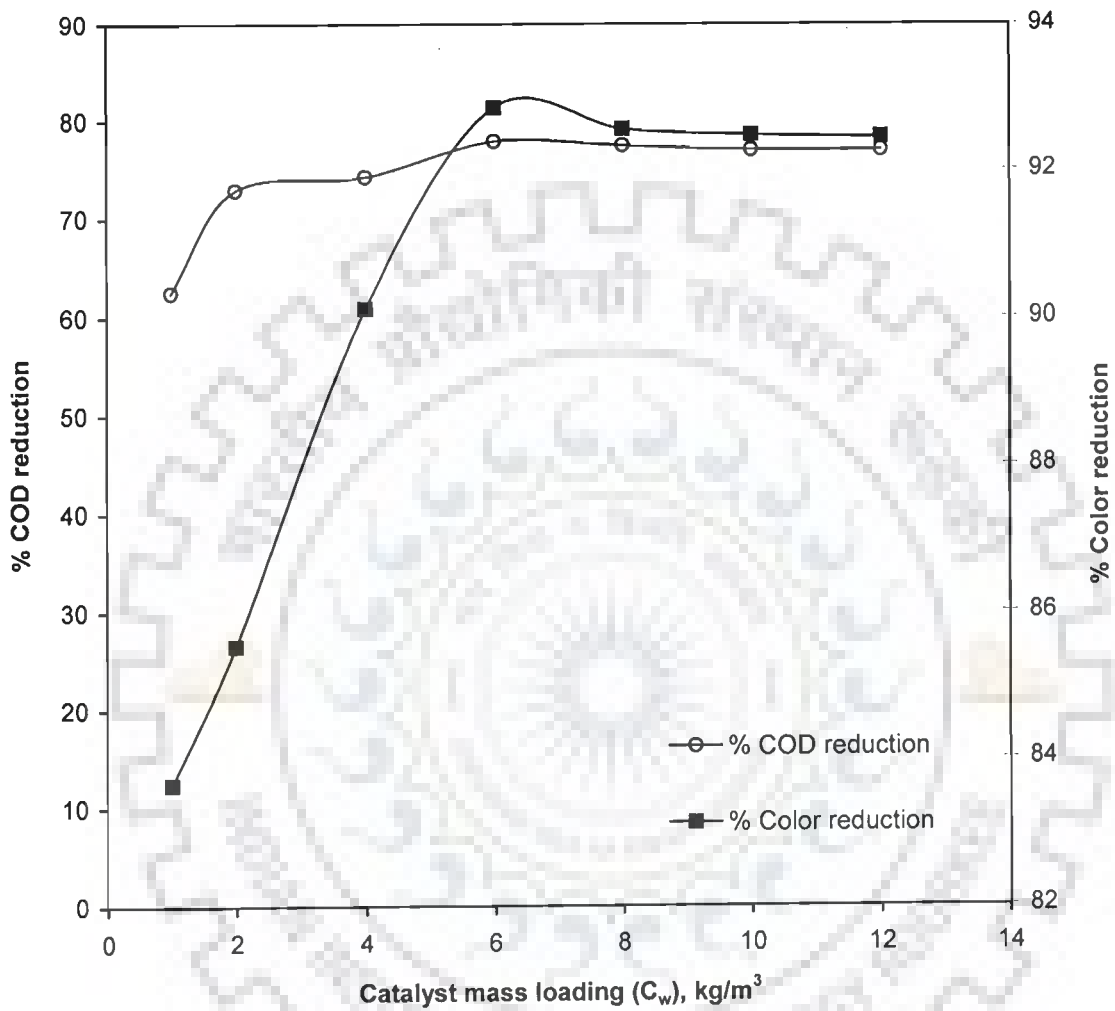
Figure 4.3 Effect of catalyst mass loading (copper sulphate) on COD and color reduction of the composite wastewater

COD_0 = 1960 mg/l, t_R = 4 h, P = atmospheric, pH_0 = 12, T_R = 95°C, Initial color concentration = 2250 PCU
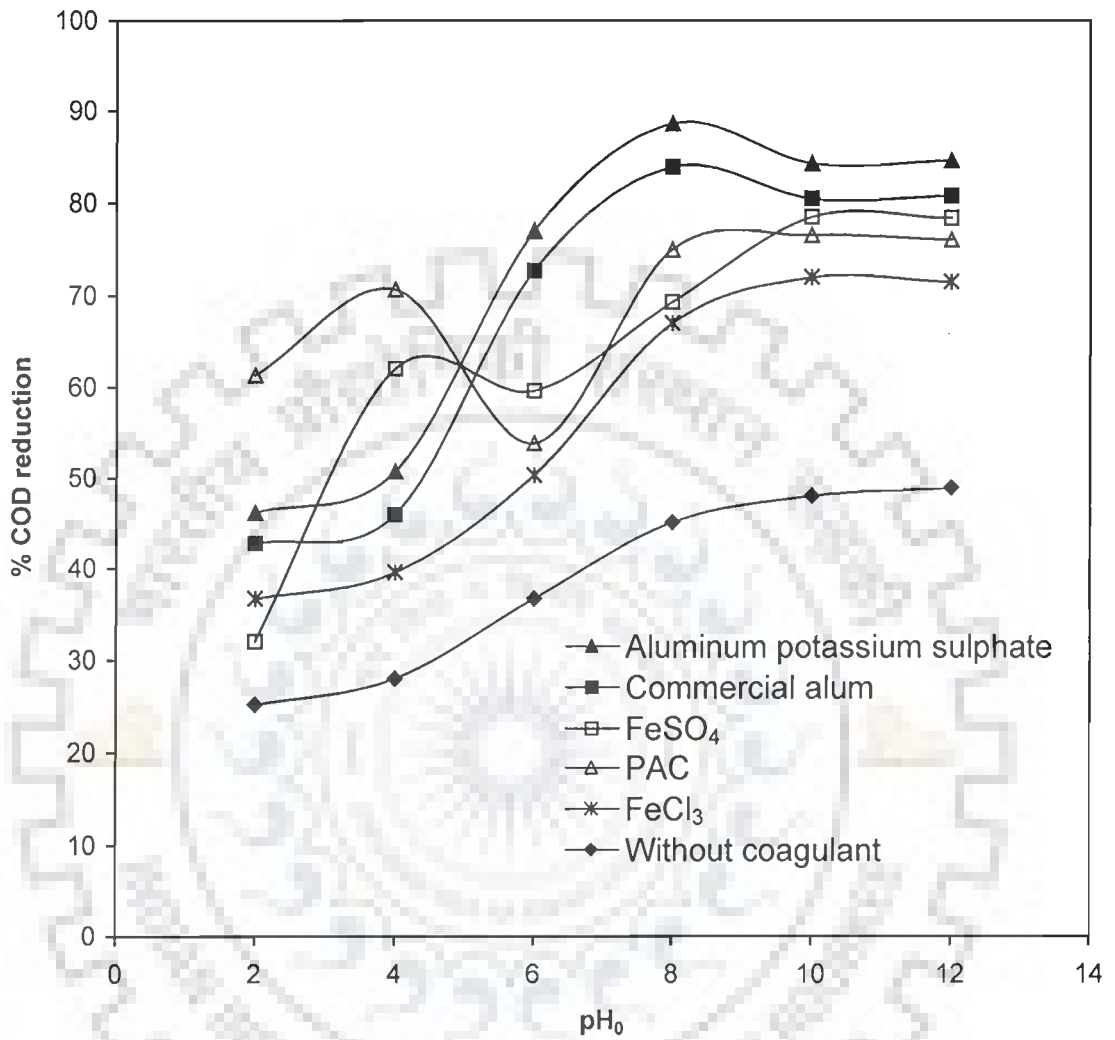
Figure 4.4(a) Effect of pH_0 on COD reduction of the composite wastewater by using different coagulants

$COD_0 = 1960$ mg/l, $t_R = 1$ h, P = atmospheric, $C_w = 5$ kg/m^3
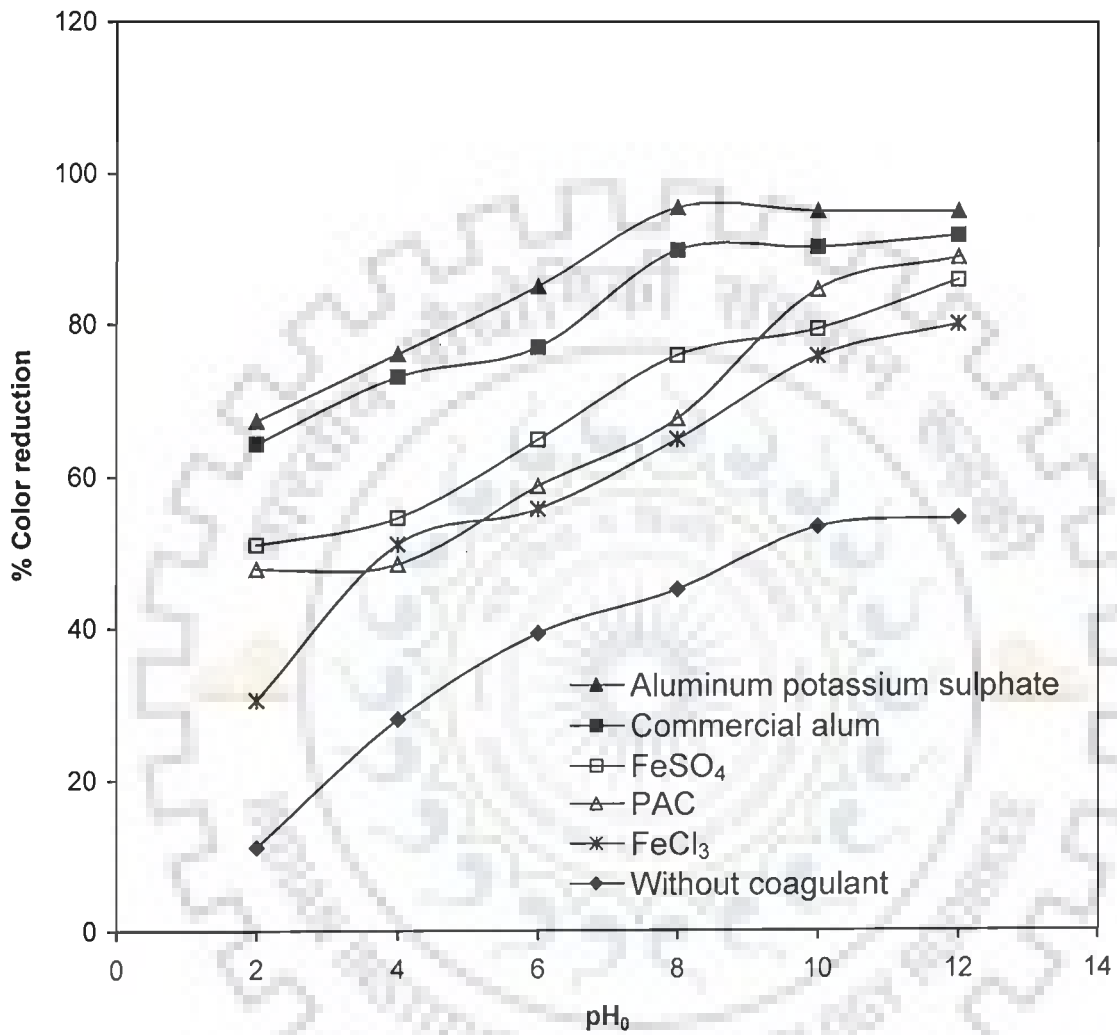
Figure 4.4(b) **Effect of pH_0 on color reduction of the composite wastewater by using different coagulants**

COD_0 = 1960 mg/l, t_R = 1 h, P = atmospheric, C_w = 5 kg/m^3,

Initial color concentration = 2250 PCU
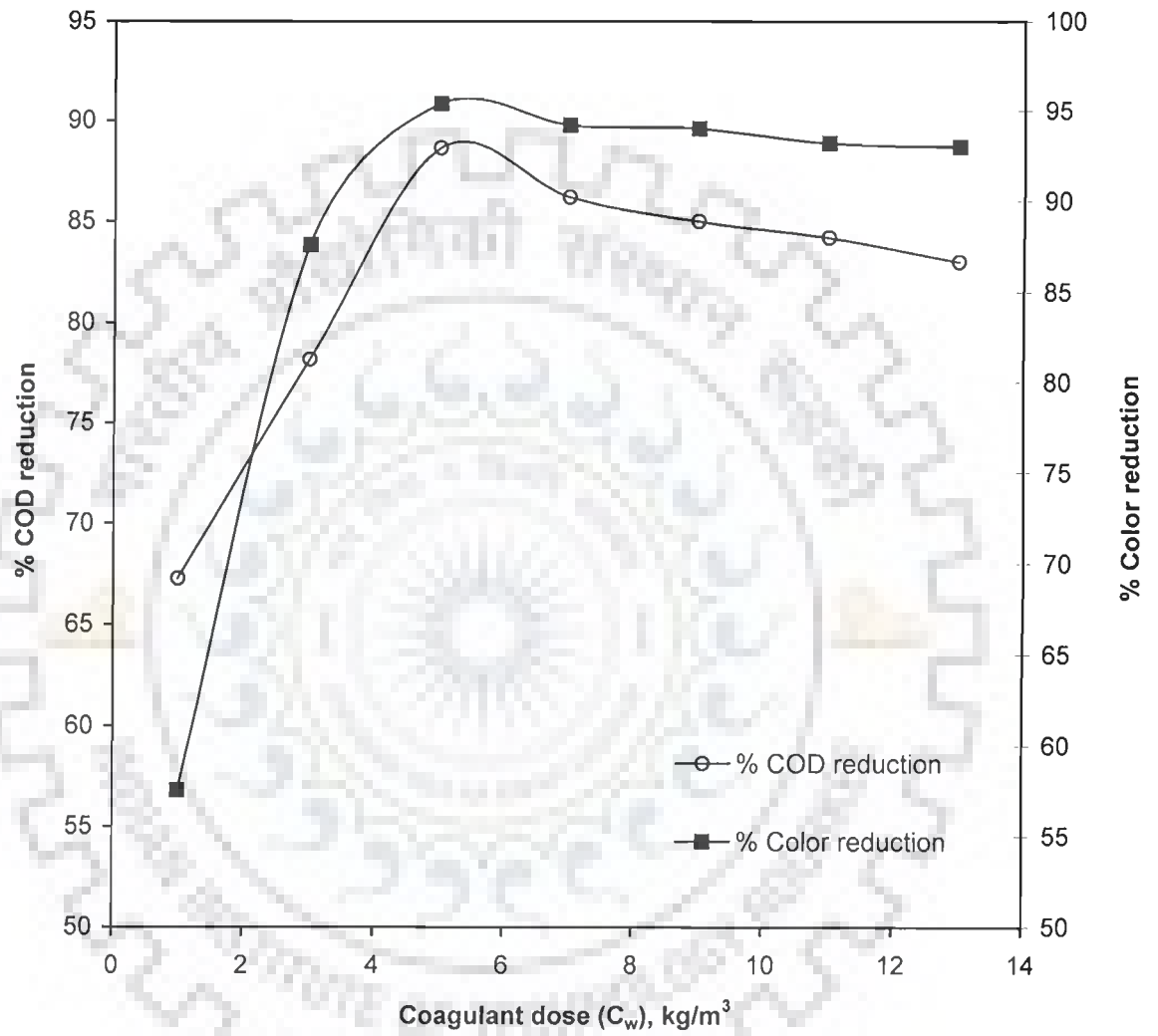
Figure 4.5 **Effect of coagulant (aluminum potassium sulphate) dose on COD and color reduction of the composite wastewater**

$COD_0 = 1960$ mg/l, $t_R = 1$ h, P = atmospheric, $pH_0 = 8$, T = 18°C, Initial color concentration = 2250 PCU

Figure 4.6 Time course of COD reduction by coagulation of the composite wastewater and the supernatant after catalytic thermolysis (Coagulant = aluminum potassium sulphate, C_w = 3 kg/m³, pH_0 = 8, T = 18°C)

Figure 4.7   Time course of color reduction by coagulation of the composite wastewater and the supernatant after catalytic thermolysis (Coagulant = aluminum potassium sulphate, C_w = 3 kg/m^3, pH$_0$ = 8, T = 18°C, Initial color concentration = 2250 PCU)

4.1.4 FTIR Analysis of Dried Residues of Composite Wastewater Before and After Treatment

The FTIR analysis was conducted to identify the functional group of the compounds present in the dried liquor and the solid residues formed due to catalytic thermolysis and coagulation. A comparison of the FTIR spectra of the dried fresh wastewater and that of the precipitate obtained after treatment gave an idea on the removal of the functional groups of compounds from the dried fresh effluent.

Composite wastewater after drying at ~45 °C for 36 h exhibits a broad band at ~3450 cm^{-1} due to ν(OH) of water. This is further supported by the presence of a sharp band at 1635 cm^{-1} due to δ(OH) mode. A weak intensity band at 1544 cm^{-1} suggests the presence of conjugated C=C bond while the weak bond at ~2900 cm^{-1} indicates the presence of CH$_2$ groups in waste. The waste material also exhibits medium intensity band at 1120 cm^{-1} possibly due to the presence of sulphate group.

On treatment with copper sulphate by catalytic thermolysis most of the IR peaks become intense. The sharp band present at 1114 cm^{-1} in the sample suggests the presence of sulphate group possibly in the coordinated form. The waste also displays a broad band at ~3400 cm^{-1} due to ν(OH), 1639 cm^{-1} due to δ(OH), 1555 cm^{-1} due to ν(C=C) and ~2900 cm^{-1} due to ν(CH$_2$). The presence of two to three medium intensity bands in the 400-600 cm^{-1} wave number in both the samples possibly suggests that hydroxyl groups are coordinated to metal ions present in the sample.

The coagulated sample also exhibits all these bands which were found in the sample after catalytic thermolysis. The sample displays ν(OH) at 3450 cm^{-1}, δ(OH) at 1637 cm^{-1}, ν(CH$_2$) at 2900 cm^{-1} and 1550 cm^{-1} due to ν(C=C). The presence of 1136 cm^{-1} peak due to sulphate group suggests that sulphate is coordinated to metal ion. Again the presence of medium intensity band at 620 cm^{-1} indicates the coordination of hydroxyl group with metal ions.

FTIR traces are presented in Figures 4.8(a-c).

95
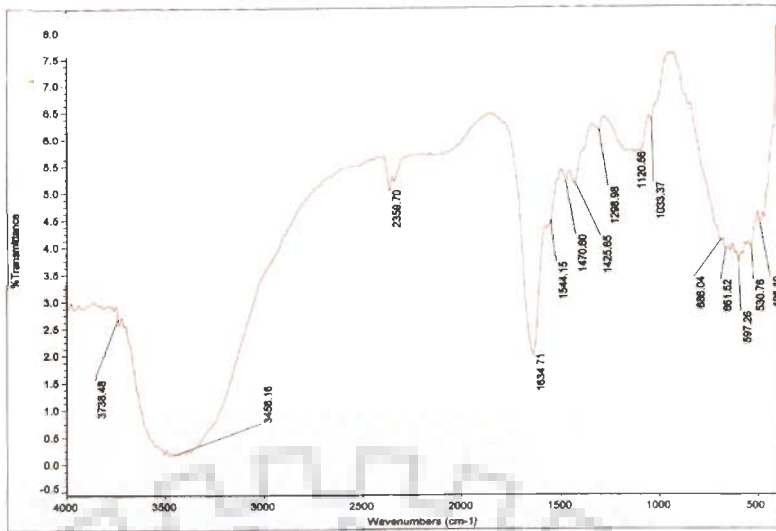
(a) Dried composite wastewater
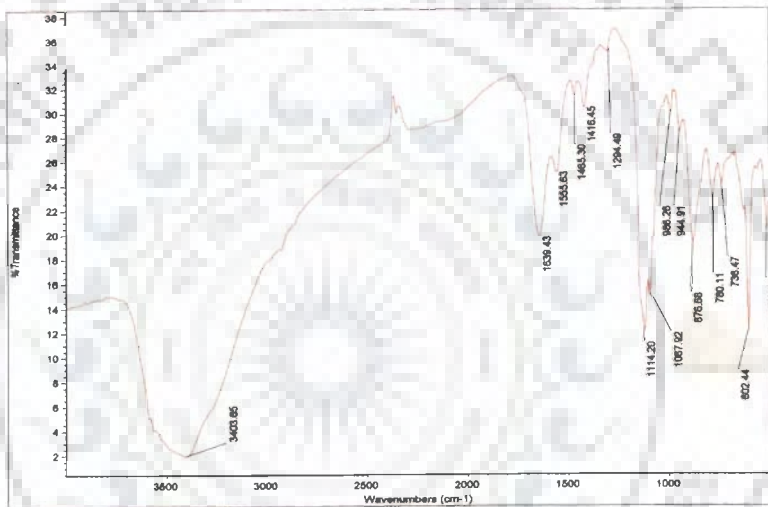
(b) After catalytic thermolysis
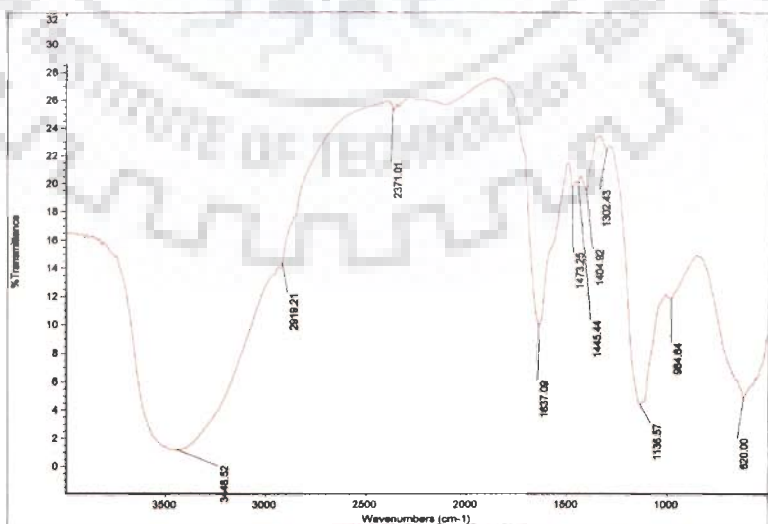
(c) After coagulation

Figure 4.8 FTIR spectra of composite wastewater

4.2 TREATMENT OF DYEING WASTEWATER OF A COTTON TEXTILE MILL USING CATALYTIC THERMOLYSIS AND COAGULATION

The effluent volume containing dyes when released into water bodies, constitutes only a small proportion of effluent. However, the dyes are visible even in small quantities due to their color brilliance. The color interferes with the photooxidation due to the interference with solar radiation and the dyes are health hazards. The biological treatment methods are incapable of removing dyes from effluent. Physicochemical methods have been suggested to be effective only if the effluent volume is small (Robinson et al., 2001). Adsorption and coagulation also pose problems in the regeneration of the adsorbents and the treatment, disposal and management of flocculated sludge. It is therefore desired to search for processes that are cost effective and present less post-treatment problems.

4.2.1 Catalytic Thermolysis

4.2.1.1 Effect of pH_0

Catalytic thermolysis experiments were conducted at 95 °C for 4 h with a $C_w = 2$ kg/m^3 to study the effect of pH_0 ($2 \leq pH_0 \leq 12$) on COD and color reduction of dyeing wastewater. After each experiment, a portion of the treated effluent was taken out and centrifuged. The clear liquid was separated and its COD and color were determined. The results are shown in Figure 4.9(a, b). Figure 4.9(a) shows a slow increase in COD reduction from pH_0 2 to pH_0 4, which rises at a faster rate between pH_0 4 and pH_0 8. From pH_0 8 to pH_0 12 almost no increase in COD reduction is seen. This trend is uniformly followed for all the catalysts. CuSO$_4$ shows the best removal of COD (~52 %) at pH_0 8. The final pH of the treated wastewater showed a decrease in pH except that for CuO treated wastewater. The results are presented in Table 4.2. The

reasons for this phenomena may be attributed to the dissociation of sulfate/chlorides into corresponding ions and thereby forming H_2SO_4/HCl which are responsible for the reduction of the pH of the solution. Carboxylic acids may also have formed out of the degradation of high molecular weight organics.

Table 4.2 Variation in pH of the treated dyeing wastewater with various catalysts

| pH_0 | Final pH (pH_f) of the wastewater after treatment with | | | | | | |
	$CuSO_4$	$FeSO_4$	$FeCl_3$	CuO	ZnO	PAC	Without catalyst
2	1.96	2.08	1.75	3.07	2.98	1.98	2.00
4	3.94	3.68	3.64	5.30	3.66	3.9	3.98
6	5.84	5.92	5.52	8.57	5.52	5.64	6.10
8	7.97	7.92	7.72	9.17	7.94	7.82	8.00
10	9.56	9.24	9.40	9.95	9.86	9.81	9.98
12	11.24	10.2	11.55	11.65	11.64	11.65	11.99

When the initial effluent was heated without any catalyst, under the identical conditions as mentioned above, the maximum COD reduction obtained at pH_0 8 was 12.6 %. The pH_0 adjustment (in the range of 8-12) of the dyeing wastewater has been effective in reducing the COD and color by ~ 10 %.

The effect of pH_0 on color reduction of dyeing wastewater is shown in Figure 4.9(b). Similar trend as noted for Figure 4.9(a) for COD reduction was also observed for color reduction. $CuSO_4$ gave the best color reduction of 58.7% at pH_0 8.

Figure 4.9(a) Effect of pH$_0$ on COD reduction of the dyeing wastewater by catalytic thermolysis

COD$_0$ = 5744 mg/l, T$_R$ = 95°C, P = atmospheric, t$_R$ = 4h, C$_w$ = 2 kg/m^3
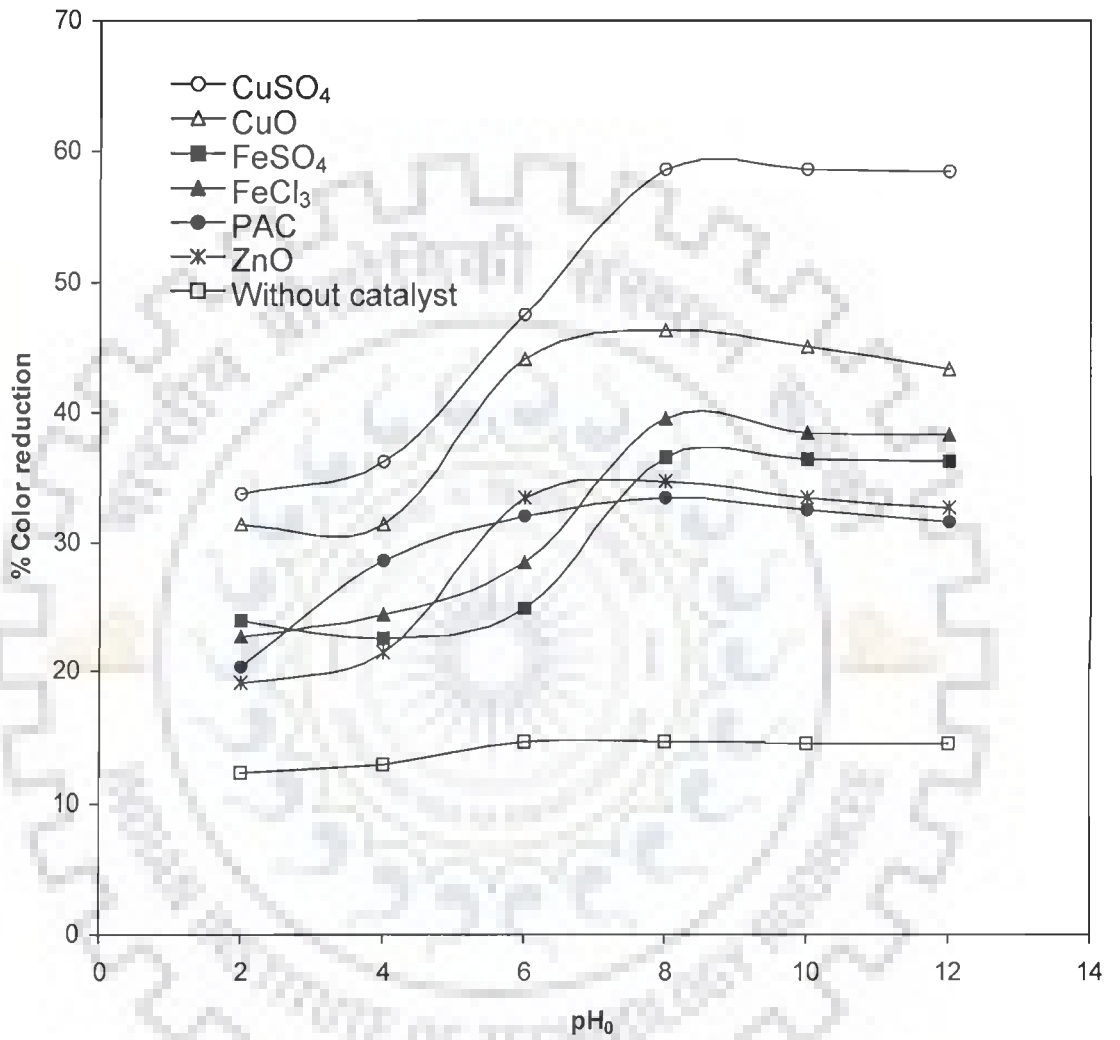
Figure 4.9(b) **Effect of pH_0 on color reduction of the dyeing wastewater by catalytic thermolysis**

$COD_0 = 5744$ mg/l, $T_R = 95^o$C, P = atmospheric, $t_R = 4$ h,

$C_w = 2$ kg/m^3, Initial color concentration = 3840 PCU

4.2.1.2 Effect of Catalyst Mass Loading (C_w)

Figure 4.10 shows the effect of $CuSO_4$ mass loading on COD as well as color reduction of dyeing wastewater during catalytic thermal treatment at 95^oC, pH_0 8 for $t_r = 4$ h. The reductions of COD and color increased with an increase in C_w from 1 kg/m^3 to 5 kg/m^3. With further increase in C_w from 5 to 8 kg/m^3, there was no increase in COD as well as color reduction. The $C_w = 5$ kg/m^3 may thus be considered as the optimum C_w at the given operating conditions. The maximum COD and color reduction obtained at 5 kg/m^3 catalyst concentration were 66.8% and 71.4 %, respectively.

4.2.1.3 Effect of temperature

Figure 4.11(a-b) present the effect of temperature of catalytic thermolysis on the COD and color reduction using $CuSO_4$ as the catalyst. The percent reductions in COD and color increased as the temperature increased from 60 to 95 ^oC. The maximum COD and color reductions at 95 ^oC were 66.8% and 71.4 %, respectively. Since the experiments were conducted at atmospheric pressure (in a glass reactor under reflux), the reaction temperature was kept below 100 ^oC.

Chen et al. (2003) observed a similar phenomena where the reduction in COD was observed during the anoxic (in the absence of oxygen) preheating period. Heating the reactor from 20 °C to the desired reaction temperature 150 °C took 1 to 2 h time. The reduction of COD during this period was found to be much less than 1 %. As the temperature increased, the COD reduction also increased and reached to ~18 percent at 300 °C. The increase in COD removal during heating of textile desizing wastewater was also observed by other investigators (Chen et al., 2000; Li et al., 2000). The phenomena of reduction in COD during heating period, in the absence of oxygen, has been indicated to be caused by the loss of volatile organic compounds with continuous stirring as well as from thermal decomposition and precipitation of catalytic thermolysis products (Skaates et al., 1981).
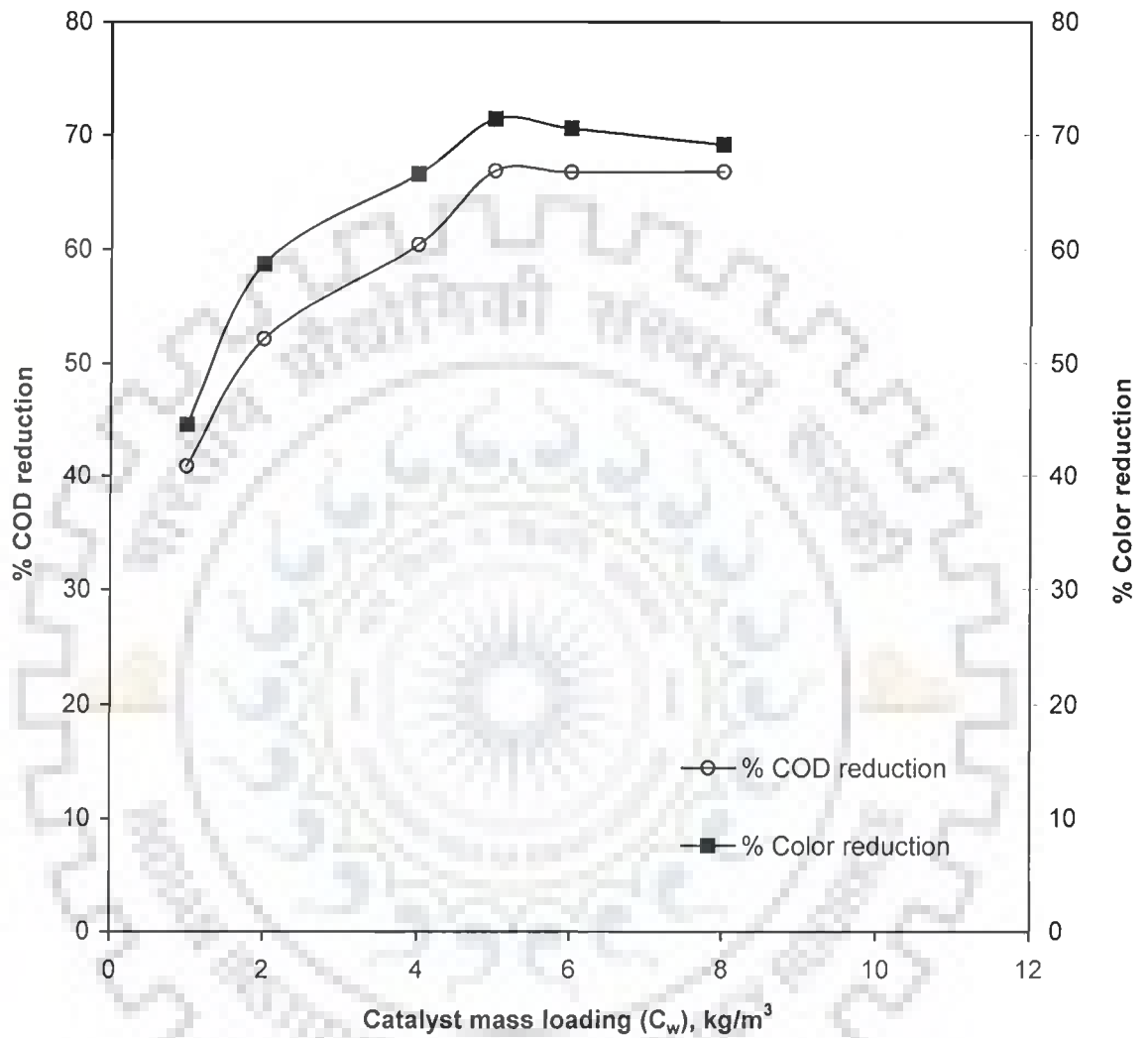
Figure 4.10 **Effect of catalyst (copper sulphate) mass loading on COD and color reduction of the dyeing wastewater**

COD_0 = 5744 mg/l, t_R = 4 h, P=atmospheric, pH_0=10,

Initial color concentration = 3840 PCU
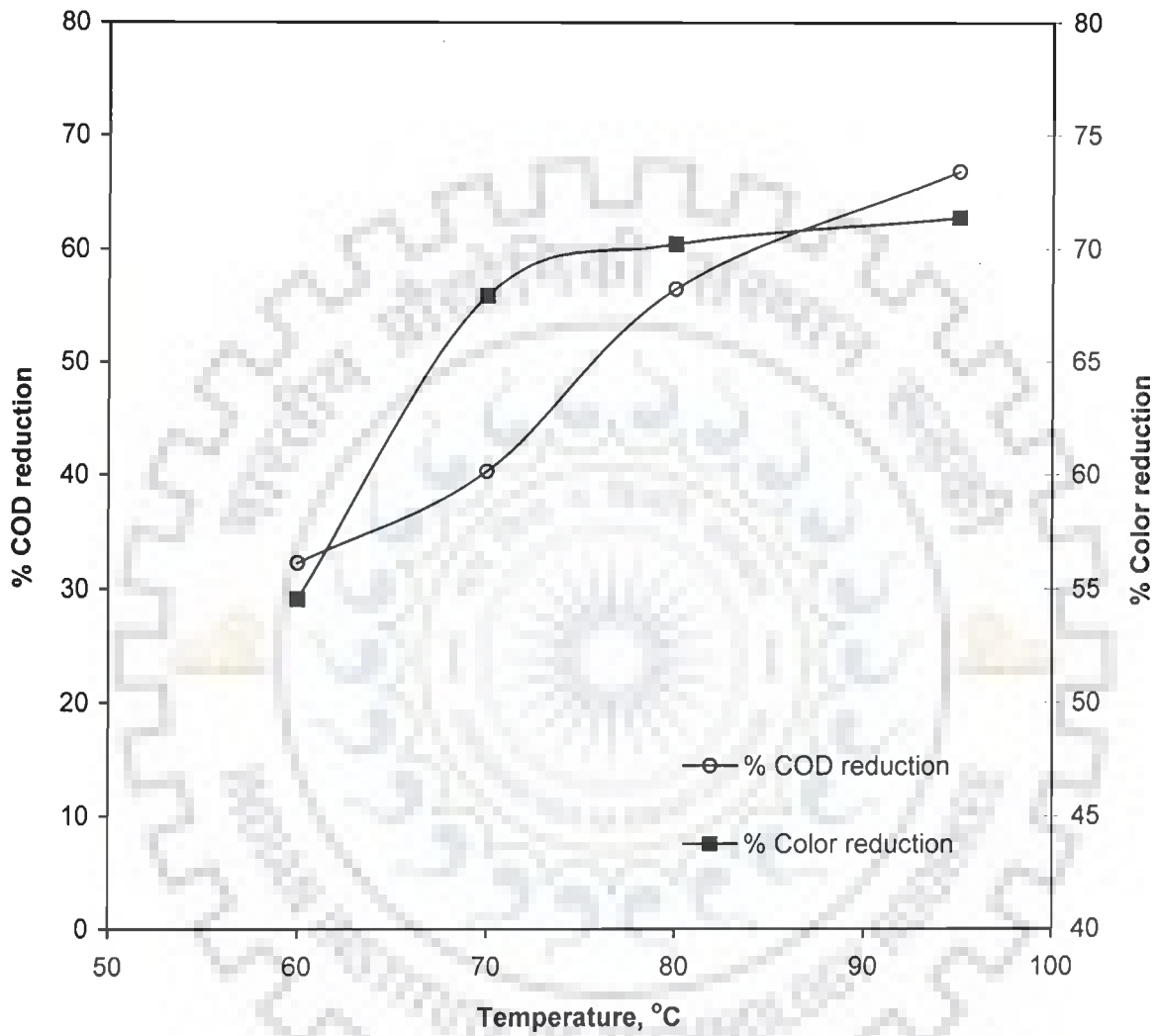
Figure 4.11(a) Effect of temperature on COD and color reduction of the dyeing wastewater of catalytic thermolysis using copper sulphate

$COD_0 = 5744$ mg/l, $t_R = 4$ h, P = atmospheric, $pH_0 = 8$,

$C_w = 5$ kg/m^3, Initial color concentration = 3840 PCU

103
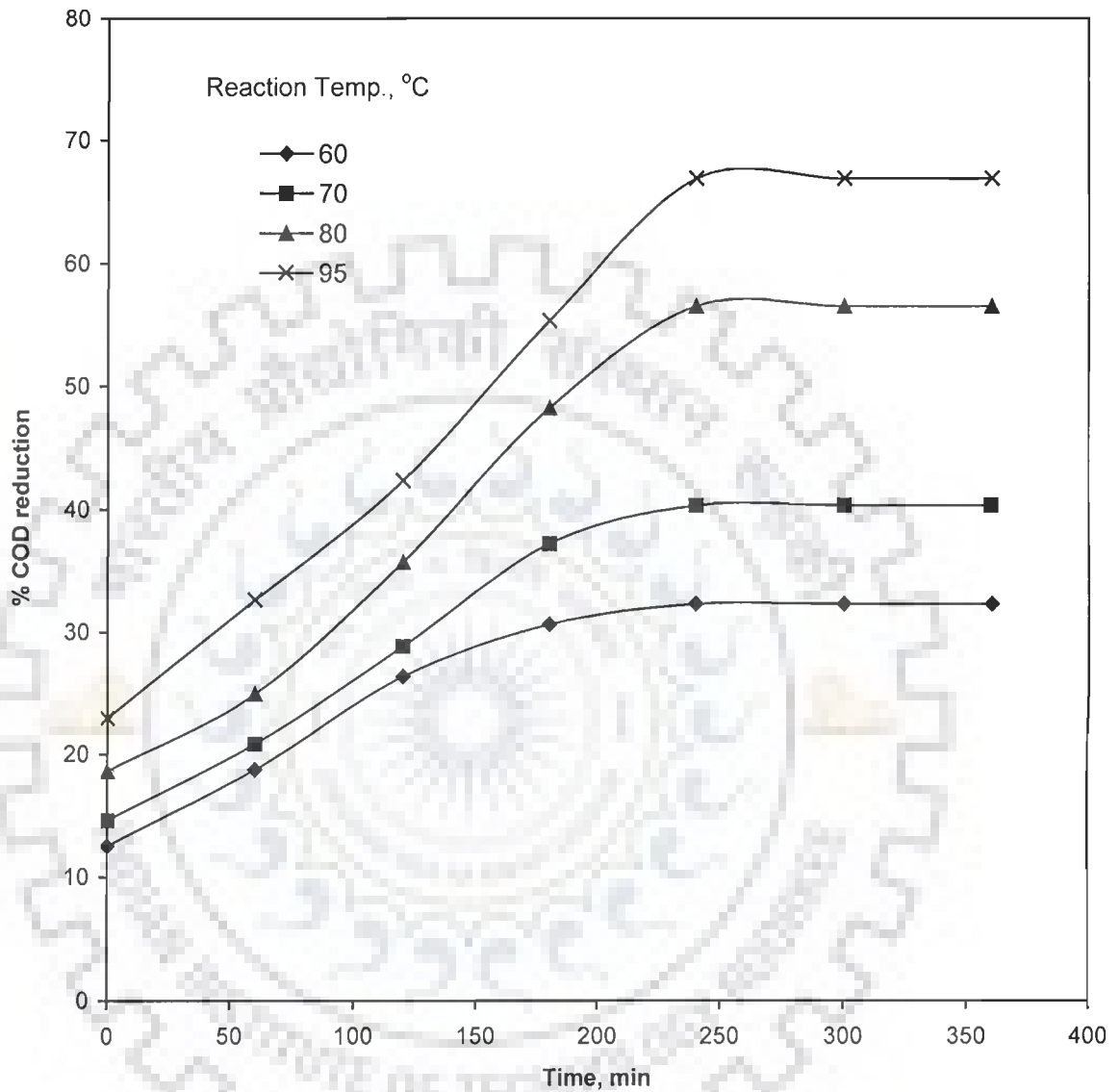
Figure 4.11(b) Effect of temperature on COD and color reduction of the dyeing wastewater of catalytic thermolysis

$COD_0 = 5744$ mg/l, P = atmospheric, $pH_0 = 8$, $C_w = 5$ kg/m³,

Initial color concentration = 3840 PCU

4.2.2 Coagulation

The effect of various coagulants such as commercial alum, aluminum potassium sulfate, PAC, $FeCl_3$, $FeSO_4$ were studied as a function of pH_0. The results are shown in Figure 4.12 and Figure 4.13 for COD and color reduction, respectively. Maximum COD and color reductions are obtained (34.57% and 60.33%, respectively) using commercial alum as a coagulant at pH_0 4 and a coagulant concentration of 3 kg/m^3. The effect of pH_0 on the dye reduction could be explained by the combined effect of (i) the ionization of amino, hydroxy and sulpho groups in the dye molecules which increases with pH in the acidic range, and (ii) the decrease in the concentration of dissolved hydrolysis products (Papic et al., 2004). Aluminum based coagulants show better results than that of iron based coagulants in the removal of COD and color of the dyeing wastewater.

Fe^{3+} has more coordination than Al^{3+} due to the presence of unfilled d-orbitals. The cationic compounds of the hydrolyzed dyes act as good reagents and electron acceptors from Al^{3+}. PAC is found to be active at pH_0 10. The multivalent Al cations of PAC coordinate with the anions present in the effluent and result in complexation. The gel structure of the PAC also enmeshes the organics present in dyeing wastewater. Thus, the complexation followed by precipitation and the capture of organics in the gel are responsible for both COD and color reduction by PAC as compared to those obtained with $FeSO_4$ and $FeCl_3$. Figures 4.14 and 4.15 reveal that the optimum pH_0 for COD and color reduction for all the five coagulants are different. Some are more active in acidic medium whereas the others are active in alkaline medium. The reduction of dissolved organics during coagulation with metal salts at different pH_0 follows two different mechanisms. At low pH, the anionic organic molecules present in the effluent coordinate with metal cations and form insoluble metal complexes at higher pH (alkaline range). The organics are adsorbed on to pre-formed flocs of metal hydroxides and get precipitated. The combined effect of the two mechanisms is that the reduction of dissolved organics with different functional groups can occur at different pH_0. The maximum COD and color removal may thus occur at a pH_0 where the combined effect of both the mechanisms is maximum.

Figure 4.12 **Effect of pH₀ on COD reduction of the dyeing wastewater by using various coagulants**

COD$_0$ = 5744 mg/l, t$_R$ = 1 h, P = atmospheric, C$_w$ = 3 kg/m^3
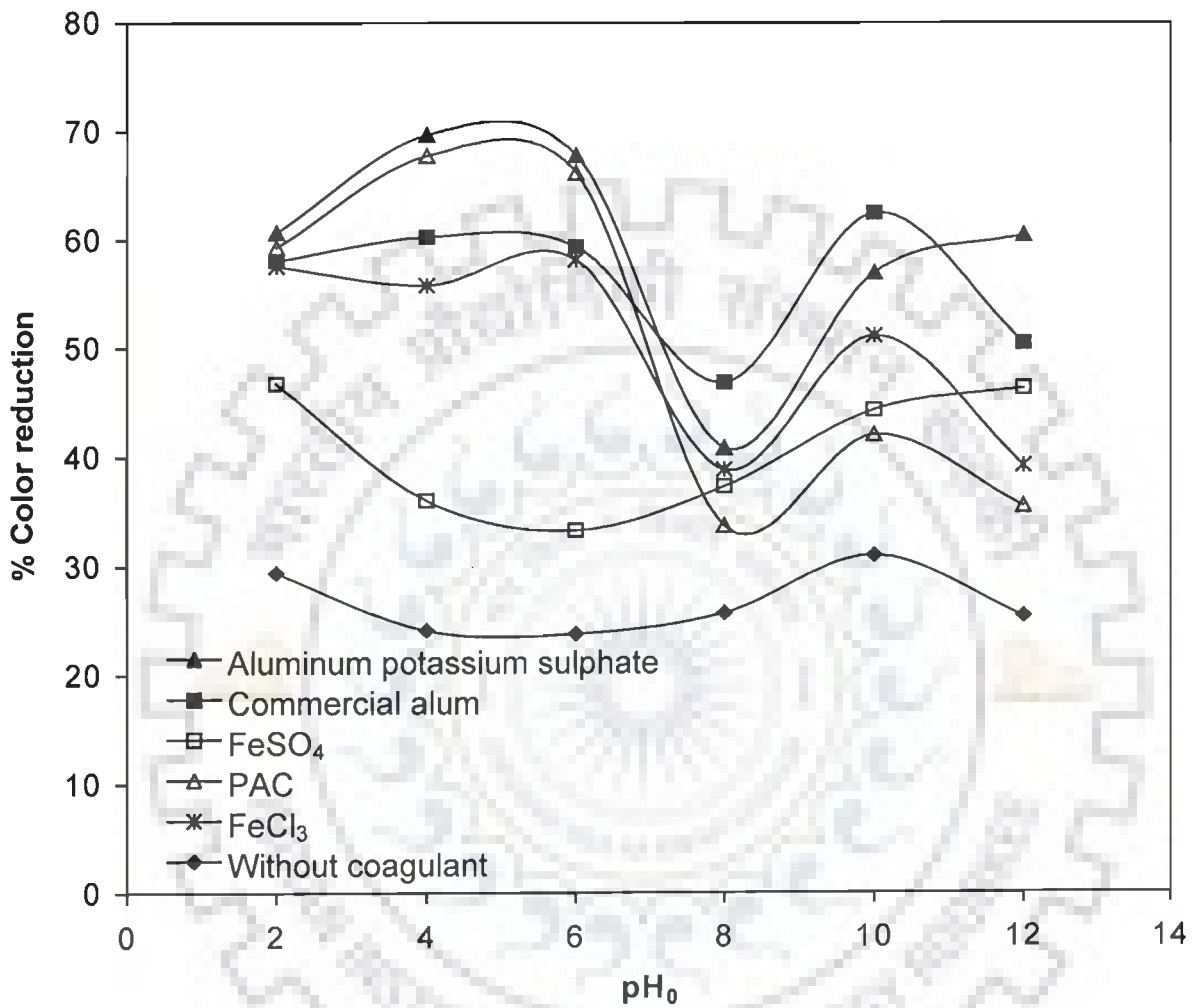
Figure 4.13 **Effect of pH₀ on color reduction of the dyeing wastewater by using various coagulants**

$COD_0 = 5744$ mg/l, $t_R = 1$ h, P = atmospheric, $C_w = 3$ kg/m^3,

Initial color concentration = 3840 PCU

4.2.2.1 Effect of coagulant dose (C_w)

During coagulation, the effluent is gently mixed which initiates floc formation, complexation and adsorption of organics resulting in precipitate formation and settling down of insoluble solids. In order to determine the optimum coagulant dose of the best coagulant (commercial alum) from amongst the various coagulant used, the effect of coagulant dose (1 to 13 kg/m^3) at optimum pH = 4 was studied. The results are shown in Figure 4.14 as percent COD as well as color reduction. It is clear that the reduction in both color and COD increases as the dose is increased from 1 to 5 kg/m^3 giving a maximum COD reduction of 58.57% and a color reduction of 74%.

With further increase in coagulant dose, the percent reduction in COD and color do not change substantially. Thus a coagulant dose of 5 kg/m^3 is assumed to be an optimum value under the prevailing treatment conditions. In coagulation process, color degradation is observed after effective COD reduction. Some metal complexes may be formed during coagulation (Liu et al., 1998). Table 4.3 shows the assay of commercial alum used for coagulation experiments. The table shows a maximum concentration of aluminum (as Al) of 16289 ppm.

Table 4.3 Assay of commercial alum used as a coagulant

	Unit (w/w)	
Aluminum content (as Al)	ppm	16289.2
Potassium content (as K)	ppm	42.183
Hydrogen (as H_2)	%	0.49
Sulphur (as S)	%	2.33
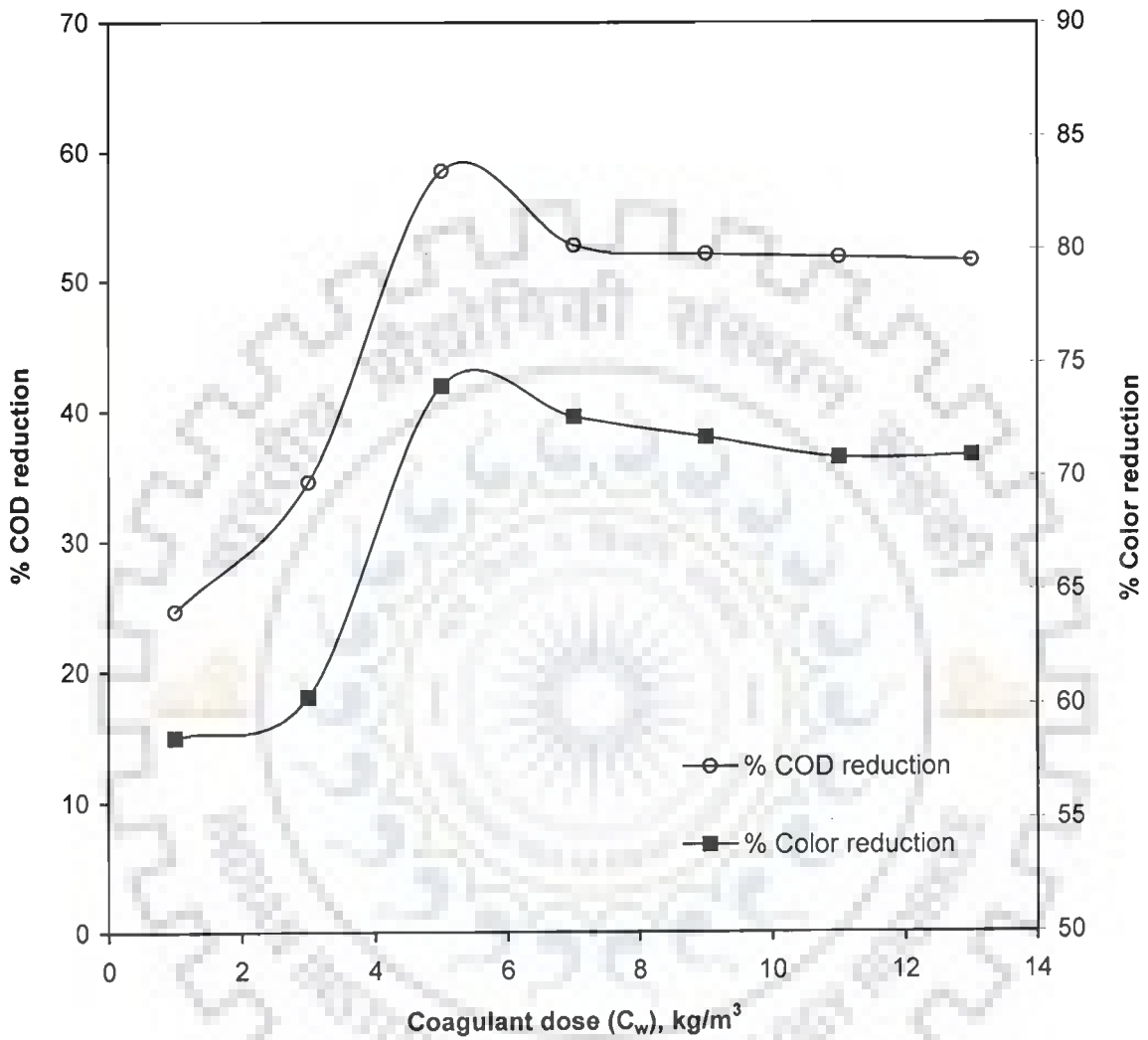
Figure 4.14 Effect of coagulant (commercial alum) dose on COD and color reduction of the dyeing wastewater

$COD_0 = 5744$ mg/l, $t_R = 1$ h, P = atmospheric, $pH_0 = 4$,

Initial color concentration = 3840 PCU
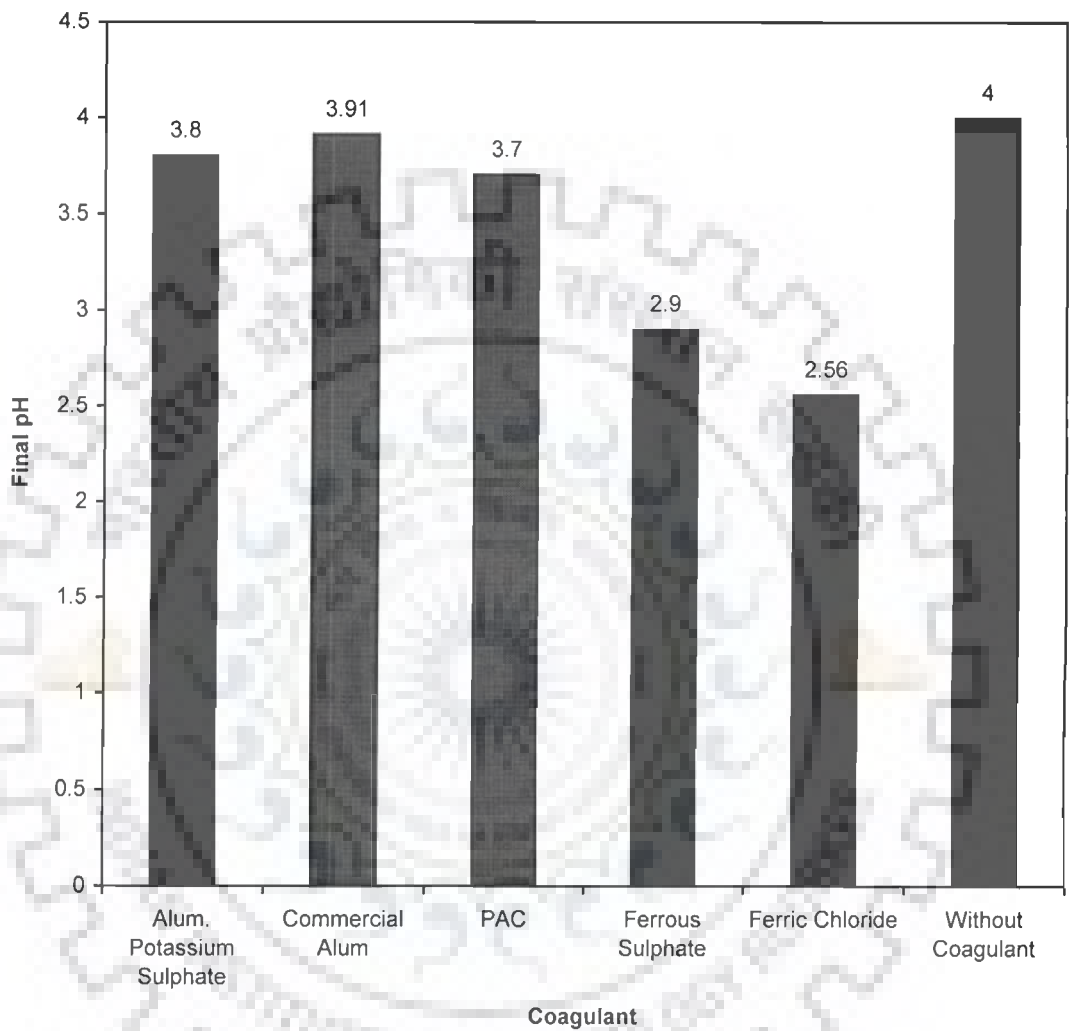
Figure 4.15 pH reduction after coagulation process

$COD_0 = 5744$ mg/l, $t_R = 1$ h, P = atmospheric, $pH_0 = 4$

It may be seen from Figure 4.15 that the addition of coagulants reduces the pH of the effluent. The final pH of the effluent after adding the coagulant was observed. It is observed from the Figure 4.15 that the pH reduction was found to be high with $FeSO_4$ and $FeCl_3$. This indicates that if Fe based coagulants are used, higher amount of alkali is required to be added to neutralize the effluent during disposal. This further indicates that commercial alum is better from the point of view of post coagulation treatments.

4.2.3 Catalytic Thermolysis followed by Coagulation

The results of catalytic thermolysis as well as coagulation done independently, as mentioned above, show maximum COD and color reduction during thermolysis of 66.85% and 71.4%, respectively, at pH 8 and catalyst concentration of 5 kg/m^3 using $CuSO_4$, whereas maximum COD and color reduction during coagulation (using commercial alum) were 58.57% and 74%, respectively at coagulant dose of 5 kg/m^3 and pH 4. In order to see the effect of combined treatment of catalytic thermolysis followed by coagulation, the catalytic thermolysis studies were conducted at the above mentioned conditions and the supernatant thus obtained was subsequently treated with the coagulant again at conditions mentioned above (except at a coagulant dose of 2 kg/m^3). A reduction in COD and color of 89.91% and 94.4%, respectively were observed as shown in Figures 4.16 and 4.17. The results thus indicate that the catalytic thermolysis followed by coagulation is an effective process for reduction of COD and color using a lower dose of coagulant, which could lead to less production of inorganic sludge and thus reducing the sludge disposal. The final COD and color observed in the treated dyeing waste were 192 mg/l and 61.5 PCU. The COD/BOD$_3$ ratio was 1.88. The prescribed limit of color in the effluent from disposal has been set at 400 PCU by Central Pollution Control Board, India.
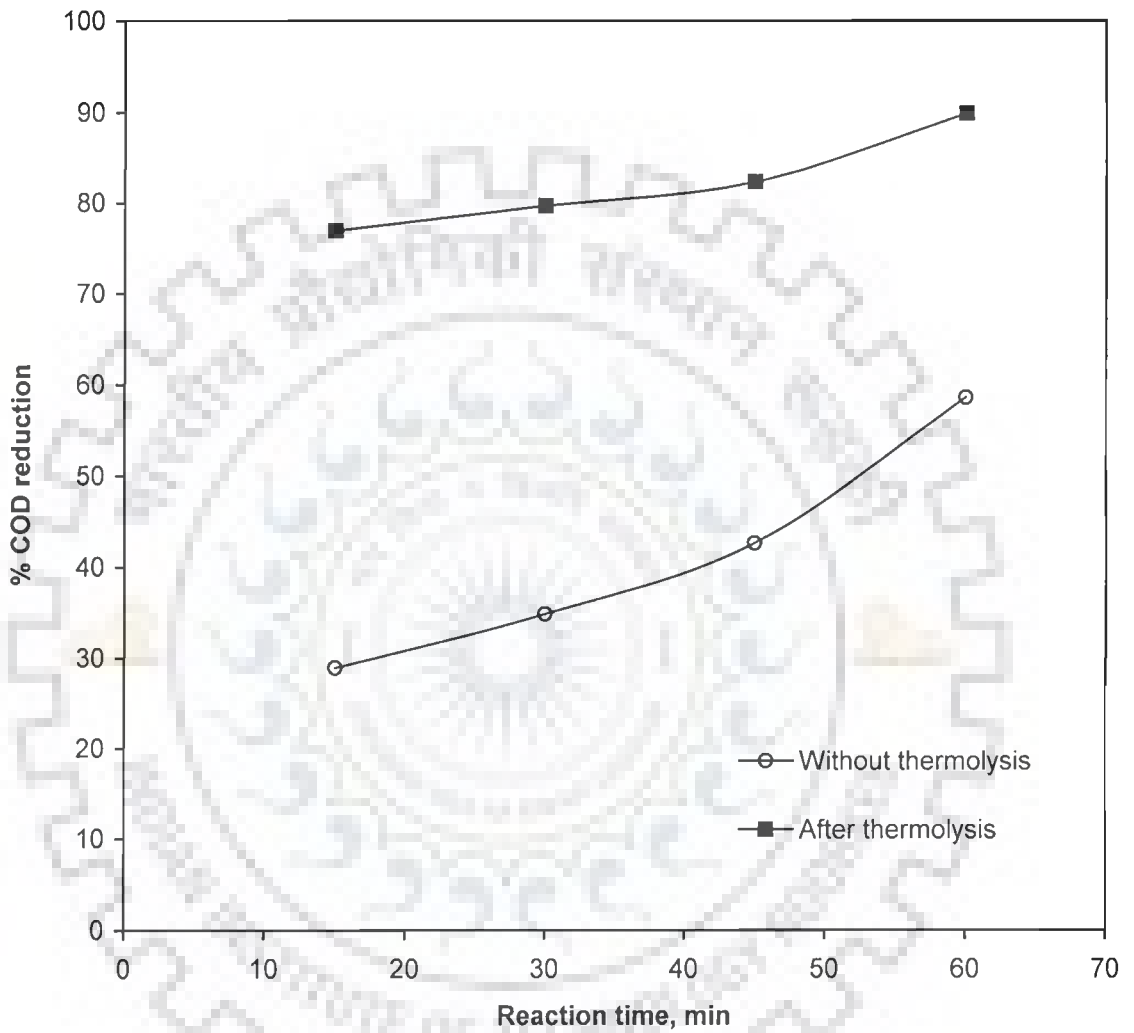
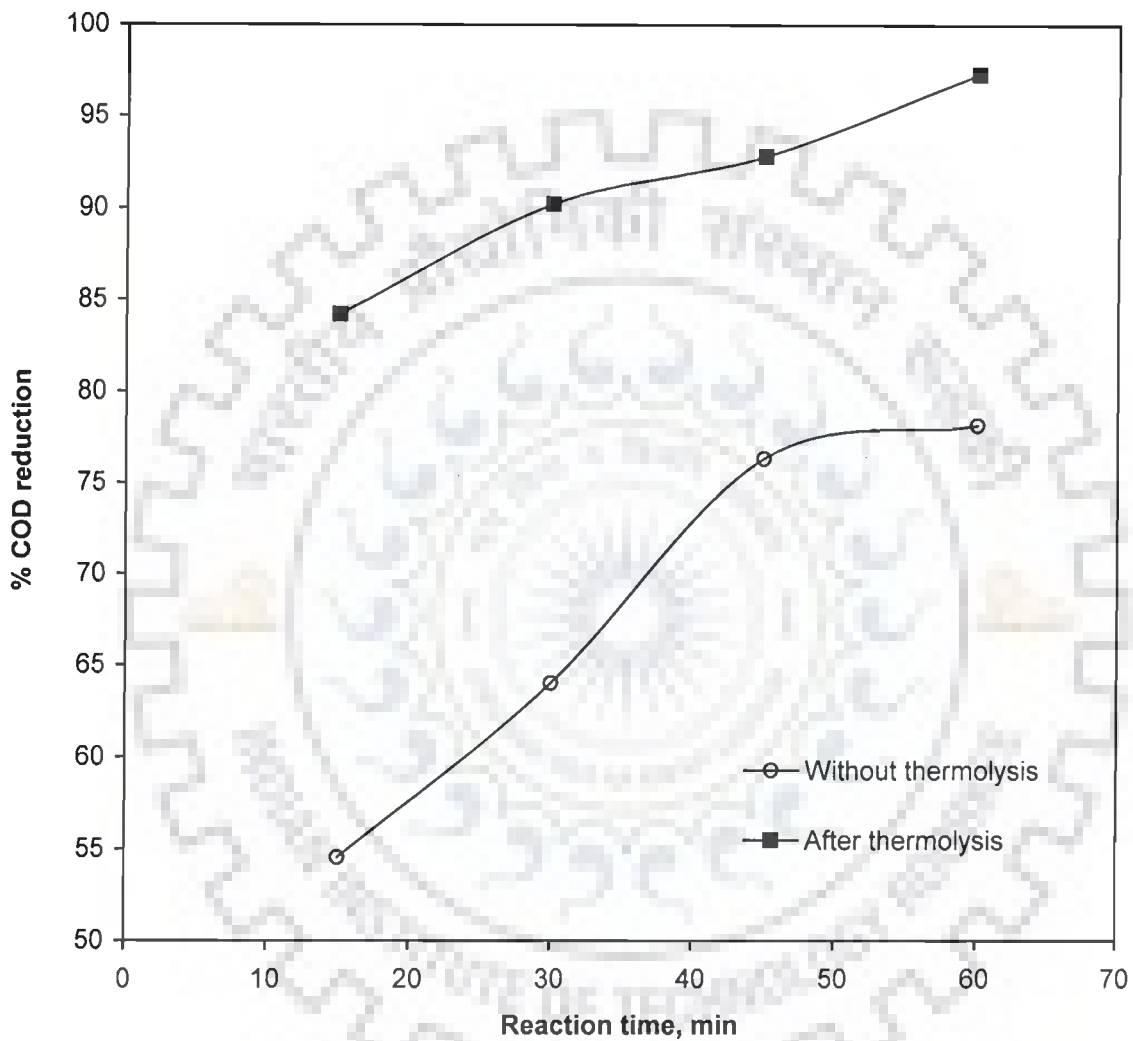**Figure 4.16**   **Time course of COD reduction by coagulation of wastewater and the supernatant after catalytic thermolysis.**

Coagulant = Commercial Alum, $pH_0 = 4$, $T_R = 18°C$, $C_w = 2$ kg/m^3
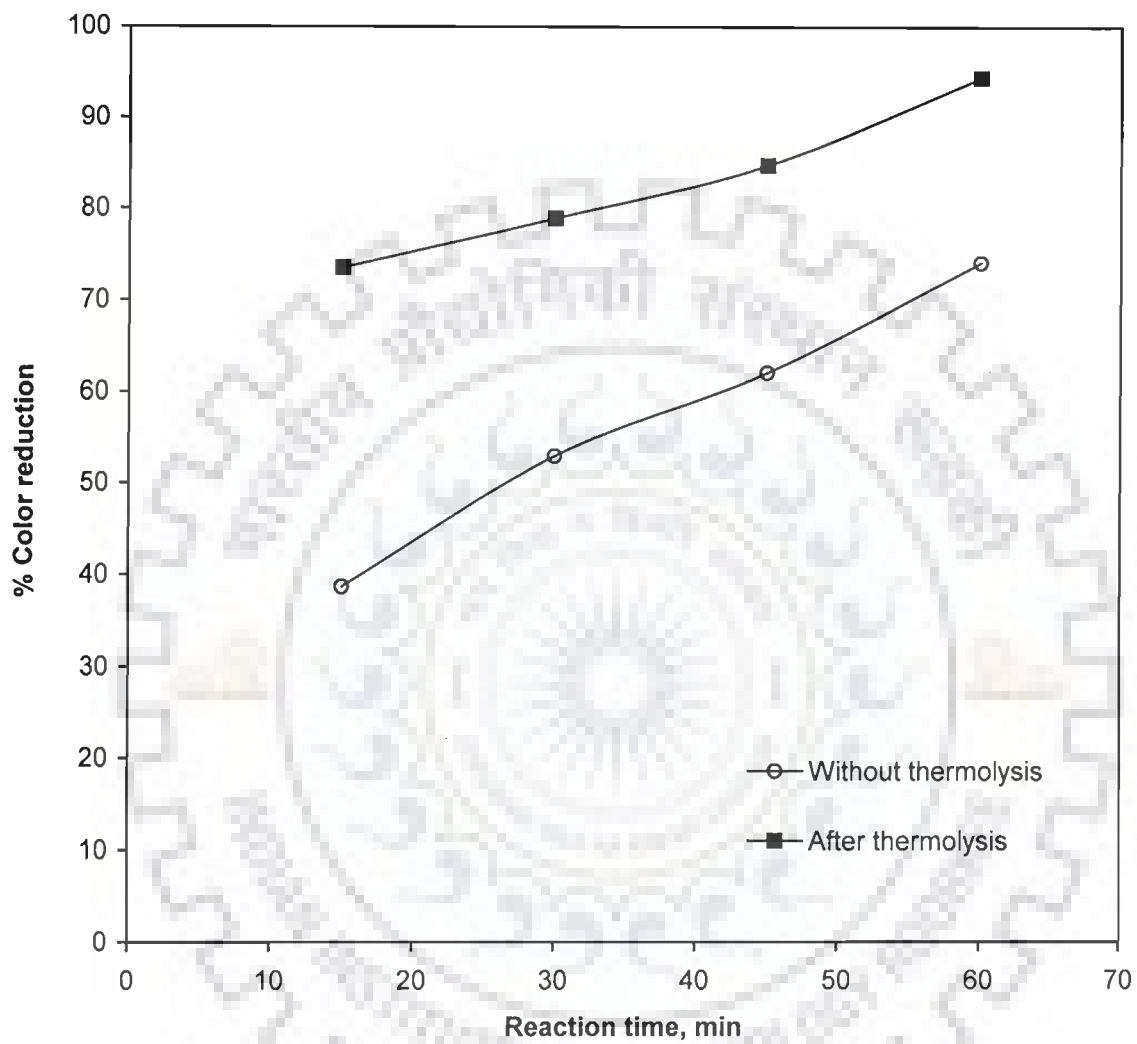
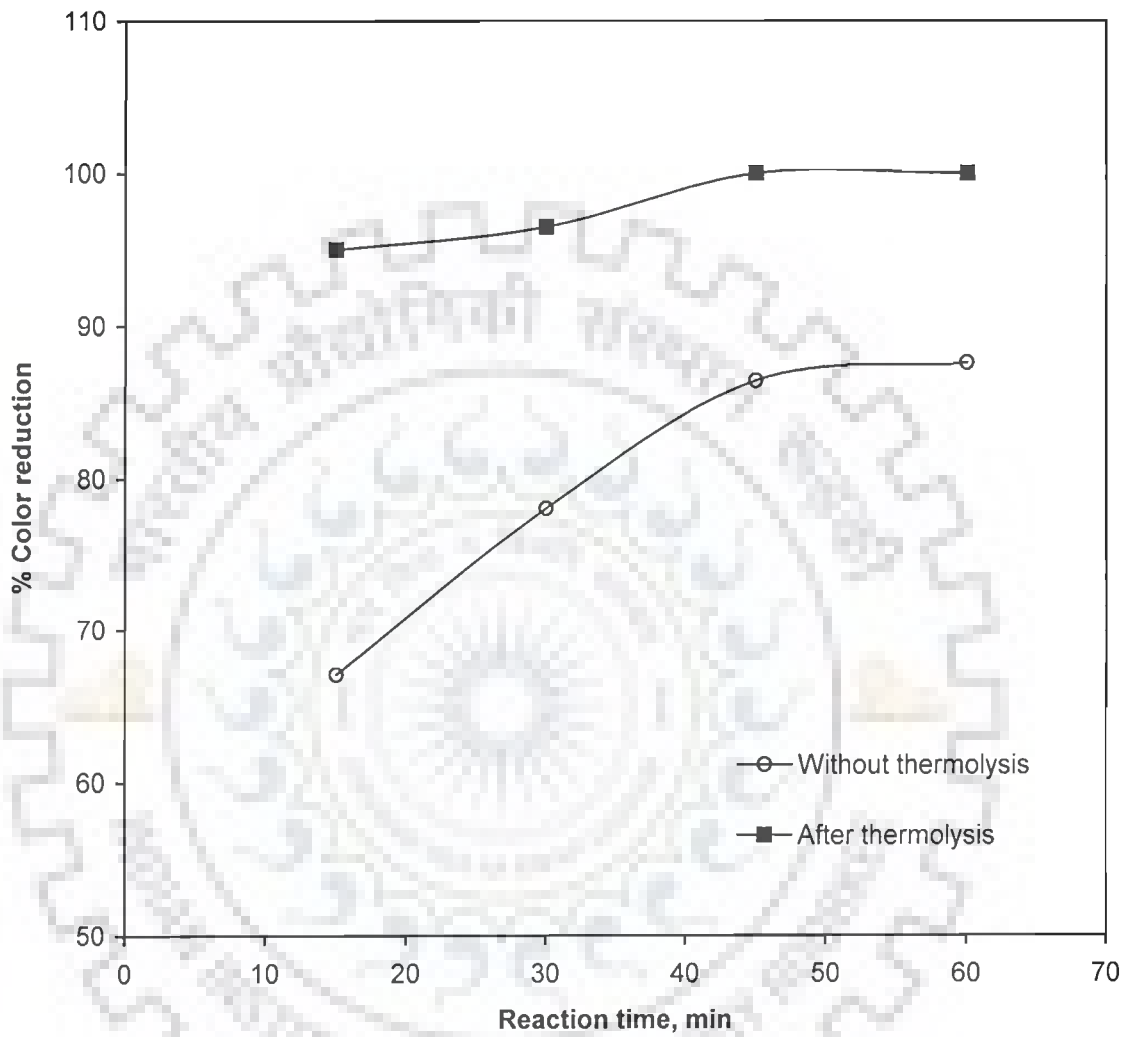**Figure 4.17** Time course of color reduction by coagulation of wastewater and the supernatant after catalytic thermolysis

Coagulant = Commercial alum, $pH_0 = 4$, $T_R = 18°C$,

$C_w = 2$ kg/m^3, Initial color concentration = 3840 PCU

4.2.4 FTIR Analysis of Dried Residues of Dyeing Wastewater Before and After Treatment

The FTIR spectra of dried dyeing wastewater (at 45 $^{\circ}$C) exhibits a strong band at 3460 cm^{-1} due to ν(OH) of either water or hydroxyl group present in dye. This dye is expected to have ring (C=N) group as a sharp band at 1618 cm^{-1} is observed due to ν(C=N) (ring). Both of these groups (hydroxyl as well as ring nitrogen) seem to be coordinated to the metal ions as four medium to sharp intense bands have been noted in the far-IR region of 420-616 cm^{-1}. The presence of band at 1138 cm^{-1} suggests the presence of sulphate group possibly attached to the metal ions. Conjugated C=C bond present in dye is confirmed by the presence of a medium intensity band at 1557 cm^{-1}. Dyeing waste also has CH$_2$ group as IR spectrum of it exhibits medium intensity bands covering the region 2848-2917 cm^{-1} as shown in Figure 4.18(a).

Thermolysis processed samples (as shown in Figure 4.18(b)) also display ν(OH) at 3450 cm^{-1}, δ(OH) at 1638 cm^{-1}, ν(CH$_2$) at 2850-2919 cm^{-1} and ν(C=C) at 1550 cm^{-1}. Coordinated azomethine group also seems to be present in the coordinated form as a weak intensity band at 568 cm^{-1} is observed. Absence of the band at 1138 cm^{-1} in this sample suggests that the removal of sulphate as water soluble components.

Coagulated sample (as shown in Figure 4.18(c)) also exhibits ν(OH) at 3450 cm^{-1}, δ(OH) at 1638 cm^{-1} and ν(CH$_2$) at 2848-2911 cm^{-1}. The presence of azomethine group at 1619 cm^{-1} and supported metal-nitrogen band 615 cm^{-1} suggest the coordination of azomethine nitrogen with coagulant. The band due to sulphato group is still present in this sample indicating their retention possibly through coordination with coagulant.
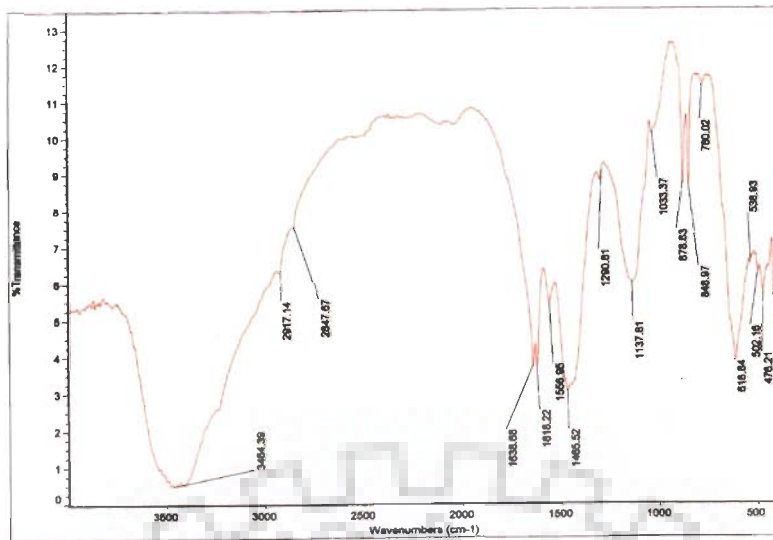
(a) Dried dyeing wastewater
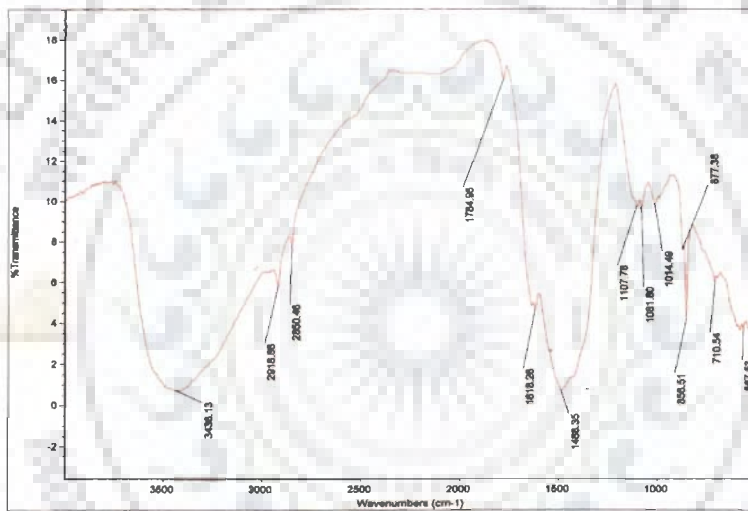
(b) After catalytic thermolysis
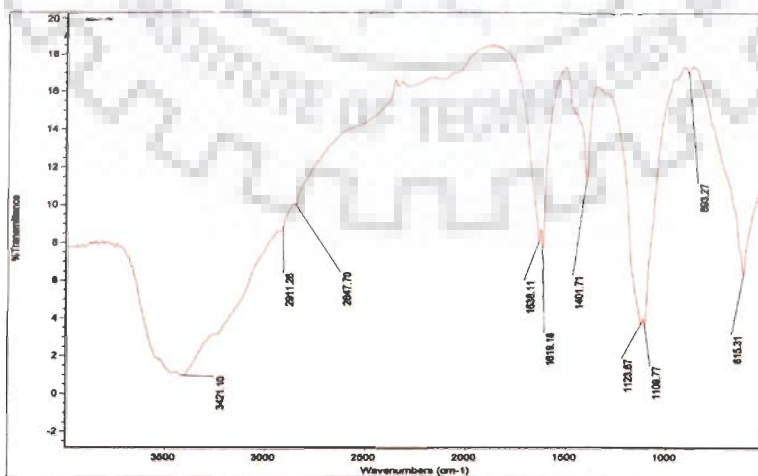
(c) After coagulation

Figure 4.18 FTIR spectra of dried dyeing wastewater

115

4.3 TREATMENT OF DESIZING WASTEWATER OF A COTTON TEXTILE MILL USING CATALYTIC THERMOLYSIS AND COAGULATION

4.3.1 Catalytic Thermolysis

4.3.1.1 Effect of pH_0 and Temperature

The effect of pH_0 on catalytic thermolysis of the desizing wastewater with and without catalyst was studied in the AGR at atmospheric pressure and 95 °C. The results are shown in Figure 4.19 as percent COD reduction in the final filtrate as a function of pH_0, while keeping other parameters fixed. All the experiments were carried out for a treatment time t_R = 4h, measured from zero time with the initial COD (COD_0) at 2884 mg/l and the catalyst mass loading (C_w) at 4 kg/m^3. The highest COD reduction of 71.6% with $CuSO_4$ as catalyst was obtained at pH_0 4. pH_0 4 was also found to give highest COD reduction with ZnO and $FeSO_4$. However, CuO showed maximum reduction at pH_0 12 and alum in the pH_0 range 6-8. It is found that excepting $CuSO_4$, all other catalysts have only marginal effect on the COD reduction over that observed without any catalyst. The highest COD removal was not more than ~20% (using $FeSO_4$, which is much less than that for $CuSO_4$. In view of these results, further experiments on the effect of variation in parameters were performed with $CuSO_4$ at pH_0 4.

It was also found that the preheating period upto 95 °C is sufficient for effecting the COD removal of 71.6% and no further increase in COD removal is observed even when the reactor is maintained at this temperature for further 4 h. The COD reduction during preheating to 60, 70, 80 and 95 °C were 27.8%, 38.5%, 49.7% and 71.63%, respectively (Figure 4.20). This leads to the conclusion that the thermochemical precipitation is a very fast (instantaneous) process and would need a very small reactor vessel in comparison to those for other catalysts.

116

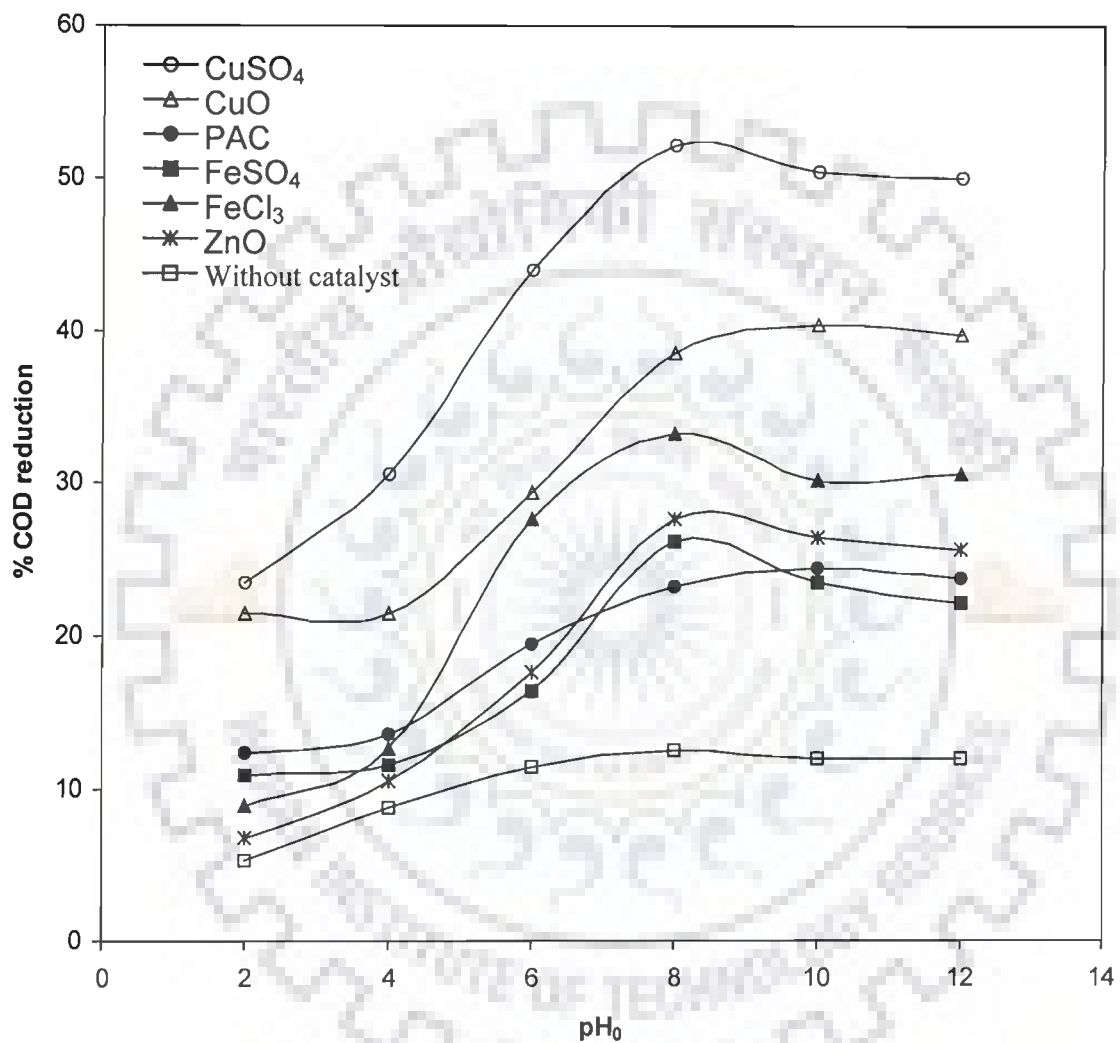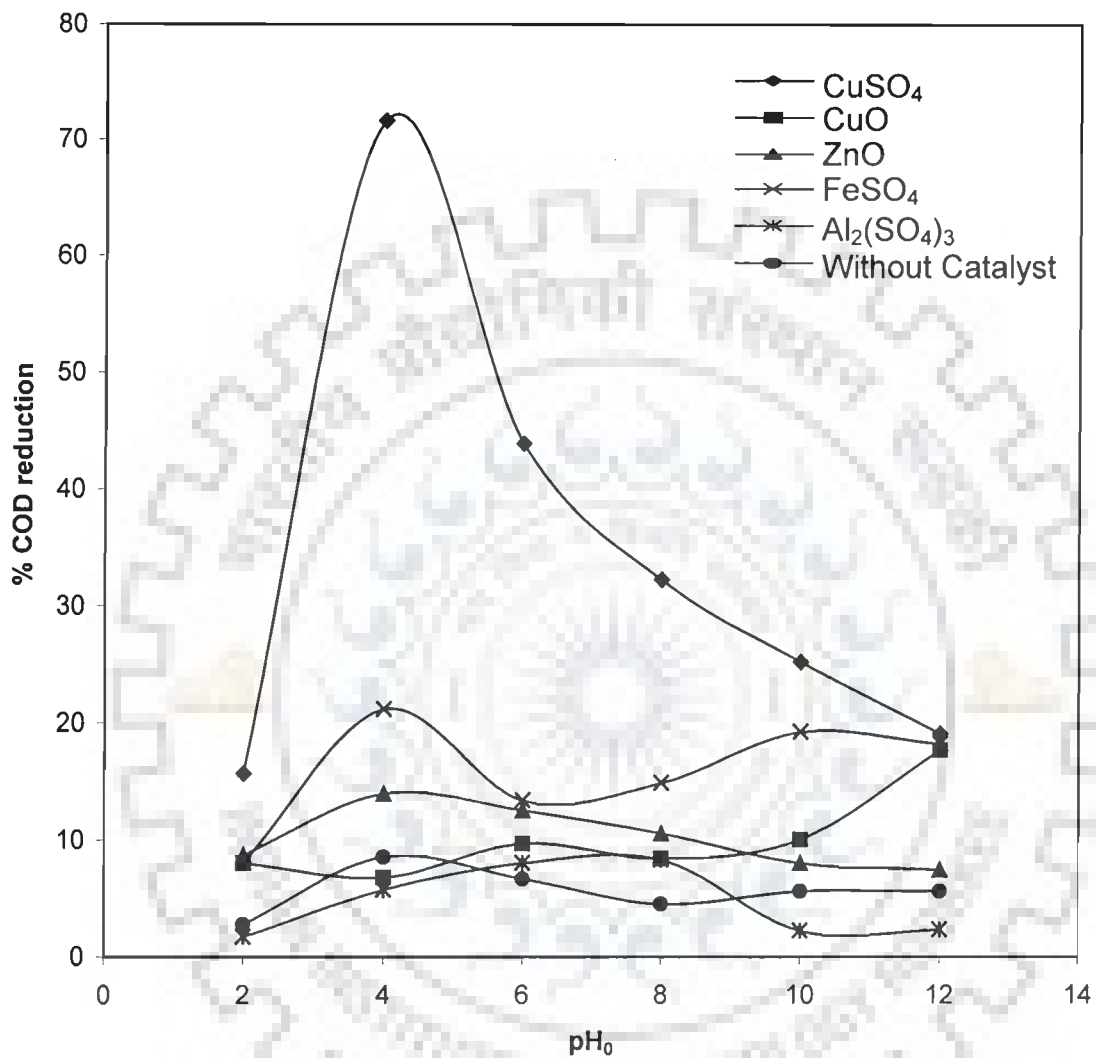**Figure 4.19**   Effect of pH_0 on COD reduction of the desizing wastewater by catalytic thermolysis

$COD_0 = 2884$ mg/l, $T_R = 95^{\circ}C$, P = atmospheric, $t_R = 4$ h,

$C_w = 4$ kg/m^3
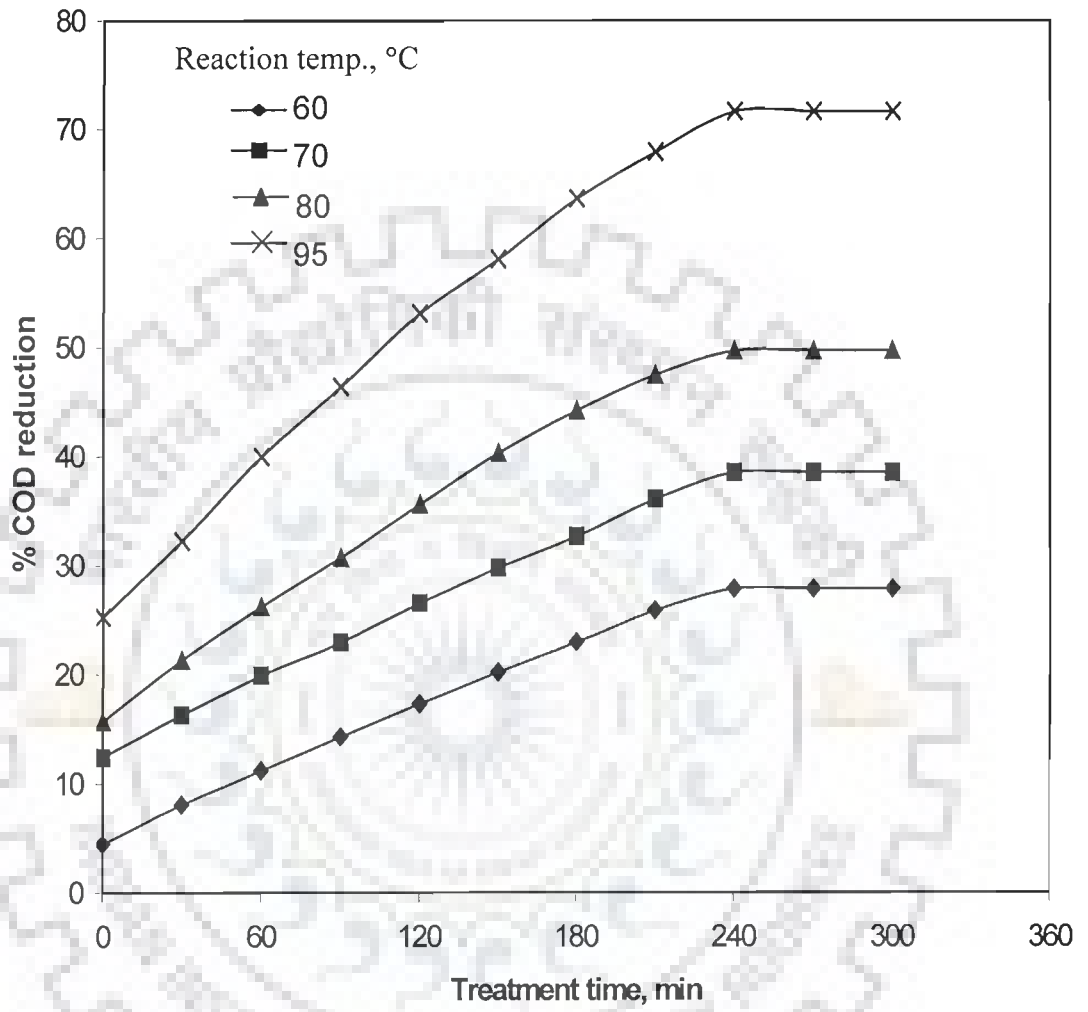
Figure 4.20   Effect of Temperature on COD reduction of the desizing wastewater of catalytic thermolysis

COD_0 = 2884 mg/l, t_R = 4 h, P = atmospheric, pH_0 = 4,

C_w = 4 kg/m^3

4.3.2 Effect of Catalyst Mass Loading (C_w)

The effect of copper sulfate mass loading on the COD reduction of desizing wastewater was observed at a temperature of 95 ^oC. The C_w was varied from 1 to 8 kg/m^3, while the pH_0 of the wastewater was kept at 4 for all the experimental runs. With C_w = 1 kg/m^3, only 44.96% reduction was observed. The solid precipitate obtained was in very small quantity and the color got converted into sea green after the completion of the reaction. However, at C_w = 2 kg/m^3, a COD reduction of 55.7% was obtained with a small amount of precipitated solid residue. With an increase in C_w to 4 kg/m^3, a maximum of 71.63% COD reduction was obtained, as shown in Figure 4.21. Beyond C_w = 4 kg/m^3, no increase in the COD reduction was observed. The final pH of the treated wastewater increases from its initial value. In some catalysts, the final pH of the treated wastewater decreased from its initial value. This trend may be attributed to the enhanced formation of SO_4^{2-} ions and/or the formation of carboxylic acids (Garg et al., 2005). As the COD_0 of the wastewater increases, comparatively larger chemical mass loading is required for optimum COD reduction. It is also found that the percent COD reduction due to thermochemical precipitation increases as the COD_0 of the effluent is increased.

4.3.3 Effect of pH_0 on the Color Reduction

The effect of pH_0 on the color reduction for a treated desizing wastewater having a COD_0 value of 2884 mg/l is shown in Figure 4.22. A maximum color removal of 87.2% was obtained at pH_0 4 and a minimum color reduction of 78.18% was found at pH_0 12 using copper sulfate as catalyst. This phenomena may be explained due to the increased concentration of copper ion present in the supernatant, affecting lower adsorption of color on the precipitate. Several researchers have reported a color removal of the order of 70 to 100% using different coagulants (Georgiou et al., 2003; Selcuk, 2005; Uddin et al., 2003; Kang et al., 2002) and operating conditions.
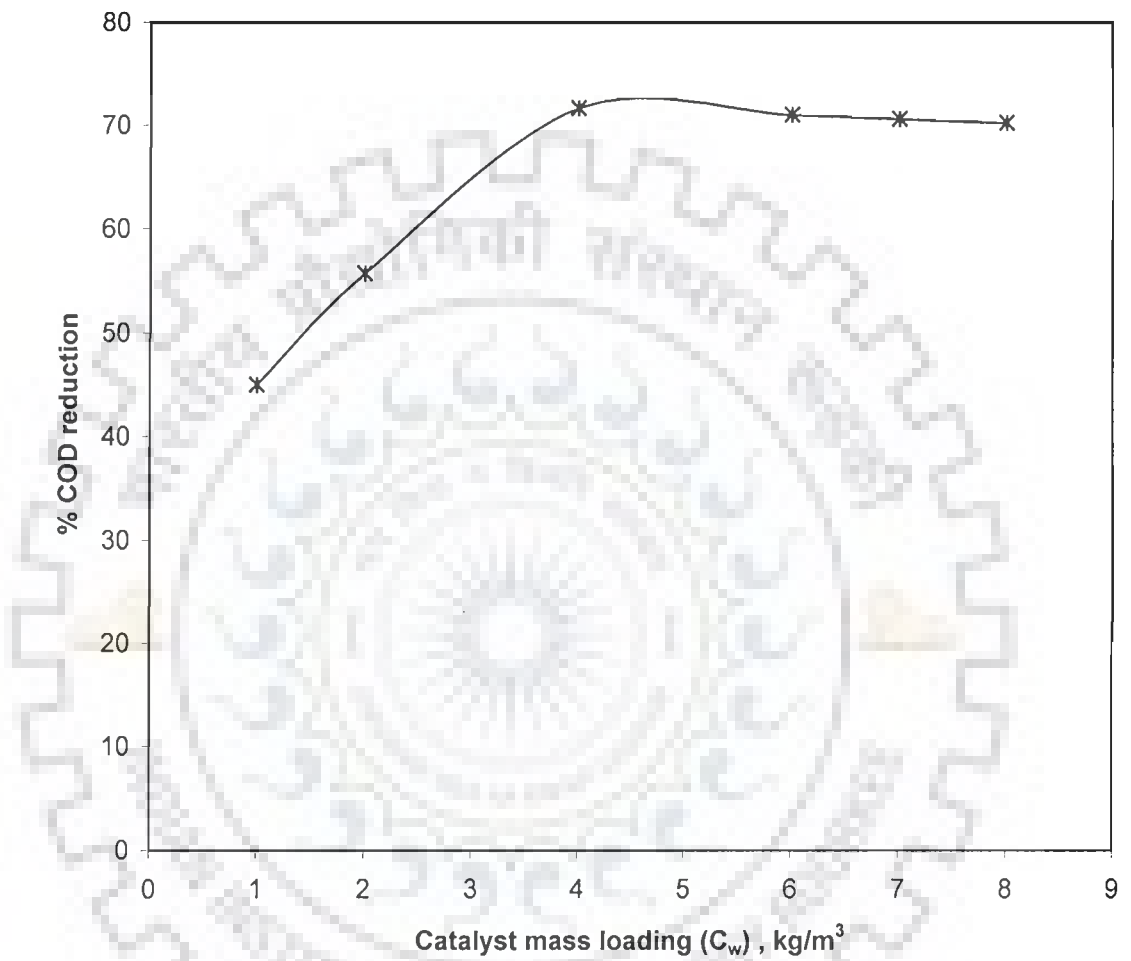
Figure 4.21   Effect of catalyst (copper sulphate) mass loading on COD reduction of the desizing wastewater

COD$_0$ = 2884 mg/l, t$_R$ = 4 h, P = atmospheric, pH$_0$ = 4, T$_R$ = 95°C
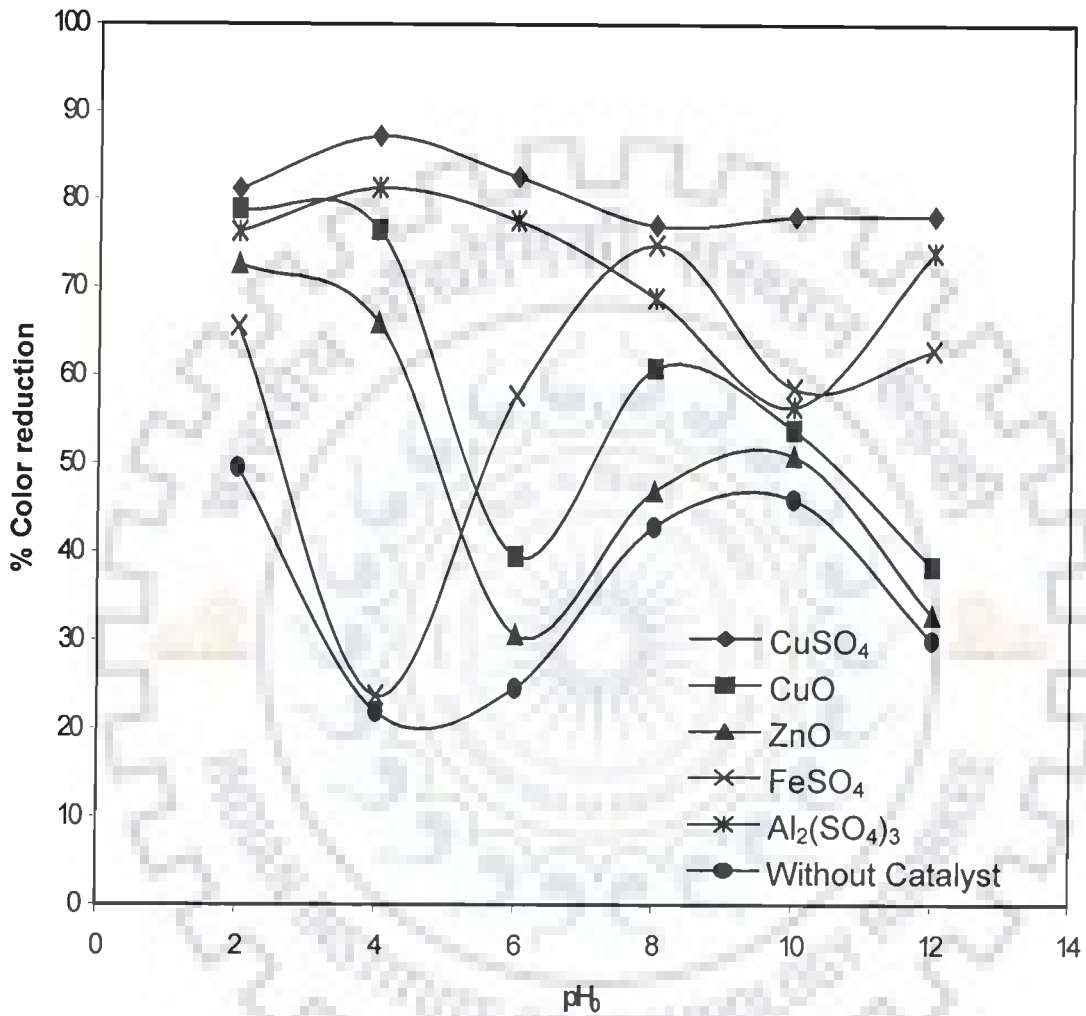
Figure 4.22 Effect of pH$_0$ on color removal of the desizing wastewater by using catalytic thermolysis

t_R = 4 h, P = atmospheric, pH$_0$ = 4, T_R = 95°C, C_w = 4 kg/m^3,

Initial color concentration = 520 PCU

4.3.4 Analysis of Precipitated Sludge and the Supernatant left after the Precipitation

During the use of $CuSO_4$ as chemical agent for the precipitation of dissolved solids, certain amount of Cu^{2+} ions remain in the solution or filtrate (supernatant). The amount of Cu^{2+} ions in the solutions varies with the pH of the solution, as shown in Figure 4.23.
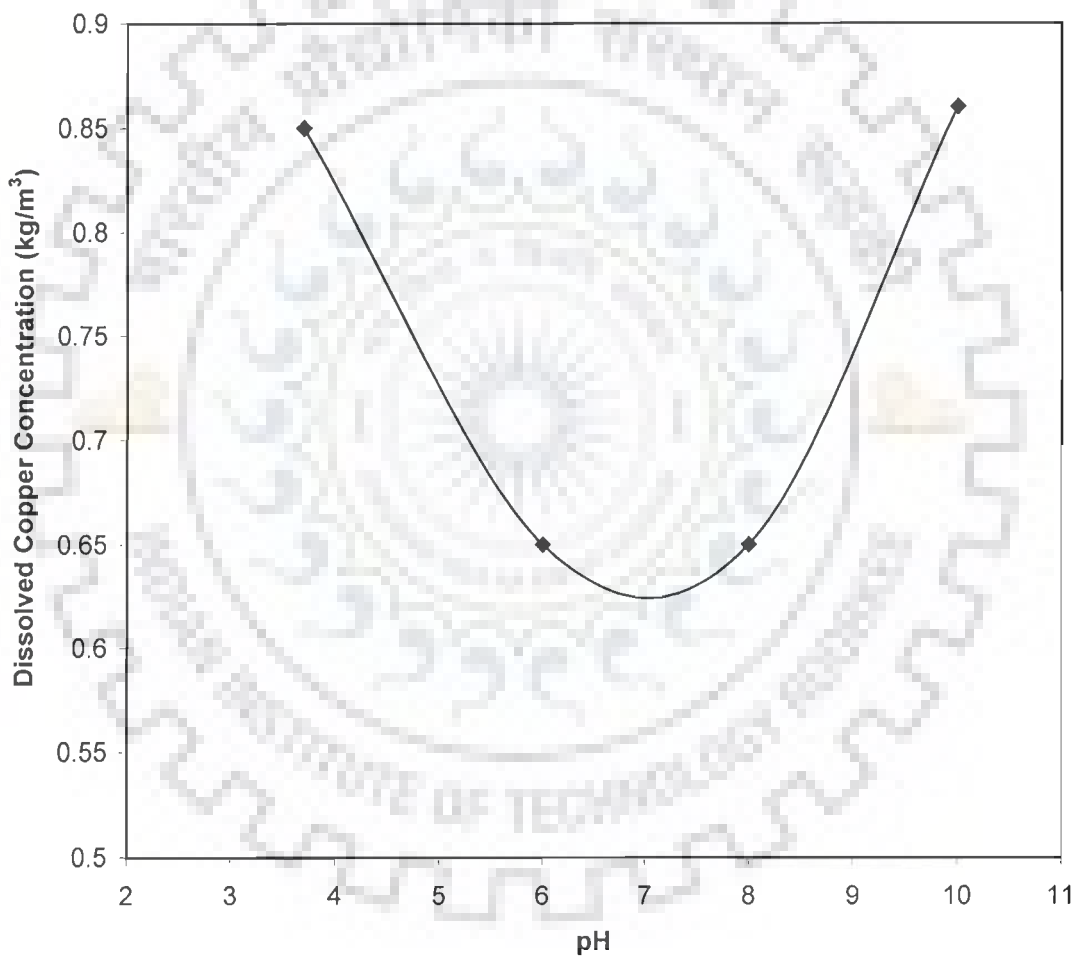
Figure 4.23 Copper concentration in the supernatant (filtrate) as a function of pH (initial $CuSO_4$ concentration = 4 kg/m^3)

The initial Cu^{2+} concentration added to the desizing wastewater was 1.107 kg/m^3 (corresponding to 4 kg/m^3 of $CuSO_4.5H_2O$). The pH of the thermally

pretreated solution was 3.7. In a study, a small amount (50 ml) of the solution was taken and the pH were adjusted to values 6.0, 8.0 and 10.0. The solutions were allowed to remain for 2 h and then filtered, and the Cu^{2+} ion concentration in the filtrate was measured. The copper concentration was found to be almost the same at pH 6 and 8 (at around 0.65 kg/m^3) but at pH 3.7 and 10 the majority of the copper remain in the solution (0.85 and 0.86 kg/m^3, respectively). The presence of Cu^{2+} ions in the solution imparts toxicity to it. However, for the situation where the supernatant is to be taken for catalytic wet oxidation/coagulation (secondary treatment), Cu^{2+} ion concentration in the supernatant may serve as the catalyst/coagulant (Garg et al., 2005, 2007).

It is suggested that in alkaline environment, copper sulfate gets hydrolyzed and forms copper hydroxides, which are insoluble in water. The hydroxide is somewhat amphoteric, dissolving in excess sodium hydroxide solution to form trihydroxycuprate $[Cu(OH)_3]$ and tetrahydroxycuprate $[Cu(OH)_4]$. Thus, in a basic environment, the majority of copper is present in precipitated hydroxide form and very little copper is present in dissolved form in the solution.

Similar results were obtained for composite and dyeing wastewater at corresponding optimum $CuSO_4$ concentration and pH. The copper concentration in the case of supernatant obtained after catalytic thermolysis of composite and dyeing wastewater were 0.06 kg/m^3 and 0.045 kg/m^3, respectively.

4.3.5 Coagulation of Desizing Wastewater

The treatment of fresh desizing wastewater ($COD_0 = 2884$ mg/l) was carried out using different coagulants, such as commercial alum, aluminum potassium sulfate, $FeSO_4$, $FeCl_3$ and PAC. The effect of process parameters, such as, pH, coagulant dose as well as reaction time were observed.

4.3.5.1 Effect of pH_0

The results of the variation of % COD reduction and % color reduction as a function of pH_0 are presented in Figures 4.24(a-b). The pH of the initial feed effluent were varied from 2 to 12, keeping the coagulant dose fixed at 3 kg/m^3 in each run. It has been generally observed that the % reductions reach two maximums, one in acidic region and the other in alkaline region. The maximum COD reduction of 52.46% was observed using commercial alum at pH_0 4. This was followed by aluminum potassium sulfate (pH_0 4), FeCl$_3$ (pH_0 6), PAC (pH_0 6), FeSO$_4$ (pH_0 4) and without coagulant (pH_0 4). The maximum reduction in COD obtained in absence of a coagulant was 19.9% at pH_0 4.

Similar trend was observed during variation in % color reduction as a function of pH_0. The maximum % color reduction of 79% was observed using commercial alum at pH_0 4. This was followed by aluminum potassium sulfate (pH_0 4), PAC (pH_0 4), FeSO$_4$ (pH_0 2), FeCl$_3$ (pH_0 6) and no coagulant (pH_0 4).

4.3.5.2 Effect of Coagulant Dose (C_w)

During these runs the coagulant dose was varied from 1 to 7 kg/m^3 and the pH of the initial effluent was fixed at 4. The results for % COD as well as % color reduction are shown in Figure 4.25 using commercial alum as coagulant. It is observed that the % COD reduction as well as % color reductions increase linearly with increase in coagulant dose from 1 to 5 kg/m^3. The rising trend, however, do not continue beyond 5 kg/m^3, getting almost no increase in the reduction of both the parameters. The maximum COD reduction observed at a coagulant dose of 5 kg/m^3 was 58.34% whereas the color reduction at these conditions was 85%.
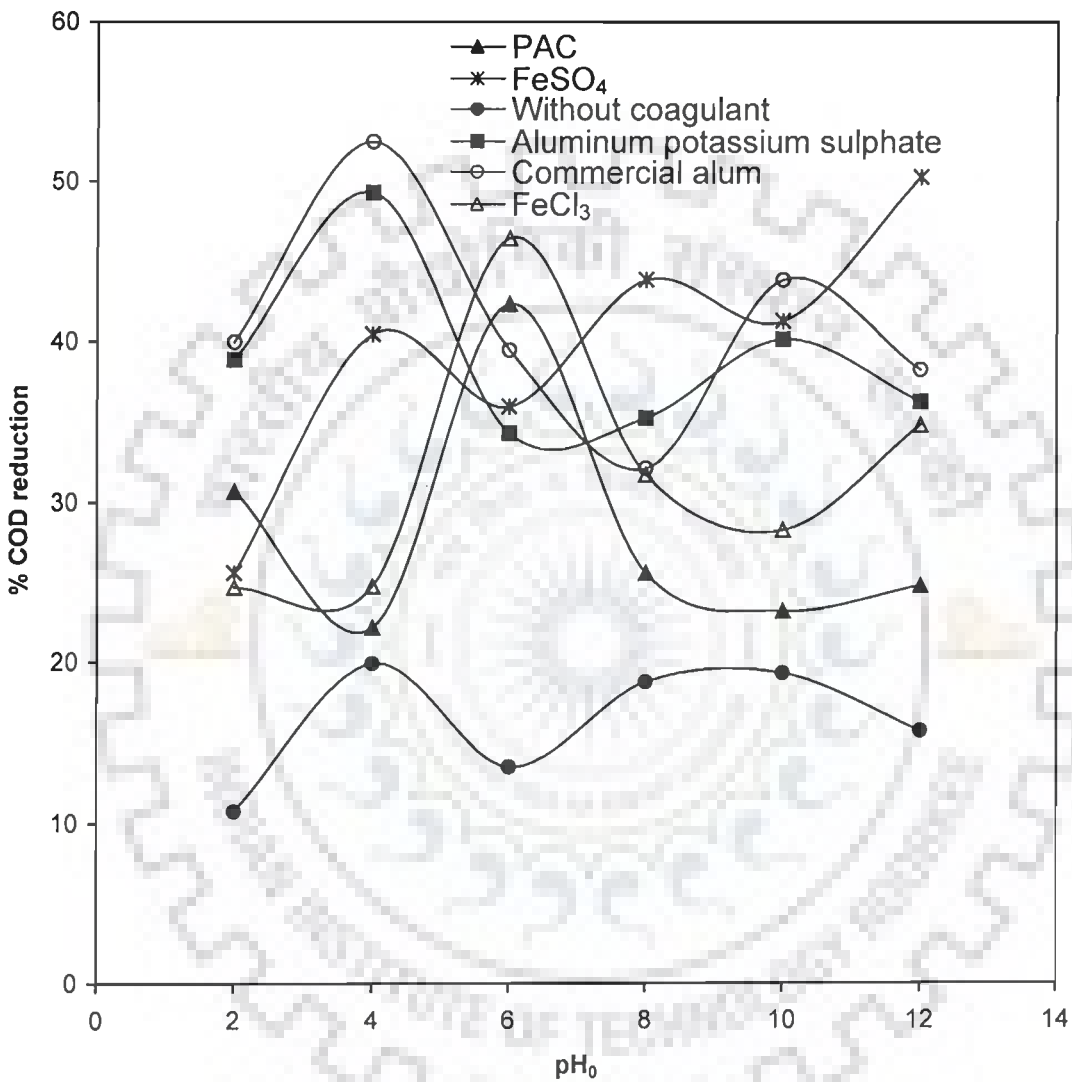
Figure 4.24(a) Effect of pH$_0$ on COD reduction of the desizing wastewater by using different coagulants

P = atmospheric pressure, COD$_0$ = 2884 mg/l, C$_w$ = 3 kg/m^3
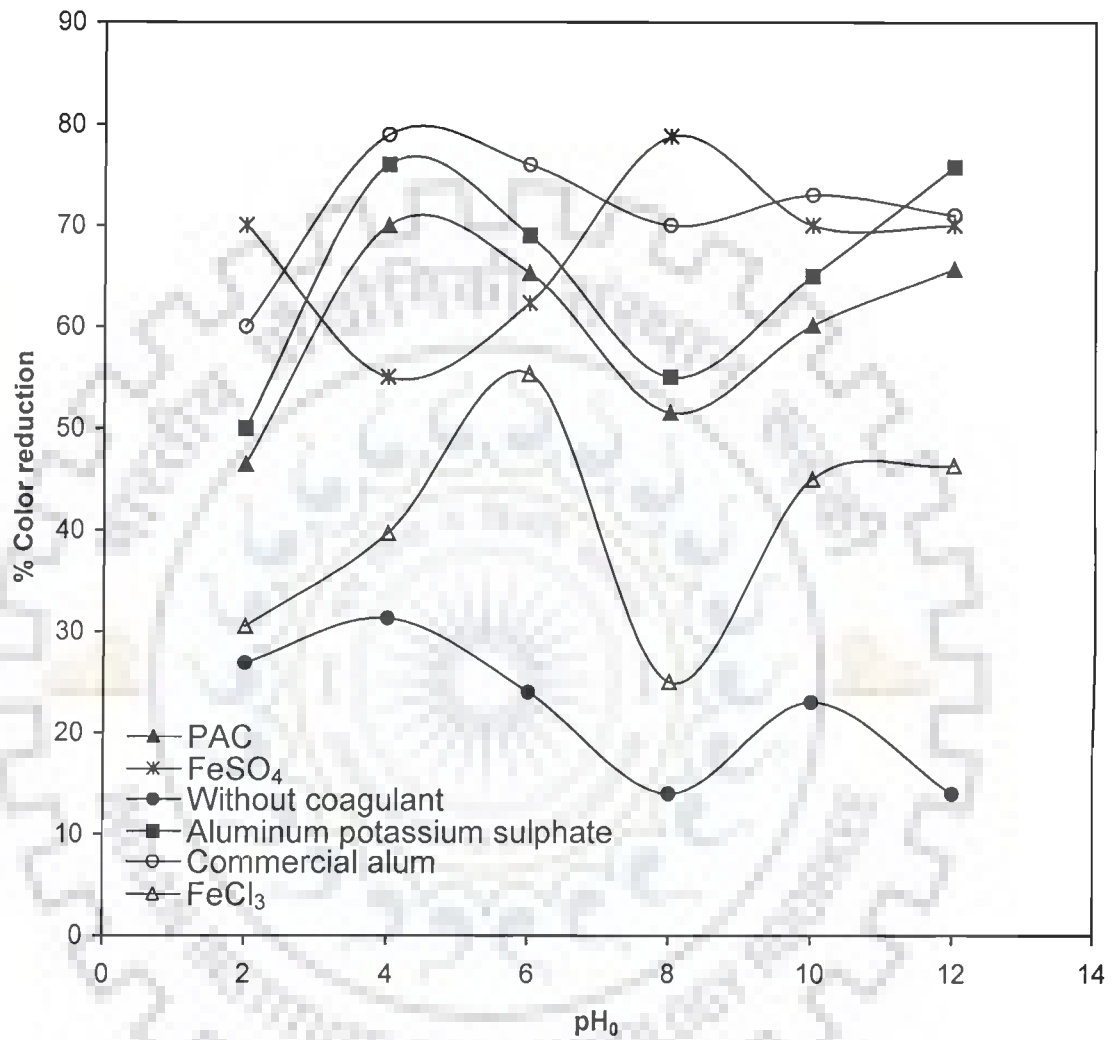
Figure 4.24(b) Effect of pH_0 on color reduction of the desizing wastewater by using different coagulants

P = atmospheric pressure, COD_0 = 2884 mg/l, C_w = 3 kg/m³,

Initial color concentration = 520 PCU
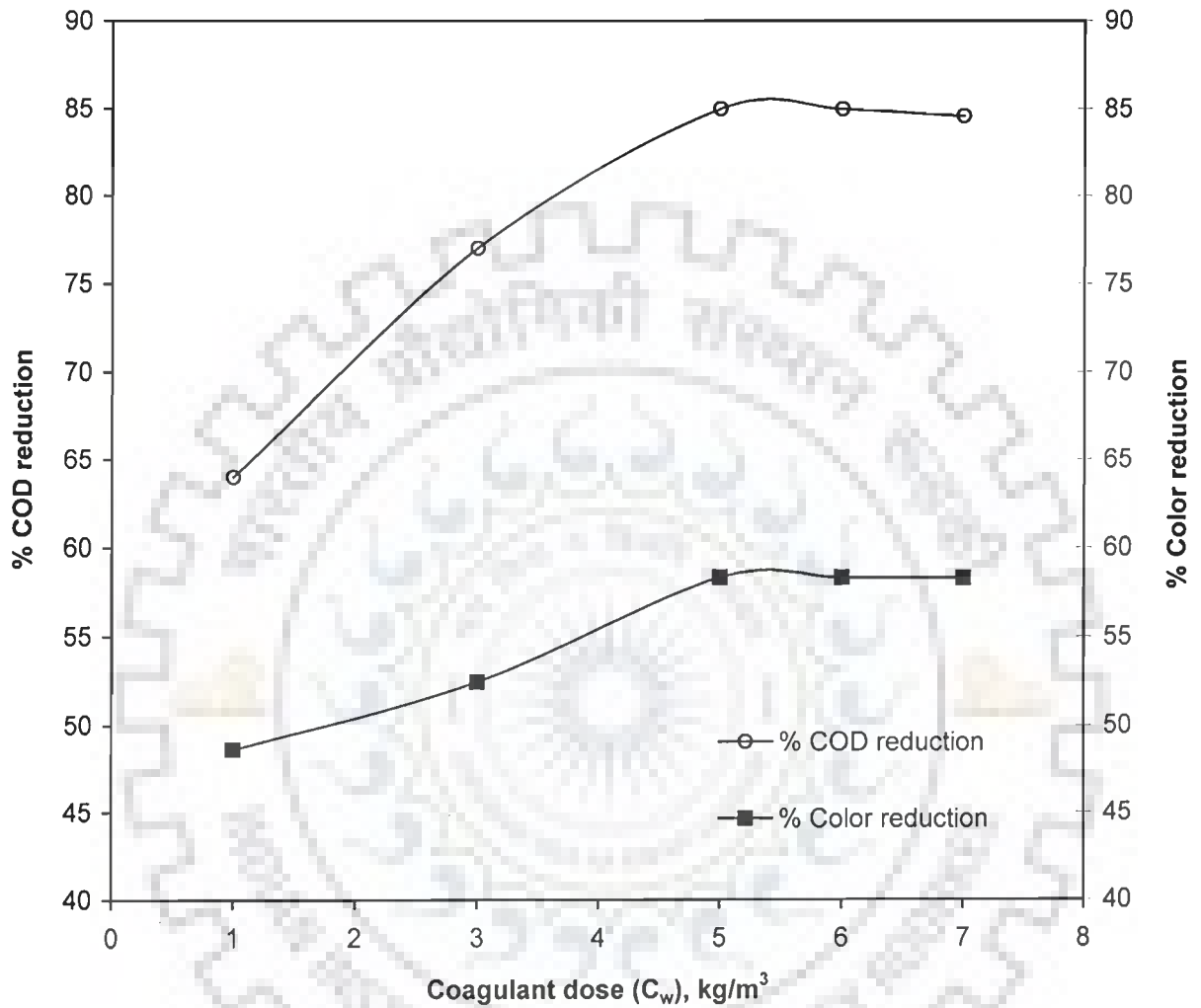
Figure 4.25 Effect of coagulant (commercial alum) dose on COD and color reduction of the desizing wastewater

P = atmospheric pressure, COD_0 = 2884 mg/l, pH = 4,

Initial color concentration = 520 PCU

4.3.6   Catalytic thermolysis followed by Coagulation

Figures 4.26(a-b) show the results of % COD as well as % color reductions as a function of time during the treatment of desizing wastewater (COD_0 = 2884 mg/l). The plots compare the result of coagulation with and without catalytic thermolysis. It is observed that coagulation of the supernatant obtained after catalytic thermolysis is more effective in treating the effluent than the individual processes. The figures demonstrate a reaction time of 60 min is enough to achieve the steady state operation.

The application of coagulation to the supernatant obtained after thermolysis show a removal of 87.96 % COD and 96.0 % color at above mentioned conditions except at a coagulant dose of 1 kg/m^3. The amount of inorganic sludge obtained due to the addition of coagulant is, thus, drastically reduced due to the reduced amount (almost 25%) of coagulant. The COD and color of the final effluent were found to be 98.6 mg/l and   2.67 PCU, respectively and the COD/BOD_3 ratio was 1.36.
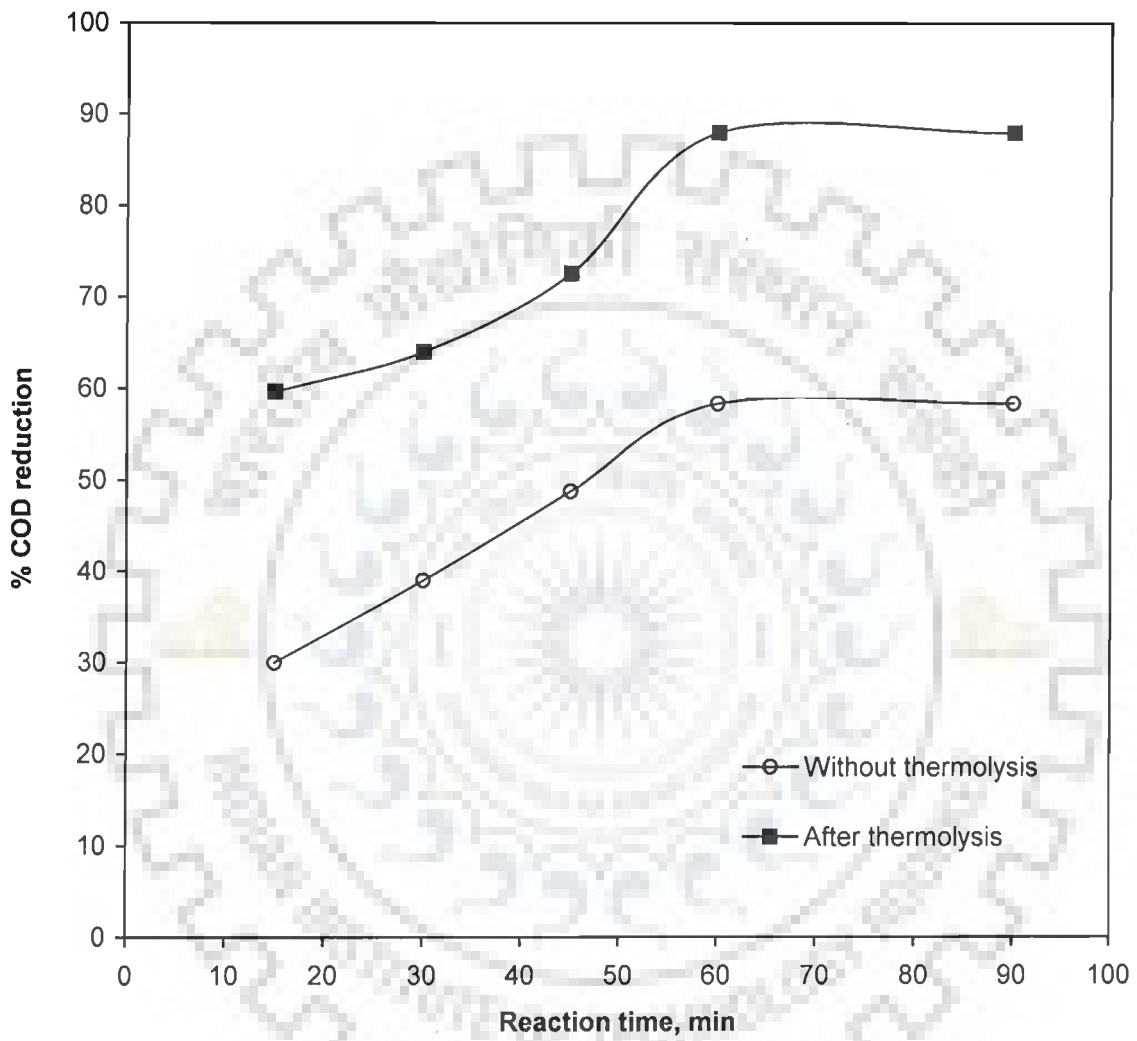
Figure 4.26(a) Reduction of COD with time by coagulation using commercial alum as coagulant

P = atmospheric pressure, COD_0 = 2884 mg/l, pH = 4, T = 18°C.
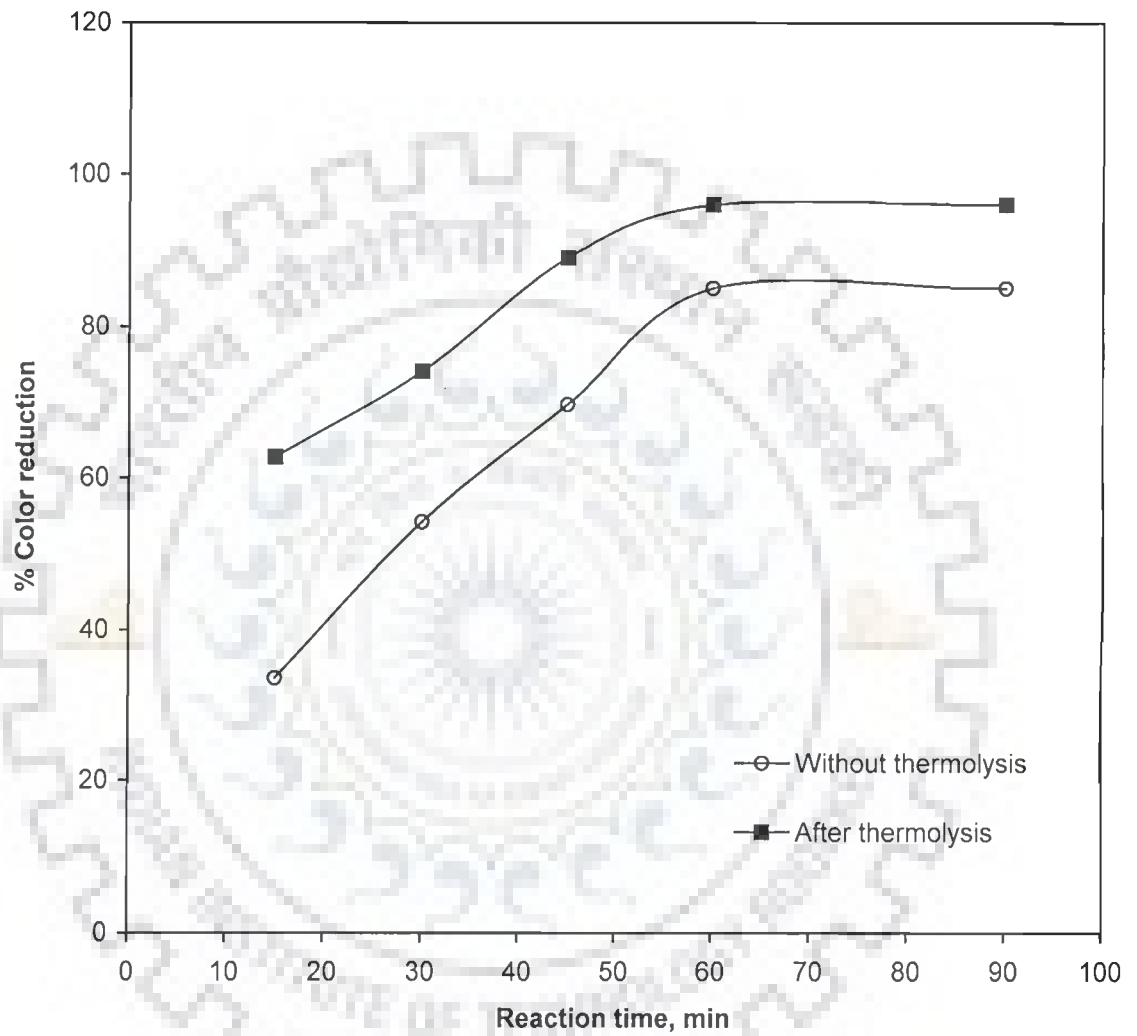
Figure 4.26(b) Reduction of color with time by coagulation using commercial alum as coagulant

P = atmospheric pressure, COD_0 = 2884 mg/l, pH = 4, T = 18°C,

Initial color concentration = 520 PCU

4.3.7 FTIR Analysis of Dried Residues of Desizing Wastewater Before and After Treatment

IR spectral studies of waste samples (before and after treatment) provide useful information on the presence of different functional groups. For example, desizing wastewater sample exhibits a broad band covering the region 3300-2800 cm^{-1} suggesting the presence of hydrogen bonded ν(OH) group. A broad band at ~1600 cm^{-1} due to δ(OH) further suggest the presence of hydroxyl group (Figure 4.27a). A strong band at 1124 cm^{-1} confirms the presence of sulfate group possibly attached with metal ions. In addition, the presence of C=C (conjugated carbon-carbon bond) is indicated by the presence of medium intensity band at 1582 cm^{-1}.

On treatment with $CuSO_4$ resulted in the separation of sludge which on drying gave relative sharper but still broad band at ~3400 cm^{-1}. This is possibly due to breaking of hydrogen bond and presence of either free hydroxyl or coordinated hydroxyl group. This also suggests the precipitation of component bearing hydroxyl group present in either complexed or free form. Absence of band due to sulphate group in this component indicates the removal of sulphate group as water soluble component. The band at 1086 cm^{-1} is possibly due to the presence of metal oxide, which is further supported by the appearance of two bands at 619 and 461 cm^{-1} due to ν(M-O) (Figure 4.27b).

A broad band appearing in the 3400 cm^{-1} region in dried desizing wastewater (Figure 4.27c) suggests the presence of ν(OH) due to the presence of hydroxyl groups from different components. Treatment with commercial alum and copper sulphate showed a decrease in the ν(OH) peak in the spectra. This decrease in broadness indicates the precipitation of a particular type of component. The band covering the region 2850-2924 cm^{-1} in dried desizing waste as well as solid residue after the treatment indicates the presence of - CH_2 group.
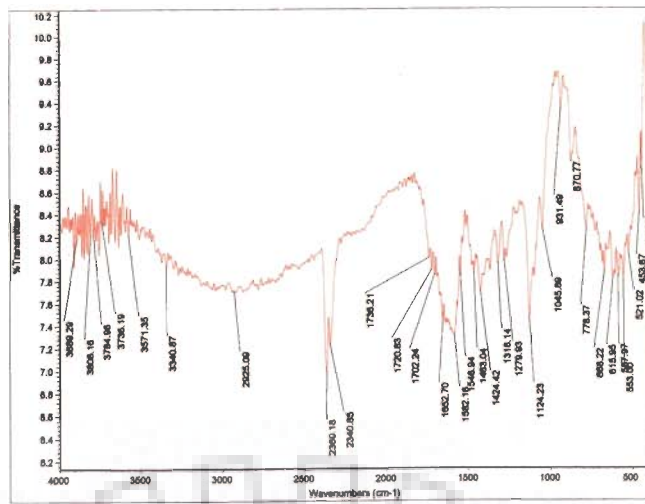
(a) Dried desizing wastewater
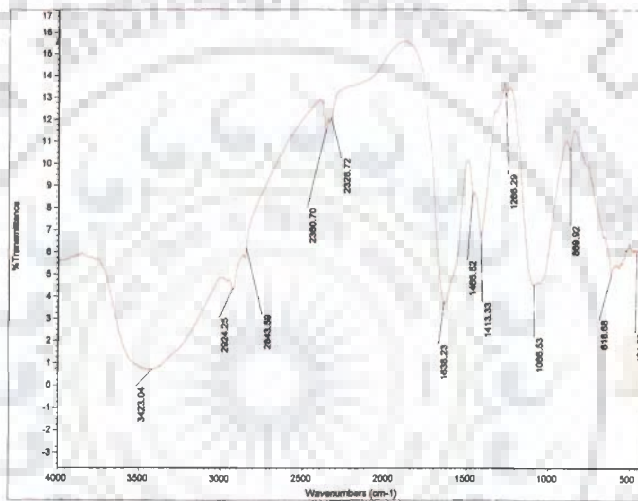
(b) After catalytic thermolysis
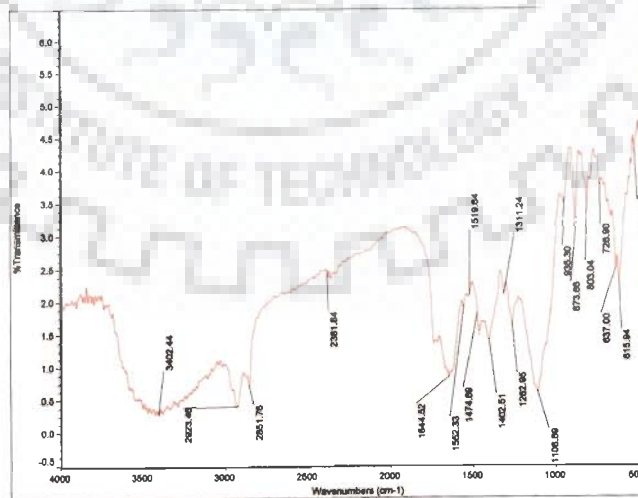
(c) After coagulation

Figure 4.27 FTIR spectra of desizing wastewater

132

A medium intensity band at 1552 cm^{-1} is assigned to C = C conjugate bond. This bond is slightly shifted to higher wave number due to adjustment of current after coordination of part of the – OH group with metal. The presence of two bands at 1680 and 1450 cm^{-1} in the dried sample are due to antisymmetric and symmetric modes of carboxylic acid. It is expected that glucoisosacchararinic acid having carboxylic group may be present in the cellulose derivatives. The Δ(antisym-sym) value of 230 cm^{-1} suggests the monodentate coordination of carboxylate group with metal salt on treatment. Presence of sulphate group as a sharp band still appears at 1109 cm^{-1} due to ν(S=O).

Interestingly, the bands appearing at 2341 and 2360 cm^{-1} in both of the above wastes/sludges are absent suggesting either the conversion of this group to other components or their removal during treatment.

4.4   MECHANISM OF COAGULATIVE TREATMENT

The chemical aspects of coagulation can be explained by an examination of the hydrolysis of metal ions. The hydrolytic reactions of metal ions like Al have been used extensively to explain coagulation mechanisms of humic substances (Hundt and O'Melia, 1988; Dempsey *et al.,* 1984; Edwards and Amirtharajah, 1985; Mangravite *et al.,* 1975). The particular form of the Al species present at a given pH is assumed to be responsible for the actual coagulation process under similar conditions.

The interpretation of hydrolysis study results for water treatment plant conditions is not straightforward. Even when Al hydrolysis is studied under conditions similar to those in water treatment, it is not sure that similar species will exist in the presence of other substances since hydrolysis and interactions between Al and other materials are complex reactions.

Aluminum species are found to be present in deionized water in the form of Al^{3+}, $Al(OH)^{2+}$, $Al(OH)_2^+$, $Al(OH)_{3(S)}$, $Al(OH)_4^-$, etc. (Benschoazn and Edzwald, 1990). In tap water, the species may be carbonate, bicarbonate, sulfate, chloride, etc. depending upon the presence of these anions in the water. The concentration of the hydrolyzed aluminum species depends on the aluminum concentration, and the solution pH. The speciation of Al(III) ions in deionized water is presented in Figure 4.28. The percentage of Al^{3+} hydrolytic products was calculated from the following stability constants (Duan and Gregory, 2003):

$$Al^{3+} + H_2O \rightleftharpoons Al(OH)^{2+} + H^+ \qquad pK_1 = 4.95$$

$$Al(OH)^{2+} + H_2O \rightleftharpoons Al(OH)_2^+ + H^+ \qquad pK_2 = 5.6$$

$$Al(OH)_2^+ + H_2O \rightleftharpoons Al(OH)_3 + H^+ \qquad pK_3 = 6.7$$

$$Al(OH)_3 + H_2O \rightleftharpoons Al(OH)_4^- + H^+ \qquad pK_4 = 5.6$$

The distribution of various Fe^{3+} species as a function of *pH* as calculated from the following stability constants has been presented in Figure 4.29:

$$Fe^{3+} + H_2O \rightleftharpoons Fe(OH)^{2+} + H^+ \qquad pK_1 = 2.2$$

$$Fe(OH)^{2+} + H_2O \rightleftharpoons Fe(OH)_2^+ + H^+ \qquad pK_2 = 3.5$$

$$Fe(OH)_2^+ + H_2O \rightleftharpoons Fe(OH)_3 + H^+ \qquad pK_3 = 6$$

$$Fe(OH)_3 + H_2O \rightleftharpoons Fe(OH)_4^- + H^+ \qquad pK_4 = 10$$
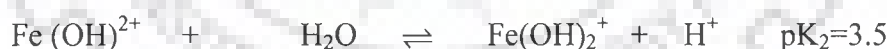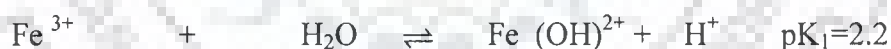
Martin (1991) has pointed out a significant difference in the hydrolysis behavior of Al and Fe, which is apparent in Figures 1 to 3. The hydrolysis constants for Al cover a much narrower range than those for Fe. The latter are spaced over approximately 8 pH units, whereas all of the Al deprotonations are 'squeezed' into an interval of less than 1 unit. Martin (1991) explained this feature by the transition from the octahedral

hexahydrate $Al^{3+}.6H_2O$ to the tetrahedral $Al(OH)_4^-$. This makes the successive

hydrolysis steps co-operative in nature. All of the hydrolysed species for Fe^{3+} retain the

octahedral co-ordination and the stepwise deprotonations show the expected spread of

pK values. This difference is clearly seen in the plots of species distributions in Figure

4.28 & 4.29, which show the mole fraction of the various soluble hydrolysis products in

equilibrium with the amorphous precipitate. The ferric species each attain significant

relative concentrations in solution at appropriate pH values, whereas for Al, apart from

a narrow pH region approximately 5–6, the dominant soluble species are Al^{3+} and

$Al(OH)_4^-$ at low and high pH, respectively.

The percentage of Fe^{2+} hydrolytic products was calculated from the following

stability constants, and is presented in Figure 4.30 (Benjamin, 2002):

$$Fe^{2+} \quad + \quad H_2O \quad \rightleftharpoons \quad Fe(OH)^+ + \quad H^+ \quad pK_1=9.5$$

$$Fe(OH)^+ \quad + \quad H_2O \quad \rightleftharpoons \quad Fe(OH)_2 + \quad H^+ \quad pK_2=11.07$$

$$Fe(OH)_2 \quad + \quad H_2O \quad \rightleftharpoons \quad Fe(OH)_3^- + \quad H^+ \quad pK_3=10.43$$
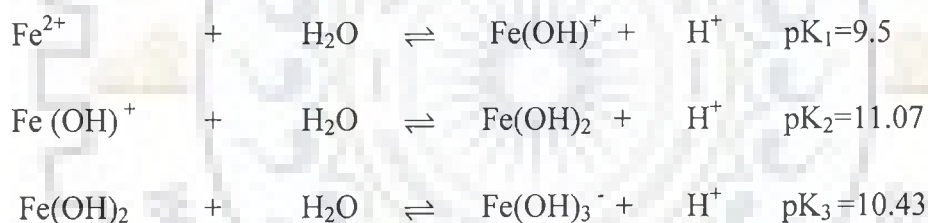
The percentage of Cu^{2+} hydrolytic products was calculated from the following

stability constants, and is presented in Figure 4.31 (Benjamin, 2002):

$$Cu^{2+} \quad + H_2O \quad \rightleftharpoons \quad Cu(OH)^+ \quad + \quad H^+ \quad pK_1=8$$

$$Cu(OH)^+ \quad + H_2O \quad \rightleftharpoons \quad Cu(OH)_2 \quad + \quad H^+ \quad pK_2=5.68$$

$$Cu(OH)_2 \quad + H_2O \quad \rightleftharpoons \quad Cu(OH)_3^- \quad + \quad H^+ \quad pK_3=13.22$$

$$Cu(OH)_3^- \quad + H_2O \quad \rightleftharpoons \quad Cu(OH)_4^{2-} \quad + \quad H^+ \quad pK_4=12.70$$
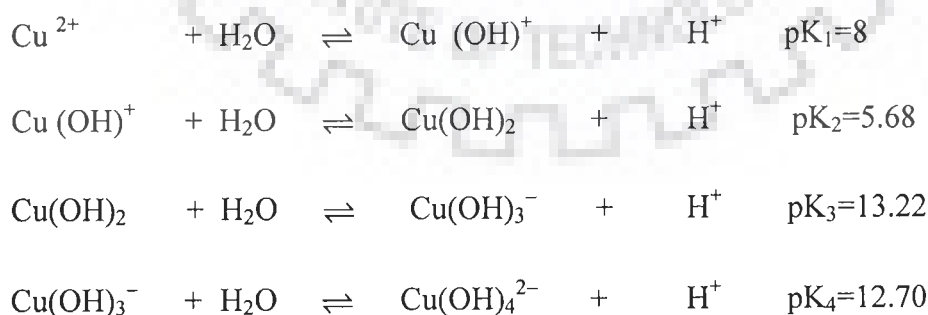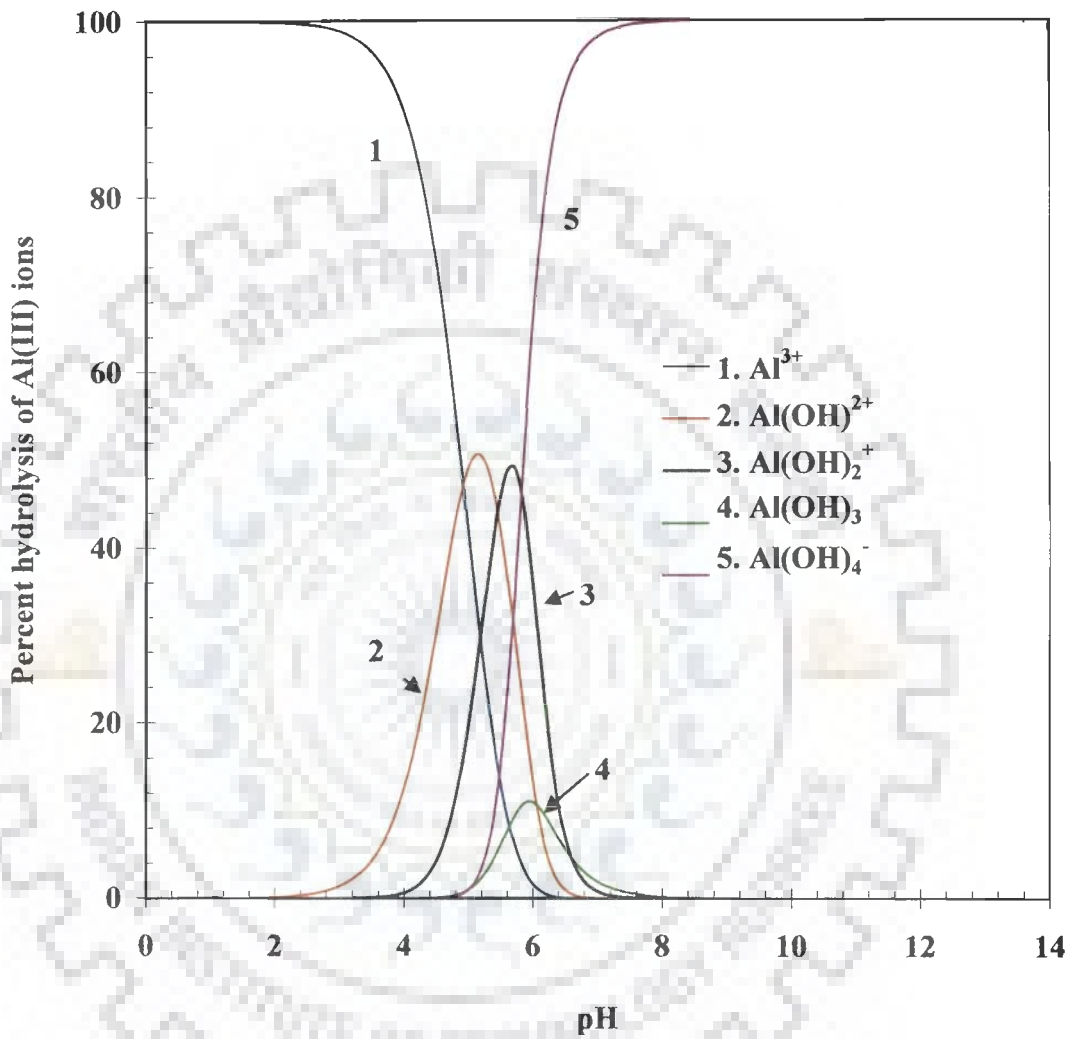
Fig. 4.28 Speciation diagram of Al(III) ion
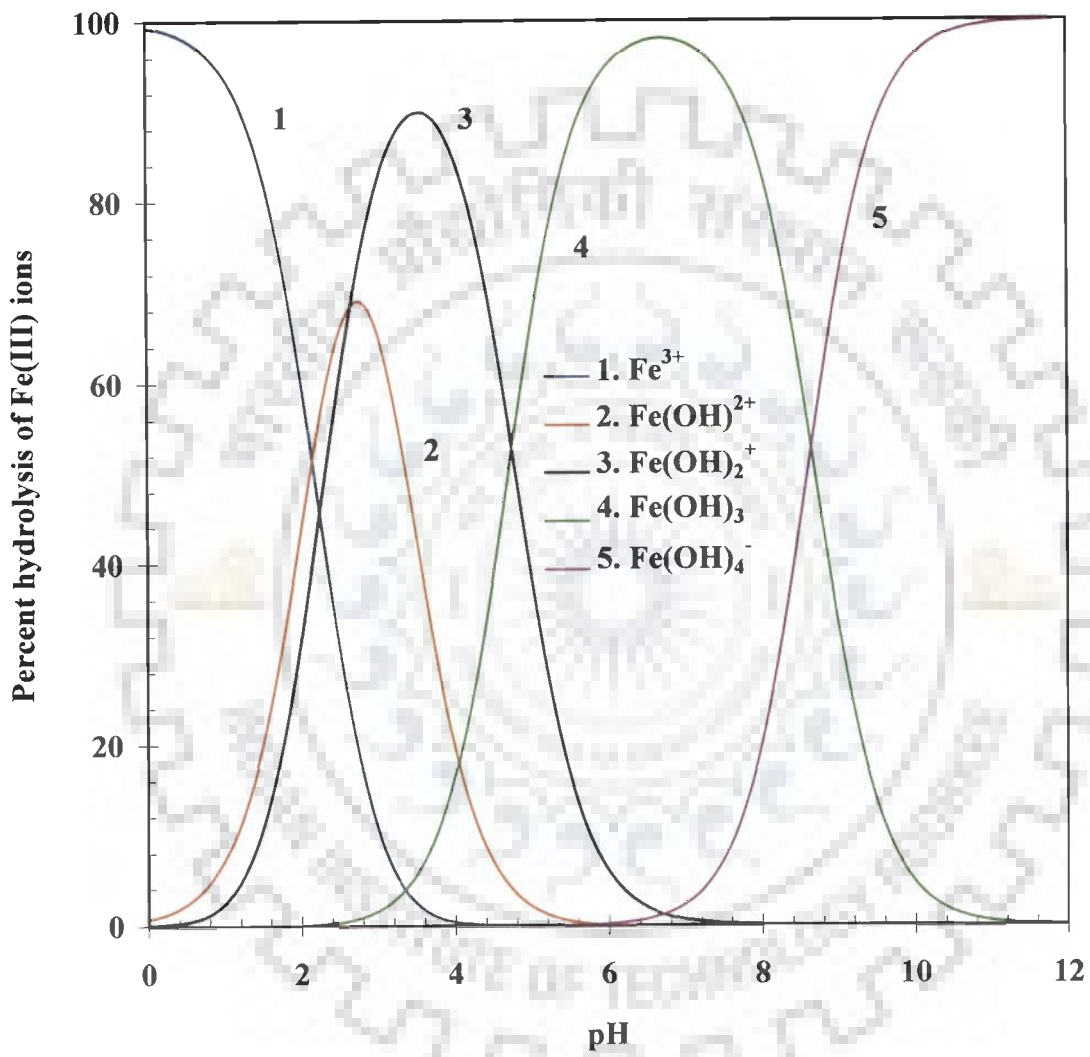
Fig. 4.29 Speciation diagram of Fe(III) ion

137
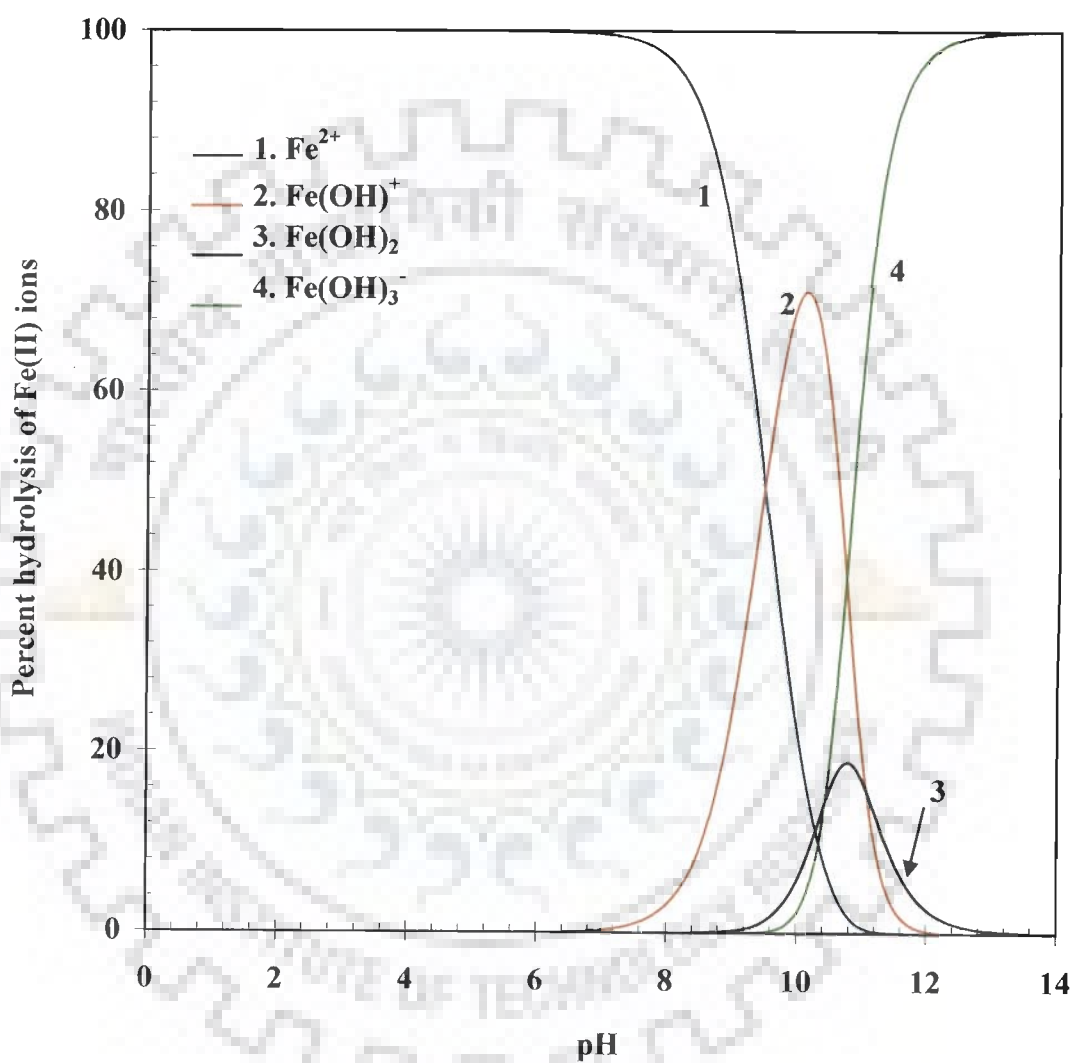
Fig. 4.30 Speciation diagram of Fe(II) ion
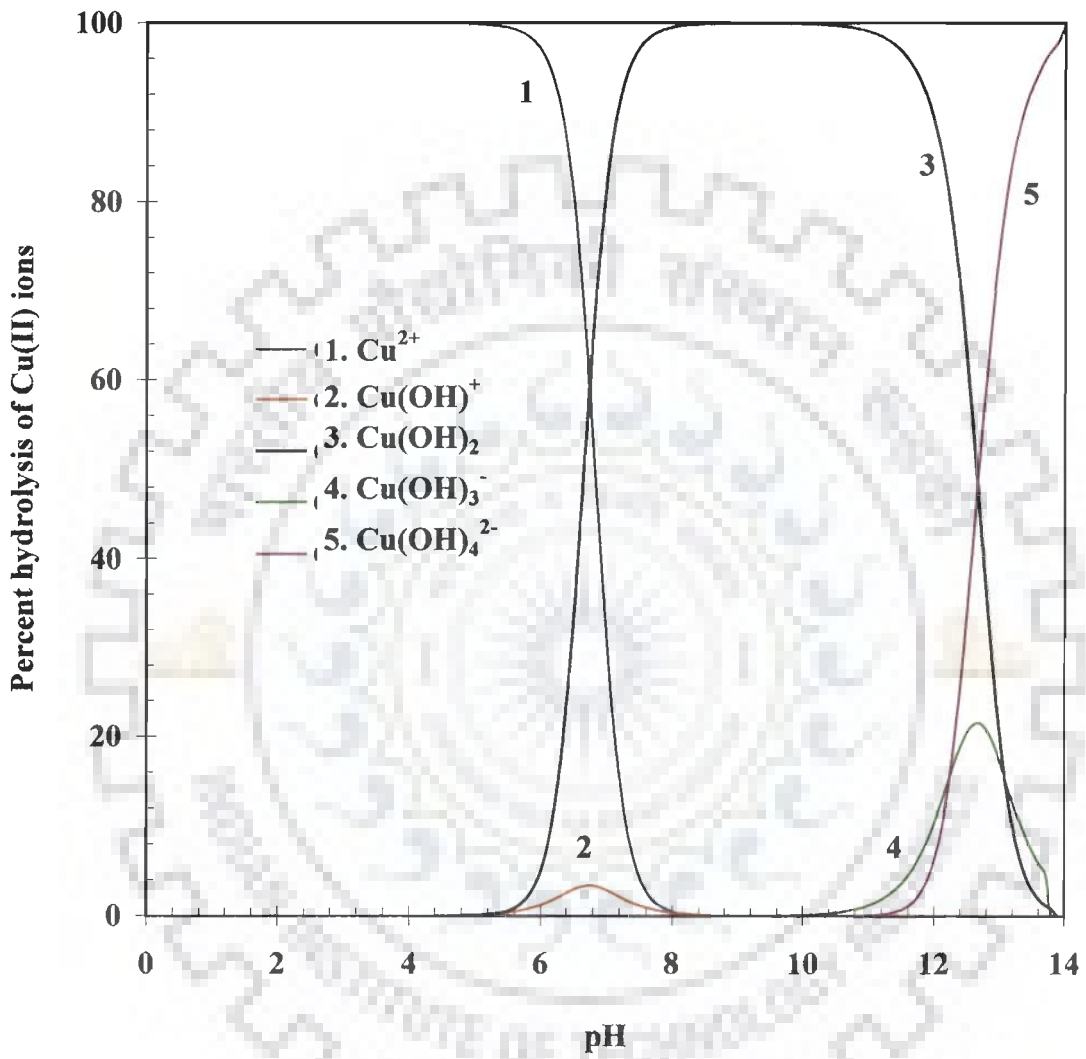
Fig. 4.31 Speciation diagram of Cu(II) ion

4.4.1 Mechanism of Coagulative Treatment of Composite Wastewater

The effect of pH on the COD and color reduction during coagulation of the fresh composite wastewater is presented in Figures 4.32(a-b). The coagulants used included aluminum potassium sulphate $[KAl(SO_4)_2.16H_2O]$, commercial alum $[Al_2(SO_4)_3.nH_2O]$, $FeSO_4.7H_2O$, $FeCl_3$ and PAC $[(Al_2(OH)_nCl_{6-n}]_m$.

A general trend of increase in COD reduction with an increase in pH_0 (from 2 to 12) was observed. The major increase was from pH_0 4 to pH_0 10. Aluminum potassium sulphate was found to be the best coagulant giving 84-88% COD reduction and about 95% color reduction at pH_0 8.

For a number of coagulants, pH_0 8 happens to be the optimum pH for both COD and color reduction. The reduction in COD is much higher under alkaline conditions than those under acidic conditions. A similar trend was also observed for color reduction with PAC and $FeSO_4$.

It is evident from Figure 4.33 that at pH > 8.0, $Al(OH)_4^-$ is the main component of aluminum present in the water. The natural pH of the composite wastewater is 9.1 (Table 4.4), therefore, the major colloids present are negatively charged at pH 8.0. The first layer of cations attracted to the negatively charged surface are "bound" to the colloid and travel with it, should displacement of the colloid relative to the water occur.

The aquometallic ion, $Al(OH)_4^-$, thus formed is soluble in water (Duang and Gregory, 2003). It becomes part of the ionic cloud surrounding the colloid and, because of its great affinity for surfaces, gets adsorbed onto the surface of the colloid where it neutralizes the surface charge. Once the surface charge has been neutralized, the ionic cloud dissipates and the electrostatic potential disappears so that contact occurs freely. It may, therefore, be inferred that the charge neutralization is the main mechanism for

the COD reduction at pH 8.0 by aluminum potassium sulphate [$KAl(SO_4)_2.16H_2O$] and commercial alum [$Al_2(SO_4)_3.nH_2O$].

4.4.2 Mechanism of Coagulative Treatment of Dyeing Wastewater

The effect of various coagulants on COD and color reduction of dyeing wastewater is shown, respectively, in Figures 4.34 and 4.35. Maximum COD and color reductions are obtained (34.57% and 60.33%, respectively) using commercial alum as a coagulant at pH_0 4 and a coagulant concentration of 3 kg/m^3. The effect of pH_0 on the color reduction could be explained by the combined effect of (i) the ionization of amino, hydroxy and sulpho groups present in the dye molecules which increases with pH in the acidic range, and (ii) the decrease in the concentration of dissolved hydrolysis products (Papic et al., 2004). Aluminum based coagulants show better results than those of iron based coagulants in the removal of COD and color of the dyeing wastewater.

The cationic compounds of the hydrolyzed dyes act as good reagents and electron acceptors from Al^{3+}. The Al cations get associated and form complexes with hydrolyzed dye species. The local negative charge of these groups are neutralized by Al cations, resulting in colloid destabilization and precipitation of metal (cations)-organics (anions) complexes. This phenomenon induces sweep flocculation and the enhancement, adsorption and bridging of both particulate organics and inorganic solids to form large, amorphous flocs (Jeckel, 1986). The large amorphous mass enmeshes the organics present in dyeing wastewater. Thus, the complexation followed by precipitation and the capture of organics in the gel are responsible for both COD and color reduction by aluminum based coagulants compared to those obtained with $FeSO_4$ and $FeCl_3$.

Figures 4.36 and 4.37 reveal that the optimum pH_0 for COD and color reduction for all the five coagulants are different. Some are more active in acidic medium whereas the others are active in alkaline medium. The reduction of dissolved organics during coagulation with metal salts at different pH_0 follows two different mechanisms. At low pH, the anionic organic molecules present in the effluent coordinate with metal cations and form insoluble metal complexes. At higher pH (alkaline range), the organics are adsorbed on to pre-formed flocs of metal hydroxides and get precipitated. The combined effect of the two mechanisms is that the reduction of dissolved organics with different functional groups can occur at different pH_0. The maximum COD and color removal may thus occur at a pH_0 where the combined effect of both the mechanisms is maximum.

4.4.3 Mechanism of Coagulative Treatment of Desizing Wastewater

The treatment of fresh desizing wastewater was carried out using coagulants, such as commercial alum, aluminum potassium sulfate, $FeSO_4$, $FeCl_3$ and PAC. The results of the variation of COD reduction as well as color reduction as a function of pH_0 are presented in Figures 4.38(a-b). It has been generally observed that the percent reductions reach two maximums, one in acidic region and the other in alkaline region. The maximum COD reduction of 52.46% was observed using commercial alum at pH_0 4. This was followed by aluminum potassium sulfate (pH_0 4), $FeCl_3$ (pH_0 6), PAC (pH_0 6) and $FeSO_4$ (pH_0 4).

The natural pH of the desizing wastewater is 4.0 (Table 4.5). The adsorption of natural organic matter present in the wastewater on the colloids will give a negative surface charge (Duan and Gregory, 2003). It is evident from Figure 4.39 that at pH ~ 4.0, Al^{3+} is the main component of aluminum present in the water. It is predicted that

142

this metallic anion gets adsorbed onto the negatively charged cations causing charge neutralization. This may allow different colloids to come together and enhance the COD and color reduction at pH $\sim$ 4.0. Heterocoagulation may also explain this behaviour. Heterocoagulation occurs between two different types of particles. When the two particles have different charges, both the van der Walls and the electrostatic forces act and this provide the conditions for an effective coagulation (Sundin, 2000).

4.5 KINETICS OF CATALYTIC THERMOLYSIS PROCESS OF COMPOSITE, DYEING AND DESIZING WASTEWATER

The catalytic thermolysis process can be represented for textile wastewater (composite wastewater, dyeing wastewater and desizing wastewater) as

$$\text{Complex organic matter} \xrightarrow[\text{Heat + } H_2O]{\text{Catalyst}}$$

$$\text{solid residue + smaller organic molecules + water + gas} \qquad (1)$$
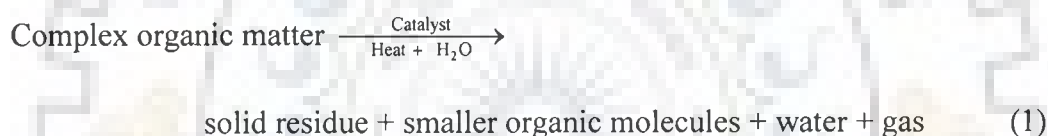
This reaction (1) can be written by a simple reaction as

$$A \xrightarrow[\text{Heat + } H_2O]{\text{Catalyst}} B + C + D \qquad (2)$$
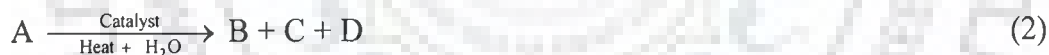
Where, A represents the complex organics effluent, B the solid residue, C the smaller organic molecules and D the gas. Gas formation is too little and is, therefore, ignored. The kinetics of catalytic thermolysis process may be represented by a simple power law rate equation :

$$-\frac{dC_A}{dt} = k\, C_A^n \qquad (3)$$

where n is the reaction order with respect to COD and k is the reaction rate constant. As observed in catalytic thermolysis study, the majority of the catalyst gets complexed with the solid residue and the residual copper is present in the solution. From the mechanistic point of view, the representation of the complex formation and COD

reduction can not be made completely to our satisfaction. Since the catalyst is not lost during catalytic thermolysis and the power law model seems to adequately and satisfactorily represent the global kinetics of catalytic thermolysis, the sample kinetics seems to be useful. Taking lumped organics to be represented by the COD of the composite wastewater, C_A may be written as (COD), and equation (3) can be rewritten as

$$-\frac{d(COD)}{dt} = k\,(COD)^n \tag{4}$$

Figures 4.39-4.41 show the variation of COD reduction with time during catalytic thermolysis of composite, dyeing and desizing wastewater, respectively. These figures show that in all the cases, the COD reduction is fast during the initial reaction period. Later on, the reaction becomes slow and sluggish. Thus, the COD reduction is a two step process. This two step process manifests for all treatment temperatures and pH_0. Since the plot of COD reduction versus time is not linear, it is not a zero order reaction as reported by Lele et al. (1989) for non-catalytic thermal pretreatment of composite wastewater. Daga et al. (1986) have reported first order kinetics for hydrolysis (catalytic thermolysis) of composite wastewater.

Belkacemi et al. (1999) and Chaudhari et al. (2005) also reported kinetics for catalytic thermolysis of grass and molasses-based alcohol distillery liquors. Chen et al. (2003) have reported first order kinetics for thermal treatment and wet air oxidation of printing and dyeing wastewater. Based on the previous studies and the nature of the curve (COD reduction versus time), the COD reduction process in composite, dyeing and desizing wastewaters can be represented adequately by the first order reaction.
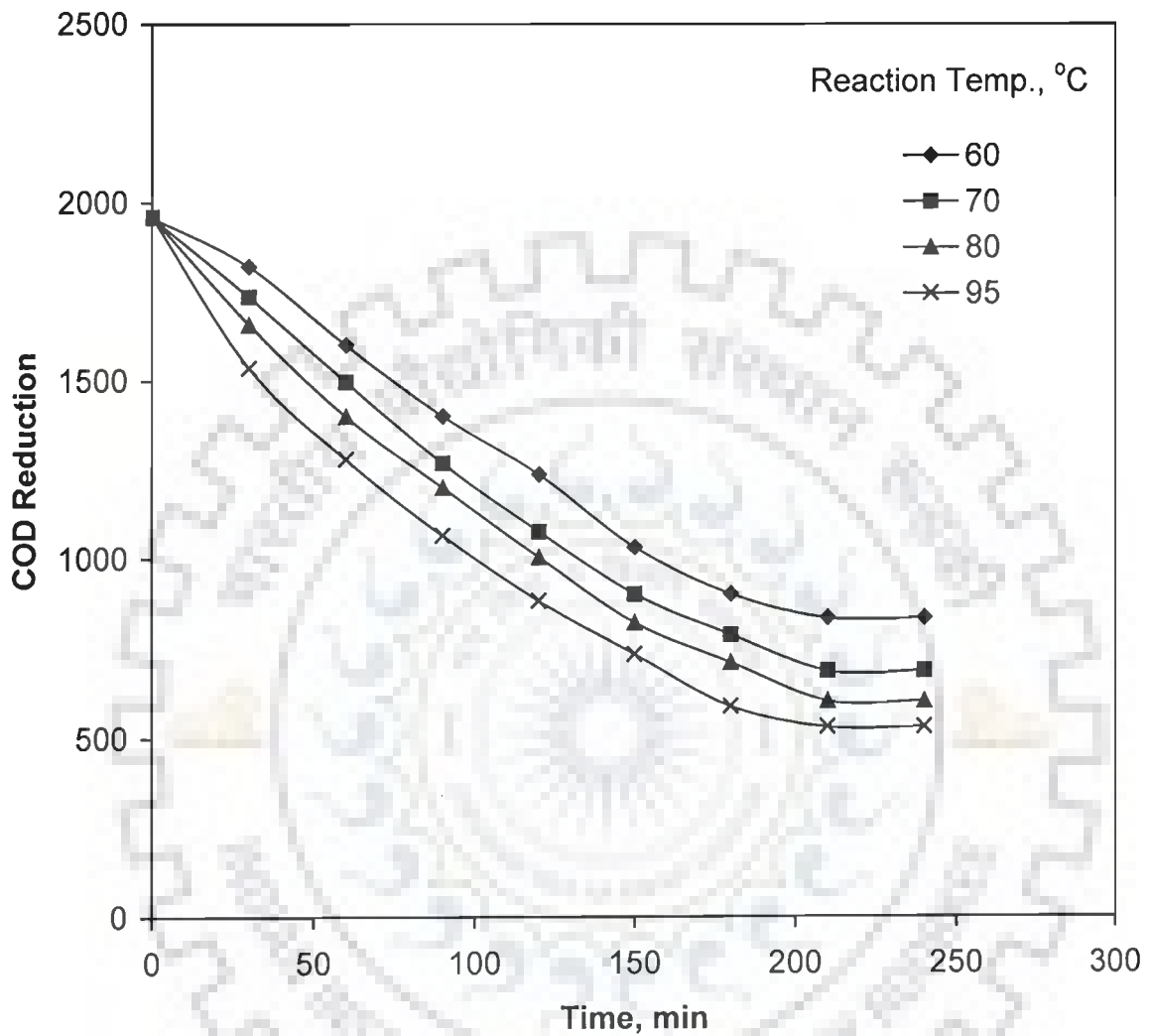
Figure 4.32   Effect of temperature on the reduction of COD with time during catalytic thermolysis of composite wastewater

$COD_0 = 1960$ mg/l, $pH_0 = 12$, $C_w = 6$ kg/m^3, p = atmospheric pressure.
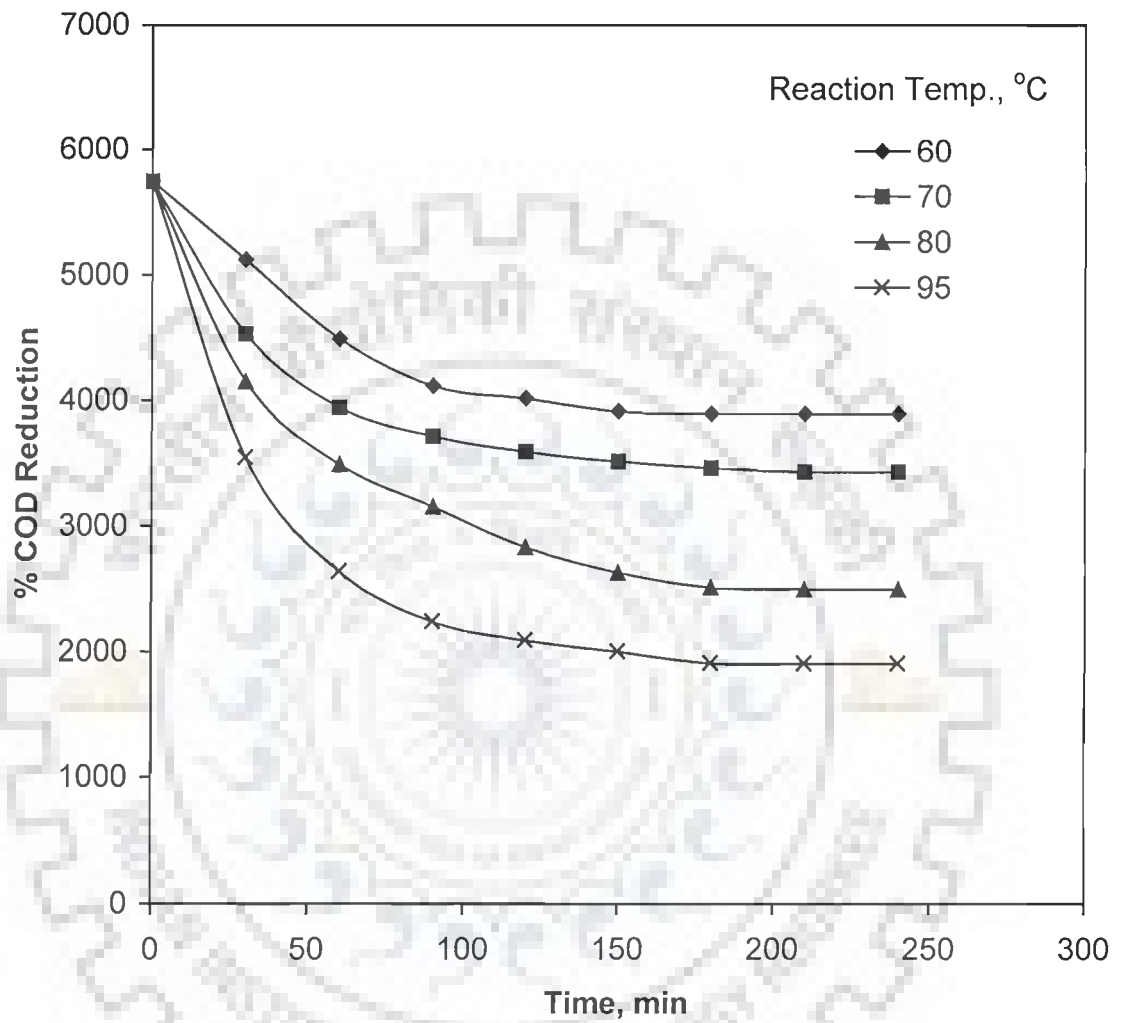
Figure 4.33 Effect of temperature on the reduction of COD with time during catalytic thermolysis of dyeing wastewater

$COD_0 = 5744$ mg/l, $pH_0 = 8$, $C_w = 5$ kg/m^3, P = atmospheric pressure.
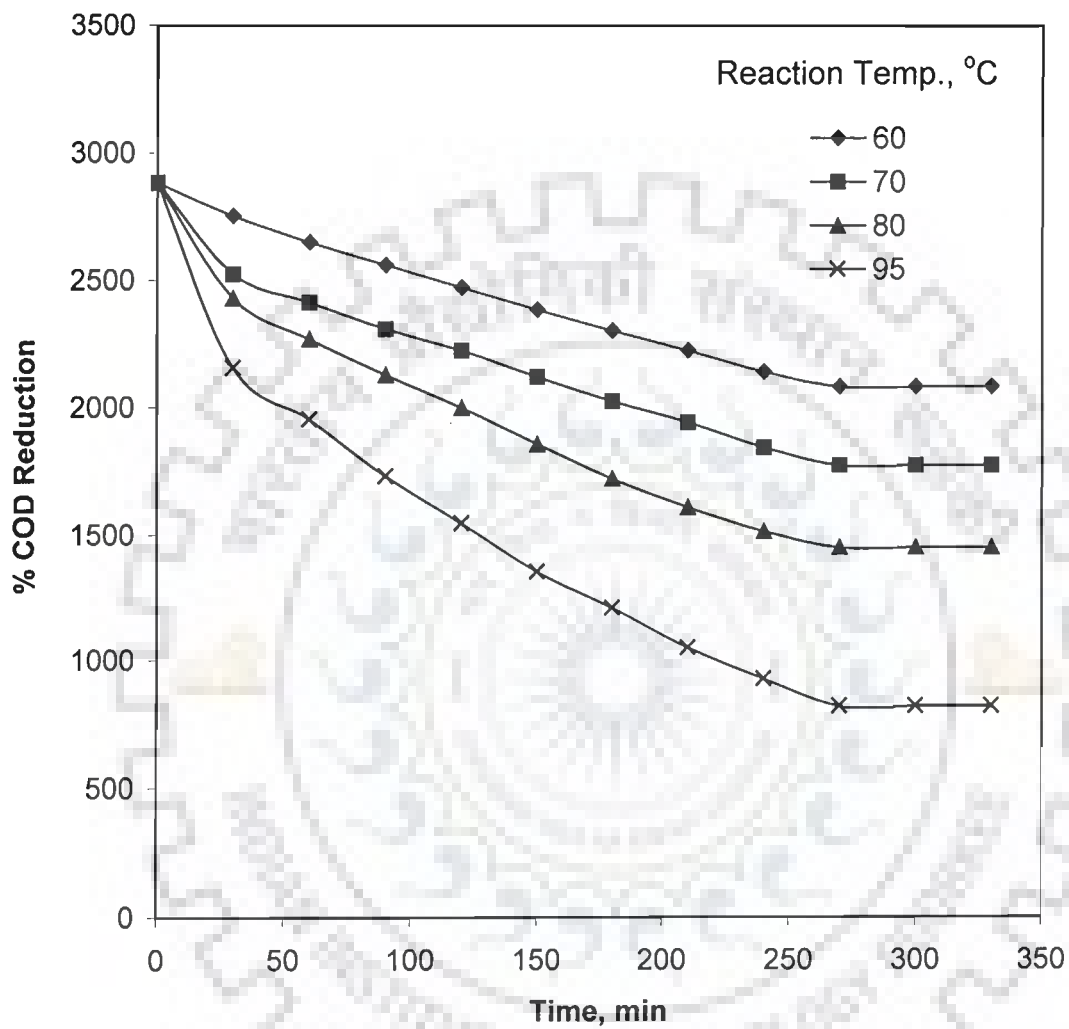
Figure 4.34 Effect of temperature on the reduction of COD with time during catalytic thermolysis of desizing wastewater

COD_0 = 2884 mg/l, pH_0 = 4, C_w = 4 kg/m^3, P = atmospheric pressure.
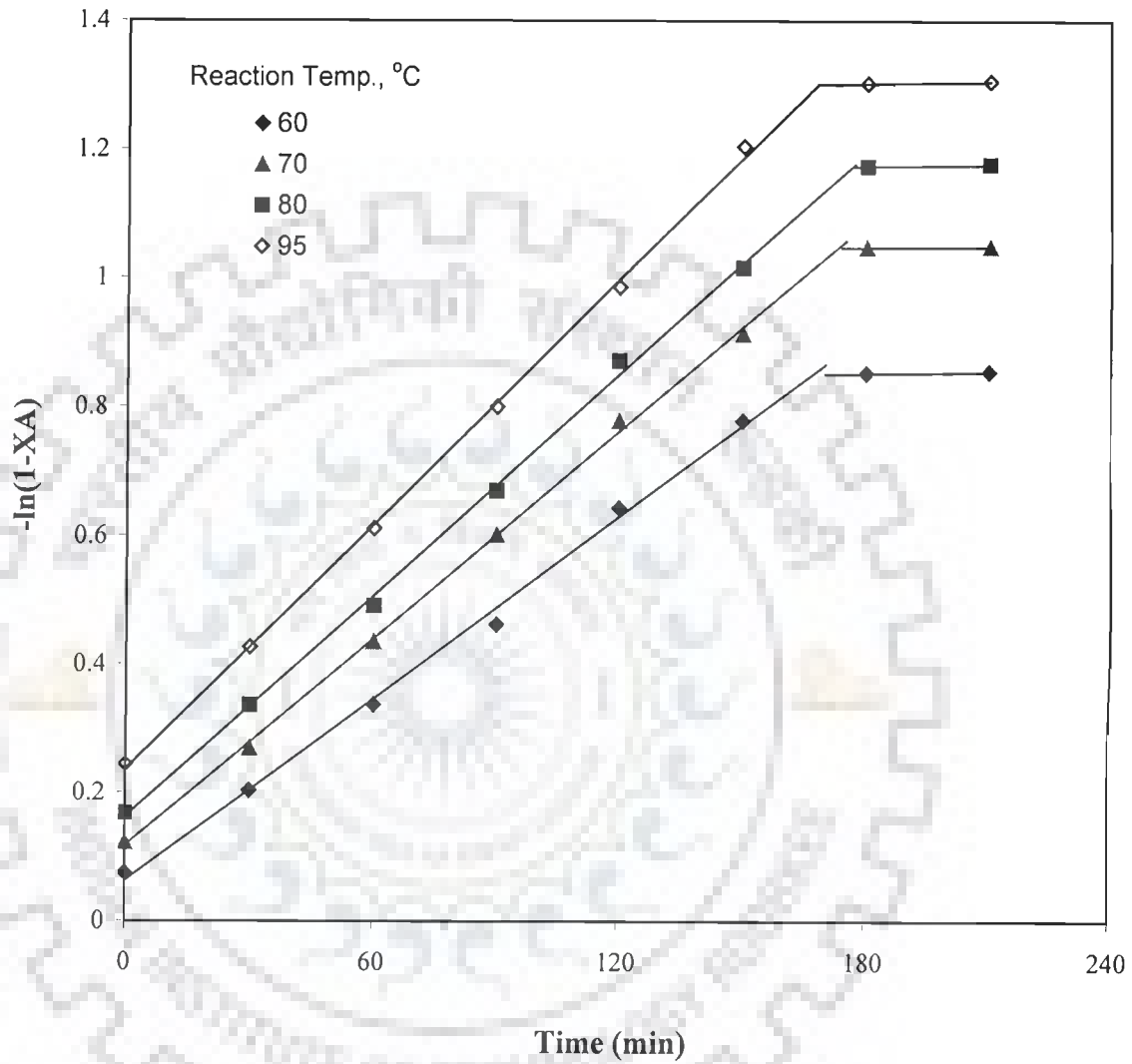
Figure 4.35 First order kinetics for catalytic thermolysis of composite wastewater with respect to organic substrate

COD$_0$ = 1960 mg/l, pH$_0$ = 12, C$_w$ = 6 kg/m^3, p = atmospheric pressure.
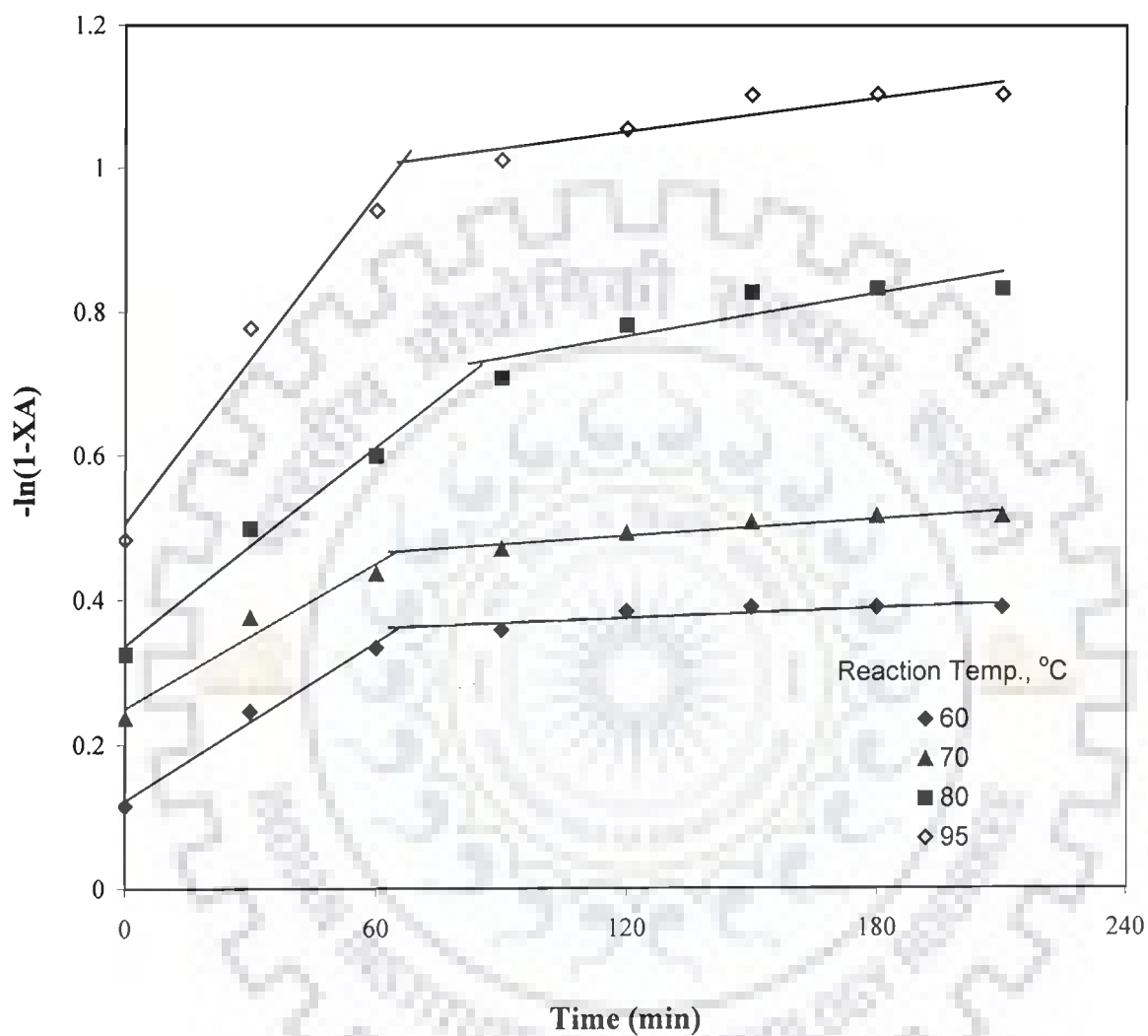
Figure 4.36 First order kinetics for catalytic thermolysis of dyeing wastewater with respect to organic substrate

COD_0 = 5744 mg/l, pH_0 = 8, C_w = 5 kg/m^3, P = atmospheric pressure.
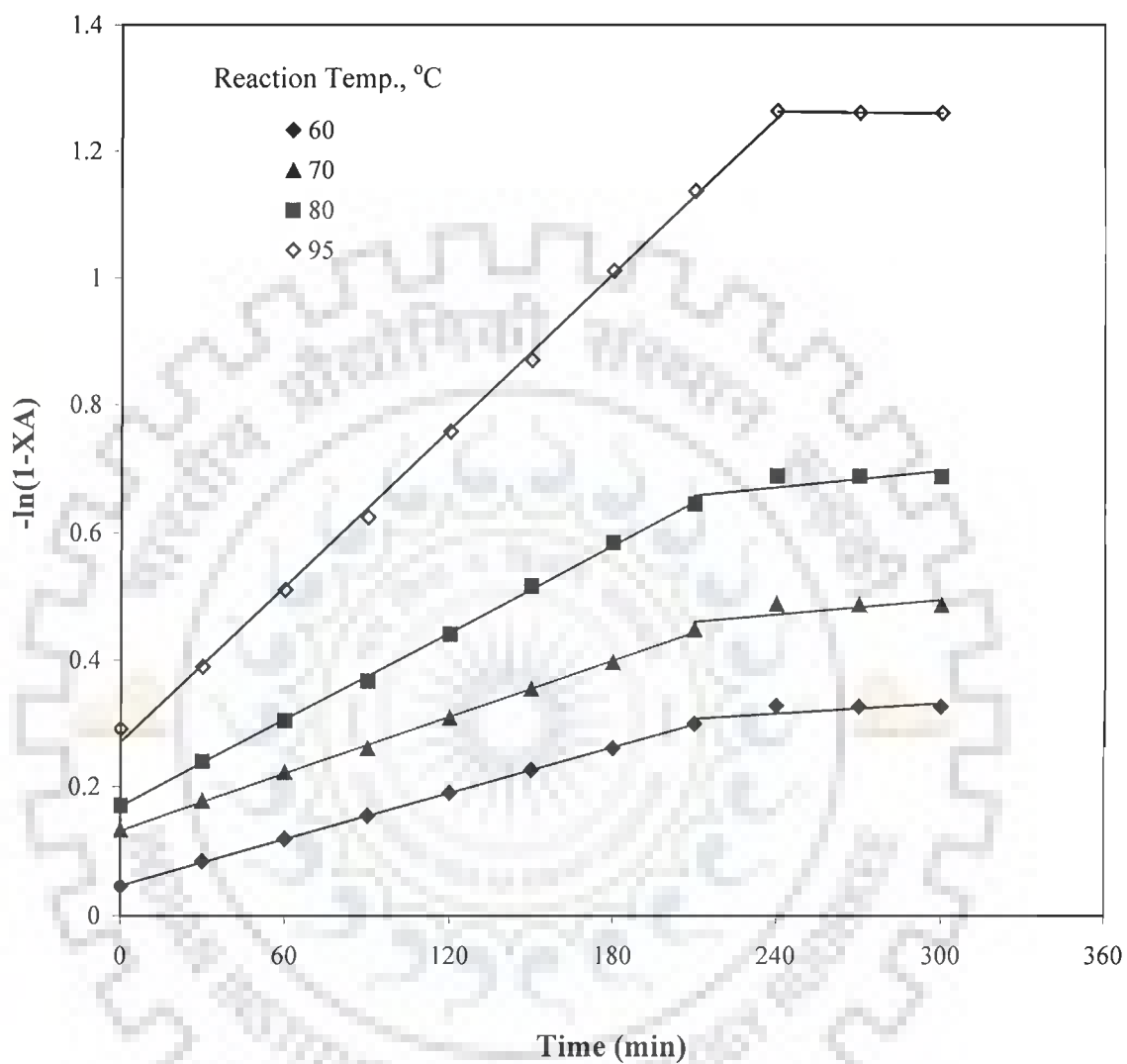
Figure 4.37 **First order kinetics for catalytic thermolysis of desizing wastewater with respect to organic substrate**

$COD_0 = 2884$ **mg/l, pH$_0$ = 4, C$_w$ = 4 kg/m^3, P = atmospheric pressure.**

Thus, equation (4) may be written as

$$-\frac{d(COD)}{dt} = k\,(COD) \tag{5}$$

Integration of equation (5) gives

$$-\ln(1-X) = k\,t \tag{6}$$

where, $X = 1 - \dfrac{(COD)}{(COD_0)}$

The specific rate constant k can, thus be estimated by plotting $[-\ln(1-X)]$ against treatment time, t. Figure 4.31-4.33 show the plot of $[-\ln(1-X)]$ versus t at various experimental conditions for the treatment of composite, dyeing and desizing wastewater, respectively.

These figures also show a two-step reaction mechanism, the data being represented by two simple straight lines. Thus, both the steps can be represented by first order kinetic constants k_1 and k_2, as determined for different reaction temperatures. The values of k_1, k_2 and k_1/k_2 for the composite, dyeing and desizing wastewater are shown in Table 4.4, 4.5 and 4.6, respectively.

Table 4.4 First order rate constants k_1 and k_2 for the first and second reaction steps during catalytic thermolysis of composite wastewater ($COD_0 = 1960$ mg/l, $pH_0 = 12$, $C_w = 6$ kg/m^3, pressure = atmospheric)

Rate constant at different temperatures			
Temperature (^{o}C)	k_1 (min^{-1})	k_2 (min^{-1})	k_1/k_2
60	0.00473	0.00008	59.21
70	0.00538	0.00005	110.88
80	0.00574	0.00011	52.04
95	0.00635	0.00013	50.64

Table 4.5 First order rate constants k_1 and k_2 for the first and second reaction steps during catalytic thermolysis of dyeing wastewater ($COD_0 = 5744$ mg/l, $pH_0 = 8$, $C_w = 5$ kg/m^3, pressure = atmospheric)

Rate constant at different temperatures			
Temperature ($^\circ$C)	k_1 (min^{-1})	k_2 (min^{-1})	k_1/k_2
60	0.00365	0.00023	16.027
70	0.00332	0.00038	8.673
80	0.00457	0.00100	4.554
95	0.00764	0.00078	9.723

Table 4.6 First order rate constants k_1 and k_2 for the first and second reaction steps during catalytic thermolysis of desizing wastewater ($COD_0 = 2884$ mg/l, $pH_0 = 4$, $C_w = 4$ kg/m^3, pressure = atmospheric)

Rate constant at different temperatures			
Temperature ($^\circ$C)	k_1 (min^{-1})	k_2 (min^{-1})	k_1/k_2
60	0.00119	0.00027	4.409
70	0.00148	0.00038	3.915
80	0.00228	0.00043	5.354
95	0.00406	0.00123	3.311

The activation energy and the frequency factor may be determined by Arrhenius equation as

$$k = k_0 \exp\left(-\frac{E}{RT}\right) \tag{7}$$

where T is in K, E is the activation energy and k_0 is the frequency factor. Thus, a plot of ln k against $1/T$ should give the frequency factor and the activation energy. Figures 4.38-4.40 show the ln k versus 1/T plot for composite, dyeing and desizing wastewater, respectively. The activation energy, E for the first and second steps for composite wastewater is found to be 8.34 and 19.24 kJ/mol, respectively. The corresponding values of the frequency factor are 0.098 and 0.065 m^{-1} respectively. The value of E for

first and second step is found to be 23.00 and 39.57 kJ/mol; and 36.64 and 42.36 kJ/mol respectively for dyeing and desizing wastewater. The corresponding values of the frequency factors are 12.59 and 429.92 m^{-1} and 614.96 and 1057.17 m^{-1}, respectively, for dyeing and desizing wastewater.

The kinetic equation for the catalytic thermolysis process of the composite, dyeing and desizing wastewater in the temperature range of 60 to 95 °C and the atmospheric pressure and at corresponding optimum C_w of 6 kg/m^3, 5 kg/m^3 and 4 kg/m^3 and at pH$_0$ 12, 8 and 4, respectively, are thus given as

For composite wastewater

First step

$$r_1 = -\left(\frac{d(COD)}{dt}\right) = 0.098 \exp\left[-\frac{1003}{T}\right][COD] \tag{8}$$

Second step

$$r_2 = -\left(\frac{d(COD)}{dt}\right) = 0.065 \exp\left[-\frac{2314}{T}\right][COD] \tag{9}$$

For dyeing wastewater

First step

$$r_1 = -\left(\frac{d(COD)}{dt}\right) = 12.59 \exp\left[-\frac{2766}{T}\right][COD] \tag{10}$$

Second step

$$r_2 = -\left(\frac{d(COD)}{dt}\right) = 429.92 \exp\left[-\frac{4759}{T}\right][COD] \tag{11}$$

For desizing wastewater

First step

$$r_1 = -\left(\frac{d(COD)}{dt}\right) = 614.96 \exp\left[-\frac{4407}{T}\right][COD] \tag{12}$$

Second step

$$r_2 = -\left(\frac{d(COD)}{dt}\right) = 1057.17 \exp\left[-\frac{5095}{T}\right][COD] \tag{13}$$

153
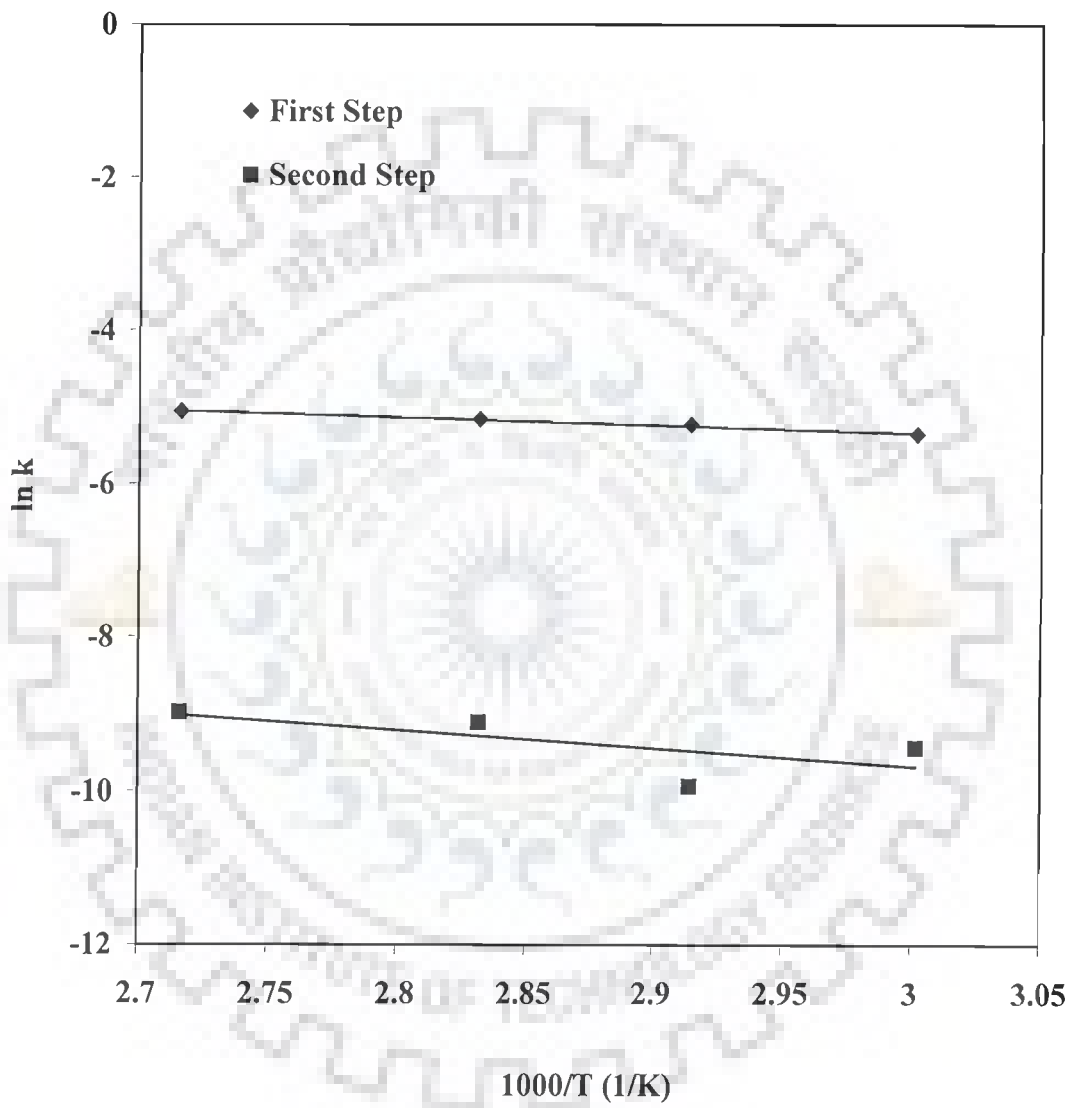
Figure 4.38 Arrhenius plot for catalytic thermolysis of composite wastewater
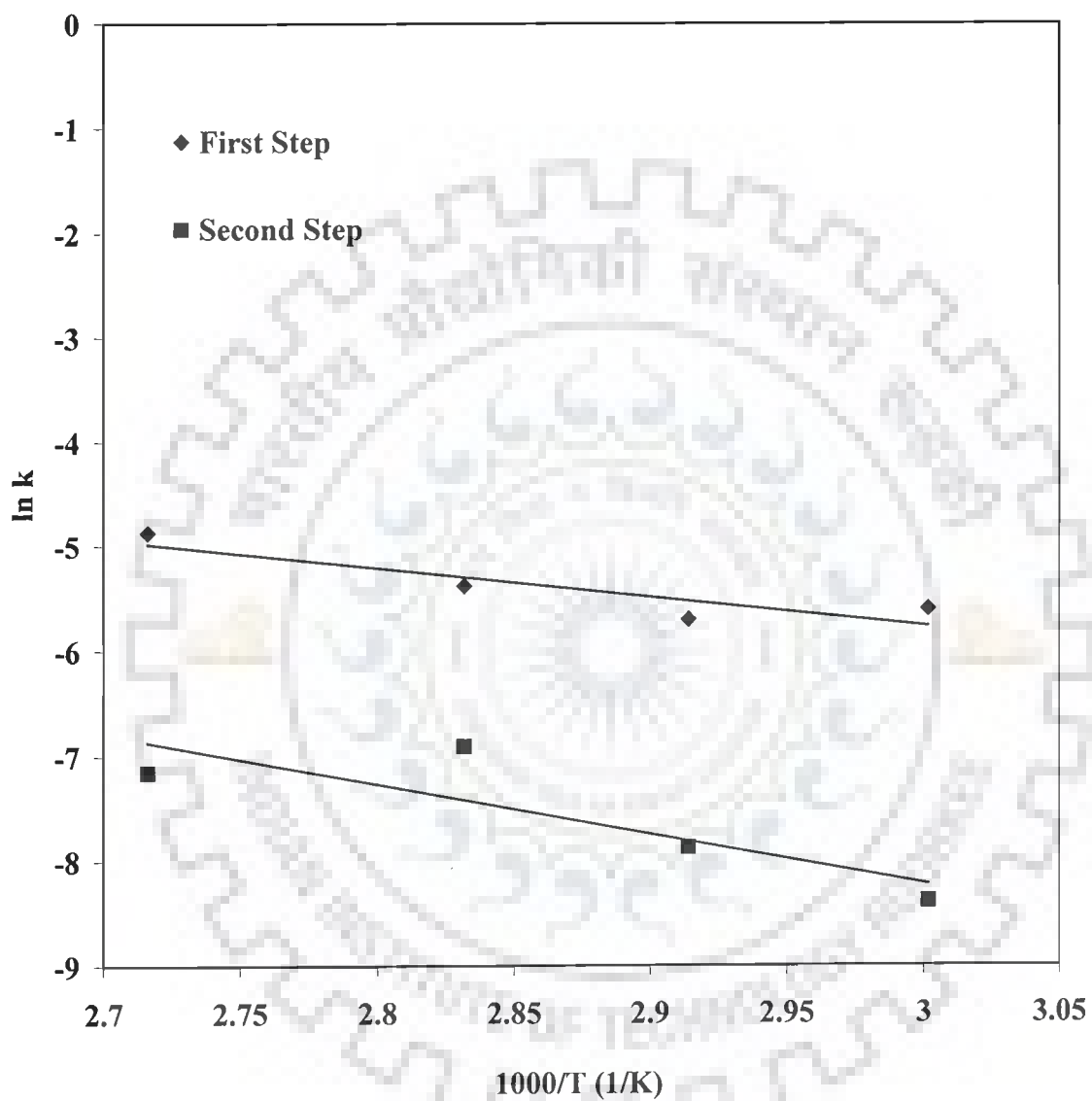
Figure 4.39 Arrhenius plot for catalytic thermolysis of dyeing wastewater
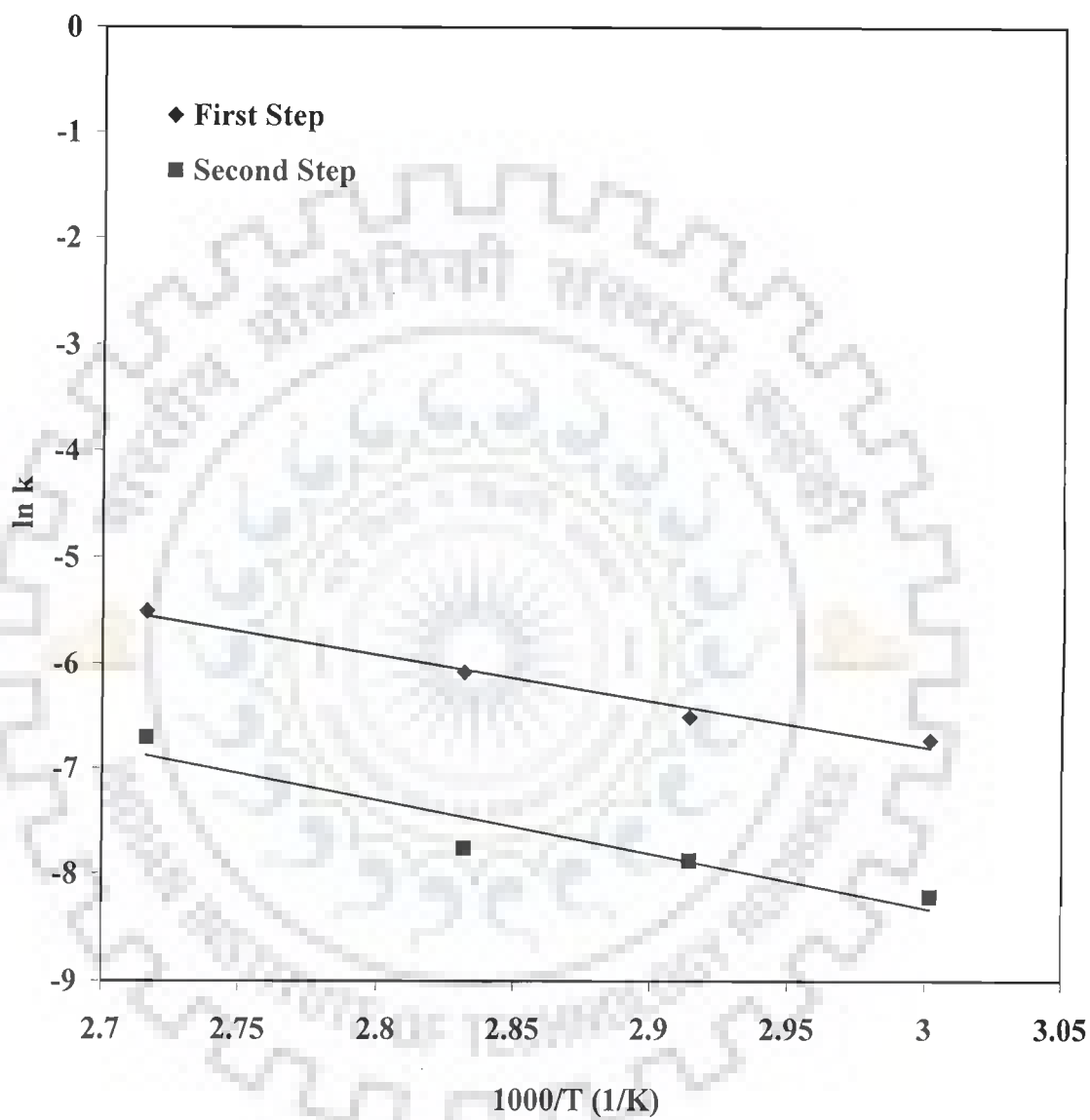
Figure 4.40 Arrhenius plot for catalytic thermolysis of desizing wastewater

4.6   SETTLING CHARACTERISTICS OF THE PRECIPITATE IN THE TREATED EFFLUENT

A faster settling of the treated effluent is desirable. The settling characteristics are strongly affected by the treatment parameters (Foust et al., 1960; Merta and Ziolo, 1985; Richardson et al., 2003). Various methods have been suggested for calculating compression zone height in continuous thickeners from the batch sedimentation data Fitch, 1983; Font, 1990; Font et al., 1999; Larue and Vorobiev, 2003). The method proposed by Richardson et al. (2003) to design a continuous thickener based on single batch sedimentation test seems to be the most appropriate. The settling of an effluent is strongly influenced by its pH.

The effect of pH on the settling characteristics of the precipitate obtained after treatment by thermolysis/coagulation of wastewater at different pH (pH = 2-12) were conducted in a 100 ml measuring cylinder. The settling rate was observed to be strongly dependent on pH. This may probably be due to the variation in size and compactness of aggregated flocs. Figures 4.41 through 4.42 show the behavior of treated effluent during sedimentation.

The calculation of sedimentation velocity (u_c), concentration C(t), and the sedimentation flux were done using the Kynch theory (Richardson et al., 2003). The sedimentation velocity (u_c) was found as the slope of the tangent at a given solids concentration, C. The concentration of sludge at a time t was determined using following relationship :

$$C = C_0 \text{ (total height)/(height of suspension after time t)} \qquad (14)$$

The concentration of the solids required in the underflow, C_u, for the effluents treated at different pH were calculated in each case and are presented in Table 4.7-4.25. The Maximum value of $[\{(1/C) - (1/C_u)\}/u_c]$ thus determined were used to calculate the area of the sedimentation tank for any effluent flow rate by the relationship :

$$A = v_f \, C_0 \left[(1/C) - (1/C_u) \right] / u_c \qquad (15)$$

From the figures, it can also be seen that the settling rate is very fast during the zone settling region. The settling rate becomes very slow, as the solids settling enter compression region. It is also seen that the compression region for a particular settled sludge is much denser than that for the other pH settled sludge.

Using these values, the area of the sedimentation tank for any effluent flow rate can, thus, be calculated as

$$A = v_f C_0 \frac{\left(\dfrac{1}{C} - \dfrac{1}{C_u}\right)}{u_c} \qquad (16)$$

where, v_f = volumetric flow rate of the effluent (m^3/s) and C_0 is the initial solids concentration (kg/m^3).

From Table 4.7, it can be seen that for C_u = 17 kg/m^3 (for composite wastewater after thermolysis process).

$$\text{maximum value of } \frac{\left(\dfrac{1}{C} - \dfrac{1}{C_u}\right)}{u_c} = 0.264 \times 10^6, \qquad (17)$$

So, for a feed rate of Q_0 = 2 m^3/min, the area of the tank (A) can be computed by the following formula:

$$A = Q_0 C_0 \left[\frac{\left(\dfrac{1}{C} - \dfrac{1}{C_u}\right)}{u_c}\right]_{max} = 17600 \text{ m}^2 \qquad (18)$$

Similarly, from Table 4.9, for C_u = 20 kg/m^3,

$$\text{maximum value of } \frac{\left(\dfrac{1}{C} - \dfrac{1}{C_u}\right)}{u_c} = 0.07 \times 10^5, \text{ and the area of the sedimentation tank for}$$

the same feed rate of the effluent (2 m^3/min) is found to be 466 m^2. Similarly, the

$$\text{maximum value of } \frac{\left(\dfrac{1}{C} - \dfrac{1}{C_u}\right)}{u_c}, \text{ and area } A = Q_0 C_0 \left[\frac{\left(\dfrac{1}{C} - \dfrac{1}{C_u}\right)}{u_c}\right]_{max} \text{ can be calculated}$$

for different wastewaters at different pH values.
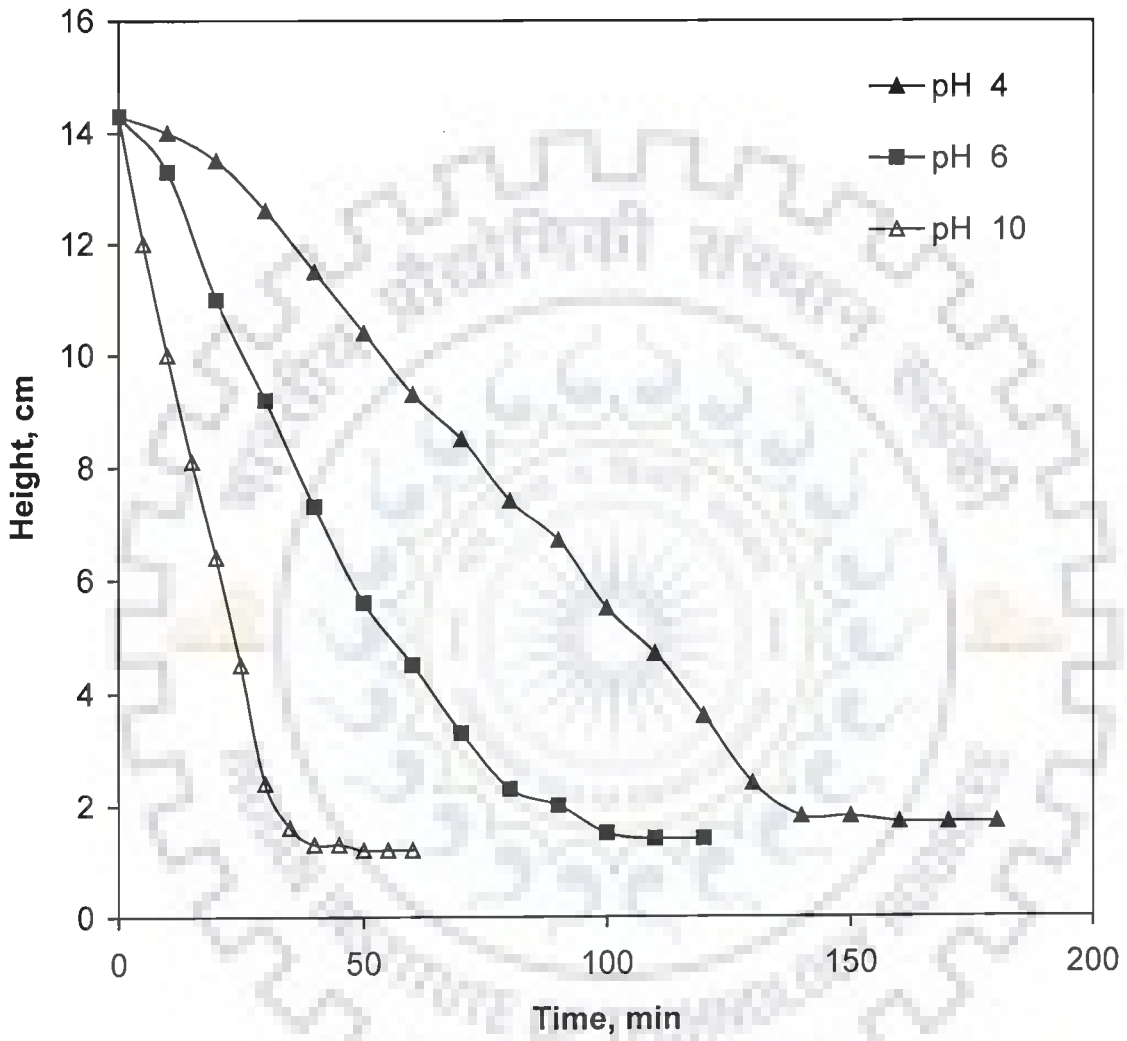
Figure 4.41   Settling characteristics of composite wastewater after thermolysis
using CuSO$_4$ as catalyst

COD$_0$ = 1960 mg/l, T = ambient temperature, P = atmospheric,
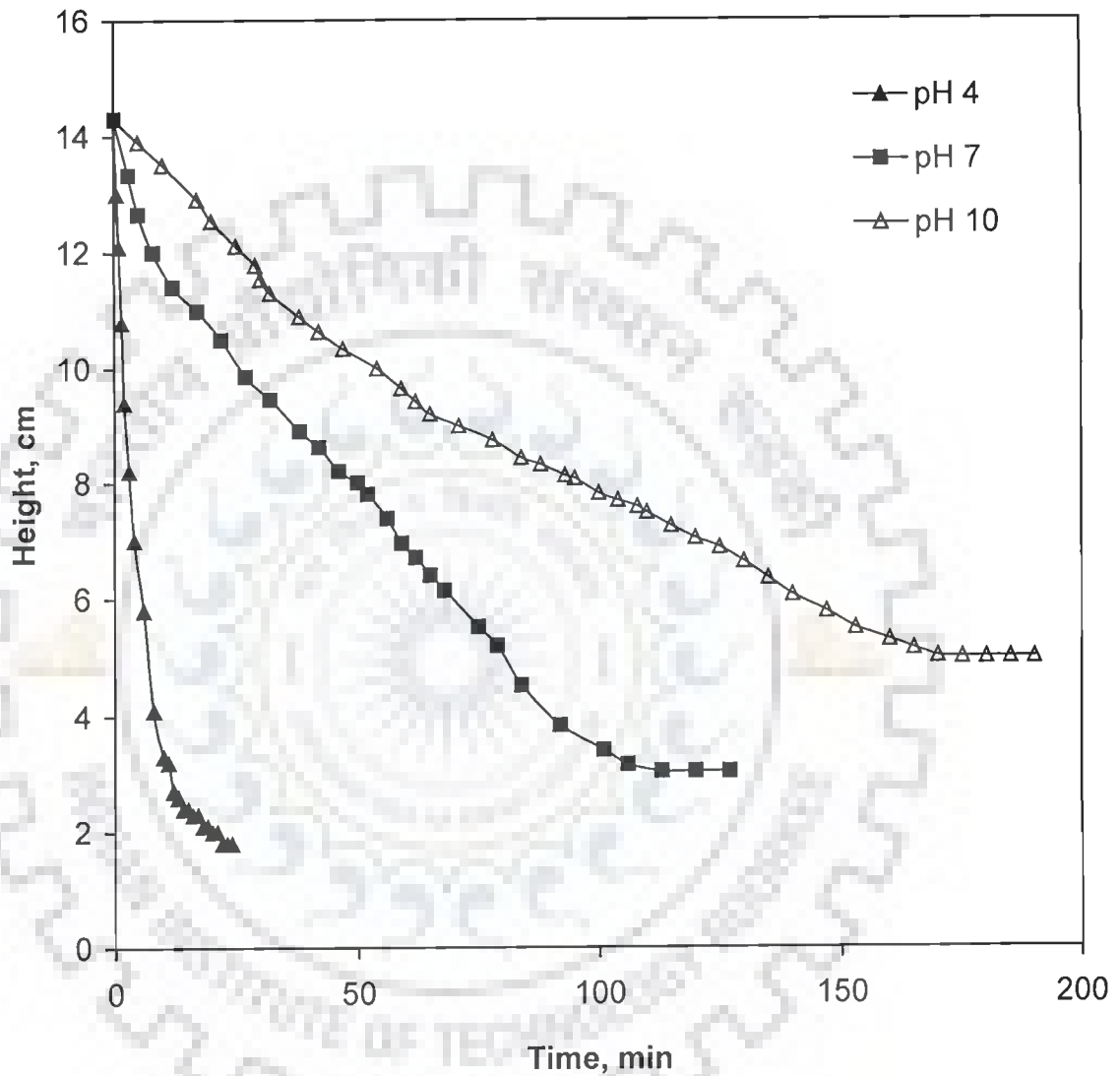
C$_w$ = 5 kg/m^3

Figure 4.42   Settling characteristics of the treated composite wastewater at different pH after coagulation using aluminum potassium sulphate as coagulant

$COD_0 = 1960$ mg/l, T = ambient temperature, P = atmospheric,
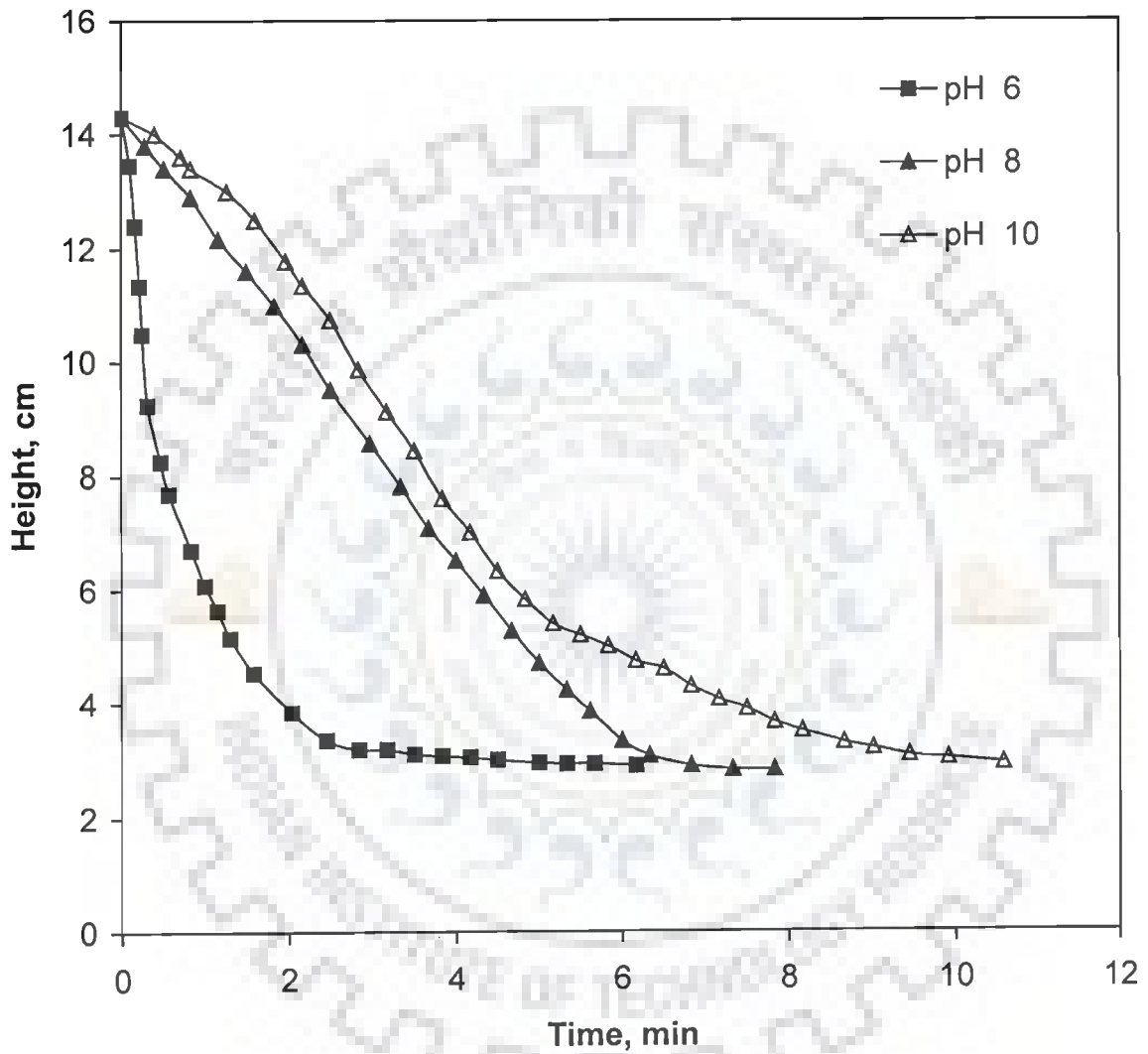
$C_w = 5$ kg/m^3

Figure 4.43 Settling characteristics of dyeing wastewater after thermolysis at different pH using $CuSO_4$ as catalyst

$COD_0 = 5744$ mg/l, P = atmospheric, $C_w = 5$ kg/m^3
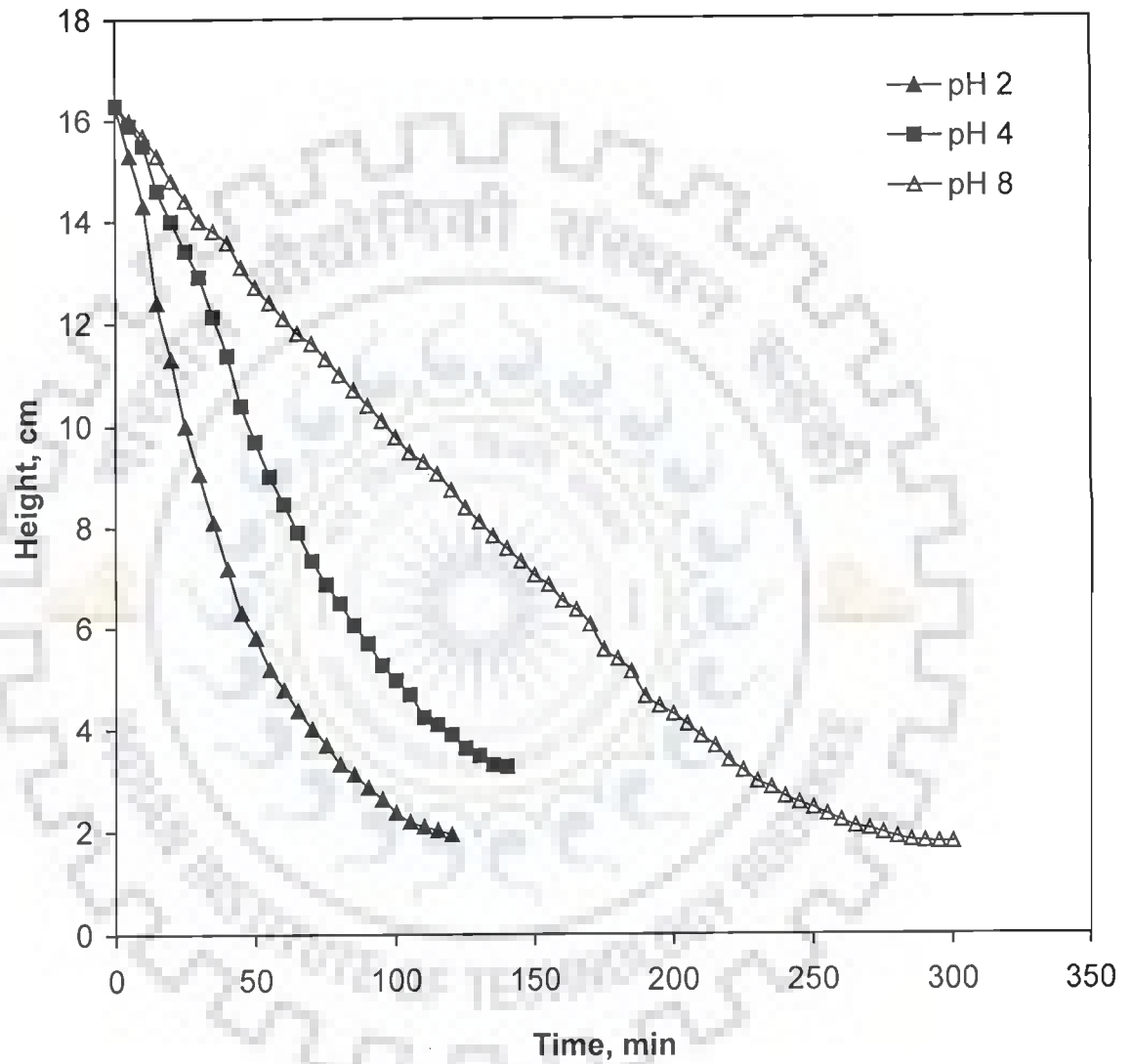
Figure 4.44 Settling characteristics of dyeing wastewater after coagulation at different pH using commercial alum as coagulant

$COD_0 = 5744$ mg/l, P = atmospheric, $C_w = 5$ kg/m^3
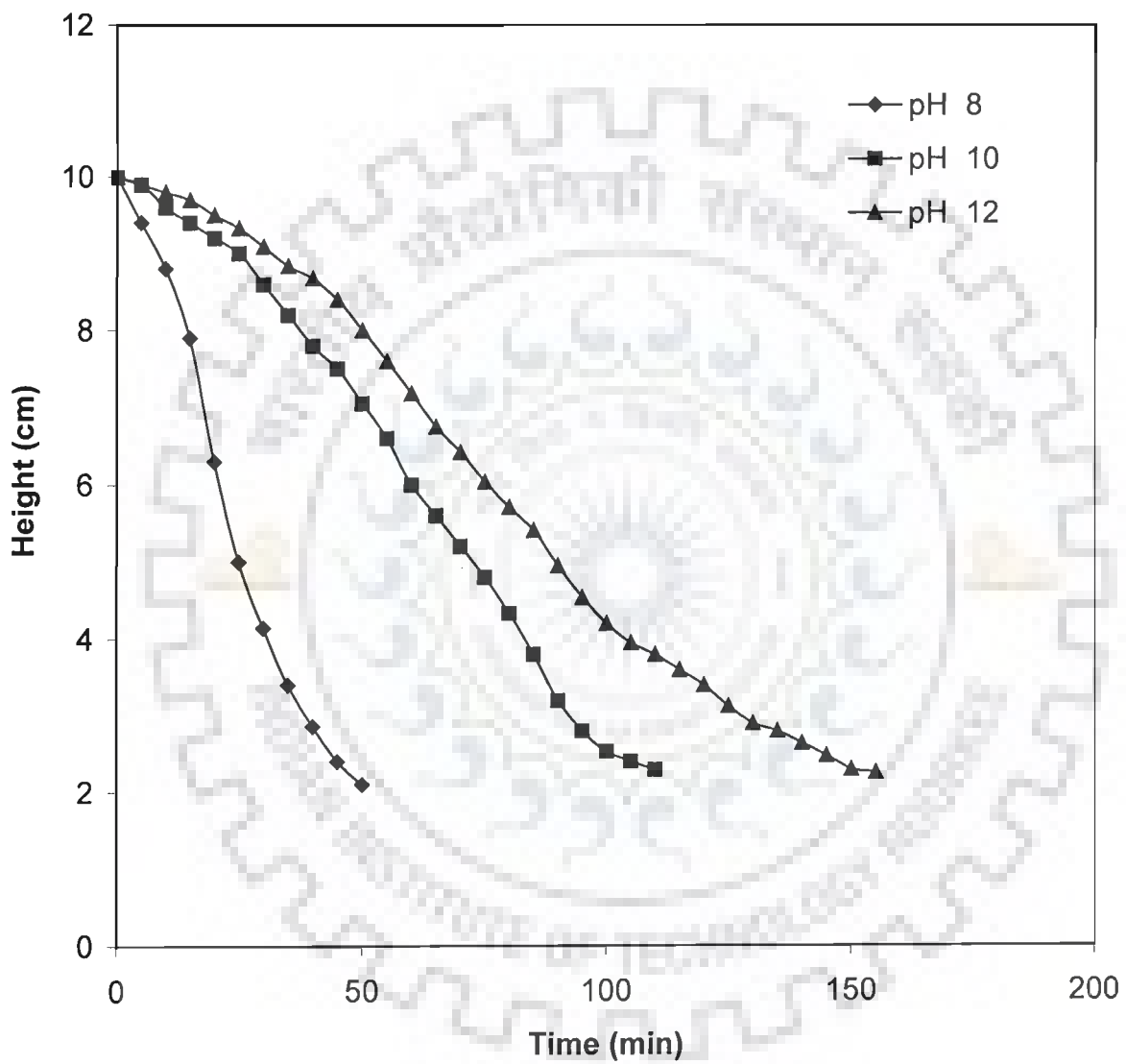
Figure 4.45 Settling characteristics of desizing wastewater after thermolysis at different pH using $CuSO_4$ as catalyst

$COD_0 = 2884$ mg/l, P = atmospheric, $C_w = 4$ kg/m^3
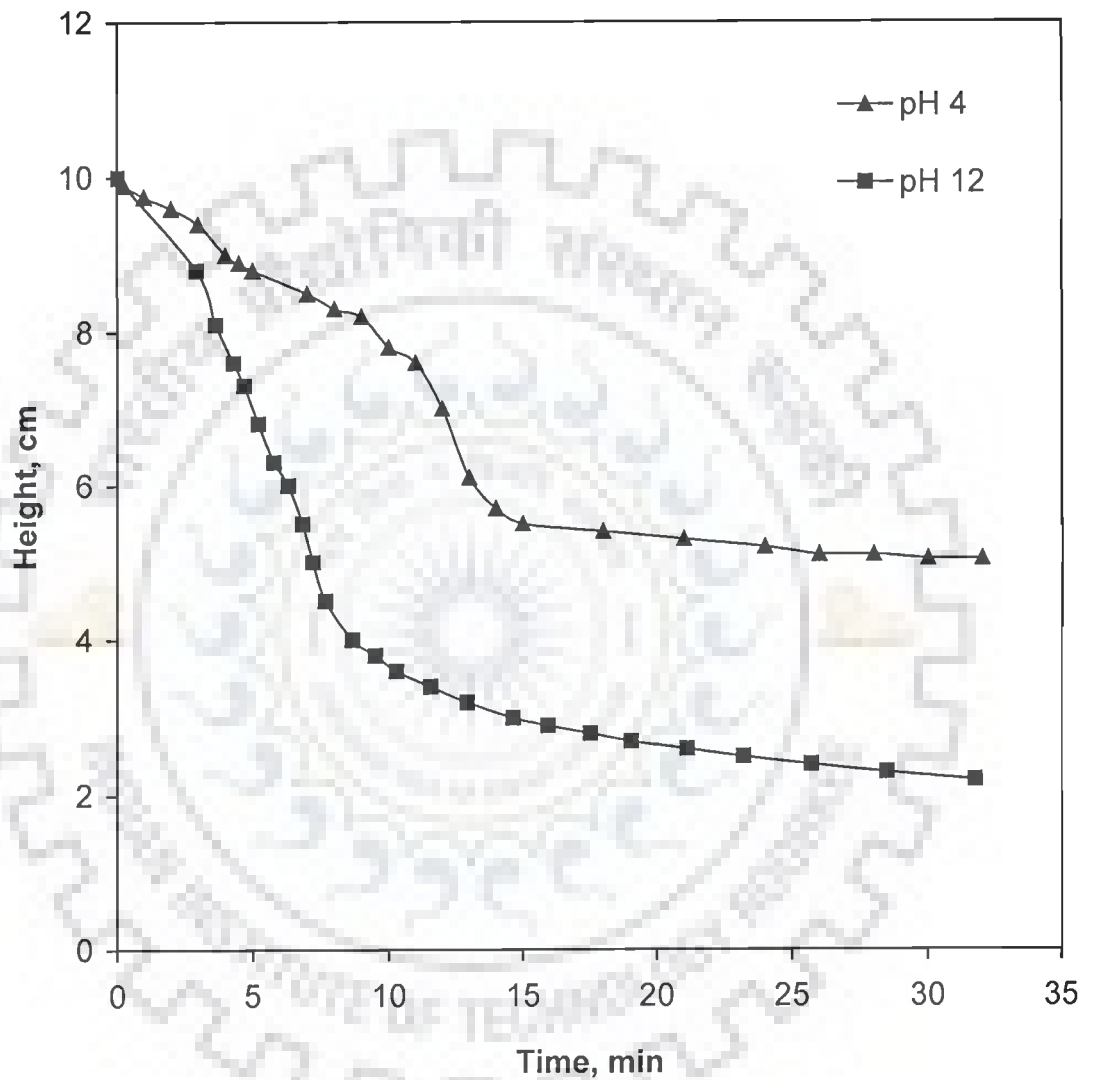
Figure 4.46   **Settling characteristics of desizing wastewater after coagulation at different pH using commercial alum as coagulant**

COD_0 = 2884 mg/l, P = atmospheric, C_w = 5 kg/m^3

Table 4.7 Settling characteristics of composite wastewater after thermolysis using copper sulphate at pH 4 and at ambient temperature ($C_0 = 2$ kg/m³, $C_u = 17$ kg/m³)

S. No.	Time (min)	Height (cm)	u_c (m/s)*10^5	C (kg/m³)	Sedimentation flux (kg/m²s) x 10^6	$1000\left(\dfrac{1}{C}-\dfrac{1}{C_u}\right)$ m³/kg	$\dfrac{u_c}{\left(\frac{1}{C}-\frac{1}{C_u}\right)}$ kg/m² s x 10^6	$\dfrac{\left(\frac{1}{C}-\frac{1}{C_u}\right)}{u_c}$ m²/s kg x 10^{-6}
1	0	14.3	1.666	2.000	3.332	0.441	3.776	0.265
2	10	14	1.666	2.043	3.403	0.431	3.868	0.259
3	20	13.5	1.666	2.119	3.529	0.413	4.032	0.248
4	30	12.6	1.666	2.270	3.782	0.382	4.364	0.229
5	40	11.5	1.666	2.487	4.143	0.343	4.853	0.206
6	50	10.4	1.666	2.750	4.582	0.305	5.466	0.183
7	60	9.3	1.666	3.075	5.123	0.266	6.255	0.160
8	70	8.5	1.666	3.365	5.606	0.238	6.989	0.143
9	80	7.4	1.666	3.865	6.439	0.200	8.333	0.120
10	90	6.7	1.666	4.269	7.112	0.175	9.496	0.105
11	100	5.5	1.666	5.200	8.663	0.133	12.481	0.080
12	110	4.7	1.666	6.085	10.138	0.106	15.790	0.063
13	120	3.6	1.666	7.944	13.235	0.067	24.847	0.040
14	130	2.4	1.666	11.917	19.853	0.025	66.394	0.015
15	140	1.8	0.041	15.889	0.656	0.004	10.040	0.100
16	150	1.8	0.041	15.889	0.656	0.004	10.040	0.100
17	160	1.7	0.041	16.824	0.695			
18	170	1.7	0.041	16.824	0.695			
19	180	1.7	0.041	16.824	0.695			

Table 4.8 Settling characteristics of composite wastewater after thermolysis using copper sulphate at pH 6 and at ambient temperature $(C_0 = 2\ kg/m^3,\ C_u = 17\ kg/m^3)$

S. No.	Time (min)	Height (cm)	u_c (m/s)*10^5	C (kg/m³)	Sedimentation flux (kg/m²s) x 10^6	$1000\left(\dfrac{1}{C}-\dfrac{1}{C_u}\right)$ m³/kg	$\dfrac{u_c}{\left(\dfrac{1}{C}-\dfrac{1}{C_u}\right)}$ kg/m² s x 10^6	$\dfrac{\left(\dfrac{1}{C}-\dfrac{1}{C_u}\right)}{u_c}$ m²/s kg x 10^{-6}
1	0	14.3	2.960	2.000	5.920	0.441	6.709	0.149
2	10	13.3	2.960	2.150	6.365	0.406	7.287	0.137
3	20	11	2.960	2.600	7.696	0.326	9.086	0.110
4	30	9.2	2.960	3.109	9.202	0.263	11.261	0.089
5	40	7.3	2.960	3.918	11.597	0.196	15.070	0.066
6	50	5.6	1.800	5.107	9.193	0.137	13.141	0.076
7	60	4.5	1.800	6.356	11.440	0.099	18.271	0.055
8	70	3.3	1.800	8.667	15.600	0.057	31.824	0.031
9	80	2.3	1.800	12.435	22.383	0.022	83.349	0.012
10	90	2	0.158	14.300	2.259	0.011	14.226	0.070
11	100	1.5	0.158	19.067	3.013	-0.006	-24.781	-0.040
12	110	1.4	0.158	20.429	3.228			

Table 4.9 Settling characteristics of composite wastewater after thermolysis using copper sulphate at pH 10 and at ambient temperature $(C_0 = 2\ kg/m^3,\ C_u = 20\ kg/m^3)$

S. No.	Time (min)	Height (cm)	u_c (m/s)*10^5	C (kg/m³)	Sedimentation flux (kg/m²s) x 10^6	$1000\left(\dfrac{1}{C}-\dfrac{1}{C_u}\right)$ m³/kg	$\dfrac{u_c}{\left(\dfrac{1}{C}-\dfrac{1}{C_u}\right)}$ kg/m² s x 10^6	$\dfrac{\left(\dfrac{1}{C}-\dfrac{1}{C_u}\right)}{u_c}$ m²/s kg x 10^{-6}
1	0	14.3	6.350	2.000	12.700	0.450	14.111	0.071
2	5	12	6.350	2.383	15.134	0.370	17.182	0.058
3	10	10	6.350	2.860	18.161	0.300	21.191	0.047
4	15	8.1	6.350	3.531	22.421	0.233	27.228	0.037
5	20	6.4	6.350	4.469	28.377	0.174	36.541	0.027
6	25	4.5	6.350	6.356	40.358	0.107	59.156	0.017
7	30	2.4	6.350	11.917	75.671	0.034	187.227	0.005
8	35	1.6	0.330	17.875	5.899	0.006	55.518	0.018
9	40	1.3	0.330	22.000	7.260			
10	45	1.3	0.330	22.000	7.260			
11	50	1.2	0.330	23.833	7.865			

Table 4.10: Settling characteristics of composite wastewater after coagulation using aluminum potassium sulphate at pH 4 and at ambient temperature ($C_0 = 2$ kg/m^3, $C_u = 15$ kg/m^3)

S. No.	Time (min)	Height (cm)	u_c (m/s)*10^5	C (kg/m^3)	Sedimentation flux (kg/m^{2}s) x 10^6	$1000\left(\frac{1}{C} - \frac{1}{C_u}\right)$ m^3/kg	$\frac{u_c}{\left(\frac{1}{C} - \frac{1}{C_u}\right)}$ kg/m^2 s x 10^6	$\frac{\left(\frac{1}{C} - \frac{1}{C_u}\right)}{u_c}$ m^2/s kg x 10^{-6}
1	0	14.3	4.444	2.000	8.888	0.433	10.255	0.098
2	0.5	13	4.444	2.200	9.777	0.388	11.457	0.087
3	1	12.1	4.444	2.364	10.504	0.356	12.469	0.080
4	1.5	10.8	4.444	2.648	11.768	0.311	14.291	0.070
5	2	9.4	4.444	3.043	13.521	0.262	16.962	0.059
6	3	8.2	1.480	3.488	5.162	0.220	6.726	0.149
7	4	7	1.480	4.086	6.047	0.178	8.310	0.120
8	6	5.8	1.480	4.931	7.298	0.136	10.872	0.092
9	8	4.1	1.480	6.976	10.324	0.077	19.298	0.052
10	10	3.3	0.128	8.667	1.109	0.049	2.627	0.381
11	11	3.2	0.128	8.938	1.144	0.045	2.831	0.353
12	12	2.7	0.128	10.593	1.356	0.028	4.614	0.217
13	13	2.6	0.128	11.000	1.408	0.024	5.280	0.189
14	14	2.4	0.128	11.917	1.525	0.017	7.421	0.135
15	15	2.4	0.128	11.917	1.525	0.017	7.421	0.135
16	16	2.3	0.128	12.435	1.592	0.014	9.307	0.107
17	17	2.3	0.128	12.435	1.592	0.014	9.307	0.107
18	18	2.1	0.128	13.619	1.743	0.007	18.935	0.053
19	19	2.1	0.128	13.619	1.743	0.007	18.935	0.053
20	20	2	0.128	14.300	1.830	0.003	39.223	0.025
21	21	2	0.128	14.300	1.830	0.003	39.223	0.025
22	22	1.8	0.128	15.889	2.034			
23	23	1.8	0.128	15.889	2.034			
24	24	1.8	0.128	15.889	2.034			

Table 4.11 **Settling characteristics of composite wastewater after coagulation using aluminum potassium sulphate at pH 7 and at ambient temperature ($C_0 = 2$ kg/m^3, $C_u = 19$ kg/m^3)**

S. No.	Time (min)	Height (cm)	u_c (m/s)*10^5	C (kg/m^3)	Sedimentation flux (kg/m^{2}s) x 10^6	$1000\left(\dfrac{1}{C}-\dfrac{1}{C_u}\right)$ m^3/kg	$\dfrac{u_c}{\left(\dfrac{1}{C}-\dfrac{1}{C_u}\right)}$ kg/m^2 s x 10^6	$\dfrac{\left(\dfrac{1}{C}-\dfrac{1}{C_u}\right)}{u_c}$ m^2/s kg x 10^{-6}
1	0	14.3	5.128	2.000	10.256	0.389	13.186	0.076
2	3	13.33	5.128	2.146	11.002	0.355	14.446	0.069
3	5	12.65	5.128	2.261	11.594	0.331	15.483	0.065
4	8	12	5.128	2.383	12.222	0.308	16.624	0.060
5	12	11.41	1.562	2.507	3.915	0.288	5.427	0.184
6	17	11	1.562	2.600	4.061	0.274	5.711	0.175
7	22	10.5	1.562	2.724	4.255	0.256	6.101	0.164
8	27	9.86	1.562	2.901	4.531	0.234	6.685	0.150
9	32	9.46	1.562	3.023	4.722	0.220	7.111	0.141
10	38	8.9	1.562	3.213	5.019	0.200	7.807	0.128
11	42	8.62	1.562	3.318	5.183	0.190	8.209	0.122
12	46	8.2	1.562	3.488	5.448	0.176	8.895	0.112
13	50	8	1.562	3.575	5.584	0.169	9.264	0.108
14	52	7.8	1.562	3.667	5.727	0.162	9.665	0.103
15	56	7.38	1.562	3.875	6.053	0.147	10.631	0.094
16	59	6.95	1.562	4.115	6.428	0.132	11.843	0.084
17	62	6.7	1.562	4.269	6.668	0.123	12.683	0.079
18	65	6.4	1.562	4.469	6.980	0.113	13.864	0.072
19	68	6.14	1.562	4.658	7.276	0.104	15.081	0.066
20	75	5.52	1.562	5.181	8.093	0.082	19.073	0.052
21	79	5.2	1.562	5.500	8.591	0.071	22.091	0.045
22	84	4.53	1.562	6.313	9.862	0.047	33.037	0.030
23	92	3.84	1.562	7.448	11.634	0.023	67.460	0.015
24	101	3.41	0.285	8.387	2.390	0.008	35.100	0.028
25	106	3.16	0.285	9.051	2.579			
26	113	3.04	0.285	9.408	2.681			
27	120	3.04	0.285	9.408	2.681			
28	127	3.04	0.285	9.408	2.681			

Table 4.12 Settling characteristics of composite wastewater after coagulation using aluminum potassium sulphate at pH 10 and at ambient temperature ($C_0 = 2$ kg/m^3, $C_u = 15$ kg/m^3)

S. No.	Time (min)	Height (cm)	u_c (m/s)*10^5	C (kg/m^3)	Sedimentation flux (kg/m^{2}s) x 10^6	$1000\left(\dfrac{1}{C}-\dfrac{1}{C_u}\right)$ m^3/kg	$\dfrac{u_c}{\left(\dfrac{1}{C}-\dfrac{1}{C_u}\right)}$ kg/m^2 s x 10^6	$\dfrac{\left(\dfrac{1}{C}-\dfrac{1}{C_u}\right)}{u_c}$ m^2/s kg x 10^{-6}
1	0	14.3	1.330	2.000	2.660	0.300	4.433	0.226
2	5	13.9	1.330	2.058	2.737	0.286	4.650	0.215
3	10	13.5	1.330	2.119	2.818	0.272	4.889	0.205
4	17	12.9	1.330	2.217	2.949	0.251	5.298	0.189
5	20	12.53	1.330	2.283	3.036	0.238	5.586	0.179
6	25	12.11	1.330	2.362	3.141	0.223	5.953	0.168
7	29	11.78	1.330	2.428	3.229	0.212	6.277	0.159
8	30	11.54	1.330	2.478	3.296	0.203	6.536	0.153
9	32	11.3	1.330	2.531	3.366	0.195	6.817	0.147
10	38	10.9	1.330	2.624	3.490	0.181	7.343	0.136
11	42	10.64	0.700	2.688	1.882	0.172	4.069	0.246
12	47	10.34	0.700	2.766	1.936	0.162	4.333	0.231
13	54	10	0.700	2.860	2.002	0.150	4.678	0.214
14	59	9.65	0.700	2.964	2.075	0.137	5.094	0.196
15	62	9.42	0.700	3.036	2.125	0.129	5.411	0.185
16	65	9.2	0.700	3.109	2.176	0.122	5.753	0.174
17	71	8.99	0.700	3.181	2.227	0.114	6.122	0.163
18	78	8.74	0.700	3.272	2.291	0.106	6.629	0.151
19	84	8.43	0.700	3.393	2.375	0.095	7.387	0.135
20	88	8.31	0.700	3.442	2.409	0.091	7.730	0.129
21	93	8.12	0.700	3.522	2.466	0.084	8.342	0.120
22	95	8.07	0.700	3.544	2.481	0.082	8.519	0.117
23	100	7.81	0.700	3.662	2.563	0.073	9.579	0.104
24	104	7.69	0.700	3.719	2.603	0.069	10.162	0.098
25	108	7.58	0.700	3.773	2.641	0.065	10.763	0.093
26	110	7.48	0.700	3.824	2.676	0.062	11.375	0.088
27	115	7.24	0.700	3.950	2.765	0.053	13.171	0.076
28	120	7.03	0.700	4.068	2.848	0.046	15.282	0.065
29	125	6.87	0.700	4.163	2.914	0.040	17.409	0.057
30	130	6.63	0.700	4.314	3.020	0.032	22.000	0.045
31	135	6.35	0.700	4.504	3.153	0.022	31.778	0.031
32	140	6.06	0.700	4.719	3.304	0.012	58.882	0.017
33	147	5.78	0.700	4.948	3.464	0.002	333.667	0.003
34	153	5.5	0.700	5.200	3.640			
35	160	5.3	0.700	5.396	3.777			
36	165	5.15	0.066	5.553	0.367			
37	170	5.02	0.066	5.697	0.376			
38	175	5	0.066	5.720	0.378			
39	180	5	0.066	5.720	0.378			
40	185	5	0.066	5.720	0.378			
41	190	5	0.066	5.720	0.378			

Table 4.13 Settling characteristics of dyeing wastewater after thermolysis using copper sulphate at pH 6 and at ambient temperature ($C_0 = 4$ kg/m^3, $C_u = 19$ kg/m^3)

S. No.	Time (min)	Height (cm)	u_c (m/s)*10^5	C (kg/m^3)	Sedimentation flux (kg/m^{2}s) x 10^6	$1000\left(\dfrac{1}{C}-\dfrac{1}{C_u}\right)$ m^3/kg	$\dfrac{u_c}{\left(\dfrac{1}{C}-\dfrac{1}{C_u}\right)}$ kg/m^2 s x 10^6	$\dfrac{\left(\dfrac{1}{C}-\dfrac{1}{C_u}\right)}{u_c}$ m^2/s kg x 10^{-6}
1	0	14.3	2.580	4.000	10.320	0.197	13.072	0.076
2	6	13.46	2.580	4.250	10.964	0.183	14.123	0.071
3	10	12.4	2.580	4.613	11.901	0.164	15.717	0.064
4	13	11.35	2.580	5.040	13.002	0.146	17.696	0.057
5	15	10.48	2.580	5.458	14.082	0.131	19.757	0.051
6	19	9.24	2.580	6.190	15.971	0.109	23.690	0.042
7	28	8.25	0.627	6.933	4.347	0.092	6.845	0.146
8	34	7.69	0.627	7.438	4.664	0.082	7.664	0.130
9	50	6.7	0.627	8.537	5.353	0.065	9.721	0.103
10	60	6.08	0.627	9.408	5.899	0.054	11.684	0.086
11	69	5.64	0.627	10.142	6.359	0.046	13.639	0.073
12	78	5.15	0.627	11.107	6.964	0.037	16.763	0.060
13	95	4.53	0.227	12.627	2.866	0.027	8.545	0.117
14	122	3.84	0.227	14.896	3.381	0.015	15.654	0.064
15	147	3.35	0.227	17.075	3.876	0.006	38.249	0.026
16	170	3.19	0.014	17.931	0.255	0.003	4.526	0.221
17	190	3.19	0.014	17.931	0.255	0.003	4.526	0.221
18	210	3.1	0.014	18.452	0.262	0.002	9.078	0.110
19	230	3.07	0.014	18.632	0.265	0.001	13.657	0.073
20	250	3.05	0.014	18.754	0.266	0.001	20.577	0.049
21	270	3	0.014	19.067	0.271			
22	300	2.95	0.014	19.390	0.275			
23	320	2.93	0.014	19.522	0.277			
24	340	2.93	0.014	19.522	0.277			
25	370	2.9	0.014	19.724	0.280			

Table 4.14 Settling characteristics of dyeing wastewater after thermolysis using copper sulphate and at pH 8 at ambient temperature ($C_0 = 4$ kg/m^3, $C_u = 19$ kg/m^3)

S. No.	Time (min)	Height (cm)	u_c (m/s)*10^5	C (kg/m^3)	Sedimentation flux (kg/m^{2}s) x 10^6	$1000\left(\dfrac{1}{C} - \dfrac{1}{C_u}\right)$ m^3/kg	$\dfrac{u_c}{\left(\dfrac{1}{C} - \dfrac{1}{C_u}\right)}$ kg/m^2 s x 10^6	$\dfrac{\left(\dfrac{1}{C} - \dfrac{1}{C_u}\right)}{u_c}$ m^2/s kg x 10^{-6}
1	0	14.3	3.660	4.000	14.640	0.197	18.544	0.054
2	17	13.8	3.660	4.145	15.170	0.189	19.403	0.052
3	31	13.4	3.660	4.269	15.623	0.182	20.150	0.050
4	50	12.9	3.660	4.434	16.229	0.173	21.169	0.047
5	70	12.16	3.660	4.704	17.216	0.160	22.881	0.044
6	90	11.6	3.660	4.931	18.048	0.150	24.373	0.041
7	110	10.98	3.660	5.209	19.067	0.139	26.269	0.038
8	130	10.3	3.660	5.553	20.325	0.127	28.720	0.035
9	150	9.5	3.660	6.021	22.037	0.113	32.260	0.031
10	178	8.56	3.660	6.682	24.457	0.097	37.725	0.027
11	200	7.81	3.660	7.324	26.806	0.084	43.620	0.023
12	220	7.08	3.660	8.079	29.569	0.071	51.444	0.019
13	240	6.51	3.660	8.786	32.159	0.061	59.824	0.017
14	260	5.9	3.660	9.695	35.483	0.051	72.453	0.014
15	280	5.27	3.660	10.854	39.725	0.040	92.655	0.011
16	300	4.7	3.660	12.170	44.543	0.030	123.916	0.008
17	320	4.22	3.660	13.555	49.609	0.021	173.093	0.006
18	337	3.85	3.660	14.857	54.377	0.015	249.385	0.004
19	360	3.33	3.660	17.177	62.868	0.006	655.303	0.002
20	380	3.07	0.116	18.632	2.161	0.001	111.565	0.009
21	410	2.9	0.116	19.724	2.288			
22	440	2.83	0.116	20.212	2.345			
23	470	2.83	0.116	20.212	2.345			

Table 4.15 Settling characteristics of dyeing wastewater after thermolysis using copper sulphate and at pH 10 at ambient temperature ($C_0 = 4$ kg/m^3, $C_u = 19$ kg/m^3)

S. No.	Time (min)	Height (cm)	u_c (m/s)*10^5	C (kg/m^3)	Sedimentation flux (kg/m^{2}s) x 10^6	$1000\left(\dfrac{1}{C}-\dfrac{1}{C_u}\right)$ m^3/kg	$\dfrac{u_c}{\left(\dfrac{1}{C}-\dfrac{1}{C_u}\right)}$ kg/m^2 s x 10^6	$\dfrac{\left(\dfrac{1}{C}-\dfrac{1}{C_u}\right)}{u_c}$ m^2/s kg x 10^{-6}
1	0	14.3	3.010	4.000	12.040	0.197	15.251	0.066
2	15	14	3.010	4.086	12.298	0.192	15.667	0.064
3	33	13.6	3.010	4.206	12.660	0.185	16.259	0.062
4	39	13.4	3.010	4.269	12.849	0.182	16.572	0.060
5	55	13	3.010	4.400	13.244	0.175	17.235	0.058
6	76	12.5	3.010	4.576	13.774	0.166	18.143	0.055
7	91	11.78	3.010	4.856	14.616	0.153	19.633	0.051
8	106	11.35	3.010	5.040	15.169	0.146	20.645	0.048
9	130	10.73	3.010	5.331	16.046	0.135	22.304	0.045
10	154	9.86	3.010	5.801	17.462	0.120	25.137	0.040
11	181	9.12	3.010	6.272	18.879	0.107	28.181	0.035
12	203	8.43	3.010	6.785	20.424	0.095	31.769	0.031
13	230	7.6	3.010	7.526	22.654	0.080	37.515	0.027
14	250	7.01	3.010	8.160	24.561	0.070	43.049	0.023
15	270	6.33	3.010	9.036	27.199	0.058	51.867	0.019
16	290	5.83	3.010	9.811	29.532	0.049	61.065	0.016
17	310	5.4	1.230	10.593	13.029	0.042	29.444	0.034
18	330	5.2	1.230	11.000	13.530	0.038	32.134	0.031
19	350	5	1.230	11.440	14.071	0.035	35.364	0.028
20	370	4.74	1.230	12.068	14.843	0.030	40.681	0.025
21	390	4.6	1.230	12.435	15.295	0.028	44.264	0.023
22	410	4.29	1.230	13.333	16.400	0.022	54.988	0.018
23	430	4.06	1.230	14.089	17.329	0.018	67.039	0.015
24	450	3.89	1.230	14.704	18.086	0.015	79.998	0.013
25	470	3.66	1.230	15.628	19.223	0.011	108.328	0.009
26	490	3.5	1.230	16.343	20.102	0.009	143.738	0.007
27	520	3.3	0.205	17.333	3.553	0.005	40.508	0.025
28	541	3.2	0.205	17.875	3.664	0.003	61.887	0.016
29	567	3.07	0.205	18.632	3.820	0.001	197.163	0.005
30	595	3.02	0.205	18.940	3.883	0.000	1237.744	0.001
31	635	2.93	0.205	19.522	4.002			

Table 4.16 Settling characteristics of dyeing wastewater after coagulation using commercial alum at pH 2 and at ambient temperature ($C_0 = 4$ kg/m³, $C_u = 19$ kg/m³)

S. No.	Time (min)	Height (cm)	u_c (m/s)*10^5	C (kg/m³)	Sedimentation flux (kg/m²s) x 10^6	$1000\left(\frac{1}{C}-\frac{1}{C_u}\right)$ m³/kg	$\frac{u_c}{\left(\frac{1}{C}-\frac{1}{C_u}\right)}$ kg/m² s x 10^6	$\frac{\left(\frac{1}{C}-\frac{1}{C_u}\right)}{u_c}$ m²/s kg x 10^{-6}
1	0	16.3	4.166	4.000	16.664	0.197	21.108	0.047
2	5	15.3	4.166	4.261	17.753	0.182	22.886	0.044
3	10	14.3	4.166	4.559	18.995	0.167	24.992	0.040
4	15	12.4	4.166	5.258	21.905	0.138	30.287	0.033
5	20	11.3	4.166	5.770	24.037	0.121	34.521	0.029
6	25	10	4.166	6.520	27.162	0.101	41.353	0.024
7	30	9.06	3.102	7.196	22.323	0.086	35.934	0.028
8	35	8.1	3.102	8.049	24.969	0.072	43.323	0.023
9	40	7.17	3.102	9.093	28.208	0.057	54.100	0.018
10	45	6.3	3.102	10.349	32.103	0.044	70.509	0.014
11	50	5.8	3.102	11.241	34.871	0.036	85.395	0.012
12	55	5.18	1.113	12.587	14.009	0.027	41.505	0.024
13	60	4.78	1.113	13.640	15.182	0.021	53.817	0.019
14	65	4.37	1.113	14.920	16.606	0.014	77.329	0.013
15	70	4.01	1.113	16.259	18.097	0.009	125.458	0.008
16	75	3.69	1.113	17.669	19.666			
17	80	3.32	1.113	19.639	21.858			
18	85	3.12	1.113	20.897	23.259			
19	90	2.86	1.113	22.797	25.373			
20	95	2.63	0.460	24.791	11.404			
21	100	2.37	0.460	27.511	12.655			
22	105	2.19	0.460	29.772	13.695			
23	110	2.1	0.460	31.048	14.282			
24	115	2.02	0.460	32.277	14.848			
25	120	1.94	0.460	33.608	15.460			

Table 4.17 Settling characteristics of dyeing wastewater after coagulation using commercial alum at pH 4 and at ambient temperature ($C_0 = 4$ kg/m^3, $C_u = 19$ kg/m^3)

S. No.	Time (min)	Height (cm)	u_c (m/s)*10^5	C (kg/m^3)	Sedimentation flux (kg/m^{2}s) x 10^6	$1000\left(\dfrac{1}{C}-\dfrac{1}{C_u}\right)$ m^3/kg	$\dfrac{u_c}{\left(\dfrac{1}{C}-\dfrac{1}{C_u}\right)}$ kg/m^2 s x 10^6	$\dfrac{\left(\dfrac{1}{C}-\dfrac{1}{C_u}\right)}{u_c}$ m^2/s kg x 10^{-6}
1	0	16.3	2.223	4.000	8.892	0.197	11.263	0.089
2	5	15.9	2.223	4.101	9.116	0.191	11.625	0.086
3	10	15.5	2.223	4.206	9.351	0.185	12.010	0.083
4	15	14.61	2.223	4.463	9.921	0.171	12.966	0.077
5	20	14	2.223	4.657	10.353	0.162	13.714	0.073
6	25	13.41	2.223	4.862	10.808	0.153	14.525	0.069
7	30	12.9	2.223	5.054	11.236	0.145	15.308	0.065
8	35	12.13	2.223	5.375	11.949	0.133	16.663	0.060
9	40	11.37	2.223	5.734	12.748	0.122	18.258	0.055
10	45	10.4	2.223	6.269	13.937	0.107	20.799	0.048
11	50	9.7	2.223	6.722	14.942	0.096	23.122	0.043
12	55	9.01	2.223	7.236	16.087	0.086	25.982	0.038
13	60	8.46	2.223	7.707	17.132	0.077	28.824	0.035
14	65	7.9	2.135	8.253	17.621	0.069	31.152	0.032
15	70	7.33	2.135	8.895	18.991	0.060	35.707	0.028
16	75	6.86	1.211	9.504	11.510	0.053	23.030	0.043
17	80	6.48	1.211	10.062	12.185	0.047	25.901	0.039
18	85	6.05	1.211	10.777	13.051	0.040	30.155	0.033
19	90	5.69	1.211	11.459	13.876	0.035	34.961	0.029
20	95	5.26	1.211	12.395	15.011	0.028	43.183	0.023
21	100	4.96	1.211	13.145	15.919	0.023	51.659	0.019
22	105	4.68	1.211	13.932	16.871	0.019	63.246	0.016
23	110	4.23	0.620	15.414	9.557	0.012	50.630	0.020
24	115	4.09	0.620	15.941	9.884	0.010	61.395	0.016
25	120	3.89	0.620	16.761	10.392	0.007	88.181	0.011
26	125	3.62	0.620	18.011	11.167	0.003	214.541	0.005
27	130	3.48	0.620	18.736	11.616	0.001	834.843	0.001
28	135	3.3	0.620	19.758	12.250			
29	140	3.26	0.620	20.000	12.400			

174

Table 4.18 **Settling characteristics of dyeing wastewater after coagulation using commercial alum at pH 8 and at ambient temperature ($C_0 = 4$ kg/m³, $C_u = 30$ kg/m³)**

S. No.	Time (min)	Height (cm)	u_c (m/s)*10^5	C (kg/m³)	Sedimentation flux (kg/m²s) x 10^6	$1000\left(\dfrac{1}{C}-\dfrac{1}{C_u}\right)$ m³/kg	$\dfrac{u_c}{\frac{1}{C}-\frac{1}{C_u}}$ kg/m² s x 10^6	$\dfrac{\frac{1}{C}-\frac{1}{C_u}}{u_c}$ m²/s kg x 10^{-6}
1	0	16.3	1.277	4.000	5.108	0.217	5.894	0.170
2	10	15.7	1.277	4.153	5.303	0.207	6.155	0.162
3	20	14.8	1.277	4.405	5.626	0.194	6.594	0.152
4	30	14	1.277	4.657	5.947	0.181	7.040	0.142
5	40	13.57	1.277	4.805	6.136	0.175	7.306	0.137
6	50	12.7	0.930	5.134	4.774	0.161	5.760	0.174
7	60	12.09	0.930	5.393	5.015	0.152	6.115	0.164
8	70	11.6	0.930	5.621	5.227	0.145	6.432	0.155
9	80	11	0.930	5.927	5.512	0.135	6.870	0.146
10	90	10.4	0.930	6.269	5.830	0.126	7.371	0.136
11	100	9.78	0.930	6.667	6.200	0.117	7.971	0.125
12	110	9.29	0.930	7.018	6.527	0.109	8.520	0.117
13	120	8.73	0.930	7.468	6.946	0.101	9.248	0.108
14	130	8.1	0.930	8.049	7.486	0.091	10.231	0.098
15	140	7.57	0.930	8.613	8.010	0.083	11.236	0.089
16	150	7.03	0.930	9.275	8.625	0.074	12.485	0.080
17	160	6.52	0.930	10.000	9.300	0.067	13.950	0.072
18	170	6.05	0.930	10.777	10.022	0.059	15.641	0.064
19	180	5.37	0.930	12.142	11.292	0.049	18.969	0.053
20	190	4.64	0.930	14.052	13.068	0.038	24.582	0.041
21	200	4.29	0.930	15.198	14.134	0.032	28.647	0.035
22	210	3.85	0.592	16.935	10.026	0.026	23.021	0.043
23	220	3.38	0.592	19.290	11.420	0.019	31.988	0.031
24	230	2.96	0.592	22.027	13.040	0.012	49.066	0.020
25	240	2.67	0.592	24.419	14.456	0.008	77.715	0.013
26	250	2.45	0.592	26.612	15.754	0.004	139.512	0.007
27	260	2.21	0.227	29.502	6.697	0.001	403.647	0.002
28	270	2.04	0.227	31.961	7.255			
29	280	1.88	0.227	34.681	7.873			
30	290	1.8	0.227	36.222	8.222			
31	300	1.78	0.227	36.629	8.315			

Table 4.19 **Settling characteristics of desizing wastewater after thermolysis using copper sulphate at pH 8 and at ambient temperature (C_0 = 5 kg/m³, C_u = 20 kg/m³)**

S. No.	Time (min)	Height (cm)	u_c (m/s)*10^5	C (kg/m³)	Sedimentation flux (kg/m²s) x 10^6	$1000\left(\dfrac{1}{C}-\dfrac{1}{C_u}\right)$ m³/kg	$\dfrac{u_c}{\left(\dfrac{1}{C}-\dfrac{1}{C_u}\right)}$ kg/m² s x 10^6	$\dfrac{\left(\dfrac{1}{C}-\dfrac{1}{C_u}\right)}{u_c}$ m²/s kg x 10^{-6}
1	0	10	3.330	5.000	16.650	0.150	22.200	0.045
2	5	9.4	3.330	5.319	17.713	0.138	24.130	0.041
3	10	8.8	3.330	5.682	18.920	0.126	26.429	0.038
4	15	7.9	3.330	6.329	21.076	0.108	30.833	0.032
5	20	6.3	3.330	7.937	26.429	0.076	43.816	0.023
6	25	5	3.330	10.000	33.300	0.050	66.600	0.015
7	30	4.14	3.330	12.077	40.217	0.033	101.524	0.010
8	35	3.4	1.800	14.706	26.471	0.018	100.000	0.010
9	40	2.86	1.800	17.483	31.469	0.007	250.000	0.004
10	45	2.4	1.000	20.833	20.833			
11	50	2.1	1.000	23.810	23.810			

Table 4.20 Settling characteristics of desizing wastewater after thermolysis using copper sulphate at pH 10 and at ambient temperature ($C_0 = 5$ kg/m³, $C_u = 20$ kg/m³)

S. No.	Time (min)	Height (cm)	u_c (m/s)*10^5	C (kg/m³)	Sedimentation flux (kg/m²s) x 10^6	$1000\left(\dfrac{1}{C}-\dfrac{1}{C_u}\right)$ m³/kg	$\dfrac{u_c}{\left(\dfrac{1}{C}-\dfrac{1}{C_u}\right)}$ kg/m² s x 10^6	$\dfrac{\left(\dfrac{1}{C}-\dfrac{1}{C_u}\right)}{u_c}$ m²/s kg x 10^{-6}
1	0	10	1.263	5.000	6.315	0.150	8.420	0.119
2	5	9.9	1.263	5.051	6.379	0.148	8.534	0.117
3	10	9.6	1.263	5.208	6.578	0.142	8.894	0.112
4	15	9.4	1.263	5.319	6.718	0.138	9.152	0.109
5	20	9.2	1.263	5.435	6.864	0.134	9.425	0.106
6	25	9	1.263	5.556	7.017	0.130	9.715	0.103
7	30	8.6	1.263	5.814	7.343	0.122	10.352	0.097
8	35	8.2	1.263	6.098	7.701	0.114	11.079	0.090
9	40	7.8	1.263	6.410	8.096	0.106	11.915	0.084
10	45	7.5	1.263	6.667	8.420	0.100	12.630	0.079
11	50	7.05	1.263	7.092	8.957	0.091	13.879	0.072
12	55	6.6	1.263	7.576	9.568	0.082	15.402	0.065
13	60	6	1.263	8.333	10.525	0.070	18.043	0.055
14	65	5.6	1.263	8.929	11.277	0.062	20.371	0.049
15	70	5.2	1.263	9.615	12.144	0.054	23.389	0.043
16	75	4.8	1.263	10.417	13.156	0.046	27.457	0.036
17	80	4.33	1.263	11.547	14.584	0.037	34.508	0.029
18	85	3.8	1.263	13.158	16.618	0.026	48.577	0.021
19	90	3.2	1.263	15.625	19.734	0.014	90.214	0.011
20	95	2.8	1.263	17.857	22.554	0.006	210.500	0.005
21	100	2.53	0.400	19.763	7.905	0.001	666.667	0.001
22	105	2.4	0.400	20.833	8.333			
23	110	2.29	0.400	21.834	8.734			

Table 4.21 Settling characteristics of desizing wastewater after thermolysis using copper sulphate at pH 12 and at ambient temperature ($C_0 = 5$ kg/m³, $C_u = 20$ kg/m³)

S. No.	Time (min)	Height (cm)	u_c (m/s)*10^5	C (kg/m³)	Sedimentation flux (kg/m²s) x 10^6	$1000\left(\dfrac{1}{C}-\dfrac{1}{C_u}\right)$ m³/kg	$\dfrac{u_c}{\left(\dfrac{1}{C}-\dfrac{1}{C_u}\right)}$ kg/m² s x 10^6	$\dfrac{\left(\dfrac{1}{C}-\dfrac{1}{C_u}\right)}{u_c}$ m²/s kg x 10^{-6}
1	0	10	9.660	5.000	48.300	0.150	64.400	0.016
2	5	9.9	9.660	5.051	48.788	0.148	65.270	0.015
3	10	9.8	9.660	5.102	49.286	0.146	66.164	0.015
4	15	9.7	9.660	5.155	49.794	0.144	67.083	0.015
5	20	9.5	9.660	5.263	50.842	0.140	69.000	0.014
6	25	9.33	9.660	5.359	51.768	0.137	70.717	0.014
7	30	9.09	9.660	5.501	53.135	0.132	73.293	0.014
8	35	8.84	9.660	5.656	54.638	0.127	76.183	0.013
9	40	8.68	9.660	5.760	55.645	0.124	78.155	0.013
10	45	8.4	9.660	5.952	57.500	0.118	81.864	0.012
11	50	8	9.660	6.250	60.375	0.110	87.818	0.011
12	55	7.6	9.660	6.579	63.553	0.102	94.706	0.011
13	60	7.1	9.660	7.042	68.028	0.092	105.000	0.010
14	65	6.75	9.660	7.407	71.556	0.085	113.647	0.009
15	70	6.42	9.660	7.788	75.234	0.078	123.214	0.008
16	75	6.04	9.660	8.278	79.967	0.071	136.441	0.007
17	80	5.71	9.660	8.757	84.588	0.064	150.467	0.007
18	85	5.41	9.660	9.242	89.279	0.058	165.979	0.006
19	90	4.95	9.660	10.101	97.576	0.049	197.143	0.005
20	95	4.54	9.660	11.013	106.388	0.041	236.765	0.004
21	100	4.2	9.660	11.905	115.000	0.034	284.118	0.004
22	105	3.95	7.000	12.658	88.608	0.029	241.379	0.004
23	110	3.8	7.000	13.158	92.105	0.026	269.231	0.004
24	115	3.6	7.000	13.889	97.222	0.022	318.182	0.003
25	120	3.4	7.000	14.706	102.941	0.018	388.889	0.003
26	125	3.13	7.000	15.974	111.821	0.013	555.556	0.002
27	130	2.9	7.000	17.241	120.690	0.008	875.000	0.001
28	135	2.8	7.000	17.857	125.000	0.006	1166.667	0.001
29	140	2.64	7.000	18.939	132.576	0.003	2500.000	0.000
30	145	2.48	7.000	20.161	141.129			
31	150	2.3	1.330	21.739	28.913			
32	155	2.26	1.330	22.124	29.425			

Table 4.22 Settling characteristics of desizing wastewater after coagulation using commercial alum at pH 4 and at ambient temperature ($C_0 = 5$ kg/m^3, $C_u = 9.8$ kg/m^3)

S. No.	Time (min)	Height (cm)	u_c (m/s)*10^5	C (kg/m^3)	Sedimentation flux (kg/m^{2}s) x 10^6	$1000\left(\dfrac{1}{C}-\dfrac{1}{C_u}\right)$ m^3/kg	$\dfrac{u_c}{\left(\dfrac{1}{C}-\dfrac{1}{C_u}\right)}$ kg/m^2 s x 10^6	$\dfrac{\left(\dfrac{1}{C}-\dfrac{1}{C_u}\right)}{u_c}$ m^2/s kg x 10^{-6}
1	0	10	8.484	5.000	42.420	0.098	86.608	0.012
2	15	9.9	8.484	5.051	42.848	0.096	88.413	0.011
3	60	9.75	8.484	5.128	43.508	0.093	91.266	0.011
4	120	9.6	8.484	5.208	44.188	0.090	94.309	0.011
5	180	9.4	8.484	5.319	45.128	0.086	98.698	0.010
6	240	9	8.484	5.556	47.133	0.078	108.826	0.009
7	270	8.9	8.484	5.618	47.663	0.076	111.692	0.009
8	300	8.8	8.484	5.889	49.965	0.068	125.208	0.008
9	420	8.5	8.484	6.386	54.176	0.055	155.501	0.006
10	480	8.3	8.484	6.510	55.234	0.052	164.549	0.006
11	540	8.2	8.484	6.702	56.863	0.047	179.901	0.006
12	600	7.8	8.484	7.022	59.579	0.040	210.212	0.005
13	660	7.6	8.484	7.485	63.503	0.032	268.828	0.004
14	720	7	8.484	7.924	67.227	0.024	351.171	0.003
15	780	6.1	8.484	8.170	69.314	0.020	416.716	0.002
16	840	5.7	8.484	8.772	74.421	0.012	709.413	0.001
17	900	5.5	8.484	9.091	77.127	0.008	1065.938	0.001
18	1080	5.4	0.810	9.259	7.500	0.006	135.925	0.007
19	1260	5.3	0.810	9.434	7.642	0.004	204.588	0.005
20	1440	5.2	0.810	9.615	7.788	0.002	413.437	0.002
21	1560	5.1	0.810	9.804	7.941			
22	1680	5.1	0.810	9.804	7.941			
23	1800	5.05	0.810	9.901	8.020			
24	1920	5.05	0.810	9.901	8.020			

Table 4.23 **Settling characteristics of desizing wastewater after coagulation using commercial alum at pH 12 and at ambient temperature ($C_0 = 5$ kg/m^3, $C_u = 20$ kg/m^3)**

S. No.	Time (min)	Height (cm)	u_c (m/s)*10^5	C (kg/m^3)	Sedimentation flux (kg/m^{2}s) x 10^6	$1000\left(\frac{1}{C}-\frac{1}{C_u}\right)$ m^3/kg	$\dfrac{u_c}{\left(\frac{1}{C}-\frac{1}{C_u}\right)}$ kg/m^2 s x 10^6	$\dfrac{\left(\frac{1}{C}-\frac{1}{C_u}\right)}{u_c}$ m^2/s kg x 10^{-6}
1	0.000	10.000	1.510	5.000	7.550	0.150	10.067	0.099
2	2.933	8.800	1.510	5.682	8.580	0.126	11.984	0.083
3	3.650	8.100	1.510	6.173	9.321	0.112	13.482	0.074
4	4.300	7.600	1.510	6.579	9.934	0.102	14.804	0.068
5	4.683	7.300	1.510	6.849	10.342	0.096	15.729	0.064
6	5.200	6.800	1.510	7.353	11.103	0.086	17.558	0.057
7	5.783	6.300	1.510	7.937	11.984	0.076	19.868	0.050
8	6.300	6.000	1.510	8.333	12.583	0.070	21.571	0.046
9	6.817	5.500	1.510	9.091	13.727	0.060	25.167	0.040
10	7.217	5.000	1.510	10.000	15.100	0.050	30.200	0.033
11	7.667	4.500	1.510	11.111	16.778	0.040	37.750	0.026
12	8.667	4.000	0.033	12.500	0.406	0.030	1.083	0.923
13	9.517	3.800	0.033	13.158	0.428	0.026	1.250	0.800
14	10.300	3.600	0.033	13.889	0.451	0.022	1.477	0.677
15	11.567	3.400	0.033	14.706	0.478	0.018	1.806	0.554
16	12.933	3.200	0.033	15.625	0.508	0.014	2.321	0.431
17	14.650	3.000	0.076	16.667	1.267	0.010	7.600	0.132
18	15.950	2.900	0.076	17.241	1.310	0.008	9.500	0.105
19	17.533	2.800	0.076	17.857	1.357	0.006	12.667	0.079
20	19.050	2.700	0.076	18.519	1.407	0.004	19.000	0.053
21	21.133	2.600	0.076	19.231	1.462	0.002	38.000	0.026
22	23.217	2.500	0.076	20.000	1.520			
23	25.717	2.400	0.076	20.833	1.583			
24	28.500	2.300	0.076	21.739	1.652			
25	31.783	2.200	0.076	22.727	1.727			

4.7 FILTERABILITY OF THE TREATED SLURRY OBTAINED AFTER CATALYTIC THERMOLYSIS/COAGULATION

Filtration is one of the steps used to clarify the treated effluent. The filterability studies are important to decide upon the optimal treatment process parameters which could produce a treated effluent with flocs having faster filtration.

The gravity filtration of the slurry was carried out at room temperature on an ordinary filter paper supported on a Büchner funnel, under constant pressure filtration. The filtrate volume obtained as a function of time was observed and a plot between $\Delta t / \Delta V$ and V was drawn for the effluents treated at different pH. The plot in Figure 4.47 shows a linear relationship. It is evident that the filterability of the treated effluent gets improved with an increase in the pH_0. pH 10 seems to offer least resistance to filtration. The filtration resistances for the filter media as well as the filter cake were obtained using the filtration equation (MaCabe et al., 2001).

$$dt / dV = k_p V + \beta \tag{19}$$

$$\text{where, } k_p = C \alpha \mu / A^2 (-\Delta p) \tag{20}$$

$$\text{and } \beta = \mu R_m / A(-\Delta p) \tag{21}$$

where k_p (slope) and β (intercept) were determined by the plot of equation (19) as shown in Figures 4.47-4.52. The values of α and R_m were calculated from k_p and β and are presented in Tables 4.24-4.26 for the sludge obtained after catalytic thermolysis and coagulation of textile mill wastewaters.
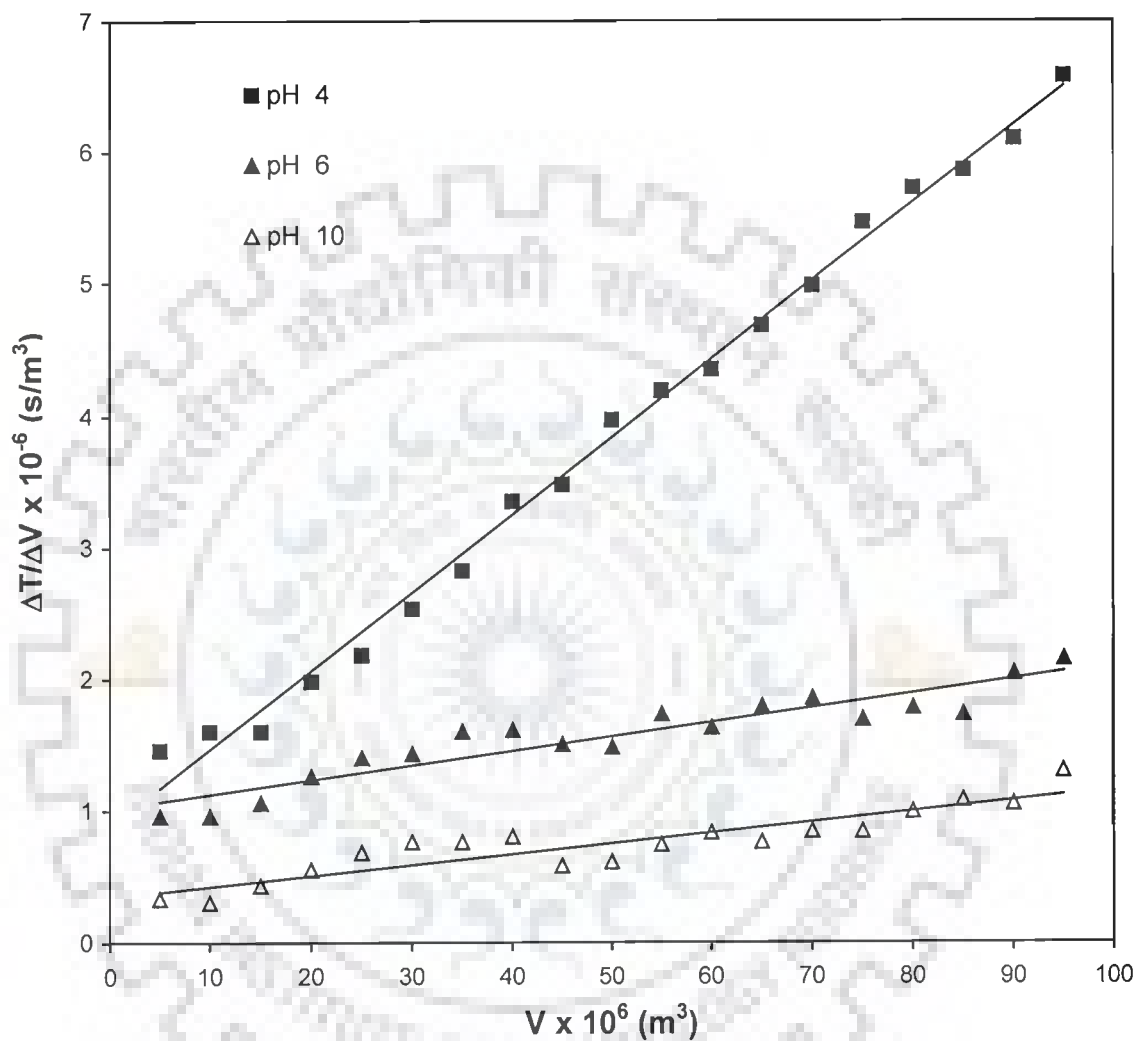
Figure 4.47 Effect of pH_0 on the filterability of the composite wastewater after catalytic thermolysis using copper sulphate as catalyst
$COD_0 = 1960$ mg/l, T = ambient temperature, P = atmospheric, $C_w = 5$ kg/m^3
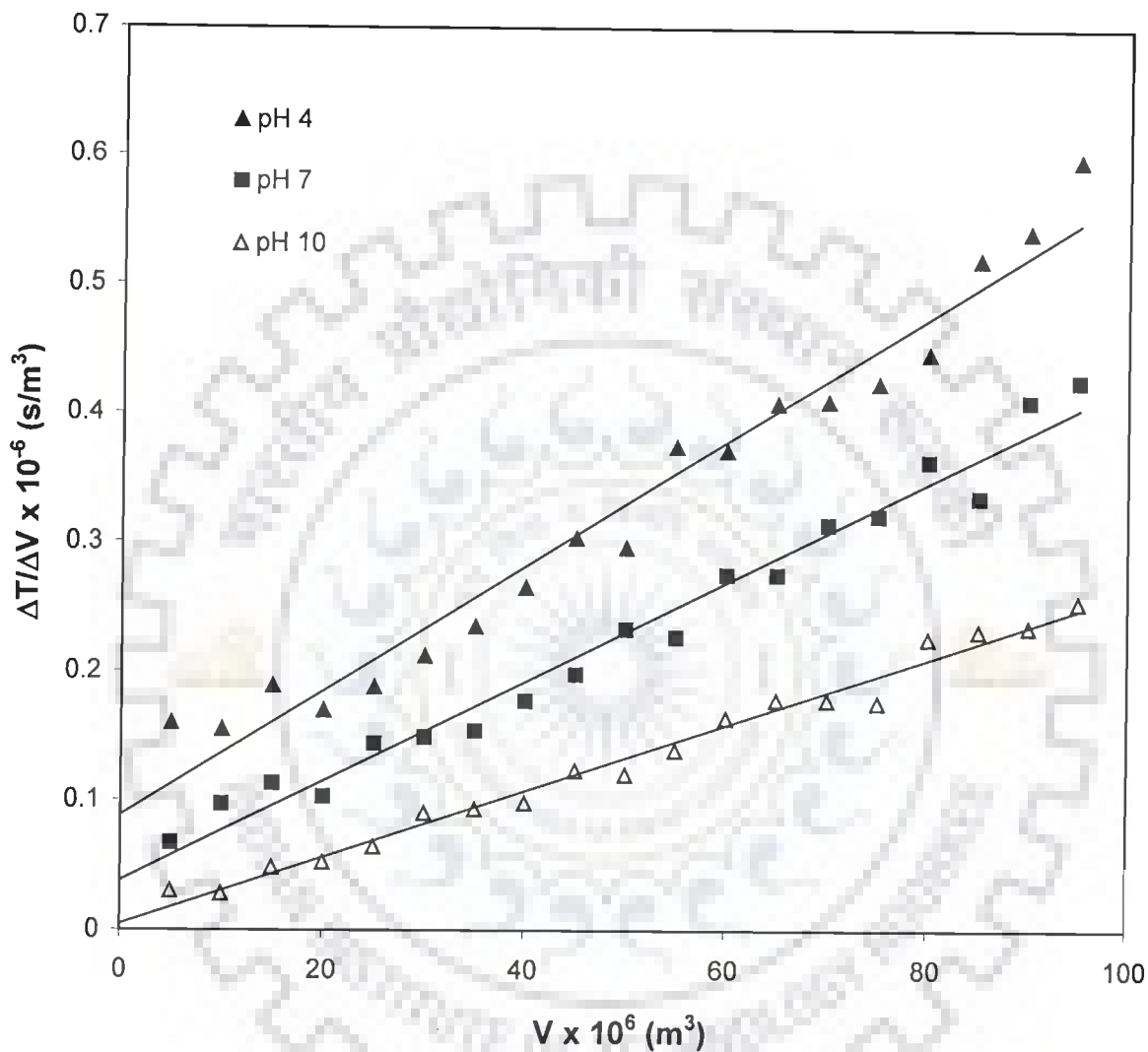
Figure 4.48 Filterability characteristics of slurry of composite wastewater in the treated effluent at ambient temperature using aluminum potassium sulphate as coagulant

$COD_0 = 1960$ mg/l, P = atmospheric, $C_w = 5$ kg/m^3
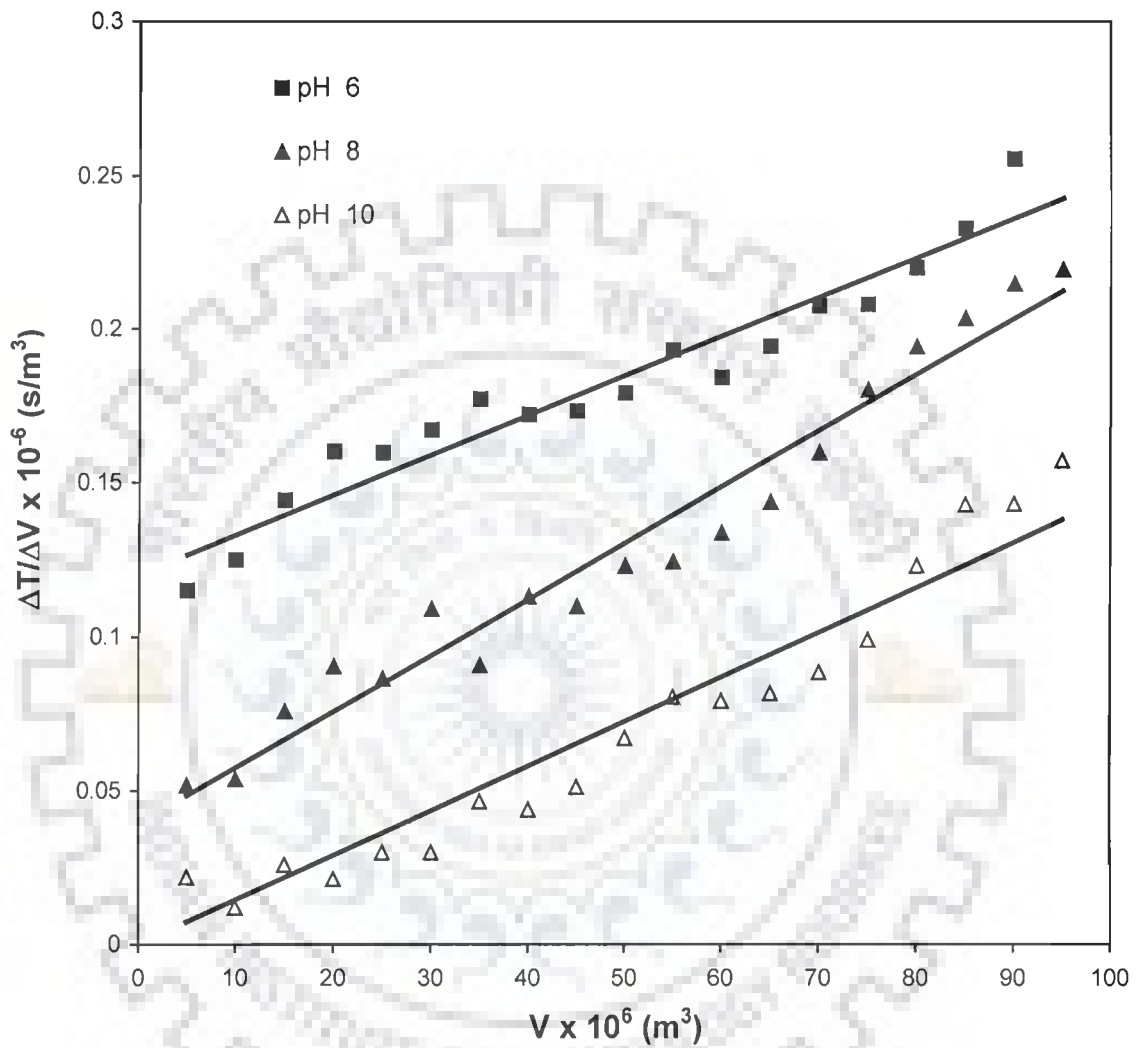
Figure 4.49 Filterability characteristics of slurry of dyeing wastewater in the treated effluent at ambient temperature using copper sulphate as catalyst

$COD_0 = 5744$ mg/l, P = atmospheric, $C_w = 5$ kg/m^3
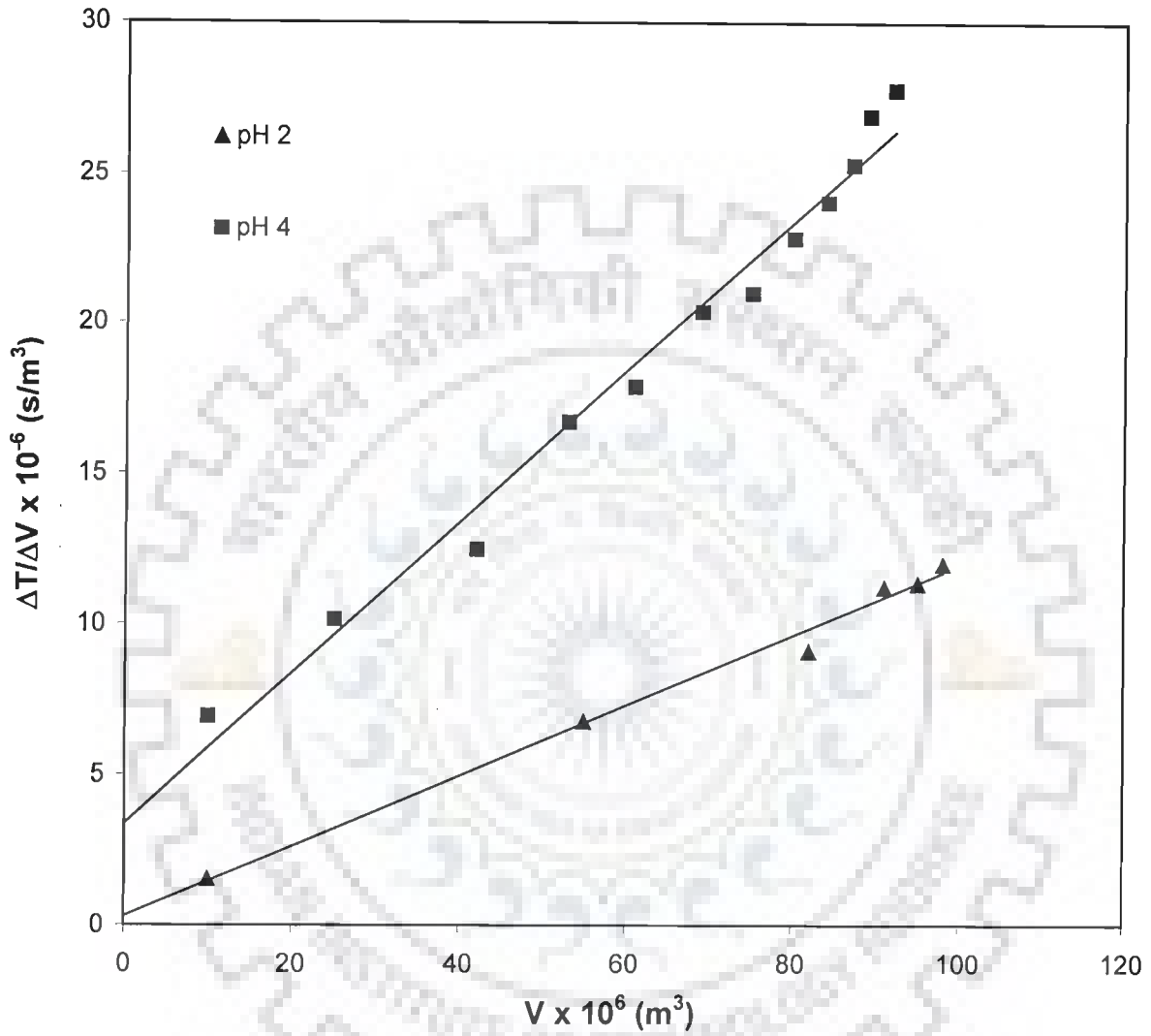
Figure 4.50 Filterability characteristics of slurry of dyeing wastewater in the treated effluent at ambient temperature using commercial alum as coagulant

$COD_0 = 5744$ mg/l, P = atmospheric, $C_w = 5$ kg/m^3
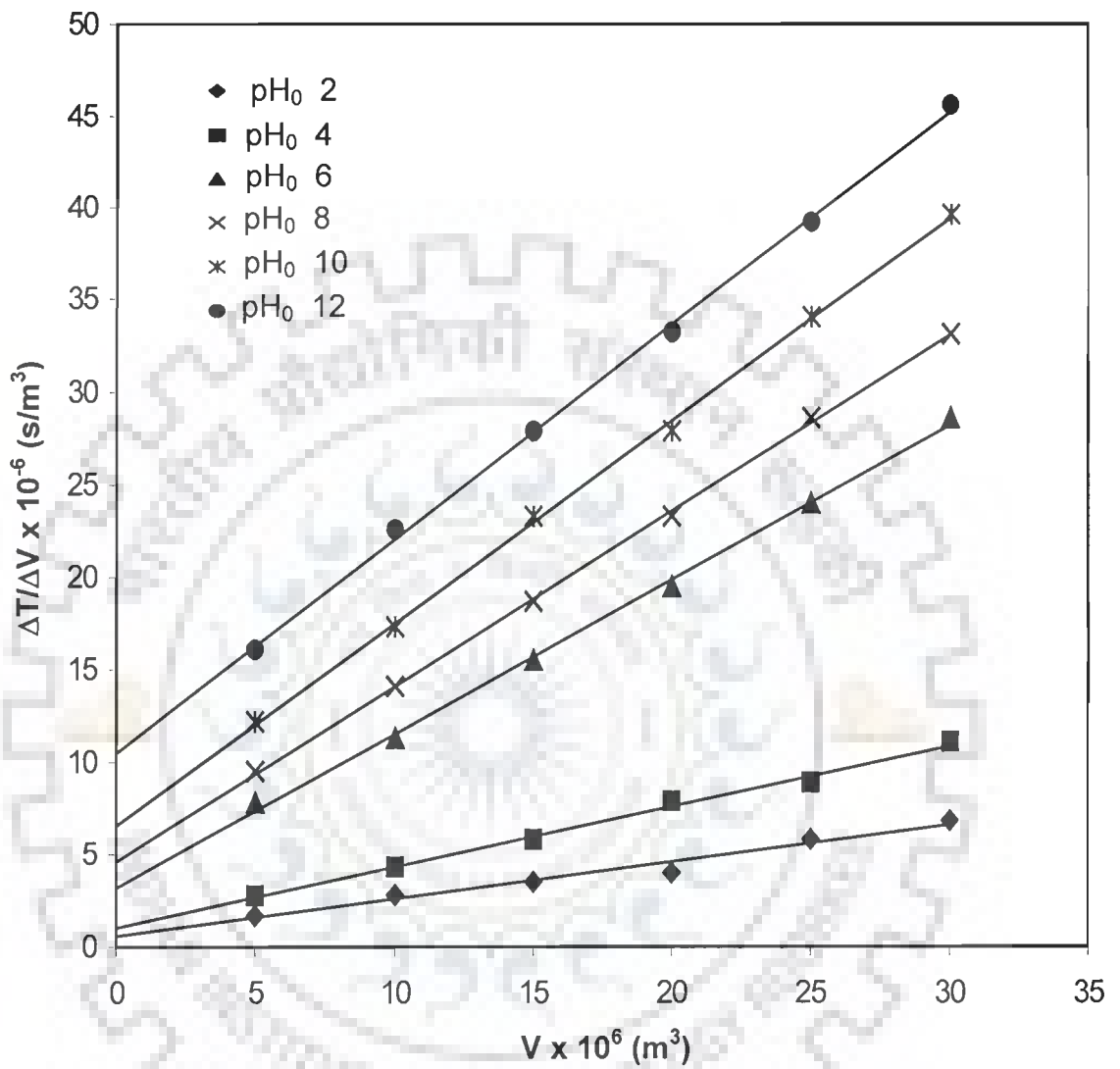
Figure 4.51 Effect of pH_0 on the filterability of the desizing wastewater after catalytic thermolysis

$T_R = 95^oC$, P = atmospheric pressure, $COD_0 = 2884$ mg/l, $C_w = 4$ kg/m^3
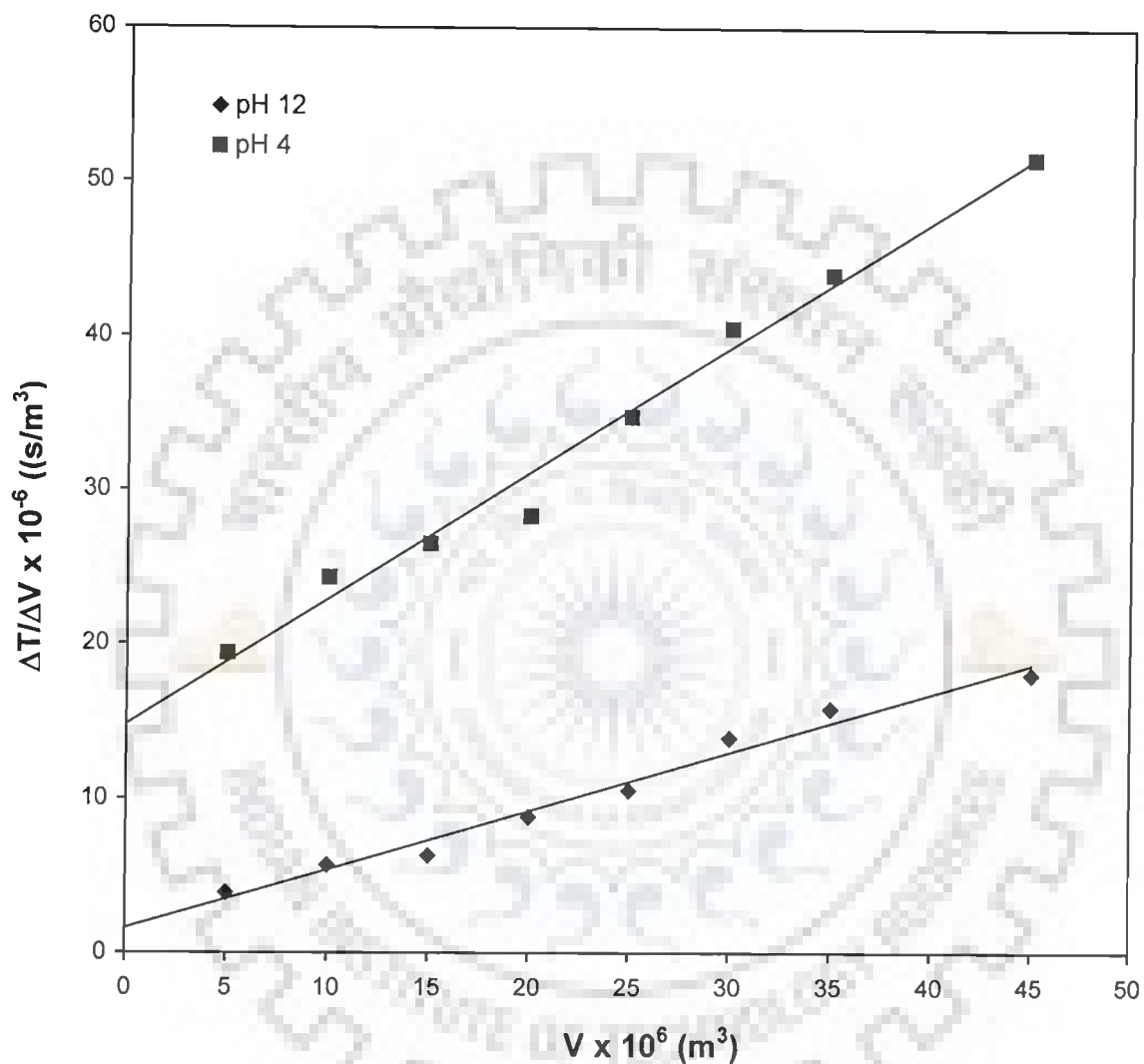
Figure 4.52 Effect of pH_0 on the filterability of the desizing wastewater after coagulation

$COD_0 = 2884$ mg/l, P = atmospheric pressure, $C_w = 5$ kg/m^3

Table 4.24 Filterability characteristics of the slurry of composite wastewater after treatment: Effect of the initial pH (pH_0)[a]

Catalytic thermolysis

pH_0	$k_p \times 10^{-12}$ s/m^6	$\beta \times 10^{-6}$ s/m^3	C kg/m^3	$\mu \times 10^3$ PaS	$\alpha \times 10^{-10}$ m/kg	$R_m \times 10^{-8}$ m^{-1}
4	0.5	0.9	1.65	1.83	10.67	4.53
6	0.12	1.0	1.61	1.85	2.36	4.98
10	0.71	0.4	1.69	1.80	1.34	2.04

Coagulation

pH_0	$k_p \times 10^{-12}$ s/m^6	$\beta \times 10^{-6}$ s/m^3	C kg/m^3	$\mu \times 10^3$ PaS	$\alpha \times 10^{-10}$ m/kg	$R_m \times 10^{-8}$ m^{-1}
4	0.4	0.9	1.65	1.83	0.91	0.47
7	0.3	0.8	1.61	1.85	0.72	0.14
10	0.2	0.6	1.69	1.80	0.48	0.38

[a] $A = 6.358 \times 10^{-3}$ m^2

Table 4.25 Filterability characteristics of the slurry of dyeing wastewater after treatment: Effect of the initial pH (pH_0)

Catalytic thermolysis

pH_0	$k_p \times 10^{-12}$ s/m^6	$\beta \times 10^{-6}$ s/m^3	C kg/m^3	$\mu \times 10^3$ PaS	$\alpha \times 10^{-10}$ m/kg	$R_m \times 10^{-8}$ m^{-1}
6	0.125	0.12	6.34	1.96	0.058	0.563
8	0.178	0.04	6.96	1.987	0.075	0.185
10	0.138	0.00	6.10	1.951	0.067	0.000

Coagulation

pH_0	$k_p \times 10^{-12}$ s/m^6	$\beta \times 10^{-6}$ s/m^3	C kg/m^3	$\mu \times 10^3$ PaS	$\alpha \times 10^{-10}$ m/kg	$R_m \times 10^{-8}$ m^{-1}
2	0.111	0.26	3.8	1.75	9.78	13.85
4	0.243	3.42	3.6	1.73	22.92	18.23

Table 4.25 Filterability of the slurry of desizing wastewater after treatment: Effect of the initial pH (pH_0)

Catalytic thermolysis

pH_0	$k_p \times 10^{-12}$ s/m^6	$\beta \times 10^{-6}$ s/m^3	C kg/m^3	$\mu \times 10^3$ PaS	$\alpha \times 10^{-10}$ m/kg	$R_m \times 10^{-8}$ m^{-1}
2	0.2	0.6	0.3666	0.9639	331.74	5.738
4	0.3284	1.0513	0.4666	0.9315	442.87	10.404
6	0.8349	3.1733	1.5	0.9829	331.925	29.764
8	0.9491	4.6067	4.333	1.0126	125.83	41.941
10	1.0954	6.5467	4.4	1.0842	134.59	55.667
12	1.1577	10.507	4.6	1.132	130.316	85.569

Coagulation

pH_0	$k_p \times 10^{-12}$ s/m^6	$\beta \times 10^{-6}$ s/m^3	C kg/m^3	$\mu \times 10^3$ PaS	$\alpha \times 10^{-10}$ m/kg	$R_m \times 10^{-8}$ m^{-1}
4	0.833	15	4.5	1.96	55.35	70.55
12	0.348	2	4.7	1.98	21.91	93.12

4.8 ELEMENTAL AND COMPOSITIONAL CHARACTERIZATION OF THE SOLID RESIDUE OBTAINED AFTER TREATMENT

The C, H, N, S and proximate analyses of the settled precipitate and the wastewater (composite, dyeing and desizing) are presented in Tables 4.26 through 4.31. The heating values of the precipitate and the wastewater are also given and compared with those of Indian coal. The elemental analysis (Table 4.26, 4.28 and 4.30) shows that there are enhancements in carbon and hydrogen composition in the precipitate and that its heating value compares well with that of Indian coal.

The carbonaceous load of the treated wastewater after filtration has gone down considerably as the supernatant is much leaner in carbon and hydrogen composition. The proximate analysis, as shown in Tables 4.27, 4.29 and 4.31, indicate considerably lower ash content in the precipitate than that in the wastewater, except in desizing wastewater, and considerably higher fixed carbon content in the precipitate than that in the wastewater.

Table 4.26   Elemental analysis of composite wastewater and precipitate formed after treatment

Material	C (%)	H (%)	N (%)	S (%)	Heating value of residue (MJ/kg)
Catalytic thermolysis (with copper sulphate)					
Composite wastewater (dried)	10.65	3.013	0.00	7.094	7.2
Precipitate	14.32	0.28	0.00	5.045	16.0
Supernatant	2.975	0.169	0.00	4.887	-
Indian coal	4.887	5.01	0.80	1.70	20.90
Coagulation (with aluminum potassium sulphate)					
Precipitate	7.74	2.97	0.07	7.40	12.0

Table 4.27   Proximate analysis (moisture-free basis) of composite wastewater and precipitate formed after treatment

Material	Ash %	Volatile matter %	Fixed carbon %
Catalytic thermolysis (with copper sulphate)			
Composite wastewater (dried)	46.0	37.0	5.0
Precipitate	41.6	43.6	9.2
Coagulation (with aluminum potassium sulphate)			
Precipitate	48.7	35.3	10.4

Table 4.28 Elemental analysis of dyeing wastewater and precipitate formed after treatment

Material	C (%)	H (%)	N (%)	S (%)
Catalytic thermolysis (with copper sulphate)				
Dyeing wastewater (dried)	0.114	17.57	0.00	0.00
Precipitate	3.083	3.287	0.00	0.00
Supernatant	1.53	0.05	0.00	0.00
Indian coal	4.887	5.01	0.80	1.70
Coagulation (with commercial alum)				
Precipitate	0.85	8.79	0.00	0.00

Table 4.29 Proximate analysis (moisture-free basis) of dyeing wastewater and precipitate formed after treatment

Material	Ash %	Volatile matter %	Fixed carbon %
Catalytic thermolysis (with copper sulphate)			
Dyeing wastewater (dried)	91.1	5.74	0.09
Precipitate	47.0	31.0	10.0
Coagulation (with commercial alum)			
Precipitate	82.48	5.88	9.2

Table 4.30 Elemental analysis of desizing wastewater and precipitate formed after treatment

Material	C (%)	H (%)	N (%)	S (%)	Heating value of solids (MJ/kg)
Catalytic thermolysis (with copper sulphate)					
Desizing wastewater (dried)	17.10	3.14	0.85	0.80	4.3
Precipitate	22.21	3.59	0.98	1.76	8.5
Supernatant	3.46	1.21	0.00	0.86	-
Indian coal	50.00	5.01	0.80	1.70	20.90
Coagulation (with commercial alum)					
Precipitate	0.85	19.92	0.00	0.00	-

Table 4.31 Proximate analysis (Moisture-free basis) of desizing wastewater and precipitate formed after treatment

Material	Ash %	Volatile matter %	Fixed carbon %
Catalytic thermolysis (with copper sulphate)			
Desizing wastewater (dried)	25.3	47.0	7.5
Precipitate	26.4	38.2	29.44
Coagulation (with commercial alum)			
Precipitate	25.48	45.0	10.15

4.9 THERMAL DEGRADATION OF SLUDGE OBTAINED AFTER CATALYTIC THERMOLYSIS AND COAGULATION

The thermogravimetric studies (TGA, DTA and DTGA) were conducted for the precipitated sludges of the dyeing, desizing and composite waste waters in order to study the combustion characteristics and the prospect of being used as a solid fuel. The information on the temperature of dehydration and volatilization (removal of volatiles), their rates and heats evolved/consumed during the process were obtained. The kinetic analysis and reaction mechanisms of thermal degradation and oxidation have been proposed for residue degradation using thermogravimetry.

191

4.9.1 TGA/DTA/DTGA of sludge of Composite Wastewater by Catalytic Thermolysis and Coagulation

The TGA, DTA and DTGA curves were obtained for the precipitated sludge at 10 °C/min heating rate and 200 ml/min air flashing rate and are presented in Figure 4.53(a). The nature of TGA trace shows dehydration and volatilization (removal of volatiles) of the sample up to a temperature of 180 °C losing about 93.17% of its weight. Between 180 °C and 240 °C the residue oxidizes losing about 20% of its original weight. The peak rate of weight loss at T_{max} = 227 °C is 5 mg/min. The oxidation is found uniform and exothermic with a heat evolution of 889 MJ/kg. The peak of exotherm being at a temperature of T_p = 242 °C. The oxidation of the residue seems to become slower between 240 °C and 366 °C, losing weight of about 10% with a marginal heat of exothermic reaction of 119 MJ/kg at the peak temperature 326 °C. The oxidation continued at very slow rate from 366 °C to 990 °C, losing a maximum weight of less than 7%, leaving the ash fraction of ~44.1% as the residue.

Figure 4.53(b) shows the TGA, DTA and DTG traces of the composite wastewater under similar heating conditions. In contrast to the TGA behavior of the precipitate, the composite wastewater TGA trace shows only about 0.62% decrease in weight upto 82 °C. However, there has been a sudden drop in the weight of about 11% from 82 °C to 117 °C on account of vaporization of volatiles and moisture.

The maximum rate of weight loss of 0.5 mg/min at 106 °C was observed with an endothermic heat requirement of 365 MJ/kg recorded at the peak temperature of 107 °C. The rate of weight loss from 117 °C onwards was extremely slow upto 699 °C losing weight of only 7%. Beyond 699 °C there has been a steady weight loss of about 20% upto 890 °C. The maximum rate of weight loss of about 0.35 mg/min was observed at around 870 °C. This might be due to the molecular level rearrangement.

The comparison of the thermal analysis of the two residues (precipitate as well as composite wastewater) shows that the precipitate obtained after catalytic thermolysis gets oxidized at a higher temperature range than that of the composite wastewater. This may be due to the presence of more stable compounds formed during catalytic thermolysis in presence of copper catalysts.
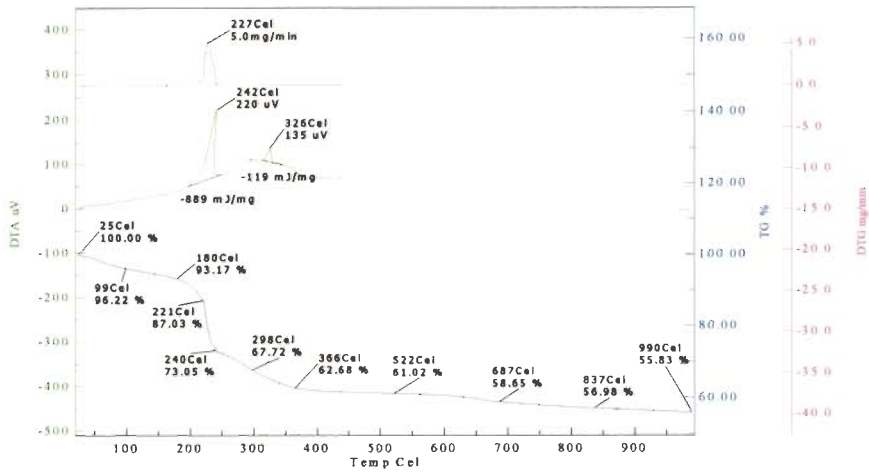
Figure 4.53(a) TGA-DTA of composite wastewater sludge obtained after catalytic thermolysis (Sample weight : 10.89 g, Atmosphere : Air at 200 ml/min)

Figure 4.53(b) TGA-DTA of dried composite wastewater (Sample weight : 10.89 g, Atmosphere : Air at 200 ml/min)
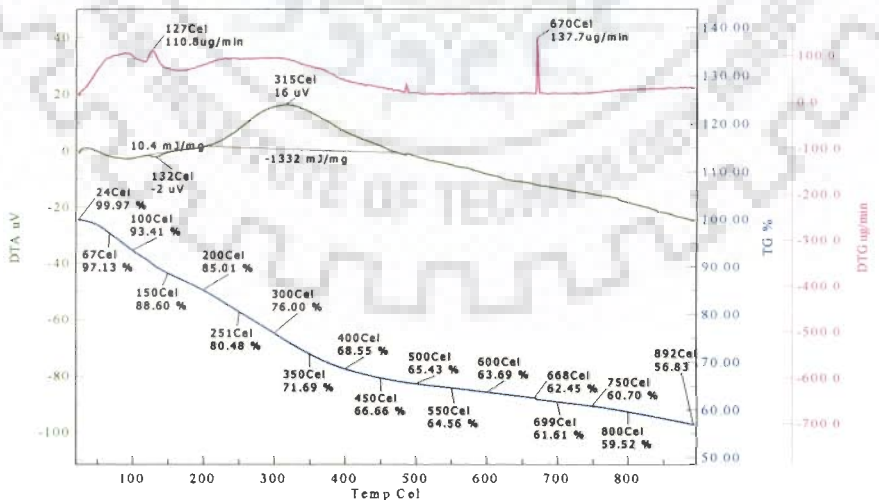
Figure 4.53(c) TGA/DTG/DTA of composite wastewater sludge obtained after coagulation (Sample weight : 9.83 mg, Atmosphere : Air at 200 ml/min)

193

The TGA traces of composite wastewater sludge show a steady weight loss of 31.5% between 24 °C to 400 °C with a weight loss of 110.8 mg/min recorded at T_{max} = 127 °C with an endothermic heat requirement of 10.4 MJ/kg and an identical rate of weight loss with an exothermic heat loss of 1332 MJ/kg at T_{max} = 315 °C. The rate of heat loss continued steadily between 400 to 900 °C at a much slower rate losing weight of around 11.7% only during this period. The maximum weight loss observed in this period was 137.7 µg/min at T_{max} = 670 °C as shown in Figure 4.53(c).

4.9.2 TGA/DTA/DTGA of sludge of Dyeing Wastewater by Catalytic Thermolysis and Coagulation

Thermogravimetric analysis of sludge provides useful information on the kinds of materials present in it and their detection at various temperatures. To collect information on such materials, sludge sample was heated at a rate of 10 °C/min under purified air with a rate of 200 ml/min. The TGA profile presented in Figure 4.54(a) shows the endothermic weight loss of 7.3% in the temperature range 100-200°C. This is possibly due to dehydration of sample alongwith removal of organic volatiles. A weight loss of 24.98% occurs endothermically in the temperature range 200-280 °C. The peak rate of weight loss at T_{max} = 255 °C is 0.5 mg/min. The endothermic weight loss with heat requirement of 526 MJ/kg suggest the involvement of energy in the oxidation of low C and H containing organic substance followed by their removal.

As absorption of energy is relatively high, a partial oxidative decomposition of high concentration of dye may also be considered alongwith low hydrocarbons. The weight remains constant on further increment of temperature upto 417 °C and then a sharp weight loss of 5.23% in a very narrow temperature range of 417-420 °C with a peak rate of 2.4 mg/min occurs. This weight loss may possible be due to further decomposition of remainder of decomposed dye or decomposition of dye coordinated with metal ions present in the sludge. The complete decomposition of such metal

194

coordinated dye occurs above 770 °C and continues till the formation of metal oxide at about 1000 °C. The residue due to metal oxide obtained at this temperature is 8.5%.

Figure 4.54(b) shows the thermogravimetric traces of the dyeing wastewater at identical heating conditions. The TGA curve shows only about 3.86% decrease in weight upto 110 °C. From 110 °C to 791 °C there has been very little weight drop of 11.57%. From 791 °C onwards and upto 933 °C, a percent weight loss of the order of 65.84% at a rate of 1.0 mg/min (at 907 °C) was recorded. This is the maximum weight loss observed during the entire process. This may once again be attributed to the oxidation of metal ions coordinated to dye present in the dyeing wastewater.

Figure 4.54(c) shows the thermogravimetric traces of the dyeing wastewater sludge after completion of coagulation process. At identical heating conditions, the TGA curves show only 2.73% decrease in weight upto 125 °C on account of evaporation of moisture with an endothermic weight loss of 0.072 mg/min and heat requirement of 45.5 MJ/kg at $T_{max} = 62$ °C. The drying rate continued upto 325 °C with a marginal weight loss of 6.7%. The rate of weight loss observed was very slow with the heat requirement of 33.4 MJ/kg at $T_{max} = 149$ °C. This zone represented the removal of organic volatiles. During the entire operation of heating upto 900 °C, there has been sudden drop in the weight at three more locations (i) between 325 to 385 °C, (ii) between 506 to 601 °C and (iii) between 743 to 900 °C loosing weights of 4.61%, 4.88% and 0.96%, respectively. The rate of weight loss during these three zones were between 0.34 – 0.64 mg/min, 0.35-0.50 mg/min (endothermic heat requirement of 52.5 MJ/kg at $T_{max} = 603$ °C) and 0.11 mg/min (endothermic heat requirement of 103 MJ/kg at $T_{max} = 779$ °C), respectively. These zones correspond to evaporation of higher hydrocarbons and re-adjustment of molecules.

Figure 4.54(a) TGA-DTA of dyeing residue obtained after catalytic thermolysis (Sample weight : 10.36 mg, Atmosphere : Air at 200 ml/min)
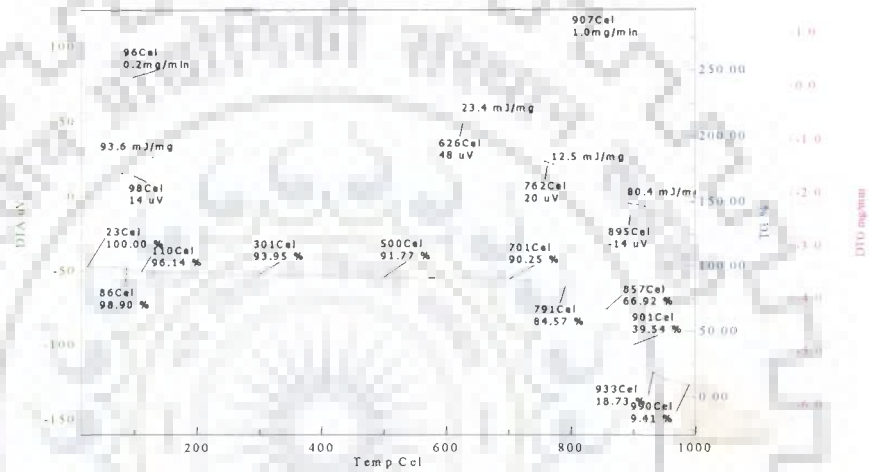
Figure 4.54(b) TGA-DTA of dried dyeing wastewater (Sample weight : 10.26 mg, Atmosphere : Air at 200 ml/min)
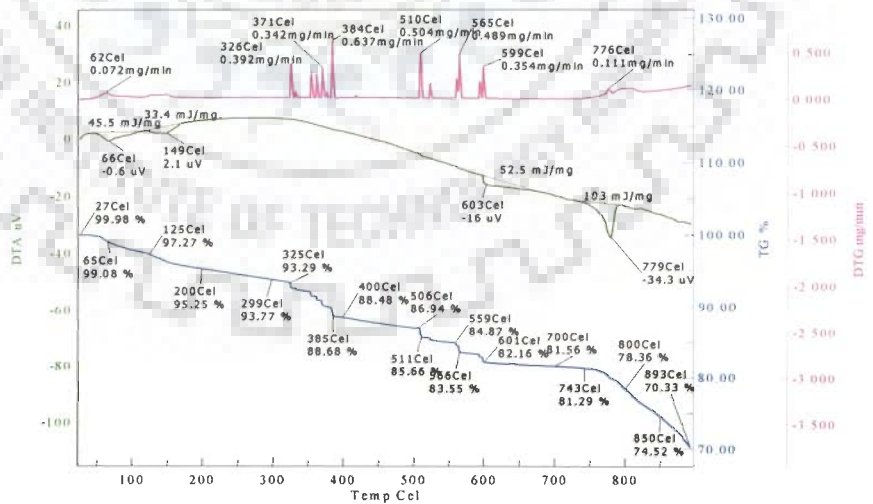
Figure 4.54(c) TGA/DTG/DTA of dyeing wastewater sludge obtained after coagulation (Sample weight : 12.44 mg, Atmosphere : Air at 200 ml/min)

196

4.9.3 TGA/DTA/DTGA of Sludge of Desizing Wastewater by Catalytic Thermolysis and Coagulation

Figure 4.55(a) shows the thermogravimetric analysis (TGA), differential thermogravimetric analysis (DTGA) and differential thermal analysis (DTA) curves for the precipitated sludge at 10°C/min heating rate with 200 ml/min air flushing rate. The nature of the TGA trace shows dehydration and volatalization (removal or volatiles) of the sample and other components upto a temperature of 193°C, losing about 88.11% of its weight. In this regime, the precipitate is unstable. Between 193°C to 464°C, the precipitate oxidizes, losing about 28% of its original weight. The peak rate of weight loss of 351.9 μg/min is at a temperature T_{max} = 237°C. The oxidation is found to be uniform and exothermic with a heat evolution of 1.77 MJ/kg, the peak of the exotherm being at a temperature of T_p = 241°C. The oxidation seems to be completed at 464°C, and the traces of TG, DTG and DTA reflect this fact. It is found that the organics of the precipitate get oxidized catalytically, leaving the ash fraction as the residue.

Figure 4.55(b) shows the TGA, DTG and DTA behaviors of the desizing wastewater under similar linear heating and air flushing rate conditions. In contrast to the TGA trace of the precipitate, the desizing TG trace shows only about 3% decrease in weight upto 117°C. Beyond 117°C, a gradual decrease in residual sample weight is observed upto a temperature of 297°C, shedding about 56% of the sample weight. Thereafter, the weight loss rate is extremely slow, and upto 680°C, the weight loss is only 23.52%. This shows that the desizing wastewater sample loses moisture at an almost steady rate upto 117°C along with volatalization of light volatiles upto 297°C, and thereafter the sample becomes dry and stable. At 520°C, the oxidation of the dry sample started, and the sample lost weight (~ 10.62% weight loss) over a temperature

range of $520^\circ C - 680^\circ C$ (a temperature span of $160^\circ C$). The maximum weight loss rate was 245 µg/min at T_{max} of $177^\circ C$ followed by 159 µg/min and 0.1 mg/min at $272^\circ C$ and $539^\circ C$, respectively (see DTGA trace). The peak temperature for the exothermic reaction as exemplified by the DTA curve was at $T_p = 518^\circ C$ with heat releases of 3.08 MJ/kg. Beyond $680^\circ C$, the weight loss is steady but very slow, giving off ~ 8% weight from $680^\circ C$ to $825^\circ C$ and 15.47% weight loss observed between $825^\circ C$ to $992^\circ C$ (over a temperature increase of $167^\circ C$).

A comparison of Figures 4.55(a) and 4.55(b) brings out clearly the fact that the residue obtained after catalytic thermolysis gets oxidized at a higher temperature range than that of the desizing wastewater. This may be due to the presence of more stable compounds formed during catalytic thermolysis in presence of copper catalyst.

The TGA curves of the desizing wastewater sludge shows a weight loss of around 3.6% due to evaporation of moisture upto $100\ ^\circ C$. The rate of weight loss has been very slow from 100 to $322\ ^\circ C$ there has been a very high weight loss of about 60%, possibly due to the loss of volatile hydrocarbons with an exothermic heat loss of 1185 MJ/kg. The rate of weight loss was 2.395 mg/min at $T_{max} = 312\ ^\circ C$. Between 322 to $451\ ^\circ C$ there has been a steady weight loss of 14.25% with exothermic heat loss of 660 MJ/kg at $T_{max} = 413\ ^\circ C$. The maximum rate of weight loss recorded at this temperature was 0.185 mg/min. From 451 to $900\ ^\circ C$, there has been less than 5% weight loss. The TG curve therefore indicate two major zones : (i) 100 to $320\ ^\circ C$, (ii) 320 to $451\ ^\circ C$, where there has been weight loss possibly due to evaporation of volatile hydrocarbons of low and high molecular weights, respectively, as shown in Figure 4.55(c).
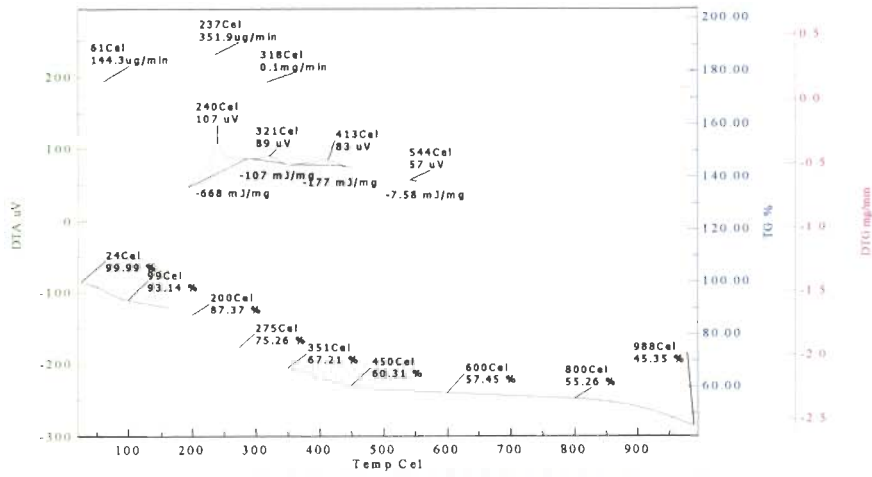
Figure 4.55(a) TGA-DTA of desizing residue obtained after catalytic thermolysis (Sample weight : 10.53 mg, Atmosphere : Air at 200 ml/min)
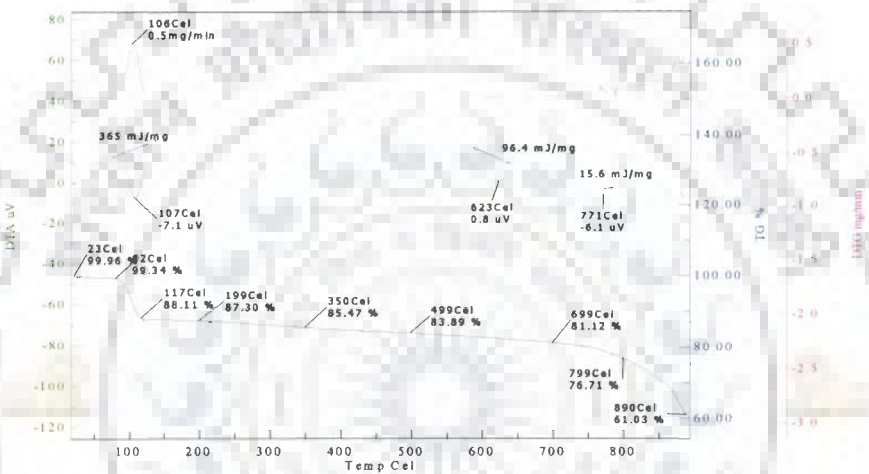

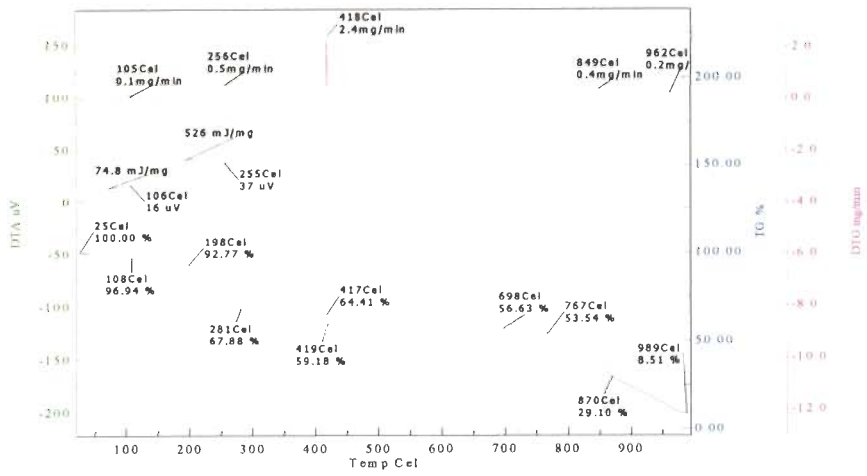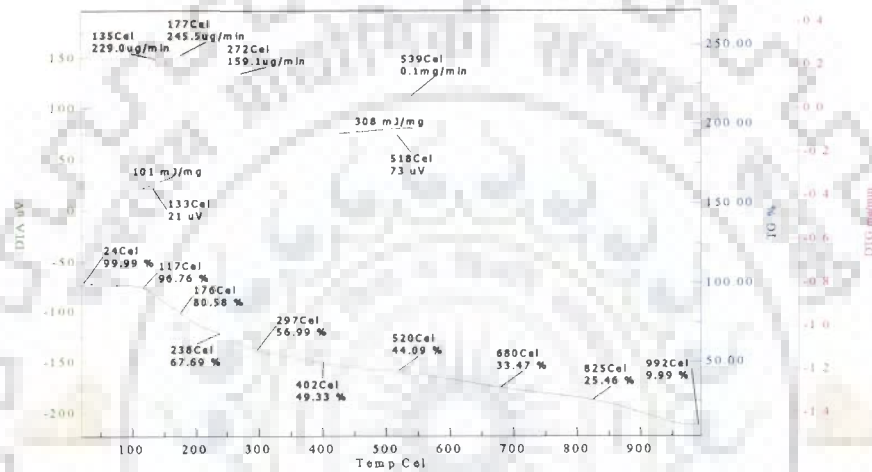**Figure 4.55(b) TGA-DTA of dried desizing wastewater (Sample weight : 11.73 mg, Atmosphere : Air at 200 ml/min)**
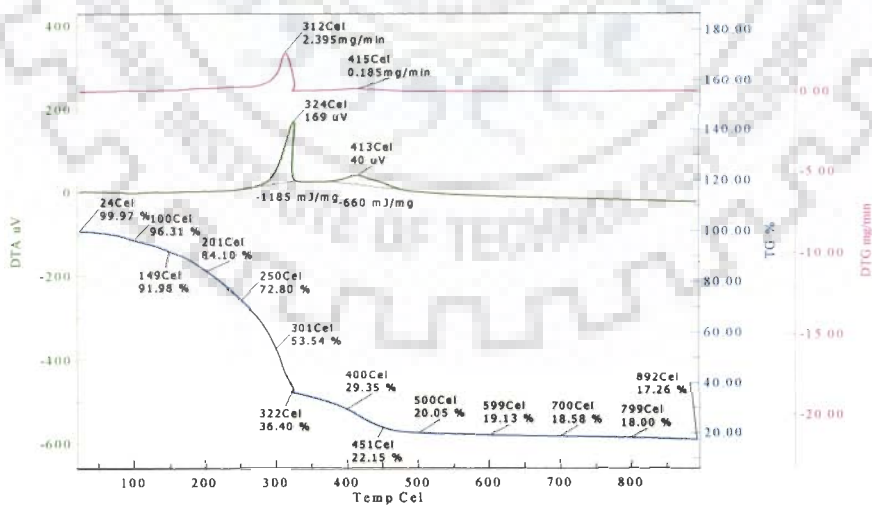
Figure 4.55(c) TGA/DTG/DTA of desizing wastewater sludge obtained after coagulation (Sample weight : 11.14 mg, Atmosphere : Air at 200 ml/min)

199

4.10 KINETICS OF THERMAL DEGRADATION AND OXIDATION

Dynamic thermogravimetry has been widely used to study the kinetics of thermal decomposition/degradation reactions for inorganic and organic chemicals, coal, biomass materials and petroleum products (Sestak, 1984; Srivastava and Jalan, 1994, 1999; Srivastava et al., 1996; Safi et al., 2004; Gangavati et al., 2005).

Several methods of kinetic analysis and reaction mechanisms have been proposed for biomass degradation using thermogravimetry. For a one step irreversible reaction model, differential and integral methods have been suggested for the determination of kinetic parameters, namely, the order of reaction, frequency factor, the specific reaction rate constant, activation energy, entropy change, enthalpy change, change in Gibb's free energy, steric factor and its dependence on temperature using Arrhenius equation. The frequency factor or pre-exponential factor, k_0, has either been used as a function of temperature or as a constant. Generally, Arrhenius equation is used to represent the variation of the specific reaction rate constant with temperature, with k_0 as a constant. Thermogravimetric data can be analyzed by using different kinetic models, which includes the nuclei growth (Vlaev et al., 2003; Safi et al., 2004; Gangavati et al., 2005).

The kinetics of the thermal degradation is determined with reference to peak temperature by using the methods described elsewhere (Vlaev et al., 2003; Gangavati et al., 2005). Although, several mechanistic models have been proposed to study the kinetics of thermal degradation using dynamic thermogravimetry, a single-step, irreversible, global reaction model of the type

$$aA(s) \ \rightarrow \ bB(s) + cC(g) \tag{22}$$

describes the degradation behavior successfully. Here, A is the biomass, B is the solid residue and C is the gas. Here, the lumped mass of the sample components designated as A is shown to degrade under oxidizing environment as the temperature increases.

For the reaction, the decomposition of the solid can be described by a general rate expression as

$$\frac{dX}{dt} = k\,f(X) \qquad (23)$$

where, X is the fractional conversion of A (adsorbent) at time t. X is calculated as

$$X = \frac{W_i - W_\tau}{W_i - W_f}$$

where, W_i, W_τ and W_f are the initial, actual (at any time, t) and final weight of the sample, respectively. f(X) is the conversion function, the type of which depends on the reaction mechanism; k the temperature dependent rate constant; T the absolute temperature; t the time and X the degree of transformation. The temperature dependence of the rate constant is usually described by the Arrhenius Equation:

$$k = k_0 \exp\left(-\frac{E}{RT}\right) \qquad (24)$$

where, k_0 is pre-exponential or frequency factor, E the activation energy and R the universal gas constant (8.314 J/mol K). Under constant heating rate:

$$\frac{dT}{dt} = q = \text{Constant} \qquad (25)$$

and after substitution in Eq. (23) and some transformations, we get

$$\int_o^X \frac{dX}{f(X)} = \frac{k_0}{q} \int_o^T \exp\left(-\frac{E}{RT}\right) dT \qquad (26)$$

The right hand side of Eq. (26) has no exact analytical solution, but making some variable substitutions and applying Cauchy's rule the expression integration can be approximated as (Coats and Redferm, 1964):

$$\frac{k_0}{q} \int_o^T \exp\left(-\frac{E}{RT}\right) dT \cong \frac{k_0 RT^2}{qE}\left(1 - \frac{2RT}{E}\right)\exp\left(-\frac{E}{RT}\right) \qquad (27)$$

If the solution of the integral on the left-hand-side of Eq. (26) is denoted with:

$$g(X) = \int_o^X \frac{dX}{f(X)} \tag{28}$$

Then, taking logarithms after division by T^2, Eq. (26) is transformed into

$$\ln \frac{g(X)}{T^2} = \ln\left(\frac{k_0 R}{qE}\alpha_T\right) - \frac{E}{RT} \tag{29}$$

Thus, a plot of $\ln[g(X)/T^2]$ against $1/T$ should be a straight line with a slope of $(-E/R)$ since $\ln\left(\dfrac{k_0 R}{qE}\alpha_T\right)$ is nearly a constant.

Ozawa (1965) method is used by the Perkin Elmer Pyris Diamond "TD/DTA kinet" software to calculate activation energy and the frequency factor by assuming first order global mass loss kinetics. It is obtained by integrating Eq. (26) using the Doyle's approximation (Doyle 1961 & 1965). The result of the integration after taking logarithms is

$$\log q = \log \frac{k_0 E}{g(x) R} - 2.315 - 0.4567E \tag{30}$$

Assuming $\log \dfrac{k_0 E}{g(x) R}$ to be constant, Eq. (30) is rewritten as

$$\log q = -0.4567 \frac{E}{RT} + \text{constant} \tag{31}$$

It follows that if several measurements are made at various heating rates and the relation between $\log q$ and $1/T$ of each pair of data is plotted on y-x coordinates, the activation energy of the specimen can be obtained from the slope of a plotted line.

The formal expressions of the functions $f(X)$ and $g(X)$ (Eqs. 26 and 28) depend on the conversion mechanism and its mathematical model. The latter usually represents the limiting stage of the reaction – the chemical reaction, random nucleation and nuclei growth; phase boundary reaction or diffusion. If the correct $g(X)$ is used, the plot of

$\ln[g(X)/T^2]$ against 1/T should give a straight line with high correlation coefficient of the linear regression analysis, from which the values of E and k_0 can be obtained. Tables 4.33-4.41 show some of the most common kinetic models and their algebraic expressions.

The other kinetic parameters of the process can be calculated using the fundamental equation of the theory of the active complex (preceding state).

$$k = \frac{\chi e k_B T}{h} \exp\left(\frac{\Delta S^\#}{R}\right) \exp\left(-\frac{E}{RT}\right) \tag{32}$$

where χ is a transmission coefficient which is unity for monomolecular reactions, k_B the Boltzmann constant, h the corresponding Plank constant, e = 2.7183 is the Neper number and $\Delta S^\#$ is the change of entropy for the active complex formation from the reactants.

Taking into account the pre-exponential constant k_0 from the Arrhenius Eqs. (24) and (32), the following expression is obtained:

$$A = \frac{\chi e k_B T}{h} \exp\left(\frac{\Delta S^\#}{R}\right) \tag{33}$$

and $\Delta S^\#$ can be calculated as

$$\Delta S^\# = R \left(\ln k_0 - \ln \frac{\chi e k_B T}{h} \right) \tag{34}$$

Since $E = \Delta H^\# - RT$ (35)

the $\Delta H^\#$ and $\Delta G^\#$ for the active complex formation can be calculated using the well known thermodynamical equation :

$$\Delta G^\# = \Delta H^\# - T \Delta S^\# \tag{36}$$

$\Delta G^{\#}$, $\Delta H^{\#}$ and $\Delta S^{\#}$ were calculated at $T = T_p$ (T_p is the DTG peak temperature), since this temperature characterizes the highest rate of the oxidation process and, therefore, is its important parameter. The steric factor for a particular temperature zone of degradation of the material selected, is given by $P_s = \exp(\Delta S^{\#}/R)$. This factor is necessary to determine whether the oxidation taking place in the zone selected is slow or fast. If it is closer to unity for the zone selected in comparison to the other zone, then we can say that the zone selected is faster and the other zone is slow.

In order to avoid poor parameter estimation due to improper scaling, the reparameterization has been used for the determination of the best fit values of n, k_0, E, k, $-\Delta S^{\#}$, $\Delta H^{\#}$, $\Delta G^{\#}$ and P_s:

$$a_1 = -\frac{E}{10^3 R}; \quad a_2 = \ln \frac{k_0 R}{\beta' E} b; \quad x = \frac{10^3}{T} \tag{37}$$

where $b = 1 - 2(RT/E)$; for Coats and Redfern approximation

$$= \frac{1 - 2(RT/E)}{1 - 5(RT/E)^2}; \text{ for Agarwal and Sivasubramanian approximation.}$$

Thus, the integral equation for the determination of kinetic parameters with either of the above approximations is manipulated with the rescaled parameters as

$$y = a_1 x + a_2 \tag{38}$$

where, $y = \ln[g(X)/T^2]$ for n^{th} order single step irreversible reaction

where, $y = \ln[\{1 : (1-x)^{1-n'}/(1-n')T^2\}]$, for $n' \neq 1$

and for first order degradation

$$y = \ln[-\ln(1-x)/T^2] \text{ for } n' = 1.$$

The best fit values of a_1 and a_2 are obtained by using least square technique which gives coefficient of correlation, $r = \frac{\Sigma(XY)}{\sqrt{\Sigma X^2 \, \Sigma Y^2}}$ (39)

where, $X = x - \bar{x}$ and $Y = y - \bar{y}$

where, $\bar{x}$ = mean of x and $\bar{y}$ = mean of y.

The value of n', which gives the highest (or closest to 1.0) value of r^2 (correlation factor) for the best fit of the experimental data plotted as Eq. (35) is chosen for the determination of a_1 and a_2, the activation energy, E and the pre-exponential factor, k_0.

The kinetic parameters for the oxidation of the three residues, as determined by various methods, for 50 K/min heating rate is given in Table 4.32. The kinetic and thermodynamic parameters were also evaluated at other heating rates, viz., 10 and 100 K/min.

Table 4.32 Different kinetic models for the thermal degradation

Mechanism	Symbol	$f(X)$	$g(X)$
Diffusion			
One way	D1	$1/2X$	X^2
Two way	D2	$[-\ln(1-X)]^{-1}$	$X+(1-X)\ln(1-X)$
Three way	D3	$2(1-X)^{2/3}(1-(1-X)^{1/3})^{-1}$	$(1-(1-X)^{1/3})^2$
Ginstling-Brounshtein equation	G-B	$(2/3)(1-X)^{1/3}/1-(1-X)^{1/3}$	$1-2X/3-(1-X)^{2/3}$
Zhuravlev diffusion	Z-D	$(2/3)(1-X)^{5/3}[1-(1-X)^{1/3}]^{-1}$	$[(1-X)^{-1/3}-1]^2$

The kinetic parameters obtained from different models are given in Table 4.33 through 4.41. From Table 4.33, it may be seen that at the heating rate 10 °C/min, for the solid residue of fresh composite wastewater without treatment, the activation energy (E) remains constant at around 121 kJ/mol. The pre-exponential factor (k_0) is found to be the minimum (6.89×10^{13} min^{-1}) for Ginstlling-Brounstein (G-B) model and the maximum (4.98×10^{14} min^{-1}) for one way transport diffusion (D1) model. The change in entropy is constant at around -250 J/(mol K). The enthalpy change and the change in Gibb's free energy is found to be constant at around 118 kJ/mol and 212 kJ/mol. The D1 model fitted best with $R^2 = 1$ for thermal oxidation kinetics.

For solid residue of composite wastewater after catalytic thermolysis treatment with copper sulphate, the maximum value of pre-exponential factor (k_0) = 942.4 min^{-1} is found to be for D1 model and minimum value of 137.3 min^{-1} for G-B model. The reaction rate constant is found maximum (0.04 min^{-1}) for D1 model and minimum (0.0005 min^{-1}) for G-B model. The E remains constant around 42 kJ/mol. The enthalpy change and the change in Gibb's free energy is found to be constant around 38 kJ/mol and 166 kJ/mol. The steric factor does not vary much and lies in the range of 3.83 x 10^{-14} – 3.96 x 10^{-14} for all the kinetic models. The D1 model fitted best with $R^2 = 1$.

For the solid residue of composite wastewater after coagulation with aluminum potassium sulphate, the maximum value of k_0 = 145.96 min^{-1} is found to be for G-B model and minimum value is 137.3 min^{-1} for Zhurav-Diffusion (Z-D) model. The reaction rate constant is found maximum (2.04 min^{-1}) for D1 model and minimum (0.36 min^{-1}) for G-B model. The minimum value of E = 32.89 is found for D1 model and highest value of 39.01 kJ/mol for Z-D model. The D1 model again fitted best with $R^2 = 1$ for thermal oxidation kinetics of solid residue of composite wastewater after coagulation with aluminum potassium sulphate.

The TG/DTA/DTG analysis of (a) solid residue of fresh dyeing and desizing wastewaters without treatment; (b) solid residue of dyeing and desizing wastewaters after catalytic thermolysis treatment with copper sulphate; and (c) solid residue of dyeing and desizing wastewaters after coagulation with commercial alum were also performed for heating rate of 10 °C/min. The data obtained are presented in Tables 4.36 through 4.41. It can be seen from these tables that D1 model with $R^2 = 1$ fitted best for all solid residues. Therefore, D1 model is appropriate to represent the oxidation kinetics of solid residues of fresh composite, dyeing and desizing wastewaters without treatment; for the solid residue of these wastewaters after catalytic thermolysis treatment with copper sulphate; and for the solid residue after coagulation with commercial alum.

Table 4.33 **Kinetic parameters calculated for the solid residue of composite wastewater without treatment (Sample weight = 10888 μg, final weight of the residue = 6646 μg, DTG peak temperature = 105.6 °C, air flow rate = 200 ml/min, heating rate = 10 °C/min)**

S. No.	Parameters	Different models				
		D1	D2	D3	G-B	Z-D
1	n'	1	1	1	1	1
2	k^0 (min^{-1})	4.97742×10^{14}	2.93536×10^{14}	7.71355×10^{13}	6.89788×10^{13}	1.08144×10^{14}
3	E_a (kJ/mol)	120.28	120.703	121.133	120.847	122
4	k (min^{-1})	0.0128288	0.00661389	0.00151614	0.00148506	0.00161406
5	ΔS (J/mol K)	-250.525	-250.598	-250.783	-250.799	-250.736
6	ΔH (kJ/mol)	117.131	117.555	117.985	117.698	118.851
7	ΔG (kJ/mol)	212.017	212.469	212.969	212.688	213.818
8	P_s	8.19313×10^{-14}	8.12133×10^{-14}	7.94244×10^{-14}	7.92766×10^{-14}	7.98729×10^{-14}
9	r^2	1	0.892548	0.892348	0.892483	0.891883

n' = Order of reaction; k^0 = frequency factor; E_a = Activation energy; k = Reaction rate constant; ΔS = Change in entropy; ΔH = Change in enthalpy; ΔG = Gibbs free energy; P_s = Steric factor; r^2 = Correlation factor; D1 = One way transport diffusion model ; D2 = Two way transport diffusion model; D3 = Three way transport diffusion model; G-B = Ginstling-Brounstein diffusion model; Z-D = Zhuravlev diffusion model.

Table 4.34 Kinetic parameters calculated for the solid residue of the solid residue of composite wastewater after catalytic thermolysis treatment with copper sulphate (Sample weight = 12171 µg, final weight of the residue = 6794 µg, DTG peak temperature = 227 °C, air flow rate = 200 ml/min, heating rate = 10 °C/min)

S. No.	Parameters	Different models				
		D1	D2	D3	G-B	Z-D
1	n'	1	1	1	1	1
2	k^0 (min^{-1})	942.405	576.642	157.667	137.312	240.001
3	E_a (kJ/mol)	41.7915	42.2912	42.8054	42.4625	43.8487
4	k (min^{-1})	0.040688	0.0220771	0.00533429	0.00504483	0.00631799
5	ΔS (J/mol K)	-256.577	-256.645	-256.824	-256.844	-256.766
6	ΔH (kJ/mol)	37.6332	38.1329	38.6471	38.3043	39.6905
7	ΔG (kJ/mol)	165.96	166.494	167.098	166.765	168.112
8	P_s	3.9566×10^{-14}	3.92434×10^{-14}	3.84044×10^{-14}	3.8316×10^{-14}	3.86743×10^{-14}
9	r^2	1	0.645802	0.65189	0.647846	0.663854

n' = Order of reaction; k^0 = frequency factor; E_a = Activation energy; k = Reaction rate constant; ΔS = Change in entropy; ΔH = Change in enthalpy; ΔG = Gibbs free energy; P_s = Steric factor; r^2 = Correlation factor; D1 = One way transport diffusion model ; D2 = Two way transport diffusion model; D3 = Three way transport diffusion model; G-B = Ginstling-Brounstein diffusion model; Z-D = Zhuravlev diffusion model.

Table 4.35 Kinetic parameters calculated for the solid residue of composite wastewater after coagulation with aluminum potassium sulphate using various proposed models (Sample weight = 9827 µg, final weight of the residue = 5583 µg, DTG peak temperature = 670 °C, air flow rate = 200 ml/min, heating rate = 10 °C/min)

S. No.	Parameters	Different models				
		D1	D2	D3	G-B	Z-D
1	n'	1	1	1	1	1
2	k^0 (min^{-1})	135.402	112.982	44.1941	30.2983	145.96
3	E_a (kJ/mol)	32.8964	34.274	35.7986	34.7816	39.014
4	k (min^{-1})	2.04473	1.4314	0.461024	0.35981	1.01065
5	ΔS (J/mol K)	-262.124	-262.149	-262.279	-262.331	-262.113
6	ΔH (kJ/mol)	25.0508	26.4285	27.953	26.936	31.1684
7	ΔG (kJ/mol)	272.407	273.808	275.455	274.488	278.514
8	P_s	2.03032×10^{-14}	2.0242×10^{-14}	1.99278×10^{-14}	1.98028×10^{-14}	2.03286×10^{-14}
9	r^2	1	0.717962	0.740607	0.725599	0.782682

n' = Order of reaction; k^0 = frequency factor; E_a = Activation energy; k = Reaction rate constant; ΔS = Change in entropy; ΔH = Change in enthalpy; ΔG = Gibbs free energy; P_s = Steric factor; r^2 = Correlation factor; D1 = One way transport diffusion model ; D2 = Two way transport diffusion model; D3 = Three way transport diffusion model; G-B = Ginstling-Brounstein diffusion model; Z-D = Zhuravlev diffusion model.

Table 4.36 Kinetic parameters calculated for the solid residue of dyeing wastewater without treatment (Sample weight = 10262 µg, final weight of the residue = 965 µg, DTG peak temperature = 907 °C, air flow rate = 200 ml/min, heating rate = 10 °C/min)

S. No.	Parameters	Different models				
		D1	D2	D3	G-B	Z-D
1	n'	1	1	1	1	1
2	k^0 (min^{-1})	1.52504	0.798111	0.185727	0.180102	0.203822
3	E_a (kJ/mol)	29.2052	29.3316	29.459	29.3741	29.7149
4	k (min^{-1})	0.0777287	0.0401579	0.0092245	0.00902291	0.00986258
5	ΔS (J/mol K)	-264.605	-264.694	-264.896	-264.901	-264.884
6	ΔH (kJ/mol)	19.3935	19.5198	19.6472	19.5623	19.9032
7	ΔG (kJ/mol)	331.667	331.899	332.265	332.185	332.506
8	P_s	1.5065×10^{-14}	1.49033×10^{-14}	1.45455×10^{-14}	1.45381×10^{-14}	1.45681×10^{-14}
9	r^2	1	0.613735	0.615496	0.614323	0.619

n' = Order of reaction; k^0 = frequency factor; E_a = Activation energy; k = Reaction rate constant; ΔS = Change in entropy; ΔH = Change in enthalpy; ΔG = Gibbs free energy; P_s = Steric factor; r^2 = Correlation factor; D1 = One way transport diffusion model ; D2 = Two way transport diffusion model; D3 = Three way transport diffusion model; G-B = Ginstling-Brounstein diffusion model; Z-D = Zhuravlev diffusion model.

Table 4.37 Kinetic parameters calculated for the solid residue of dyeing wastewater after catalytic thermolysis treatment with copper sulphate using various proposed models (Sample weight = 11254 µg, final weight of the residue = 1110 µg, DTG peak temperature = 898 °C, air flow rate = 200 ml/min, heating rate = 10 °C/min)

S. No.	Parameters	Different models				
		D1	D2	D3	G-B	Z-D
1	n'	1	1	1	1	1
2	k^0 (min^{-1})	4.84816	2.52353	0.583947	0.5684	0.633379
3	E_a (kJ/mol)	37.8534	37.9615	38.0704	37.9978	38.2888
4	k (min^{-1})	0.0993601	0.051147	0.0117039	0.0114775	0.012413
5	ΔS (J/mol K)	-264.381	-264.471	-264.674	-264.678	-264.663
6	ΔH (kJ/mol)	28.1164	28.2246	28.3334	28.2608	28.5519
7	ΔG (kJ/mol)	337.746	337.96	338.306	338.238	338.512
8	P_s	1.54763×10^{-14}	1.53088×10^{-14}	1.49398×10^{-14}	1.49331×10^{-14}	1.49601×10^{-14}
9	r^2	1	0.66399	0.66525	0.664411	0.667761

n' = Order of reaction; k^0 = frequency factor; E_a = Activation energy; k = Reaction rate constant; ΔS = Change in entropy; ΔH = Change in enthalpy; ΔG = Gibbs free energy; P_s = Steric factor; r^2 = Correlation factor; D1 = One way transport diffusion model ; D2 = Two way transport diffusion model; D3 = Three way transport diffusion model; G-B = Ginstling-Brounstein diffusion model; Z-D = Zhuravlev diffusion model.

Table 4.38 Kinetic parameters calculated for the solid residue of dyeing wastewater after coagulation with commercial alum using various proposed models (Sample weight = 12438 µg, final weight of the residue = 8748 µg, DTG peak temperature = 384 °C, air flow rate = 200 ml/min, heating rate = 10 °C/min)

S. No.	Parameters	Different models				
		D1	D2	D3	G-B	Z-D
1	n'	1	1	1	1	1
2	k^0 (min^{-1})	5.37129 x 10^{12}	1.30781 x 10^{16}	2.89056 x 10^{20}	1.27406 x 10^{17}	1.40218 x 10^{32}
3	E_a (kJ/mol)	73.8164	93.5088	120.481	102.354	184.049
4	k (min^{-1})	7.30099 x 10^6	4.83906 x 10^8	7.68359 x 10^{10}	9.3422 x 10^8	3.30477 x 10^{17}
5	ΔS (J/mol K)	37.8461	102.676	185.844	121.602	409.554
6	ΔH (kJ/mol)	68.352	88.0444	115.016	96.8892	178.585
7	ΔG (kJ/mol)	43.4775	20.5604	-7.13072	16.9658	-90.5963
8	P_s	94.8303	230894	5.10329 x 10^9	2.24936 x 10^6	2.47555 x 10^{21}
9	r^2	1	1	1	1	1

n' = Order of reaction; k^0 = frequency factor; E_a = Activation energy; k = Reaction rate constant; ΔS = Change in entropy; ΔH = Change in enthalpy; ΔG = Gibbs free energy; P_s = Steric factor; r^2 = Correlation factor; D1 = One way transport diffusion model ; D2 = Two way transport diffusion model; D3 = Three way transport diffusion model; G-B = Ginstling-Brounstein diffusion model; Z-D = Zhuravlev diffusion model.

Table 4.39 Kinetic parameters calculated for the solid residue of desizing wastewater without treatment (Sample weight = 10539 μg, final weight of the residue = 3420 μg, DTG peak temperature = 271 °C, air flow rate = 200 ml/min, heating rate = 10 °C/min)

S. No.	Parameters	Different models				
		D1	D2	D3	G-B	Z-D
1	n'	1	1	1	1	1
2	k^0 (min^{-1})	19985.1	11688	3047.27	2739.4	4207.3
3	E_a (kJ/mol)	58.4128	58.8283	59.2521	58.9695	60.1085
4	k (min^{-1})	0.0493487	0.0263287	0.00625045	0.00598111	0.00714161
5	ΔS (J/mol K)	-256.855	-256.929	-257.115	-257.13	-257.07
6	ΔH (kJ/mol)	53.8888	54.3042	54.7281	54.4455	55.5844
7	ΔG (kJ/mol)	193.656	194.112	194.637	194.363	195.469
8	P_s	3.82659 x 10^{-14}	3.79253 x 10^{-14}	3.7085 x 10^{-14}	3.70193 x 10^{-14}	3.7285 x 10^{-14}
9	r^2	1	0.85485	0.857617	0.855778	0.863047

n' = Order of reaction; k^0 = frequency factor; E_a = Activation energy; k = Reaction rate constant; ΔS = Change in entropy; ΔH = Change in enthalpy; ΔG = Gibbs free energy; P_s = Steric factor; r^2 = Correlation factor; D1 = One way transport diffusion model ; D2 = Two way transport diffusion model; D3 = Three way transport diffusion model; G-B = Ginstling-Brounstein diffusion model; Z-D = Zhuravlev diffusion model.

Table 4.40 **Kinetic parameters calculated for the solid residue of desizing wastewater after catalytic thermolysis treatment with copper sulphate using various proposed models (Sample weight = 11739 µg, final weight of the residue = 5309 µg, DTG peak temperature = 237 °C, air flow rate = 200 ml/min, heating rate = 10 °C/min)**

S. No.	Parameters	Different models				
		D1	D2	D3	G-B	Z-D
1	n'	1	1	1	1	1
2	k^0 (min^{-1})	389.578	251.106	72.5556	60.9041	123.744
3	E_a (kJ/mol)	37.4975	38.1157	38.7565	38.3292	40.0617
4	k (min^{-1})	0.0563714	0.0314068	0.00780231	0.00724351	0.00978202
5	ΔS (J/mol K)	-256.864	-256.925	-257.097	-257.121	-257.023
6	ΔH (kJ/mol)	33.2561	33.8743	34.5151	34.0878	35.8203
7	ΔG (kJ/mol)	164.295	164.944	165.673	165.258	166.94
8	P_s	3.82235×10^{-14}	3.79448×10^{-14}	3.71677×10^{-14}	3.70594×10^{-14}	3.74999×10^{-14}
9	r^2	1	0.653182	0.661313	0.655916	0.67725

n' = Order of reaction; k^0 = frequency factor; E_a = Activation energy; k = Reaction rate constant; ΔS = Change in entropy; ΔH = Change in enthalpy; ΔG = Gibbs free energy; P_s = Steric factor; r^2 = Correlation factor; D1 = One way transport diffusion model ; D2 = Two way transport diffusion model; D3 = Three way transport diffusion model; G-B = Ginstling-Brounstein diffusion model; Z-D = Zhuravlev diffusion model.

Table 4.41 Kinetic parameters calculated for the solid residue of desizing wastewater after coagulation with commercial alum using various proposed models (Sample weight = 11146 µg, final weight of the residue = 1924 µg, DTG peak temperature = 312 °C, air flow rate = 200 ml/min, heating rate = 10 °C/min)

S. No.	Parameters	Different models				
		D1	D2	D3	G-B	Z-D
1	n'	1	1	1	1	1
2	k^0 (min^{-1})	8835.38	6305.34	2044.99	1589.17	4461.64
3	E_a (kJ/mol)	52.7445	53.7142	54.7478	54.0583	56.885
4	k (min^{-1})	0.174602	0.102104	0.0267818	0.0239782	0.0376733
5	ΔS (J/mol K)	-257.579	-257.626	-257.782	-257.817	-257.674
6	ΔH (kJ/mol)	47.8751	48.8448	49.8784	49.1889	52.0156
7	ΔG (kJ/mol)	198.737	199.734	200.859	200.19	202.933
8	P_s	3.50715×10^{-14}	3.48749×10^{-14}	3.42265×10^{-14}	3.4083×10^{-14}	3.46744×10^{-14}
9	r^2	1	0.878864	0.885633	0.881184	0.897881

n' = Order of reaction; k^0 = frequency factor; E_a = Activation energy; k = Reaction rate constant; ΔS = Change in entropy; ΔH = Change in enthalpy; ΔG = Gibbs free energy; P_s = Steric factor; r^2 = Correlation factor; D1 = One way transport diffusion model ; D2 = Two way transport diffusion model; D3 = Three way transport diffusion model; G-B = Ginstling-Brounstein diffusion model; Z-D = Zhuravlev diffusion model.

Chapter-5

CONCLUSIONS AND RECOMMENDATIONS
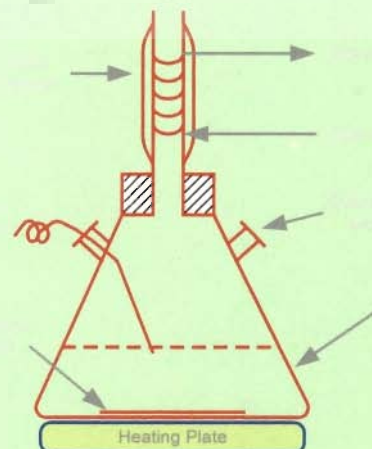
Chapter – 5

CONCLUSIONS AND RECOMMENDATIONS

5.1 CONCLUSIONS

In the present work, studies were conducted for the reduction of COD and color of composite, dyeing and desizing wastewater, the kinetics of these processes, thermogravimetric studies of the dried residues, settling and filterability studies of slurry produced, determination of various functional groups present in the treated effluent, determination of metal concentration and C, H, N, S compositions in treated effluent as well as sludge, mechanism of thermolysis and coagulative processes, etc. On the basis of these studies on the treatment of textile mill wastewaters using catalytic thermolysis and coagulation, following conclusions can be drawn :

5.1.1 Treatment of Composite Wastewater

Following conclusions were drawn from the treatment of composite wastewater of a cotton textile mill using catalytic thermolysis accompanied with/without coagulation.

- ❖ Among the various catalysts used during thermolysis, copper sulfate was found to be the most active in treating composite waste giving about 77.9% COD as well as 92.85% color reduction, respectively using the catalyst concentration of 6 kg/m^3 at pH 12 and 95 °C temperature.

- ❖ The settling rate of the slurry obtained is strongly influenced by treatment pH. Based on the sedimentation flux calculations, the slurry obtained at pH 10 settled much faster than that at other pH.

❖ The filterability of the treated effluent gets improved with an increase in the initial pH (pH_0). Based on the values of specific cake resistance and filter medium resistance, pH 10 seems to offer least resistance to filtration.

❖ During coagulation aluminum potassium sulfate is found to be the best among other coagulants studied, resulting in 88.62% COD reduction and 95.4% color reduction of the fresh effluent at pH 8 and a coagulant concentration of 5 kg/m^3.

❖ Coagulation when applied to clear fluid (supernatant) obtained after catalytic thermal treatment (at above mentioned operating conditions except at lower coagulant concentration of 3 kg/m^3) resulted in a reduction of about 97.3% COD and close to 100% color.

❖ The residual COD was found to be 11.7 mg/l in the final effluent, whereas, the COD/BOD$_3$ ratio was 1.67. A value of less than 2 of COD/BOD$_3$ ratio is desirable to make the effluent biodegradable. The sludge produced from the coagulation unit would contain lower inorganic mass coagulant, requiring reduced disposal problems. The solid residue from the thermolysis, which is rich in organics, can be used as a solid fuel with high calorific value of about 16 MJ/kg, close to that of Indian coal.

❖ During catalytic thermal treatment using copper sulfate as catalyst, the copper gets leached out and the residue obtained is rich in copper. This residue can be blended with organic manure to be used in agriculture.

5.1.2 Treatment of Dyeing Wastewater

❖ During thermolysis of the fresh dyeing effluent, copper sulfate was found to be the best catalyst giving about 66.85% COD as well as 71.4% color reduction at a catalyst concentration of 5 kg/m^3, pH 8 and 95 °C temperature.

❖ The settleability as well as filterability of the slurry obtained is strongly influenced by pH of the solution. The slurry obtained at pH 6 settled much faster than those obtained at other pH.

❖ During coagulation commercial alum is found to be the best among other coagulants studied, resulting in 58.57% COD reduction and 74% color reduction at pH 4 and a coagulant concentration of 5 kg/m^3.

❖ Coagulation of the supernatant obtained after catalytic thermolysis at above mentioned operating conditions (except at lower coagulant concentration of 2 kg/m^3) resulted in a reduction of about 89.91% COD and 94.4% color. The final COD and color was found to be 192 mg/l and 61.5 PCU, respectively in the treated effluent. The COD/BOD$_3$ ratio was 1.88.

❖ Thermolysis followed by coagulation has, thus, been the most effective process in removing COD as well as color at a lower dose of coagulant. The sludge thus produced contains lower inorganic mass coagulant and, therefore, less amount of sludge containing dye coordinated metal ions to be disposed.

5.1.3 Treatment of Desizing Wastewater

❖ Thermolysis experiments at moderate temperatures (60-95 °C) and atmospheric pressure in the presence of a CuSO$_4$ catalyst showed that the desizing wastewater from a textile mill can be pretreated to reduce its COD and color. A maximum removal of about 71.6% of COD and 87.2% of color was achieved with a catalyst concentration of 4 kg/m^3 at

95 °C and initial pH (pH_0) 4. The results on the effect of variation of catalyst mass loading revealed that 4 kg/m^3 is the critical chemical concentration. The final pH of the treated effluent slightly increases above its pH_0.

❖ The elemental analysis of the desizing wastewater, filtrate and sludge shows carbon, hydrogen and sulfur enrichment in the sludge in relation to desizing wastewater itself. Thus the COD reduction is accompanied with the formation of a settleable solid residue, which is enriched in carbon and hydrogen.

❖ The residual copper concentration in the filtrate after the thermolysis can be utilized as a catalyst in the secondary treatment, e.g., in coagulation/ wet oxidation. Copper in the filtrate can also be reduced by pH adjustment. The sludge obtained after thermolysis has high heating value and can be used as a fuel.

❖ During coagulation of fresh effluent, the maximum COD reduction obtained was 58.34% using commercial alum at coagulant dose 5 kg/m^3 and pH 4. The maximum % color reduction at these conditions was 85%.

❖ The application of coagulation to the supernatant obtained after thermolysis show a removal of 87.96 % COD and 96.0 % color at above mentioned conditions except at a coagulant dose of 1 kg/m^3. The amount of inorganic sludge obtained due to the addition of coagulant is, thus, drastically reduced due to the reduced amount (almost 25%) of coagulant. The COD and color of the final effluent were found to be 98.6 mg/l and 2.67 PCU, respectively and the COD/BOD_3 ratio was 1.36.

Table 5.1 compares the COD and color reduction of composite, dyeing and desizing wastewater by thermolysis and/or coagulation at optimum conditions.

Table 5.1 COD and color reduction of composite, dyeing and desizing wastewater by catalytic thermolysis and coagulation either alone or in combination

S. No.	Wastewater	Catalyst/coagulant used	Initial COD (mg/l)	Initial color (PCU)	Catalyst/coagulant conc. (kg/m³)	Optimum pH	Temp. (°C)	% COD reduction	% color reduction	Residual COD (mg/l)	Residual color (PCU)	Residual BOD_3 (mg/l)	Residual COD/BOD_3 ratio
(A) Thermolysis													
1.	Composite	CuSO₄	1960	2250	6	12	95	77.90	92.85	433	795	-	-
2.	Dyeing	CuSO₄	5744	3840	5	8	95	66.85	71.40	1904	1098	-	-
3.	Desizing	CuSO₄	2884	520	4	4	95	71.60	87.20	819	66.6	-	-
(B) Coagulation													
1.	Composite	Aluminium potassium sulphate	1960	2250	5	8	ambient	88.62	95.4	223	103.5	-	-
2.	Dyeing	Commercial alum	5744	3840	5	4	ambient	58.57	74.0	2380	998.4	-	-
3.	Desizing	Commercial alum	2884	520	5	4	ambient	58.34	85.0	1201.5	78	-	-
(C) Coagulation of supernatant of thermolysis													
1.	Composite	Aluminium potassium sulphate	433	795	3	8	ambient	97.30	100	11.7	Not detectable	7	1.67
2.	Dyeing	Commercial alum	1904	1098	2	4	ambient	89.91	94.4	192	61.5	102	1.88
3.	Desizing	Commercial alum	819	66.6	1	4	ambient	87.96	96.0	98.6	2.67	72	1.36

Allowable limit of effluent discharge as prescribed by Central Pollution Control Board, India (1986) : COD = 300 mg/l, BOD_3 = 150 mg/l and color = 400 PCU.

➢ Thermolysis followed by coagulation can be less expensive treatment scheme, in which the need of biological oxidation can be eliminated and the generation of solid waste can be reduced.

➢ FTIR analysis showed the type and intensity of various bonds and groups present in the precipitate formed during treatment of composite, dyeing and desizing wastewater by thermolysis/coagulation process.

➢ The overall thermal degradation characteristics are found to be well represented by diffusion model for the fresh dried wastewater (composite, dyeing and desizing) and precipitates formed during thermolysis and coagulation process using various catalysts and coagulants.

➢ The kinetic analysis of catalytic thermolysis process shows a two-step mechanism in treating all the three effluents. Both the steps followed a first order kinetics. The kinetic equations of the two steps have been presented. The activation energies of the first step ranged between 8.34-36.64 kJ/mol whereas for second step between 19.24-42.36 kJ/mol.

➢ C, H, N, S and heating value of the sludge were also observed to characterize the dried sludge and its prospective use as solid fuel.

➢ In the light of the dyeing and desizing operations being hot processes, these wastewaters discharged from the plant are at sufficiently hot conditions. This may allow its treatment by thermolysis on the site of the plant by the addition of suitable catalyst. This way the process can be energy efficient.

➢ The chemical aspects of coagulation has been explained by an examination of the hydrolysis of metal ions. Aluminum based coagulants show better results than that of iron based coagulants in the removal of COD and color of the textile wastewater.

5.2   RECOMMENDATIONS

On the basis of the present studies, following recommendations may be made for the future studies :

➢   Although the combined treatment of catalytic thermolysis accompanied with coagulation has been found to be an effective process for removal of COD as well as color from textile mill wastewater, it is proposed that other treatment methods, such as, Fenton process, membrane process and elctrocoagulation method be tested and compared.

➢   Detailed mechanism of catalytic thermolysis process should be studied.

➢   The catalyst gets complexed with the organic and inorganic present in the effluent. Therefore, the catalyst with various porous support materials may be used during catalytic thermolysis to avoid loss of catalyst.

➢   Due to several drawbacks of using aluminum and ferric salts, such as residual metal in treated water etc., alternative rapidly available coagulants may be developed to replace aluminum and ferric salt, such as natural coagulants of vegetable and mineral origin.

REFERENCES
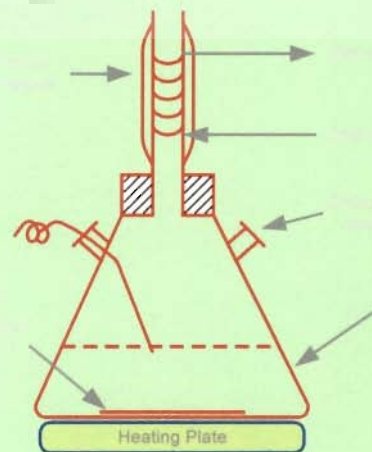
REFERENCES

1. Alaton I. A. and Alaton I., Degradation of xenobiotics originating from the textile preparation, dyeing and finishing industry using ozonation and advanced oxidation, Ecotoxicology and Environmental Safety (2007).

2. Andrade L. S., Ruotolo L. A. M., Filho R. C. R., Bocchi N., Biaggio S. R., Iniesta J., Garcia V. G., Montiel V., On the performance of Fe and Fe,F doped Ti-Pt/PbO$_2$ electrodes in the electrooxidation of the blue reactive 19 dye in simulated textile wastewater, Chemosphere, 66, 2035-2043 (2007).

3. Andrzejewska A., Krysztafkiewicz A. and Jesionowski T., Treatment of textile dye wastewater using modified silica, Dyes and Pigments, 75, 116-124 (2007).

4. Arslan I. and Balcioglu I. A., Oxidative treatment of simulated dyehouse effluent by UV and near-UV light assisted Fenton's reagent, Chemosphere, 39(15), 2767-2783 (1999).

5. Arslan I., Treatability of a simulated disperse dye-bath by ferrous iron coagulation, ozonation, and ferrous iron-catalyzed ozonation, Journal of Hazardous Materials, 85(3), 229-241 (2001).

6. Baban A., Yediler A., Lienert D., Kemeredere N., Kettrup A., Ozonation of high strength segregated effluents from a woolen textile dyeing and finishing plant, Dyes and Pigments, 58, 93-98 (2003).

7. Balcioglu I. A. and Arslan I., Application of photocatalytic oxidation treatment to pretreated and raw effluents from the Kraft bleaching process and textile industry, Environmental Pollution, 103, 261-268 (1998).

8. Bali U. and Karagozoglu B., Performance comparison of Fenton process, ferric coagulation and H$_2$O$_2$/pyridine/Cu(II) system for decolorization of Remazol Turquoise Blue G-133, Dyes and Pigments, 74, 73-80 (2007).

9. Banat F., Asheh S. A. and Qtaishat M., Treatment of waters colored with methylene blue dye by vacuum membrane distillation, Desalination, 174, 87-96 (2005).

10. Bandala E. R., Pelaez M. A., Lopez A. J. G., Salgado, M. de J. and Moeller G., Photocatalytic decolourisation of synthetic and real textile wastewater containing benzidine-based azo dyes, Chemical Engineering and Processing (2007) (in press).

11. Belkacemi K., Larachi F., Hamoudi S., Turcotte G. and Sayari A., Inhibition and deactivation effects in catalytic wet oxidation of high-strength alcohol-distillery liquors, Ind. Eng. Chem. Res., 38, 2268-2274 (1999).

12. Belkacemi K., Larachi F., Hamoudi S., Turcotte G. and Sayari A., Catalytic wet oxidation of high-strength alcohol-distillery liquors, Applied Catalysis A : General 199, 199-209 (2000).

13. Benjamin M. M., Water Chemistry, McGraw Hill International Edition, 644 p.p. (2002).

14. Bes-Piá A., Mendoza-Roca J. A., Alcaina-Miranda M. I., Iborra-Clar A. and Iborra-Clar M. I., Reuse of wastewater of the textile industry after its treatment with a combination of physico-chemical treatment and membrane technologies, Desalination, 149, 169-174 (2002).

15. Bes-Piá A., Mendoza-Roca J. A., Alcaina-Miranda M. I., Iborra-Clar A. and Iborra-Clar M. I., Combination of physico-chemical treatment and nanofiltration to reuse wastewater of a printing, dyeing and finishing textile industry, Desalination, 157, 73-80 (2003).

16. Chang W. S., Hong S. W. and Park J., Effect of zeolite media for the treatment of textile wastewater in a biological aerated filter, Process Biochemistry, 37, 693-698 (2002).

17. Chaudhari P. K., Mishra I. M. and Chand S., Catalytic thermal treatment (catalytic thermolysis) of a biodigester effluent of an alcohol distillery plant, Ind. Eng. Chem. Res., 44, 5518-5525 (2005).

18. Chen G., Chai X., Yue P.L. and Mi Y., Treatment of textile desizing wastewater by pilot scale nanofiltration membrane separation, Journal of Membrane Science, 127, 93-99 (1997).

19. Chen G., Lei L., Hu X. and Yue P. L., Kinetic study into the wet air oxidation of printing and dyeing wastewater, Separation and Purification Technology, 31, 71-76 (2003).

20. Chen X., Shen Z., Zhu X., Fan Y. and Wang W., Advanced treatment of textile wastewater for reuse using electrochemical oxidation and membrane filtration, Water SA, 31(1), 127 (2005).

21. Chun H. and Yizhong W., Decolorization and biodegradability of photocatalytic treated azo dyes and wool textile wastewater, Chemosphere, 39 (12), 2107-2115 (1999).

22. Daga N. S., Prasad, C. V. S., Joshi J. B., Kinetics of hydrolysis and wet-air oxidation of alcohol distillery waste, Indian Chemical Engineer, 28(4), 22-31 (1986).

23. Damas S. B., Iborra-Clar M. I., Bes-Pia A., Alcaina-Miranda M. I., Mendoza-Roca J. A., Iborra-Clar A., Study of preozonation influence on the physical-chemical treatment of textile wastewater, Desalination, 182, 267-274 (2005).

24. Dantas T. L. P., Mendonca V. P., Jose H. J., Rodrigues A. E. and Moreira R. F. P. M., Treatment of textile wastewater by heterogeneous Fenton process using a new composite Fe_2O_3/carbon, Chemical Engineering Journal, 118, 77-82 (2006).

25. Dempsey B. A., Ganho R. M. and O'Melia C. R. (1984) The coagulation of humic substances by means of aluminum salts. J. Am. Wat. Wks Ass. 76(4), 141-150.

26. Dhale A. D. and Mahajani V. V., Treatment of distillery waste after bio-gas generation : wet oxidation, Indian J. Chemical Technology, 7(1), 11-18 (2000).

27. dos Santos A. B., Bisschops I. A. E., Cervantes F. J. and van Lier J. B., Effect of different redox mediators during thermophilic azo dye reduction by anaerobic granular sludge and comparative study between mesophilic ($30^{o}C$) and thermophilic (55 ^{o}C) treatments for decolorisation of textile wastewaters, Chemosphere, 55, 1149-1157 (2004).

28. Edwards G. A. and Amirtharajah A. (1985) Removing color caused by humic acids. J. Am. War. Wks Ass. 77(3), 50-57.

29. ElDefrawy N. M. H. and Shaalan H. F., Integrated membrane solutions for green textile industries, Desalination, 204, 241-254 (2007).

30. El-Daley H. A., Habib A.F.M. and El-Din M.A.B., Kinetic investigation of the oxidative decolorization of direct green 28 and direct blue 78 by hydrogen peroxide, Dyes and Pigments, 66, 161-170 (2005).

31. Fitch B., Kynch Theory and Compression Zones, AIChE J. 29, 940 (1983).

32. Fongsatitkul P., Elefsiniotis P., Yamasmit A. and Yamasmit N., Use of sequencing batch reactors and Fenton's reagent to treat a wastewater from a textile industry, Biochemical Engineering Journal, 21, 213-220 (2004).

33. Font R., Calculation of the compression zone height in continuous thickeners, AIChE J., 36, 3 (1990).

34. Font R., García P. and Rodriguez M., Sedimentation test of metal hydroxides: hydrodynamics and influence of pH, Colloids and Surfaces A: Physicochemical and Engineering Aspects, 157, 73 (1999).

35. Foust A. S., Wenzel L. A., Clump C. W., Maus L., Anderson L. B., Principles of Unit Operations, Wiley, New York (1960).

36. Gangavati P. B., Safi M. J., Singh A., Prasad B. and Mishra I. M., Pyrolysis and thermal oxidation kinetics of sugar mill press mud, Thermochimica Acta, 428(1-2), 63-70 (2005).

37. Gao B. Y., Wang Y., Yue Q. Y., Wei J. C. and Li Q., Color removal from simulated dye water and actual textile wastewater using a composite coagulant prepared by ployferric chloride and polydimethyldiallylammonium chloride, Separation and Purification Technology, 54, 157-163 (2007).

38. Gao B. Y., Yue Q. Y., Wang Y., Zhou W. Z., Color removal from dye-containing wastewater by magnesium chloride, Journal of Environmental Management, 82, 167-172 (2007).

39. Garg A., Chand S., Mishra I. M., Catalytic wet oxidation of the pretreated synthetic pulp and paper mill effluent under moderate condition, Chemosphere 66, 1799-1805 (2007).

40. Garg A., Mishra I. M. and Chand S., Thermochemical precipitation as a pretreatment step for the chemical oxygen demand and color removal from pulp and paper mill effluent, Ind. Eng. Chem. Res., 44, 2016-2026 (2005).

41. Georgiou D., Aivazidis A., Hatiras J. and Gimouhopoulos K., Treatment of cotton textile wastewater using lime and ferrous sulfate, Wat. Res., 37, 2248-2250 (2003).

42. Gordon, Waste color removal from textile effluents, American Dyestuff Reporter, 29-34, April 1979.

43. Grimau V. L. and Gutierrez M. C., Decolorization of simulated reactive dyebath effluents by electrochemical oxidation assisted by UV light, Chemosphere, 62, 106-112 (2006).

44. Hachem C., Bocquillon F., Zahraa O. and Bouchy M., Decolorization of textile industry wastewater by the photocatalytic degradation process, Dyes and Pigments, 49, 117-125 (2001).

45. Hundt T. R. and O'Melia C. R., Aluminum-fulvic acid interactions: mechanisms and applications. J. Am.War. Wks Ass. 80(4), 176-186 (1988).

46. Jalan R. K. and Srivastava V. K., Studies on pyrolysis of a single biomass cylindrical pellet – kinetic and heat transfer effects, Energy Conversion & Management, 40, 467-494 (1999).

47. Jekel, M.R., Interaction of humic acids and aluminium salts in the flocculation process, Water Res., 20, 1535-1542 (1986).

48. Jia J., Yang J., Liao J., Wang W. and Wang Z., Treatment of dyeing wastewater with ACF electrodes, Wat. Res., 33(3), 881-884 (1999).

49. Jinming Duan and John Gregory, Coagulation by hydrolysing metal salts, Advances in Colloid and Interface Science 100 –102, 475–502 (2003).

50. John E. Van Benschoten I and James K. Edzwald, Chemical aspects of coagulation using aluminum salts I. Hydrolytic reactions of alum and polyaluminum chloride WaT. Res. 24(2), 1519-1526 (1990).

51. Kang S. F., Liao C. H. and Chen M. C., Pre-oxidation and coagulation of textile wastewater by the Fenton process, Chemosphere, 46, 923-928 (2002).

52. Kang S. F., Liao C. H., Po S. T., Decolorization of textile wastewater by photo-fenton oxidation technology, Chemosphere, 41, 1287-1294 (2000).

53. Kapdan I. K. and Alparslan S., Application of anaerobic-aerobic sequential treatment system to real textile wastewater for color and COD removal, Enzyme and Microbial Technology, 36, 273-279 (2005).

54. Karcher S., Kornmuller A. and Jekel M., Screening of commercial sorbents for the removal of reactive dyes, Dyes and Pigments, 51, 111-125 (2001).

55. Kim S. Y., An J. Y. and Kim B. W., The effects of reductant and carbon source on the microbial decolorization of azo dyes in an anaerobic sludge process, Dyes and Pigments (2006) (in press).

56. Kim S., Kim T. H., Park C. and Shin E. B., Electrochemical oxidation of polyvinyl alcohol using a RuO$_2$/Ti anode, Desalination, 155, 49-57 (2003).

57. Kim S., Park C., Kim T.H., Lee J. and Kim S. W., COD reduction and decolorization of textile effluent using a combined process, Journal of Bioscience and Bioengineering, 95(1), 102-105 (2003).

58. Kim T. H., Park C., Lee J., Shin E. B., Kim S., Pilot scale treatment of textile wastewater by combined process (fluidized biofilm process – chemical coagulation – electrochemical oxidation), Wat. Res., 36, 3979-3988 (2002).

59. Kositzi M., Antoniadis A., Poulios I., Kiridis I. and Malato S., Solar photocatalytic treatment of simulated dyestuff effluents, Solar Energy, 77, 591-600 (2004).

60. Kumar.P., Prasad.B., Mishra I. M., Chand S., Catalytic thermal treatment of desizing wastewater. Journal of Hazardous Materials (2007) (In press).

61. Kusvuran E., Gulnaz Q., Irmark S., Atanur O. M., Yavuz H. I. and Erbatur O., Comparison of several advanced oxidation processes for the decolorization of reactive Red 120 azo dye in aqueous solution, Journal of Hazardous Materials, 109(1-3), 85-93 (2004).

62. Kusvuran E., Irmark S., Yavuz H. I., Samil A. and Erbatur O., Comparison of the treatment methods efficiency for decolorization and mineralization of reactive black 5 azo dye, Journal of Hazardous Materials, 119 (1-3), 109-116 (2005).

63. Larue O. and Vorobiev E., Floc size estimation in iron induced coagulation using sedimentation data, Int. J. Miner. Process, 1, 1629 (2003).

64. Lei L., Hu X., Chen G., Porter J. F., Yue P. L., Wet air oxidation of desizing wastewater from textile industry, Ind. Eng. Chem. Res. 39, 2896-2901 (2000).

65. Lei L., Hu X., Chu H. P., Yue P. L., Catalytic wet air oxidation of dyeing and desizing wastewater, Water Sci. Technol. 65, 311-319 (1997).

66. Lei, L., Hu, X., Yue, P. L., "Improved wet oxidation for the treatment of dyeing wastewater concentrate from membrane separation process, Wat. Res., 32, 2753-2759 (1998).

67. Lele S. S., Rajadhyaksha P. J., Joshi J. B., Effluent treatment for alcohol distillery : thermal pretreatment with energy recovery, Environmental Progress, 8(4), 245-52 (1989).

68. Lin S. H. and Chen M. L., Purification of textile wastewater effluents by a combined Fenton process and ion exchange, Desalination, 109, 121-130 (1997).

69. Lin S. H. and Chen M. L., Treatment of textile wastewater by chemical methods for reuse, Wat. Res., 31(4), 868-876 (1997).

70. Lin S. H. and Ho S. J., Catalytic wet-air oxidation of high strength industrial wastewater, Applied Catalysis B : Environmental, 9, 133-147 (1996).

71. Lin S. H. and Lo C. C., Fenton process for treatment of desizing wastewater, Wat. Res., 31(8), 2050-2056 (1997).

72. Lin S. H. and Peng C. F., Continuous treatment of textile wastewater by combined coagulation, electrochemical oxidation and activated sludge, Wat. Res., 30(3), 587-592 (1996).

73. Lucas M. S. and Peres J. A., Degradation of reactive black 5 by Fenton/UV-C and ferrioxalate/H_2O_2/solar light processes, Dyes and Pigments, 74, 622-629 (2007).

74. MaCabe W. L., Smith J. C. and Harriot P., Unit Operations of Chemical Engineering, 6th Ed., McGraw Hill, New York (2001).

75. Malik A. and Taneja U., Utilizing Fly ash for color removal of dye effluents, American Dyestuff Reporter, 20-28, (1994).

76. Mangravite F. J. Jr, Buzzel T. D., Matijevic E. and Saxton.G. B. (1975) Removal of humic acid by coagulation and microflotation. J. Am. Wat. Wks Ass. 67(2), 88-94.

77. Manu B. and Chaudhai S., Decolorization of indigo and azo dyes in semicontinuous reactors with long hydraulic retention time, Process Biochemistry, 38, 1213-1221 (2003).

78. Marcucci M., Ciardelli G., Matteucci A., Ranieri L. and Russo M., Experimental campaigns on textile wastewater for reuse by means of different membrane processes, Desalination, 149, 137-143 (2002).

79. Marcucci M., Nosenzo G., Capannelli G., Ciabatti I., Corrieri D. and Ciardelli G., Treatment and reuse of textile effluents based on new ultrafiltration and other membrane technologies, Desalination, 138, 75-82 (2001).

80. Martin R. B., Fe^{3+} and Al^{3+} hydrolysis equilibria cooperativity in Al^{3+} hydrolysis reactions, J. Inorg. Biochem. 44, 141 (1991).

81. Meric S., Selcuk H. and Belgiorno V., Acute toxicity removal in textile finishing wastewater by Fenton's oxidation, ozone and coagulation-flocculation processes, Wat. Res., 39, 1147-1153 (2005).

82. Merta H., Ziolo J., Calculation of thickener area and depth based on the rate of batch-settling test, Chem. Eng. Sci., 40, 1301 (1985).

83. Navarro A. V., Ramirez M. Y., Salvador S. B. and Gallardo J. M., Determination of wastewater LC_{50} of the different process stages of the textile industry, Ecotoxicology and Environmental Safety, 48, 56-61 (2001).

84. Neamtu M., Siminiceanu I., Yediler A. and Kettrup A., Kinetics of decolorization and mineralization of reactive azo dyes in aqueous solution by the UV/H_2O_2 oxidation, Dyes and Pigments 53, 93-99 (2002).

85. Neamtu M., Zaharia C., Catrinescu C., Yediler A., Macoveanu M. and Kettrup A., Fe-exchanged Y zeolite as catalyst for wet peroxide oxidation of reactive azo dye Procion Marine H-EXL, Applied Catalysis B : Environmental 48, 287-294 (2004).

86. Özbelge T. A., Özbelge Ö. H. and Başkaya S. Z., Removal of phenolic compounds from rubber-textile wastewaters by physico-chemical methods, Chemical Engineering and Processing, 41, 719-730 (2002).

87. Ozer A. and Dursun G., Removal of methylene blue from aqueous solution by dehydrated wheat bran carbon, Journal of Hazardous Materials (2006) (in press).

88. Pala A. and Tokat E., Color removal from cotton textile industry wastewater in an activated sludge system with various additives, Wat. Res., 36, 2920-2925 (2002).

89. Panswad T. and Luangdilok W., Decolorization of reactive dyes with different molecular structures under different environmental conditions, Wat. Res., 34(17), 4177-4184 (2000).

90. Peavy H. S., Rowe, D. R. and Tchobanoglous G., Enviromental Engineering, McGraw Hill International Book Company, 1985, p. 137.

91. Perez M., Torrades F., Domenech X. and Peral J., Fenton and photo-Fenton oxidation of textile effluents, Wat. Res., 36, 2703-2710 (2002).

92. Pia A. B., Clar M. I. I., Clar A. I., Roca J. A. M., Uribe B. C. and Miranda M. I. A., Nanofiltration of textile industry wastewater using a physicochemical process as a pre-treatment, Desalination, 178, 343-349 (2005).

93. Pia A. B., Roca J. A. M., Alcover L. R., Clar A. I., Clar M. I. I. and Miranda M. I. A., Comparison between nanofiltration and ozonation of biologically treated textile wastewater for its reuse in the industry, Desalination, 157, 81-86 (2003).

94. Pia A. B., Roca J. A. M., Alcover L. R., Clar A. I., Clar M. I. I. and Miranda M. I. A., Nanofiltration of biologically treated textile effluents using ozone as a pre-treatment, Desalination, 167, 387-392 (2004).

95. Pradeep Kumar, Prasad B., Mishra I. M., Chand S., Catalytic thermal treatment of desizing wastewaters, Journal of Hazardous Materials (2007) (online).

96. Qin J. J., Oo M. H. and Kekre K. A., Nanofiltration for recovering wastewater from a specific dyeing facility, Separation and Purification Technology, 56, 199-203 (2007).

97. Rajkumar D. and Kim J. G., Oxidation of various reactive dyes with in situ electro-generated active chlorine for textile dyeing industry wastewater treatment, Journal of Hazardous Materials, B136, 203-212 (2006).

98. Ranganathan K., Karunagaran K. and Sharma D. C., Recycling of wastewaters of textile dyeing industries using advanced treatment technology and cost analysis – Case studies, Resources, Conservation and recycling, 50, 306-318 (2007).

99. Richardson J. F., Harker J. H. and Backhurst J. R., Coulson and Richardson's Chemical Engineering, Particle Technology & Separation Processes, Fifth edition, Vol. 2, Elsevier, a division of Reed Elsevier India Pvt. Ltd. (2003).

100. Safi M. J., Mishra I. M. and Prasad B., Global degradation kinetics of pine needles in air, Thermochimica Acta, 412(1-2), 155-162 (2004).

101. Sandhya S. and Swaminathan K., Kinetic analysis of treatment of textile wastewater in hybrid column upflow anaerobic fixed bed reactor, Chemical Engineering Journal, 122, 87-92 (2006).

102. Sanghi R., Bhattacharya B. and Singh V., Seed gum polysaccharides and their grafted co-polymers for the effective coagulation of textile dye solutions, Reactive and Functional Polymers, 67, 495-502 (2007).

103. Sayan E., Optimization and modeling of decolorization and COD reduction of reactive dye solutions by ultrasound-assisted adsorption, Chemical Engineering Journal, 119, 175-181 (2006).

104. Schroder M. Fr., Polar organic pollutants from textile industries in the wastewater treatment process – biochemical and physico-chemical elimination and degradation monitoring by LC-MS, FIA-MS and MS-MS, Trends in Analytical Chemistry, 15(8), p. 349 (1996)

105. Selcuk H., Decolorization and detoxification of textile wastewater by ozonation and coagulation processes, Dyes and Pigments, 64, 217-222 (2005).

106. Sestak, J., Thermochemical Properties of Solids, Academica : Prague (1984).

107. Silva J. P., Sousa S., Rodrigues J., Antunes H., Porter J. J., Goncalves I., Dias S. F., Adsorption of acid orange 7 dye in aqueous solutions by spent brewery grains, Separation and Purification Technology, 40, 309-315 (2004).

108. Singh V. K., Tiwari P. N., removal and recovery of chromium(VI) from industrial wastewater, J. Chem. Technol. Biotechnol., 69, 376-382 (1997).

109. Sinha A. S. K. and Shankar V., Characterization and activity of cobalt oxide catalysts for total oxidation of hydrocarbons, The Chemical Engineering Journal, 52, 115-120 (1993).

110. Sirianuntapiboon S. and Srisornsak P., Removal of disperse dyes from textile wastewater using bio-sludge, Bioresource Technology, 98, 1057-1066 (2007).

111. Srivastava, V.K. and Jalan, R.K., Predictions of concentration in the pyrolysis of biomass materials—I, Energy Conversion and Management, 35(12), 1031-1040 (1994).

112. Srivastava, V. K., Sushil and Jalan, R. K., Prediction of concentration in the pyrolysis of biomass material—II, Energy Conversion and Management, 37(4), 473-483 (1996).

113. Sundin, J. Precipitation of Kraft Lignin under Alkaline Conditions. Doctoral Thesis, Department of Pulp and Paper Chemistry and Technology. Royal Institute of Technology, Stockholm 2000.

114. Swaminathan T. and Subhramanyam P.V.R., Innovative and alternative technology for wastewater treatment and disposal – concept, assessment and application, Chemical Age of India, 33, 153-156 (1982).

115. Szpyrkowicz L., Juzzolino C. and Kaul S. N., A comparative study on oxidation of disperse dyes by electrochemical process, ozone, hypocholorite and Fenton reagent, Wat. Res., 35(9), 2129-2136 (2001).

116. Tan B. H., Teng T. T. and Omar A. K. M., Removal of dyes and industrial dye wastes by magnesium chloride, Wat. Res., 34(2), 597-601 (2000).

117. Toor A. P., Verma A., Jotshi C. K., Bajpai P. K. and Singh V., Photocatalytic degradation of Direct Yellow 12 dye using UV/TiO2 in a shallow pond slurry reactor, Dyes and Pigments, 68, 53-60 (2006).

118. Van der Bruggen B., Daems B., Wilms D. and Vandecasteele C., Mechanisms of retention and flux decline for the nanofiltration of dye baths from the textile industry, Separation and Purification Technology, 22-23, 519-528 (2001).

119. Verma V. K. and Mishra A. K., Removal of dyes by the wheat straw carbon, Ecology, Environment and Conservation, 12(4), 755-757 (2006).

120. Vlaev, L.T., Markovska, I.G. and Lyubchev, L.A., Non-isothermal kinetics of pyrolysis of rice husk, Thermochim. Acta., 406, 1-7 (2003).

121. Vlyssides A. G., Loizidou M., Karlis P. K., Zorpas A. A. and Papaioannou D., Electrochemical oxidation of a textile dye wastewater using a Pt/Ti electrode, Journal of Hazardous Materials, B70, 41-52 (1999).

122. Wu C. H., Chang H. W. and Chern J. M., Basic dye decomposition kinetics in a photocatalytic slurry reactor, Journal of Hazardous Materials, B137, 336-343 (2006).

123. Xu X. R., Li H. B., Wang W. H. and Gu J. G., Degradation of dyes in aqueous solutions by the Fenton process, Chemosphere, 57, 595-600 (2004).

124. Zylla R., Ledakowicz J. S., Stelmach E., Ledakowicz S., Coupling of membrane filtration with biological methods for textile wastewater treatment, Desalination, 198, 316-325 (2006).

CURRICULAM VITAE

NAME	:	**PRADEEP KUMAR**
FATHER'S NAME	:	Dr. Jai Chand
DATE OF BIRTH	:	5th March, 1969
MARITAL STATUS	:	Married
PERMANENT ADDRESS	:	206, Chow Mandi, Railway Road, Roorkee (U.P) PIN – 247667 Phone No. : +91 1332 273689 Mobile No.: +91 9917103555 E-Mail : ppap1234@yahoo.co.in

1. **PROFESSIONAL QUALIFICATIONS: -**

S. No.	Qualification	University/Institute	Year	% of Marks
1	**Ph. D. (Chemical Engineering)**	I.I.T Roorkee, Roorkee	2007	Submitted
2.	**M. Tech. (Chemical Engineering)**	I.I.T Roorkee, Roorkee	2002	7.67 C.G.P.A.
3.	**B. Tech. (Chemical Engineering)**	Amravati University, Maharashtra	1993	59.68%

PUBLICATIONS IN JOURNALS

INTERNATIONAL :

1. **Pradeep Kumar**, Prasad B., Mishra I.M. and Chand S., "Catalytic Thermal Treatment of Desizing Wastewaters", Journal of Hazardous Materials, 2007 (online).

2. **Pradeep Kumar**, Prasad B., Mishra I.M. and Chand S., "Treatment of Composite Wastewater of a Cotton Textile Mill by Thermolysis and Coagulation", Journal of Hazardous Materials, 2007 (online).

3. **Pradeep Kumar**, Prasad B., Mishra I.M. and Chand S., "COD and Color Reduction of Dyeing Wastewater of a Textile Mill Using Thermolysis and Coagulation", Journal of Dyes and Pigments, 2007 (under review).

(Two research papers are to be communicated soon)

NATIONAL :

4. Chaudhari P. K., **Pradeep Kumar** and Chand S., "Comparative Performance of Ion-exchanged ZSM-5 and Y-Zeolite Cataysts for Toluene Disproportionation Reaction", Journal of Scientific & Industrial Research, Vol. 61, Oct. 2002, 810-816.

5. Chaudhary R., **Pradeep Kumar** and Chand, S., "Catalytic wet air oxidation of toxic nitrogen containing compounds (pyridine) from wastewater", Journal of Scientific & Industrial Research, Vol. 65, September 2006, 757-759.

6. **Pradeep Kumar**, Raghvendra P.V.K. and Chand S., "Catalytic wet air oxidation of carboxylic acid present in wastewater" Journal of Scientific & Industrial Research, Vol. 65, Oct 2006, 838-842.